UNIVERSITY OF SUSSEX

DOCTORAL THESIS

Closed-loop photic stimulation using EEG

Author:
Philipp STREICHER

Supervisor:
Dr. Christopher BUCKLEY
Dr. David SCHWARTZMAN

A thesis submitted in fulfillment of the requirements for the degree of Doctor of Philosophy

in the

Department of Informatics

April 16, 2020

Declaration of Authorship

I, Philipp STREICHER, declare that this thesis titled, "Closed-loop photic stimulation using EEG" and the work presented in it are my own. I confirm that:

- This work was done wholly or mainly while in candidature for a research degree at this University.
- Where any part of this thesis has previously been submitted for a degree or any other qualification at this University or any other institution, this has been clearly stated.
- Where I have consulted the published work of others, this is always clearly attributed.
- Where I have quoted from the work of others, the source is always given. With the exception of such quotations, this thesis is entirely my own work.
- I have acknowledged all main sources of help.
- Where the thesis is based on work done by myself jointly with others, I have made clear exactly what was done by others and what I have contributed myself.

Signed:

Date:

"Mother Nature, truly we are grateful for what you have made us. No doubt you did the best you could. However, with all due respect, we must say that you have in many ways done a poor job with the human constitution. You have made us vulnerable to disease and damage. You compel us to age and die – just as we're beginning to attain wisdom. And, you forgot to give us the operating manual for ourselves! ... What you have made is glorious, yet deeply flawed ... We have decided that it is time to amend the human constitution ... We do not do this lightly, carelessly, or disrespectfully, but cautiously, intelligently, and in pursuit of excellence ... Over the coming decades we will pursue a series of changes to our own constitution ... We will expand our perceptual range ... improve on our neural organization and capacity ... reshape our motivational patterns and emotional responses ... take charge over our genetic programming and achieve mastery over our biological and neurological processes. "

— Max More, The Transhumanist Reader: Classical and Contemporary Essays on the Science, Technology, and Philosophy of the Human Future (2013)

UNIVERSITY OF SUSSEX

Abstract

Faculty Name
Department of Informatics

Doctor of Philosophy

Closed-loop photic stimulation using EEG

by Philipp STREICHER

Accumulating evidence indicates that neural oscillations play a central role in brain function, organising and modulating brain activity in response to both bottom-up exogenous stimuli and top-down endogenous dynamics. It has been pointed out that abnormalities in oscillatory dynamics are sometimes associated with various neuropathologies. Consequently, it has been posited that normalising pathological oscillations in these conditions may reduce negative symptoms of brain disorders.

One potential technique for this is photic brain stimulation. However, while it has been shown to be able to increase the power of targeted frequency bands during stimulation, it remains an open question as to whether it is possible to also suppress the amplitude of a frequency band by rhythmic light stimulation. In this thesis, we will explore different light stimulation protocols, assessing whether a more general control of the alpha frequency band is possible. Specifically, we are exploring the during- and post-stimulation impact of photic stimulation and the feasibility that closed-loop interaction between high-luminance LEDs and an electroencephalography (EEG) brain activity signal can both increase and decrease alpha frequency power across the visual cortex while stimulation is being applied.

Acknowledgements

I want to thank my supervisors Dr. Christopher Buckley and Dr. David Schwartzman for their fantastic support and helpful criticism. Their expert knowledge and experience has benefited me greatly, and without their guidance this work would not have been possible.

I am also indebted to Dr. Anil Seth for his support and giving me access to valuable laboratory space and equipment to conduct my experiments.

My thanks is also with my research assistants Joe, Alberto, and Gabrielle.

Most importantly, I want to express my deepest gratitude to my partner and my friends and familiy for their unwavering support.

Contents

List of Figures

List of Tables

Chapter 1

Introduction

Increasing evidence suggests that rhythmic brain activity caused by the selective (de)synchronisation of groups of neurons in response to sensory input is central to information processing in the brain. Abnormalities in these oscillations, are associated with a number of brain disorders such as attention-deficit hyperactivity (ADHD) (Arns et al., 2008) or post-traumatic stress disorder (PTSD) (Wahbeh and Oken, 2013). Therefore, a possible treatment of these conditions, may be achieved through the correction of abnormal oscillations.

1.1 A primer on neurofeedback

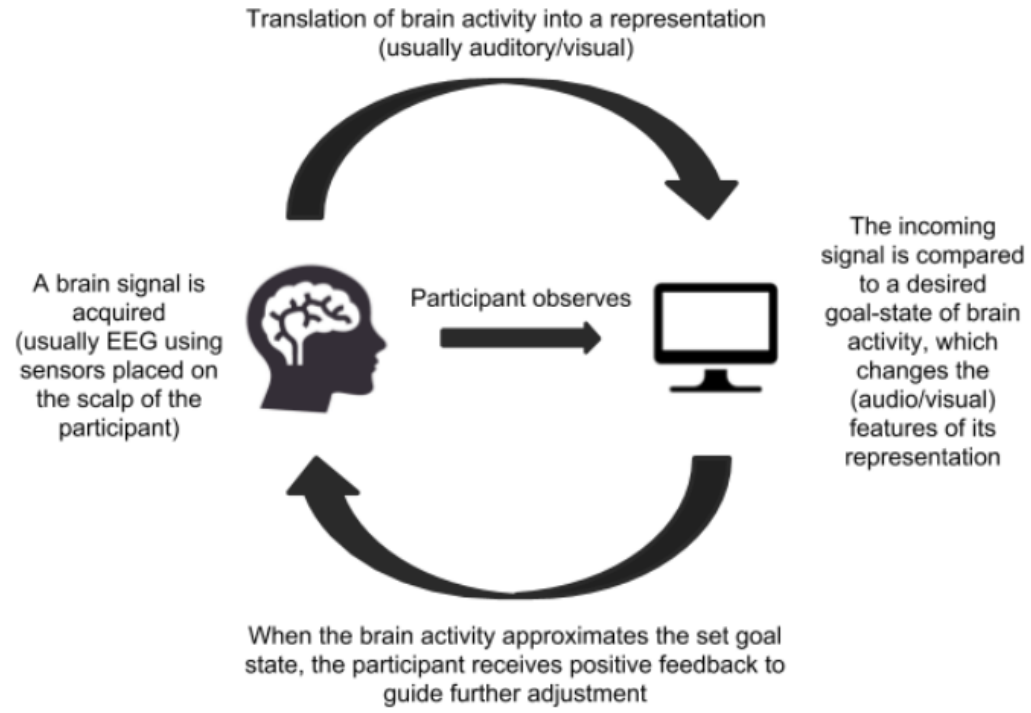

FIGURE 1.1: Principles of neurofeedback

Neurofeedback has emerged as a promising technique for this purpose. It involves giving users a representation of their brain activity, which they then attempt to consciously influence by modulating specific frequency components. On the most basic level, this approach is based on giving participants positive reinforcement as their brain activity approaches a desired goal state. Practically speaking, this might

involve a participant watching the colour of an object on a computer screen change from grey to red as the brain signal (usually EEG) more closely approximates desired criteria. This, however, also requires that the participant is able to self-regulate their brain activity in accordance with a feedback signal, which might not be practical in some cases.

1.2 Rhythmic photic brain stimulation

Rhythmic brain stimulation in the form of photic stimulation may be a viable alternative to the current use of neurofeedback in clinical practice. Applying a fixed rhythmic photic stimulation frequency has already been shown to effectively modulate the alpha frequency range (8-12 HZ) (Adrian and Matthews, 1934). In addition, the effectiveness of photic stimulation in increasing alpha amplitude has been demonstrated (Walter, Dovey, and Shipton, 1946). So far, however, there exists no light stimulation protocol that would also allow for decreasing alpha power. As normalising pathological oscillations might not only involve increasing the amplitude of a specific frequency band, such as alpha, but also to decrease it, this limits the potential clinical application of light stimulation.

1.2.1 The structure of this thesis

In this thesis, we will explore different light stimulation protocols, assessing whether a more complete control of the alpha frequency band is possible.

We first investigate fixed photic stimulation at 10 Hz, including its immediate post-stimulatory effects on alpha power, connectivity levels, and transcranial-magnetic stimulation evoked potentials. We then turn to the phase-dependency of effects, and close by proposing a novel closed-loop feedback protocol. Specifically, we put forward an alternate approach where we construct feedback-based photic stimulation directly from a real-time EEG signal, essentially mirroring neurofeedback, but circumventing the need for a participant's active involvement. Through the closed-loop interaction between high-luminance light flashes and brain activity, we seek to make the photic stimulation phase-dependent, aiming for a more complete control of alpha.

1.3 Chapter breakdown

- Chapter 1: Introduction to the thesis topic
- Chapter 2: Background information and theory

  A review on the relationship of neural oscillations to cognition and behaviour is presented, with a particular focus on the alpha frequency range, as well as an introduction to neurofeedback and photic stimulation, which have emerged as potential approaches to modulate the brains' rhythmic electrical currents.

- Chapter 3: Photic post-stimulatory alpha power suppression

  We confirm earlier findings of repetitive photic stimulation successfully entraining and enhancing alpha activity as measured over occipital electrodes (Herrmann, 2001). We show that these effects can be found beyond the occipital areas in the brain, including medial and frontal areas. For the first time we

also show evidence of significant post-stimulation effects in the form of scalp-wide alpha power suppression. We show that length of stimulation correlates with effect sizes. Finally, we demonstrate that both the alpha power enhancement and consequent suppression impact connectivity measures, as indicated by phase-lag values (PLV).

- Chapter 4: Stimulation duration and post-stimulation alpha power suppression

  We add to our findings from 3 and demonstrate that as stimulation duration increases, post-stimulation alpha power suppression effect sizes increase. Further, we find that, for equal stimulation length, post-stimulation alpha power suppression is strongly reduced in effect size at a lower luminance, implying that photic stimulation after-effects might be increased or decreased with stimulation strength.

- Chapter 5: Conscious attention and alpha power suppression

  This chapter investigates how alpha power suppression might impact behaviour. Prior research has shown that alpha levels and reaction times (RT) are negatively correlated (Nenert et al., 2012; Haig and Gordon, 1998; Callaway and Yeager, 1960), with lower pre-RT-trial alpha power being predictive of slower responses by participants. Building on this, we compare participants' performance in a RT task immediately following photic stimulation in the alpha and delta ranges. As we found post-alpha-stimulation alpha power suppression to be long-lasting in previous experiments, we assumed that, consequently, this would negatively impact RT, when compared to a control condition where we stimulate at 3 Hz, impacting the delta frequency band. Our results, however, showed no statistical difference between conditions in either reaction time or alpha levels. Indeed, post-stimulation alpha power suppression at effect sizes comparable to findings in chapter 3 was only present when participants were asked to ignore the RT task at hand after 10 Hz photic stimulation. Whenever participants were asked to respond to the RT task, alpha power suppression was either reduced or alpha levels returned to their pre-stimulation baseline entirely. This suggests that given the task-demand, exogenous suppression of alpha might be overridden endogenously.

- Chapter 6: Alpha power suppression increases amplitude and spread of TMS-evoked potentials

  We present a follow-up study, probing the impact of alpha power suppression on neural activity in absence of conscious involvement via assessing changes in amplitude and spread of transcranial magnetic stimulation-evoked potentials (TEPs). Results show that alpha power suppression following stimulation significantly increases TEP amplitude in occipital, and medial brain areas, which may be due to the reduction in alpha activity allowing a greater spread of transcranial magnetic stimulation (TMS) pulses. These results support the conclusion that photic stimulation changes the normal operation of the brain even after photic stimulation has ceased.

- Chapter 7: Phase-dependency of photic stimulation effects

  In order to investigate if the effects of photic stimulation are phase-dependent, we performed a study that regularly shifted the phase of the driving photic

stimulus by either adding an additional on- or off-cycle to a fixed 10 Hz stimulation driving signal. We found that out-of-phase stimulation by means of shifting the phase of the stimulation signal significantly changes the ERP response, with an additional off-cycle slowing down the ERP oscillation while increasing its amplitude, and an additional on-cycle speeding it up with a significantly diminished amplitude. These changes can be seen across the scalp and demonstrate that, depending on flash placement relative to endogenous oscillations, EEG brain activity can be both enhanced or suppressed.

- Chapter 8: Closed-loop photic stimulation using EEG

  We propose that the phase-dependency of photic stimulation may be best leveraged with a closed-loop interaction between the photic stimulation and the EEG signal, aiming to make every flash phase-dependent. In a proof-of-concept experiment, we found that feedback-based stimulation that lined flashes up with peaks in the EEG signal increased alpha amplitude during stimulation more effectively than a replay condition, in which the same sequence of flashes was replayed to the participant in absence of direct input from their EEG signal. Similarly, we found that feedback-based stimulation that triggered flashes at troughs of the EEG signal resulted in a significant reduction of alpha power, while a replay condition failed to bring about a significant change in alpha power relative to pre-stimulation baseline values.

- Chapter 9: Conclusion and future directions

  We summarise the findings of this thesis and conclude that they could act as a foundation for future research applying our closed-loop photic stimulation protocol in a clinical setting, to normalise brain wave activity through targeted up- and down-regulation of alpha power or the amplitude of other frequency bands. This could reduce negative symptoms of brain disorders or even enhance cognitive functions in healthy brains. Further, photic stimulation that can both enhance or suppress specific EEG frequency component activity could be used for the purpose of studying their respective proposed cognitive correlates through first modulating EEG activity, and then testing the impact of said modulation on the selected function or ability.

For a brief overview of the experiments done and their main finding, refer to table 1.1.

Chapter	Research question	Contribution
3	Does photic alpha stimulation lead to lasting effects on brain activity?	We find significant post-stimulation alpha power suppression, with concurrent increases in scalp-level neural connectivity.
4	Does stimulation length impact alpha power suppression?	There is a positive correlation between stimulation length and post-stimulation alpha power suppression effect sizes.
5	Lower alpha power and slower reaction times are often correlated. Do participants exhibit slower reaction times during alpha power suppression?	When engaged in a task, alpha power suppression was reduced, with no difference in reaction times.
6	Does alpha power suppression affect neural activity in absence of conscious involvement in a task?	During alpha power suppression (post 10 Hz stim) occipital and medial TEPs are enhanced.
7	Are the effects of photic stimulation phase-dependent?	EEG activity can both be enhanced or suppressed by varying the flash placement relative to endogenous oscillations.
8	Is it possible to both enhance or suppress alpha power during stimulation?	Lining up flashes with peaks of a real-time EEG signal increases alpha power, while lining flashes up with troughs in the signal reduces alpha power.

TABLE 1.1: Experiment overview
This thesis investigates different light stimulation protocols to assess whether photic stimulation can be used to achieve more complete control of the alpha frequency band. Chapters 3 and 4 show that photic stimulation results in entrainment of neural oscillations, and that post-stimulation effects are significant - taking the form of alpha power suppression. Chapter 6 shows that TEP peak amplitude is increased during alpha power suppression over medial and occipital areas following 10 Hz stimulation, indicating a reduction in neural inhibition. Chapter 7 and 8 give evidence that stimulation effects are phase-dependent, and that, depending on flash placement relative to endogenous oscillations, EEG activity generally and alpha amplitude specifically can be both increased and decreased during stimulation, allowing for a more complete control of alpha.

Chapter 2

Background information and theory

2.1 Introduction

Ever since Berger in 1929 discovered that brain activity could be measured from the scalp in the form of rhythmic electrical currents via electroencephalography (EEG), there existed an interest in their potential cognitive correlates and respective possible causal interrelations (Berger, 1929). Different frequency bands are proposed to have discrete properties (Klimesch, 2012), that are associated with distinct functions (Buzsaki, 2006), and their interactions are thought to mediate local and global communication in the brain (Thut, Miniussi, and Gross, 2012; Siegel, Donner, and Engel, 2012; Stein and Sarnthein, 2000). In healthy populations, the resulting EEG frequency profiles show a great degree of consistency within task/resting conditions (Fingelkurts et al., 2006), while neuropathologies like attention-deficit-hyperactivity disorder (ADHD) or post-traumatic stress disorder (PTSD) are associated with significant EEG frequency profile deviations (Arns et al., 2008; Wahbeh and Oken, 2013; Shephard et al., 2019)).

Neurofeedback (NFB) and brain stimulation techniques based on the manipulation of the brain's rhythmic electrical currents have slowly been emerging as promising techniques allowing for a correction of pathological oscillations (Choi et al., 2011; Kim et al., 2016). NFB uses representations of brain activity to allow for volitional modulation of brain activity within specific frequency bands. At the most basic level, this involves a reward signal, which is triggered once the brain activity reaches the desired state. In the case of the first NFB experiments by Kamiya in 1966 (Kamiya, 2011), high pitched clicks were used as indicators that alpha amplitude was increased successfully. Reward signals might, however, take any imaginable form, even though they are most commonly auditory, visual, or a combination of both (Marzbani, Marateb, and Mansourian, 2016). In all cases, NFB involves a change in the signal that is dependent on how closely the real-time brain activity approximates the desired criteria. An object on a screen might change form, colour, move around, or a tone might shift its pitch - as long as the participant is aware that the change is the one that is desired, it can serve as a mental guide stone for endogenous top-down brain modulation (Evans, 2007). While following these signals allows for influencing the speed and amplitude of targeted frequency components (Ros et al., 2014), NFB is only an option for those who are able to consciously self-regulate their neural activity.

Rhythmic brain stimulation techniques, such as repetitive light stimulation, on the other hand, do not necessitate conscious involvement of the user, as they simply apply a fixed stimulation frequency, which enhances the amplitude or changes the speed of the targeted frequency band (Adrian and Matthews, 1934; Walter, Dovey,

and Shipton, 1946). This happens, as brain oscillations become synchronised with a periodic external drive - a process referred to as entrainment (Thut, Schyns, and Gross, 2011). Consequently, light stimulation might constitute a viable alternative to NFB, when its learning curve proves too steep to master.

While neurofeedback can increase and decrease the power of specific frequency bands, however, light stimulation has thus far only been demonstrated to enhance frequency amplitude during stimulation (Walter, Dovey, and Shipton, 1946; Walter, 1963). This means it is limited in potential clinical application, as normalising pathological oscillations might necessitate not just a correction of deficient brain activity by enhancing the power of a targeted frequency band, but also the decrease of excess activity relative to the levels found in the EEG measurements of healthy populations. While theoretical work on the principles underlying entrainment implies that the phase differences between the periodic driving stimulus and the endogenous oscillation might drive the direction of the resulting effect (Pikovsky, Rosenblum, and Kurths, 2001), suggesting that decreasing amplitude by stimulation is potentially possible if stimulation would be phase-specific, fixed stimulation is by its nature phase-ignorant.

In addition, while the effects of NFB have shown to outlast the training session immediately after training had ceased (Choi et al., 2011), there exists no detailed investigation of the immediate post-stimulatory effects of photic stimulation. More specifically, the literature shows no documented evidence of post-stimulatory changes in speed or amplitude of the targeted frequency band, nor if stimulation strength (luminance) or length of stimulation has an impact on during- or post-stimulation outcomes of photic driving. Additionally, there is a lack of an application of more in-depth measures of brain function, such as whether light stimulation also affects connectivity measures. In addition to a lack of rigorous study of the effects of stroboscopic stimulation, there are also practical issues with this brain stimulation method. Most pressingly for matters of broad clinical application, traditional photic stimulation applied at a fixed frequency cannot adapt to differences and changes in the dynamics of the neural oscillators it attempts to entrain. This is particularly problematic, as past research (Walter, 1963) has shown that as the frequency divergence between targeted and driving oscillator increases, the effectiveness of the approach is diminished

A promising approach to address these shortcomings, might entail synthesising the approaches of photic brain stimulation and neurofeedback. To allow for a more complete manipulation of alpha in the form of both its amplitude increase and decrease, we propose a novel closed-loop feedback protocol. Specifically, we aim to make the photic stimulation dependent on a real-time EEG signal, by triggering individual light flashes when the amplitude of the signal crosses a threshold value. This may allow for the controlled manipulation of specific frequency components by both increasing and decreasing their amplitude, and hence for the treatment of pathological oscillations without the need for conscious involvement of the participant.

2.2 Discovery of EEG

In 1929, Berger first discovered that rhythmic electrical currents could be measured from the scalp surface via electroencephalography (EEG) (Berger, 1929). The standard model of EEG assumes that it measures the strength of voltage potentials at the

scalp associated with post-synaptic potentials along dendrites of pyramidal neurons, that is, their synaptic input (Lopes da Silva, 2013; Cohen, 2017).

More specifically, these brain oscillations are thought to be the result of rhythmic fluctuations in local field potentials (LFP) which are, in turn, caused by synchronous transmembrane currents in populations of neurons. It is worth noting, however, that neural processes other than postsynaptic potentials contribute to LFP, including calcium/sodium spikes, or active/passive currents (Buzsáki, Anastassiou, and Koch, 2012; Murakami, Hirose, and Okada, 2003), and that the relationship between LFP and EEG remains imperfectly understood (Mazzoni et al., 2010). Regardless, the standard model assumes that the resulting oscillations in brain activity represent cyclic changes in excitement of local neural elements (Cohen, 2017), which may have preferences to only fire at and respond to certain frequencies of activity (Mehaffey et al., 2008; Hutcheon and Yarom, 2000; Puil, Meiri, and Yarom, 1994). As excitatory neurons fire, it is argued, they activate inhibitory neurons in order to keep neuronal activity in a range that avoids run-away excitation or inhibition which brings about rhythmic patterns of brain activity (Wang, 2010). When neuronal activity is strongly synchronised across hundreds of thousands to millions of nearby neurons, it results in a signal that is measurable via EEG at the scalp level (Cohen, 2017). The neuronal oscillations measured then, are rhythmic patterns representing the degree of synchronized neuronal input to the underlying neuronal ensemble (Buzsaki and Draguhn, 2004) and are described in terms of their frequency, power, and phase. Frequency refers to the speed of the oscillation in terms of its number of cycles per second, described in units of hertz (Hz), power is the amount of energy in a specific frequency band and described as the squared amplitude of the oscillation, and phase is the position along the oscillation at any time point measured in radians or degrees (Cohen, 2014).

SUMMARY

In short, electrical brain activity can be recorded via EEG, which contains rhythmic activity that reflects oscillations which vary in power and speed.

2.2.1 Causal role of neural oscillations

The spectrum of these brain rhythms can be catalogued and grouped into five main frequency bands of delta (1-4 Hz), theta (4-8 Hz), alpha (8-12 Hz), beta (12-30 Hz), and gamma (>30 Hz) (Loomis, Harvey, and Hobart, 1935; Loomis, Harvey, and Hobart, 1937). A good estimate of the center frequency for most people of delta, theta, alpha, beta, and gamma, are 2.5, 5, 10, 20, and 40 Hz respectively (Klimesch, 2012). Each center frequency is twice as high as its neighbour, which generates a chain of harmonics following a scale-free law of doubling/halving any frequency to obtain adjacent harmonics, suggesting a fractal-like organisation. This implies that EEG activity is not an unstructured continuum but that these frequency bands have discrete properties, which is supported, in part, by the finding that each frequency band shows clear task/event related behaviour (Buzsaki, 2006). Indeed, even early on correlations between neural oscillations and mental states were found, for example, alpha waves, were shown to be modulated by mental effort or attention, decreasing in amplitude while participants were solving mental arithmetic tasks (Adrian and Matthews, 1934). Still, it remained unclear whether neural oscillations were causally involved in brain function or mere by-products. Since the early days of EEG research, however, there has been accumulating evidence that neural oscillation frequencies are an organising principle of neuronal communication, enabling normal

brain functioning (Buzsaki, 2006; Wang, 2010; Thut, Schyns, and Gross, 2011). In addition, the finding that there is remarkable cross-species conservation of neural oscillation frequencies, implies that oscillations play a fundamental role in the brain (Kay, 2015).

One proposed function of different frequency bands is that it might be their interplay that enables the dynamic and highly interlinked function of the brain, with slow frequency components of EEG signals representing global large-scale cooperative activity of neuronal populations, whereas high-frequency components mostly reflect joint activity on a local level, giving rise to the observed $1/f$ amplitude characteristics in EEG frequency spectra (Singer, 1993; Stein and Sarnthein, 2000). More specifically, lower frequencies, between 4-12 Hz, that is, from theta to alpha, are thought to enable long distance, area to area interactions, whereas higher frequency oscillations (20-100 Hz) make for local neuronal communication (Thut, Miniussi, and Gross, 2012). Coherence, or signal-similarity, in EEG oscillations of more spatially separated brain regions is, in this picture, interpreted as reflecting functional cooperation (Siegel, Donner, and Engel, 2012; Stein and Sarnthein, 2000).

This interaction between smaller local networks oscillating at higher frequencies and larger more distributed networks operating at lower frequencies, has been proposed to be enabled by cross-frequency coupling (CFC), which might be mediated by interactions between the phase and amplitude of different frequency bands (Thut, Miniussi, and Gross, 2012; Jensen and Colgin, 2007), with the excitatory phases of two frequencies either meeting frequently and regularly (harmonic), as in the interaction between alpha (around 10 Hz) and beta (roughly 20 Hz), or infrequently and irregularly (non-harmonic). Although these mechanisms are imperfectly understood, and their role in neuronal processing remains unclear, cross-frequency phase synchronisation (CFS) and phase-amplitude coupling (PAC) are two of the most documented forms of CFC (Klimesch, 2018).

PAC has been observed between gamma amplitudes, which have been shown to be coupled to the phases of delta, theta, and alpha during attentional sampling of sensory input (Lakatos et al., 2016). During, speech perception, gamma amplitude becomes locked to the phase of theta, which is thought to play an important role in speech segmentation (Gross et al., 2013; Giraud and Poeppel, 2012). CFS differs from PAC in that it depends on a stable phase-difference between the two frequency bands. This means that CFS can only materialise for harmonic couplings where the ratio of frequency m to frequency n does not equal the golden mean (Pletzer, Kerschbaum, and Klimesch, 2010)

$$m : n \neq 1.618, \tag{2.1}$$

as this avoids spurious phase-synchronisation (Klimesch, 2013). If this condition is fulfilled, however, modulation of the oscillatory phase relationships between neural populations via CFS becomes possible.

The importance of m:n frequency ratios to CFS provides a formal explanation for the demarcation of the EEG signal into the five frequency bands detailed above. In order to minimise unwanted cross-frequency band interference, the frequency boundaries, or width of the frequency band, should be set accordingly (Klimesch, 2013). Using the given center frequencies, we can then arrive at the frequency band demarcation given above by the formulas

$$ufb(i) = (1.25(2^{i+1}))/g\,, \tag{2.2}$$

and

$$lfb(i) = (1.25(2i^{-1}))/g \tag{2.3}$$

respectively, where g=1.618, and ufb(i) and lfb(i) are upper and lower frequency boundaries of domain i. The value 1.25 is the basic frequency f0 obtained by introducing the frequency domain (fd) scaling factor

$$fd(i) = s(2^i) \tag{2.4}$$

based on the assumption of the doubling of center frequencies (Klimesch, 2013). It is solved by considering the center frequency of delta as the first value (i = 1)in the harmonic series

$$fd(1) = 2.5\,, \tag{2.5}$$

leading to

$$2.5 = s(2^1)\,. \tag{2.6}$$

When solving for s this gives the basic frequency value

$$f(0) = 1.25\,, \tag{2.7}$$

which is also the scaling factor for all frequency domains via

$$fd(i) = f(0)(2^i) = 1.25(2^i)\,. \tag{2.8}$$

Applied to the alpha frequency band, for example, this would result in a center frequency of 10 Hz

$$fd(3) = f(0)(2^3) = 1.25(2^3) = 10Hz \tag{2.9}$$

and an alpha band of 8-12 Hz, as defined above, via upper and lower bounds being established with

$$ufb(3) = \beta/g = 20/1.618 \approx 12Hz \tag{2.10}$$

and

$$lfb(3) = \delta/g = 5/1.618 \approx 8Hz\,. \tag{2.11}$$

This line of reasoning provides justification for the demarcation of the alpha rhythm that we use in this thesis, asides from convention. Further, this formal model shows the plausibility of the notion of a center frequency, an assumption on the basis of which we will later use 10 Hz stimulation to drive the alpha rhythm. Most centrally, however, it also provides further explanation as to the mechanisms underlying CFS.

Practically, CFS has been observed during parametric visual working memory (VWM) tasks, showing phase interactions between alpha, beta, and gamma, possibly highlighting the functional significance of CFS in the temporal organization of neuronal processing (Siebenhühner et al., 2016).

Oscillatory cycles in the brain then, could be the basis for a recurrent temporal reference frame, allowing for coding of temporal relations between (groups of)

neural elements and the environment (Lőrincz et al., 2009; Busch, Dubois, and VanRullen, 2009). This means that information may be represented through multiplexing - through combining multiple signals into one - by relying on the hierarchical organisation of oscillations, with their impact on information processing being proportional to their magnitude ((Panzeri et al., 2010). In this way, by means of cross-frequency interaction in a multi-band neuronal workspace, oscillations could facilitate the dynamic routing or gating of information through the (de)synchronization of neuronal elements (Palva and Palva, 2007).

This new perspective tells a story of processing in the brain as a quantized system of relations shaped by rhythmic pulses. Hence, in a more complete picture, brain function might not only be based on functional anatomy and spatial connectivity, but also on its temporal structure. In other words, the language of the brain might lie in neuronal coding, but its expression is best described by its rhythmicity and timing. This rhythmicity is due to selective (de)synchronisation of the encoding of billions of neurons (Cohen, 2014).

Given the seeming importance of the rhythmic organisation of brain activity, specifically that synchronisation patterns between neural groups are modulated endogenously, shaping processing during attention and cognition (Palva and Palva, 2012), abnormal dynamics in the interplay of different frequency bands may be at the root of some neuropathologies. To the extent that specific cognitive mechanisms can be linked with brain rhythms, and an understanding can be created that also links deficiencies or excesses of activity in specific frequency bands with associated brain disorders, there lies the potential to treat neuropathologies with exogenous brain stimulation.

This endeavour is complicated by the fact that identified cognitive mechanisms far outnumber the five different frequency bands. This implies, that it is far too simplistic to expect a direct mapping between specific frequency bands and cognitive or perceptual functions (Herrmann et al., 2016). Instead EEG oscillations likely contribute to brain function depending on where in the brain they occur, as well as on their respective parameters such as amplitude, frequency, phase, coherence, and their interactions with each other. Given the assumption that different brain regions perform different and specific functions, this seems intuitively reasonable (Buzsaki, 2006). Any complete treatment of pathological oscillations is hence unlikely to be concerned with just one frequency band in isolation, but rather take into account its interplay with local and global brain dynamics. This is the reason why, in clinical practice, NFB practitioners often do not aim to modulate the speed or amplitude of a single frequency band, but rather change ratios between frequency bands, their coherence (signal similarity), phase-synchrony, or try to normalise more global parameters, such as background EEG scaling (Evans, 2007).

SUMMARY

In summary, EEG activity can be grouped into five main frequency bands, which have distinct properties and are organised in a fractal-like manner, with the center frequency of each frequency band following a scale-free law of doubling/halving in relation to preceding/succeeding center values. The width of each frequency band is such that the upper band is defined by equation 2.3, and the lower band according to equation 2.2, as to ensure that CFS can take place. CFS and PAC are two examples of CFC, and their dynamics serve as evidence that multiplexing is used in the brain in order to facilitate local- and global communication, which indicates that oscillations play a causal role in brain function. Further, the importance of temporal relations between groups of neural elements in CFS implies that oscillatory cycles are perhaps

the basis for a recurrent temporal reference frame of the brain. Given that this means that the rhythmic organisation of brain activity is important for normal brain function, aberrations in rhythmic activity might be at the root of some neuropathologies. While we can potentially normalise pathological oscillations with brain stimulation, it is not a simple matter, as our discussion of the importance of CFC has shown that it is unlikely that aberrations in a single frequency component are to blame for the emergence of a neuropathology, but that a more global account is needed as to where the interplay of various frequency bands has become pathological. For the sake of simplification, however, we will, for now, just focus on one frequency band and how it might relate to brain function and neuropathologies.

2.2.2 The alpha rhythm

A very prominent example of how an oscillatory rhythm may contribute to cognition can be found in the alpha rhythm. As, via EEG, its occipital activity can be very easily observed, it was chosen as the frequency band of focus for this thesis.

In the original EEG experiments by Berger, alpha (8-12 Hz) was shown to oscillate depending on the degree of attention paid to a stimulus (Berger, 1929). As subjects lost their attentional focus, the alpha amplitude increased. The largest increase occurred when participants closed their eyes. Following these observations, alpha was often interpreted as simply representing an idling process of the visual system. It is only recently that alpha has been reconceptualized as being involved with memory (Klimesch, 1997), attentional (Hanslmayr et al., 2011; Thut et al., 2006), and inhibitory processes (Klimesch, Sauseng, and Hanslmayr, 2007).

Accumulating evidence suggests that alpha oscillations are subserved by the thalamo-cortical loop, acting in close association with cortico-cortical networks (Steriade et al., 1990; Saalmann et al., 2012; Buzsaki, 2006). Recent findings suggest that this loop involves the lateral geniculate nucleus (LGN), the visual cortex, and the thalamic pulvinar nucleus, which acts to modulate alpha synchrony between cortical areas as a function of attentional demands (Saalmann et al., 2012). Alpha oscillations are present across the cortex, and their purported functions and mechanisms vary depending on which area of the cortex is investigated (Buzsaki, 2006). For example, alpha activity in the motor cortex expresses itself in the form of mu-waves, that, perhaps unsurprisingly, are thought to be involved in attentional demands of sensorimotor activity (Pfurtscheller and Neuper, 1994), while occipital alpha activity are thought to be associated with the processing of visual information (Mathewson et al., 2012). This is where, together with parietal areas, the largest alpha amplitude can be observed (Lopes da Silva, 2013). Besides varying in speed, power, phase and functional purpose across different brain regions (Buzsaki, 2006), alpha frequencies have also been shown to vary between individuals and across time, as alpha, first predominantly occipital in origin, slows down, and becomes more frontal with age (Gratton et al., 1992; Thorpe, Cannon, and Fox, 2016), showing that alpha is not a static phenomenon.

SUMMARY

To sum up, alpha oscillations are subserved by the thalamo-cortical loop and cortico-cortical networks, range from 8-12 Hz and are present across the cortex. They are associated with attentional, memory and inhibitory processes, although their specific function varies depending on the functional specialisation of the brain region under investigation.

2.2.2.1 Alpha as an attentional-inhibitory system

Alpha activity has been shown to display a varying response to presented stimuli or tasks (Pfurtscheller and Lopes da Silva, 1999; Mathewson et al., 2011). Measuring alpha power levels, task-active brain regions exhibit an amplitude decrease, known as an event-related desynchronization (ERD), while areas that are not task-relevant exhibit an increase in amplitude, referred to as an event-related synchronization (ERS) (Pfurtscheller and Lopes da Silva, 1999). It can be argued that alpha ERS is perhaps best framed as reflecting inhibition of neural processing (Mathewson et al., 2011). A good example of this relationship can be found during a visual reaction time task, where non-visual areas of the brain exhibit alpha ERS, while the visual cortex displays alpha ERD, with the level of alpha desynchronization being negatively correlated with reaction time speed (Nenert et al., 2012; Callaway and Yeager, 1960; Bompas et al., 2015; Haig and Gordon, 1998; Bastiaansen et al., 2001). This response makes intuitive sense, as the brain tries to minimise interference from task-irrelevant areas and focuses cognitive resources on the task-relevant visual cortex by releasing its inhibitory brake on cognition based on attentional demands. The idea that alpha may play a role in optimising distribution of computational supply matching attentional demands was first formalised under the term "focal ERD/surround ERS" by (Suffcynski et al., 1999) on the basis of neuronal network simulations. More precisely, it is argued that the antagonistic ERD/ERS pattern is a consequence of the interaction between thalamo-cortical nodes, where alpha ERD in an active node removes inhibition on the inhibitory network of neighbouring nodes, resulting in surround ERS, with the goal of facilitating task-relevant information processing (focal ERD) through the simultaneous inhibition of task-irrelevant cortical areas (surround ERS) thus optimising cognitive resource allocation to favour processing demands of task-relevant areas (Suffczynski et al., 2001; Neuper and Klimesch, 2006).

Hence, alpha might not just reflect sensory disengagement but could be an active component in cognitive control and attention through modulatory influences of both its overall power and specific phase (Mathewson et al., 2011). This mechanism of selective inhibition of neural processing, with inhibition being defined as a silencing of weakly excited cells, while pulsed patterns of action potentials (APs) are induced in cells with higher excitation levels, would aid working memory (WM) representation, arguably making alpha its most likely correlate.

SUMMARY

Alpha activity changes based on task demands or presented stimuli, as it seems to regulate memory, attentional, and inhibitory processes in relation to situational demands, aiding overall efficiency of computational processes of the brain via focal ERD/surround ERS. WM is its closest cognitive correlate.

2.2.2.2 Alpha and cognitive correlates

WM is a theoretical cognitive system that allows for the allocation of attention, temporary storage or quick processing of information, while modulating their potential integration with stored data. It is, as many theoretical systems, undergoing regular revisions, with some of its components being more controversial than others (Baddeley, 2012). For the sake of this thesis, we will describe it as comprising of slave units for auditory and visual data, a buffer that integrates information across those subsystems, and of a higher-level supervisory attentional system, to which they are subservient, and which can switch their function from storing to processing data

on demand (Norman and Shallice, 1986; Baddeley, 2000). The functionality of this higher level attentional system, dubbed the central executive, can consequently be subdivided into mechanisms of attention focusing, dividing, and switching (Baddeley, 1996). Supporting the idea that alpha might be a correlate of WM, research has demonstrated that its amplitude increases in early sensory regions in concurrence with memory load (Jensen et al., 2002). Other findings give credence to the WM-alpha-connection, by showing how alpha is modulated by attentional shifts between focused (exploitative) and exploratory processing, two core functions often assigned to the central executive component of WM (Hills, Todd, and Goldstone, 2010). When focused attention shifts inward, such as when the participant's eyes are closed (Berger, 1929) an increase in posterior and frontal alpha is observed, and when mental or sensory processing starts, frontal alpha power suppression occurs (Benedek et al., 2014). During an inward shift of attention, information from the outside world loses relevance, and the increase in alpha activity consequently could be interpreted as the successful inhibition of external input. Conversely, processing information might require an appreciation of its features and how they connect to stored data, which necessitates the decrease of inhibitory functions of the brain (and hence alpha), as the range of potential interconnectivity between new impression and stored data is broadened. Once integration of the information in the short-term memory storage (STM) of WM with long-term memory (LTM) happens, however, it would be necessary to limit the breadth of the informational network by boosting suppression of weakly excited nodes. This pruning, arguably, would have to happen for any successful LTM-STM integration. Consequently, if alpha were a correlate of WM, an increase in frontal alpha should be expected to be correlated with this shift from short- to long-term memory. This is supported by Mathewson, who found that frontal alpha power positively correlates with- and predicts learning rate both before and during a training session (Mathewson et al., 2011), and Meeuwissen et al., who showed that alpha power during long-term memory encoding was positively correlated with its success (Meeuwissen et al., 2011).

Alpha activity has not just been shown to be related to WM, it is has also been shown to be modulated by retrieval of information from LTM, which is outside the scope of WM operations. Specifically, LTM retrieval coincides with a decrease in alpha amplitude, with the ERD magnitude varying as a function of the semantic content of the information being retrieved - more semantically integrated information causes larger ERD (Klimesch, 1997). This makes sense, as more semantically integrated pieces of data would necessitate more cortical excitation than less integrated information, and consequently a decrease in inhibition reflected in alpha activity, but also highlights the fact that alpha is not identical to WM. For this reason, (Klimesch, 2012) puts forward the hypothesis that alpha activity reflects not any particular cognitive construct such as WM, but rather an attentional-inhibitory system modulating access to WM, which in turn mediates LTM-STM interaction and access to declarative LTM, procedural memory, and implicit-perceptual memory.

Going beyond memory- related processes, alpha as an attentional-inhibitory system, to maximise efficiency, also can be viewed as a preparatory mechanism that allocates cognitive resources for information processing purposes in anticipation of future demands (Rohenkohl and Nobre, 2011; Thut et al., 2006; Park et al., 2014; Buzsáki, Anastassiou, and Koch, 2012). Specifically, Rohenkohl and Nobre have shown that alpha plays a role in the generation of expectations about upcoming stimuli, noting that an unfulfilled expectation of a stimulus leads to a decrease in alpha power to a degree comparable to when the anticipated stimuli actually occurred (Rohenkohl and Nobre, 2011). This anticipatory change in alpha directly impacts

information processing, as it has been shown to be positively correlated with subsequent behavioural attentional-tasks (Thut et al., 2006) and also impacts long-term memory performance (Park et al., 2014). Consequently, we can say that it is not just temporal but also anticipatory attention that is reflected in alpha activity (Buzsaki, 2006).

Together these observations support neural oscillations as playing a causal role in cognition in general, and highlights the influence the alpha rhythm might have in modulating anticipatory, attentional, and inhibitory processes. This hypothesis suggests that there might be a certain range of oscillatory activity in the alpha band that is ideal to fulfill these functions, a certain speed of oscillation and maximum/minimum power level that would maximise the effectiveness of alpha related cognitive correlates. We speculate that these ideal parameters can be found within the normal range of alpha activity, with normal being defined as the range of oscillatory activity found clustering around the average of a randomly sampled population following a Gaussian distribution. Deviations from this distribution can therefore be viewed as abnormal, and to the extent that they are associated with brain disorders, can be deemed pathological, as alpha parameters drift further from their ideal values. This view of there being a normal distribution of typically healthy alpha is supported by the fact that EEG measures exhibit consistency within task/resting conditions in healthy populations (Fingelkurts et al., 2006). Moreover, various brain disorders have been identified that are associated with deviations from that norm - with abnormalities in the alpha rhythm. For example, a slower frequency of resting state individual alpha (IAF) is associated with attentional deficit hyperactivity disorder (ADHD) (Arns et al., 2008). If alpha acts as an attentional-inhibitory mechanism, as we have posited, then it is unsurprising that a slower IAF frequency would mean that thoughts or actions that do not pertain to the object of attentional focus would be more difficult to block out effectively. Similar problems lie at the core of post-traumatic stress disorder (PTSD), which shows an IAF with lower power and higher frequency, affecting the normal cortical inhibitory functioning, which perhaps explains why PTSD is associated with cortical hyperarousal (Wahbeh and Oken, 2013). Similarly, depression in humans is commonly associated with diminished alpha activity (Kan and Lee, 2015; Choi et al., 2011). Lastly, Alzheimer's patients show diminished IAF power compared to healthy populations (Babiloni et al., 2009), which perhaps can be linked to how alpha modulates memory encoding and retrieval, with alpha power and successful long-term memory encoding or retrieval being positively correlated, making the lack of it in patients with Alzheimer's problematic (Meeuwissen et al., 2011; Klimesch, 1997; Park et al., 2014).

As argued above in section 2.2.1, it is unlikely that a single frequency band is the sole causal agent underlying neuropathologies, the underlying oscillatory aberrations leading to the pathology are likely to be both more complicated and diverse. To give a notion of the complexity of the topic at hand, it is worth mentioning that the very notion of EEG abnormality might be a state- and task-dependent phenomenon (Arns et al., 2008), where, for example, the differences between brains of healthy subjects and patients with ADHD need to be teased out through the use of attentional tasks (Buyck and Wiersema, 2015). In addition, the resulting differences might manifest in distinct fashions, with EEG differences between healthy subjects and, for example, ADHD subjects not following a uniform pattern (Sohn et al., 2010). This implies that what we commonly identify as a single neuropathology might in fact be heterogeneous at its core. While neuropathologies may present themselves with similar symptoms, they may be caused by different underlying mechanisms and hence need to be treated on an individual basis. Even under these circumstances,

however, we are dealing with aberrant oscillations, how they could be treated, and how they might arise in the first place.

SUMMARY

WM is the closest cognitive correlate of alpha activity, as it too deals with memory, attentional, and inhibitory processes. As alpha activity is also modulated by LTM retrieval, however, alpha is unlikely to reflect a single theoretical cognitive construct, but rather a yet to be fully outlined attentional-inhibitory system mediating interaction between WM, STM, and LTM, while also aiding the allocation of cognitive resources based on temporal and anticipatory demands. Given the functional importance of alpha, deviations from normal ranges of alpha activity might play a part in disrupting the functioning of associated cognitive mechanisms, in turn giving rise to neuropathologies such as ADHD. As neuropathologies might be heterogeneous in origin even though overlap in symptoms suggests uniform causation, caution is warranted in suggesting cures. In some cases, pathological interplay of various frequency components might be a more likely culprit than aberrant activity in isolated frequency bands. Still, the association between various neuropathologies such as PTSD and aberrant alpha activity warrants further study of the effectiveness of clinical alpha modulation and how pathological oscillations might come about.

2.3 Clinical modulation of alpha

Many studies have attempted to understand abnormal oscillatory patterns and how they might come about, investigating the dynamics of degenerative encephalopathies (Stam, 2005) or studying the emergence of thalamocortical dysrhythmia (TCD) (Llinás et al., 1999). Most relevant for this thesis, as his model has the broadest explanatory power, Stam proposes that the system of the brain can be envisaged as a multidimensional energy state-space (Stam, 2005). We can think of it in a simplified manner, as a two dimensional plane. On it, the dynamic state of an oscillator, driven by random energy (noise in the system), experiences increased stability in low-potential valleys (basins of attraction) and less so in hills (repellers). These basins and repellors are numerous, and differ in their potential to withstand perturbations and give stability to the system. While the brain's organisation might be multistable, with the state of a neural oscillator traversing multiple states (Van de Ville, Britz, and Michel, 2010; Mehrkanoon, Breakspear, and Boonstra, 2014; Ghosh et al., 2008), local minima might turn out to be suboptimal for overall functioning of the system. They might, however, be stable enough that the oscillator gets stuck, unless it is disrupted by exogenous forcing. This might be why pathological oscillations can sustain themselves, even though a preferable minima exists. While this simplification of Stam's model (Stam, 2005) proposed here is not meant to be taken as a complete description of how pathological oscillations actually do arise in the brain, it can serve as a guide stone to orient our thinking. Relevant for this thesis, in line with the models predictions, alpha rhythms do exhibit distinct dynamical (non-random) state transitions (bifurcations) between low and high synchronisation states (Freyer et al., 2009; Freyer et al., 2011). This is especially relevant for our discussions of pathological oscillations, as said bifurcations have been shown to impact brain function (Kornmeier and Bach, 2012). Specifically, Kornmeier and Bach have found that alpha oscillations, among others, are predictive of perceptual transitions of the occurrence of perceptual alternations in bistable visual stimuli (such as in the Necker Cube illusion) (Kornmeier and Bach, 2012). In addition, alpha exhibits attractor properties

around distinct frequency peaks (Pradhan et al., 1995; Freyer et al., 2011; MacIver and Bland, 2014), which we can liken to minima in our two-dimensional brain-state attractor plane (BSAP).

Expanding on the BSAP model, Ros et al link the emergence of abnormal oscillatory patterns to the concept of system criticality (Ros et al., 2014). A system is said to operate at the sweet-spot of criticality, when it manages to balance order and disorder, which maximises both flexibility and stability (Pastukhov et al., 2013; Hellyer et al., 2014). Supercritical organisation is defined by brief dwell times of the oscillator state, which leads to unpredictable bifurcations and hence random noise. Conversely, systems exhibiting subcriticality are so heavily synchronised that they converge towards a global state. Alternatively, super- and subcritical regimes could be described in terms of their respective levels of coupling or synchrony of their constituent elements. For the former, with low coupling/synchronisation, you have Gaussian noise, for the latter, with high coupling/synchronisation, you have rhythmic patterns. In the middle, there is a critical region - hence the term "criticality" - where levels of informational complexity are maximised, balancing between randomness and total order (Sporns and Honey, 2006)). Although speculative, there is evidence that the healthy brain might operate near criticality in the background scaling of the EEG power spectrum: Once the prominent oscillatory peaks of the signal are removed, the resulting "pink noise" has a hyperbolic shape of $1/f$, which is typical of scale-free (fractal) dynamics, which are indicative of the self-organising dynamics of complex systems that actively maintain a critical state (Bak, Tang, and Wiesenfeld, 1988). Indeed, as reviewed by Hesse and Gross, operating near criticality would maximise the informational complexity that the brain could handle (Hesse and Gross, 2014). In line with this, Sporns et al.point out that magnetoencephalographic (MEG) records reveal large-scale functional brain networks which exhibit "small-world" structure (Sporns and Honey, 2006), that is, high levels of clustering with short path length, which are largely preserved across frequency bands and behavioural tasks. A "small-world" network organisation strikes the balance between distributed and local connectivity under the constraint of wiring costs (Bullmore and Sporns, 2009), and, again, tends towards criticality (Russo, Herrmann, and Arcangelis, 2014). Based on Stam and Ros et al. we speculate, that it is perhaps the balance between excitation and inhibition of brain activity that would result in its criticality (Stam, 2005; Ros et al., 2014), as the excitation/inhibition balance of the brain has been shown to be abnormal in a number of brain disorders (Montez et al., 2009), with subcritical or supercritical regimes of brain exhibition/inhibition balance manifesting themselves as disorders (Montez et al., 2009; Poil et al., 2012).

In line with this, this thesis speculates that restoring brain function by correcting pathological oscillations to be in line with the neural signatures found in healthy populations would push the brain near-criticality, to optimise information processing (Thatcher, North, and Biver, 2009; Shew and Plenz, 2013) - whether it is by modulating frequency power, phase-locking, the speed of an oscillator, or the background EEG scaling.

SUMMARY

Pathological alpha oscillations might come about as a consequence of the neural oscillator getting stuck in a local minima of the BSAP, which might be stable enough to not allow for an endogenous adjustment to a more ideal minima. Evidence suggests that the ideal state would approach an excitation/inhibition balance of the oscillator that brings about "small-world" network structures and brings the BSAP

close to criticality, so that flexibility and stability are both maximised. Brain functions impaired by pathological alpha oscillations may hence be restored by pushing the oscillator closer to said point on the BSAP, which might involve normalising measures such as alpha power or alpha speed.

2.3.1 Neurofeedback

Neurofeedback (NFB) might provide one such way in which abnormal oscillatory patterns of brain activity could be corrected. This technique dates back to 1966, when Kamiya (Kamiya, 2011) published first results of an experiment that aimed to allow for volitional control of brain oscillations, by providing subjects with real-time information about their current EEG alpha levels. He successfully demonstrated its viability, using auditory feedback, which allowed users, who were guided by the audio signal, to increase their alpha levels. This was later shown to work with non-human animals as well (Wyrwicka and Sterman, 1968; Fetz, 1969), where it had effects on brain function (Fairchild and Sterman, 1974), and was long-lasting (Sterman, Howe, and Macdonald, 1970). Specifically, Sterman's original experiments on using NFB on cats in order to increase the amplitude of their SMR which, similar to the alpha rhythm, seems to facilitate neural inhibition, deserves a brief mention (Sterman, LoPresti, and Fairchild, 1969). Working for NASA, Sterman, LoPresti and Fairchild were tasked to conduct research about the toxicity of rocket fuels, as they contain compounds that absorb coenzymes needed for the synthesis of inhibitory neurotransmitters (Sterman, LoPresti, and Fairchild, 1969). When an organism is exposed to those fuels, seizures ensue, which can be deadly. Because of this, Sterman, LoPresti, and Fairchild used cats to investigate the dose-response relationship, trying to evaluate which central nervous system mechanisms might mediate the effects post-exposure to monomethylhydrazine (MMH) (Sterman, LoPresti, and Fairchild, 1969; Sterman, LoPresti, and Fairchild, 2010). The finding most relevant for this thesis, is that they demonstrated that a subset of cats was not susceptible to seizures, who just happened to have gone through another experiment, where operant conditioning was used to increase their sensorimotor rhythm (SMR) amplitude a year earlier (Wyrwicka and Sterman, 1968). Sterman and Friar, inspired by their success to increase the SMR amplitude in cats, then applied SMR NFB to a patient suffering from epilepsy, significantly reducing the number of subsequent seizures after his SMR was successfully enhanced (Sterman and Friar, 1972).

This shows that NFB can modulate the alpha rhythm, and that these changes to the alpha rhythm have functional relevance, in this case the increase of the inhibitory potential of alpha, hindering the uncontrolled spread of neural activity associated with seizures, and hence their onset. In addition, this also demonstrates that changes caused by NFB can be long-lasting.

As these results demonstrate, it is possible to modulate neural oscillations using NFB. Findings by Ghaziri et al. have further demonstrated, that NFB is able to affect changes in brain plasticity, as they successfully increased gray- and white-matter volume in healthy subjects, using beta NFB training, where participants are taught how to increase their beta frequency band amplitude, which is thought to benefit the ability to pay sustained attention (Ghaziri et al., 2013). These results support NFB as an interesting candidate that can be used to optimise brain function (Gruzelier, 2014) and countering neuropathologies relating to oscillatory abnormalities (Niv, 2013). In fact, previous research applying NFB for the treatment of brain disorders, have already shown promising results (Becerra et al., 2006; Choi et al., 2011). NFB

treatment of ADHD, for example, has yielded behavioural improvements in a two-year follow-up study, which were associated with sustained normalisation of the resting-state EEG (Becerra et al., 2006). Similarly, NFB has been shown to reduce depressive symptoms by enhancing right frontal alpha amplitude (Choi et al., 2011). Not everybody might be able to self-regulate their brain activity at the same levels of effectiveness, however, making NFB limited in potential application.

SUMMARY

NFB allows for the self-guided modulation of EEG frequency components, including the normalisation of pathological alpha oscillations. Although, at this time, evidence is limited that modulation of frequency bands will improve pathological behaviour, existing research has shown that NFB-based normalisation of EEG activity is associated with long-lasting positive effects on brain function in non-human animals and human participants alike.

2.3.1.1 Hebbian versus homeostatic plasticity

As demonstrated by Choi et al., NFB can bring about long-lasting changes in alpha levels, in line with previous training (Choi et al., 2011). The amplitude enhancement of the alpha rhythm during NFB training in subjects whose alpha power is below levels expected in healthy populations, hence seems to show long-lasting change to more closely approximate normal power levels. Similarly, the NFB training of Becerra et al. (2006) showed both long-lived frequency profile changes, and increases in gray- and white-matter volume in healthy subjects (Becerra et al., 2006). Both of these pieces of evidence point towards NFB working via mechanism of NFB-induced Hebbian plasticity, following the principles that neurons that fire together, wire together, and that those who fire apart, wire apart (Hebb, 1949). In other words, oscillatory patterns brought about with NFB would, after some time, strengthen the connection between population(s) of involved neurons, making it easier for the resulting neural pattern to emerge again in the future. There is, however, evidence that implies that this perspective is incomplete. Kluetsch et al., for example, used NFB to reduce alpha amplitude in patients with PTSD (Kluetsch et al., 2014). This is a curious choice, as PTSD patients have reduced alpha levels already, when compared to healthy populations (Wahbeh and Oken, 2013). Even curiouser is that, after training had finished, the participants showed a significant increase in their alpha amplitude compared to pre-training baseline levels - alpha levels during NFB training were negatively correlated with their post-training baseline (Kluetsch et al., 2014). Rather than this being due to Hebbian forces we can speculate that this is the product of a homeostatic mechanism. Considering our discussion on the BSAP, the normal distribution of EEG activity, and the existence of center frequencies within each frequency band, we can begin to make sense of this finding. We can speculate that, if there is something like a global minimum in the BSAP which oscillators can approximate, perhaps in the form of the centre frequencies of each frequency band, they would provide an ideal baseline to ensure overall normal brain functioning. We can further speculate that Hebbian plasticity alone would be unable to reach this global minima, as the brain, relying on it alone would find itself in an infinite feedback loop away from that centre, towards excessive or deficient oscillations and consequently neuropathologies. Only the existence of some homeostatic mechanism, would keep oscillations close to their centre values. Although this interpretation is speculative, the results of Kluetsch et al. imply that, when engaging in brain modulation, we should not expect the results to follow pure Hebbian rules,

but also encompass homeostatic principles (Kluetsch et al., 2014). We may speculate that, the further it is removed from its ideal minima, homeostatic mechanisms are increasingly likely to ensure stability of the system. When the oscillator approaches the global BSAP minima, however, it can likely be moved by Hebbian forces.

SUMMARY

NFB likely involves both processes of Hebbian and homeostatic plasticity, depending on how far away the targeted oscillator is from its ideal position in the BSAP. Close to the global minima we might expect Hebbian forces, which make way for homeostatic dynamics as the oscillator deviates too strongly from its ideal center values.

2.3.1.2 Control theory and neurofeedback

The fact that NFB changes the EEG frequency profile of non-human animals (Wyrwicka and Sterman, 1968; Fetz, 1969) seems to imply that NFB largely involves implicit learning, which may in turn mean that higher cognitive processes would not play a significant role in the process. This open-loop behaviourist interpretation would hence conclude that NFB is simply about specifying a frequency band in need of repair, and then applying operant conditioning until the desired end-state is reached. In contrast to this, Ros et al postulate that NFB is better thought of as being part of a closed-loop control system, where the output affects input (Ros et al., 2014). To make this point, they point to control theory, which deals with the behaviour of dynamical systems within a feedback loop. In a control system, a controller unit adjusts the behaviour of the system by comparing the data from an output sensor and an input reference set-point, until the measured error between both equals zero. Instead of the change in the state of the oscillator being a simple stimulus-response mechanism, it might rather be that the NFB response is creating a new set-point for the brain. At first, the feedback signal reflects stochastic variability, which will sometimes reach the reward threshold, giving a cue for the brain to memorize as a set-point, which then acts as a new starting point for the next loop. Although speculative, predictions from models applying the theoretic principles of control theory to the brain have matched both behavioral (Todorov, 2004; Nagengast, Braun, and Wolpert, 2009) and neural (Héliot et al., 2010) data.

Based on this theoretical framework, Ros et al. suggest that NFB gives the control system additional information by allowing for direct sensing of oscillatory dynamics, allowing the brain to self-correct more effectively, as the necessary information for this correction - the way NFB represents brain activity in a way the participant can understand, who can then use it to further guide it consciously - would in other circumstances not be available to conscious awareness (Ros et al., 2014). The early findings of Kamiya in 1962 (Kamiya, 2011) also highlight the role that higher level cognitive processes must play in NFB, as he reported that subjects were not just able to consciously regulate their alpha levels, but also to accurately report their relative rise and fall after receiving NFB training. If higher level control processes are indeed involved, this also highlights the potential problem that NFB might come with a learning curve or initial demands on self-regulation that cannot be mastered by everyone equally, as conscious control is asked to top-down/feed-forward reproduce the set-point. Brain stimulation techniques that do not necessitate said conscious involvement would therefore have a broader clinical applicability.

SUMMARY

NFB can be thought of as a mechanism by which the control system of the brain is given more information according to which it can self-regulate. Although part of the self-regulation of brain activity - based on observing changes in its representation in NFB - might operate implicitly, evidence suggests that conscious awareness plays an important role. If this is this true, self-regulating brain activity via NFB is a skill which we can expect to be unevenly distributed as all skills are. This makes it important to provide brain stimulation techniques that work equally well for all.

2.3.2 Entrainment and rhythmic stimulation

Repetitive photic stimulation might provide a viable alternative to NFB. However, as with any form of rhythmic brain stimulation, its effectiveness relies on how rhythmic properties of neural oscillations are altered in response to stimulation and how temporal expectancies create phase locking in ongoing neural oscillations, a process referred to as entrainment (Thut, Schyns, and Gross, 2011).

During entrainment of neural oscillations by photic stimulation, occipital EEG responses recorded over visual cortex have been shown to display sharply peaked responses at the same frequency as the driving frequency, known as steady state visual evoked potentials (SSVEPs) (Thut, Schyns, and Gross, 2011). Contrary to single sensory stimuli such as a single flash, SSVEP come in quick succession, superimposing their trailing ends on the start of their successors, which produces a train of visual evoked potential waves. Consequently, while the former come in the form a transient, stimulus-induced phase-resetting, that is, an adjustment of the phase of ongoing oscillations, which is followed by fast subsequent desynchronization, as the brain frequency settles back into its natural rhythm after stimulus presentation, SSVEPs produces deviations from natural rhythms for as long as stimulation is applied (Herrmann, 2001).

Criteria that serve as evidence for successful entrainment of neural oscillations through rhythmic stimulation via SSVEPs are as follows:

1. Synchronization (phase alignment) of a neural oscillator to rhythmic perturbation can be observed via EEG measurements.

2. The effects of entrainment show frequency-specificity (stimulation is increasingly effective, as the gap between stimulation and natural frequency is diminishing).

3. Entrainment effects also show spatial-specificity (the effects of entrainment are strongest in the target area, so visual stimulation should show the strongest effects over the visual cortex).

4. It is theoretically possible for the target area to cycle at the stimulation frequency on its own, in a way that is:

   (a) Self-sustained.

   (b) Activated by a task

(Thut, Schyns, and Gross, 2011)

In addition, behavioural evidence can be used to bolster any claims of successful entrainment, as given the assumption of neural oscillations being causally involved in cognition, we should expect frequency-specific behavioural effects that emerge while stimulation is applied. Similarly, any lasting effects of stimulation should also leave an impact on how the brain processes information, possibly affecting behavioural responses.

The ability of an external rhythmic stimulus to alter endogenous oscillations via direct entrainment raises the interesting possibility that photic stimulation could be used to correct deficient or excess brain activity by modulating speed and amplitude of targeted frequency bands.

The implicit assumption behind this idea is that the stimulation frequency applied is the frequency which is both induced and enhanced in the cortical network. As this assumes a linear system, with the output mirroring the frequency of the input (phase and amplitude differences notwithstanding) this is admittedly shaky as a theoretical foundation, as even the basic mechanisms determining the firing of a neuron's action potential are nonlinear (Hodgkin and Huxley, 1952).

SUMMARY

Photic stimulation might be a NFB alternative that does not require conscious involvement. It works by entraining neural oscillations via repetitive light flashes. Entrainment refers to the process by which rhythmic properties of neural oscillators are altered in response to rhythmic stimulation. This happens as a consequence of how temporal expectancies bring about phase locking. For visual or photic stimulation, this takes the form of SSVEPs, which create trains of VEPs. Successful entrainment must show phase alignment of an endogenous neural oscillator to the stimulus, with the effects displaying frequency- and spatial-specificity. Behavioural or neural changes based on effects resulting from entrainment would further bolster claims of its effectiveness. While the theoretical possibility to use rhythmic photic stimulation to correct pathological oscillations is promising, the stimulation frequency applied will not necessarily induce or enhance the same frequency in the cortical network, as the brain is nonlinear. Any explanation of entrainment will have to take this into account.

2.3.2.1 Dynamic systems theory and rhythmic stimulation

A more realistic approach to understanding periodic forcing of oscillators is provided by dynamic systems theory, as it is concerned with systems whose internal dynamics or state variables are in flux due to their response to exogenous perturbation. In more detail, Pikovsky et al. (2001) describes it as follows: In dynamic systems theory, an oscillatory system is seen to have an internal source of energy. Hence its rhythmic activity pattern with the period T and a frequency of f = 1/T is not a reflection of a periodic input but it is self-sustained. F, is hence its natural frequency in absence of external perturbations. When a periodic force is applied to the oscillator, the change it enacts lead to synchronisation and ultimately to entrainment or phase locking. If there is a divergence between stimulation frequency and oscillator frequency, this is referred to as detuning. Put more formally, detuning is the difference between natural (NF) and stimulation frequency (SF) (detuning = SF-NF). The NF response is then described as a function of both stimulation strength of the applied perturbation, as well as the degree of detuning. If SF and NF match in frequency, SF will phase-lock the targeted oscillator, so that the difference between the phase of SF and NF is stable. If the frequency does not match, however, detuning pushes the

phase of both apart, meaning that at some point during the oscillatory cycle, the SF pushes opposite to the direction of detuning, which slowly shifts the NF via entrainment. More accurately, when SF and detuning get closer to cancelling each other out in the cycle, NF slows down. Conversely, when their forces are additive, NF accelerates. Synchronisation hence involves both acceleration and deceleration of the NF in response to the SF. In addition to affecting phase, the rhythmic external stimulation of SF also affects the amplitude of NF, as the phase changes in non-uniform rates, with either an advance or delay, depending on the SF pulses in relation to the phase of the NF. As detuning increases, a greater stimulation strength is necessary for this to happen. If it is not sufficient, NF will move towards SF without reaching it. Put differently, the stronger the stimulation strength, the broader the range of SF at which NF can become entrained.

SUMMARY

In sum, dynamic systems theory provides a more complete account of entrainment. Rather than assuming that the output mirrors the frequency of the input, detuning, which equals the difference between SF and NF, will push the phase of both apart. This in turn will cause the output to be reduced in amplitude and speed when SF and detuning approximate cancelling each other out. Conversely, amplitude and speed of the output will be increased when SF and detuning are additive. This means that entrainment is feasible, but that results will differ based on differences between NF and SF.

2.3.3 Open-loop rhythmic brain stimulation

In this thesis, rhythmic brain stimulation takes the form of repetitive photic driving. It has, in the form of photic stimulation, a long history, and was shown to be effective at modulating frequency (Adrian and Matthews, 1934; Herrmann, 2001) or increase amplitude (Walter, Dovey, and Shipton, 1946; Herrmann, 2001) of targeted oscillations during stimulation, as brain rhythms are entrained by the driving stimulus. There are, however, no known methods to use photic stimulation to also suppress activity of specific frequency bands (like alpha) during stimulation, which may be important in cases in which normalising brain activity involves correcting excessive oscillations.

Beyond these early findings, recent studies have shown that photic stimulation might be a viable tool for clinical application. Iaccarino et al. found that, when using 40 Hz light stimulation to counter the systematic lack of gamma oscillations in transgenic mice with Alzheimer's, the amyloid levels and buildup of damaged proteins was successfully reduced by more than half after daily one-hour stimulation sessions for a total duration of a week (Iaccarino et al., 2016). A study by Ismail et al., however, failed to replicate the same effects in humans, using 10 daily sessions of 2 hours of repetitive 40 Hz photic stimulation (Ismail et al., 2018). They conclude, that, for human subjects, longer treatments might be necessary to affect change. Another study by Kim et al. demonstrated that inducing alpha activity in mice by 10 Hz stimulation reduced depressive symptoms in a corticosterone (CORT)-induced mouse model of depression more effectively than fluoxetine (Kim et al., 2016). As depression in humans is commonly associated with reduced alpha activity as well, (Kan and Lee, 2015; Choi et al., 2011), these results warrant trials with human participants. Aside from trying to replicate the original findings (Kim et al., 2016) with humans, it would also be interesting to vary the stimulation frequencies methodically, to assess how different frequencies outside of the alpha range might impact

depressive symptoms. Alternatively, future research could employ a sham stimulation condition by disrupting entrainment by phase-shifting the stimulation sequence every other cycle, or changing frequencies during stimulation. As this section shows, although photic stimulation might constitute a useful tool in clinical practice, the research thus far is lacking a thorough investigation of its effectiveness and mechanisms by which it affects change in the first place

SUMMARY

Photic stimulation has been shown to modulate frequency power and speed. In studies using mice, it significantly alleviated symptoms associated with depression and Alzheimer's. Although these results have yet to be successfully replicated with human participants, this makes it a promising tool for clinical researchers. Before it can be applied as a tool for treatment of neuropathologies, its effectiveness with human participants as well as the mechanisms by which it affects change have to be investigated thoroughly. In addition, photic stimulation has so far only been shown to be able to enhance neural oscillations (in the form of enhancing alpha power, for example). Given that normalising pathological oscillations may also entail reducing excessive activity in targeted frequency bands, this limits the potential clinical applications for photic stimulation, as no stimulation protocol exists that is able to suppress neural activity during stimulation.

2.3.4 Phase-specific photic driving via closed-loop rhythmic brain stimulation

Having established that both enhancing and suppressing neural oscillations might be necessary for normalising pathological brain activity, fixed photic stimulation has limited usefulness, as it can only enhance frequency band activity during stimulation. As section 2.3.2.1 detailed, however, there is a theoretical basis for the idea that, depending on the phase-timing of photic stimulation, it could both suppress and enhance activity. Specifically, section 2.3.2.1 includes the prediction that, if the NF and SF do not match, detuning pushes the phase of both apart. When detuning and the SF force approximate canceling each other out in the cycle, this has the effect of slowing down the NF. Conversely, if detuning and SF are additive, NF accelerates. This shows that, depending on the phase-timing of the stimulation, we can expect it to impact the NF in different ways. Although this in itself only gives a prediction over the direction in which NF would shift, and not how in- or out-of-phase stimulation might impact overall power levels of the NF, an analogy might give us insight: if the oscillation of the NF is likened to a swing, and the SF is akin to a push, in- and out-of phase stimulation would differ in terms of the direction of the perturbation in relation to the endogenous NF. The more closely the perturbation approximates the peak of the NF oscillation before it is reached, the more momentum it adds to the swing. If the push is delivered just slightly past the peak, at the point when the swing is about to reverse in the direction of the perturbation, this, however, would slow down the tempo of the swing, and decrease its overall amplitude, as the swing would lose momentum. If this applies to photic stimulation as well, this would mean that stimulation that approximates (but precedes) the NF peak would enhance it, but light flashes aligned ever so slightly with the end of the peak, would have the opposite effect. Consequently, if phase can be taken into consideration during photic stimulation, a more complete modulation of brain activity becomes at least theoretically feasible.

In short, we propose that in order to most efficiently enhance neural activity, NF and SF forces should be kept additive. Conversely, when NF and SF forces cancel each other out, it, in theory, should be possible to suppress brain activity during stimulation.

Building on this idea, we posit that the shortcoming of NFB's inaccessibility to those who cannot master its learning curve, as well as the detuning problems and phase-ignorance of fixed rhythmic light stimulation can be circumvented by combining both approaches and implementing a closed-loop photic stimulation protocol, that is driven by a real-time EEG signal. By making flashes phase-specific, ensuring that NF and SF forces are additive, brain activity can, in theory, be most efficiently enhanced. In addition, by making NF and SF forces cancel each other out, we propose that it should be possible to suppress brain activity during stimulation. In other words, this approach might allow for a complete manipulation of neural oscillations, increasing and decreasing their amplitude as wanted.

SUMMARY

Open-loop photic stimulation cannot be maximally effective or complete, as only closed-loop feedback would allow to make stimulation phase-specific, ensuring that SF and NF forces are additive for efficient enhancement of neural activity, or cancel each other out for during-stimulation brain activity suppression.

2.4 Summary

EEG allows us to get a glimpse of brain dynamics as they manifest themselves through electrical activity on the scalp. The frequency bands which we can measure show well-behaved distinct features and functions, as well as complex interactions with each other. In various neuropathologies, the resulting dynamics are often warped, with frequency components displaying excessive or deficient activity. As a form of treatment, NFB allows users to normalise their brain activity, by consciously influencing features of a representation that reflects how closely the current brain signal approximates the target state. As not everybody is equally able to self-regulate their brain activity via NFB, this approach is somewhat limited. Traditional photic stimulation, on the other hand, does not require conscious control. Rather, it applies exogenous forcing at a fixed frequency, to enhance deficient rhythms. Since pathological oscillations might also need a controlled decrease of their activity, this approach also shows limitations for clinical application. A novel approach is represented through closed-loop photic stimulation, which combines elements of NFB and photic stimulation, allowing for a complete manipulation of the activity of a specific frequency bands by making each flash dependent on a real-time EEG signal. This approach would also allow for the specific increase or decrease of the amplitude of the targeted frequency band by implementing a closed-loop photic stimulation protocol.

Chapter 3

Photic post-stimulatory alpha power suppression

3.1 Abstract

10 Hz repetitive photic stimulation has been shown to increase electroencephalogram (EEG) alpha activity (8-12 Hz) (Walter, Dovey, and Shipton, 1946). This approach shows promise to correct aberrant patterns of neural oscillations in brain disorders such as ADHD (Arns et al., 2008), potentially alleviating associated negative symptoms. However, to date, neither the parameters affecting entrainment - that is, the synchronisation between the external periodic stimulation and the targeted brain oscillation leading to alpha power enhancement - nor the immediate post-stimulation effects of photic stimulation have been studied in detail, which is a necessary prerequisite for its use in any potential future clinical study. This study investigates both the direct effects of stroboscopic light stimulation as well as the neural responses once stimulation has ceased, to investigate if stroboscopic light stimulation leads to lasting effects on brain activity. To achieve this aim this study recorded EEG while participants were exposed to stroboscopic light stimulation at 10 Hz for 30, 60, and 120 seconds, to investigate whether stimulation length affects the extent to which alpha activity is increased during stimulation, and to probe differences in possible post-stimulatory effects dependent on stimulation length. The results confirm earlier findings of successful entrainment of a photic driving frequency over the visual system as measured by occipital electrodes (Herrmann, 2001). We also observed the effects of entrainment over medial and frontal regions. We found that the effect size of alpha band enhancement was dependent on the difference between individual alpha frequency (IAF) and stimulus frequency (SF). In contrast to previous results (Walter, 1963), which demonstrate that the effectiveness of stroboscopic stimulation in enhancing alpha amplitude decreases with a greater divergence between IAF and SF, we find that alpha amplitude was most enhanced by stimulating 1.5-2 Hz above the IAF, as calculated by occipital measurements. Examining the time-window immediately following stroboscopic stimulation, we observed a scalp-wide suppression of alpha activity. The suppression of alpha activity was positively correlated with stimulation length. Finally, we show that the post-stimulatory alpha power suppression increases connectivity measures, as indicated by phase-lag values (PLV). This data confirms that 10 Hz stroboscopic stimulation is able to enhance alpha amplitude during stimulation. Further, our findings imply that length of stimulation is not positively correlated with that enhancement. Most importantly, however, we have, for the first time, shown the existence of post-alpha-stimulation effects in the form of alpha power suppression. We speculate that this may be part of a homeostatic mechanism, that aims to maintain a stable range of alpha activity within the brain (Stam, 2005).

3.2 Introduction

The alpha rhythm (8-12 Hz) is one of the most prominent and stable rhythmic components of electroencephalogram (EEG) brain activity (Williams, 2001). Berger (1929) showed that it was modulated by attention, and since then it has also been shown to reflect inhibitory processes (Klimesch, Sauseng, and Hanslmayr, 2007). Moreover, accumulating evidence indicates that the alpha rhythm of the brain is not just an epiphenomenon of those cognitive states, but rather plays a causal role in their functioning (Buzsaki, 2006). These findings suggest that brain disorders which are associated with deviations from normal alpha levels such as post-traumatic stress disorder (PTSD) (Wahbeh and Oken, 2013), Alzheimer's (Babiloni et al., 2009) or attentional deficit hyperactivity disorder (ADHD) (Arns et al., 2008) could potentially be treated by normalising this frequency of brain oscillations.

One potential approach to modulate neural oscillators is repetitive photic stimulation (Walter, 1963). By applying rhythmic light flashes whose rhythmicity falls within the frequency band of the targeted neural oscillator, previous research has shown that photic stimulation results in entrainment of neural oscillators (Herrmann, 2001), modulation of their frequency (Adrian and Matthews, 1934), and enhancement of EEG frequency component amplitude (Walter, Dovey, and Shipton, 1946). This works, as the pulsing light flashes bring about steady-state visually evoked potentials (SSVEPs), which produce a train of visual evoked potential waves. While a single sensory event would yield a transient, stimulus-induced phase-resetting EEG response, that is, a phase adjustment of ongoing oscillations, which settles back into its natural rhythm after stimulus offset, the repetitive stimulation produces long-lasting deviations from said endogenous oscillations for as long as stimulation is applied (Thut, Schyns, and Gross, 2011). In other words, we assume that when an external periodic force is applied to an internal oscillator, the change it causes leads to synchronisation and entrainment or phase locking (Pikovsky, Rosenblum, and Kurths, 2001). As even the basic mechanisms determining the firing of a neuron's action potential are nonlinear (Hodgkin and Huxley, 1952), the stimulation frequency applied is not necessarily the frequency induced or enhanced. Rather, the difference between the natural (NF) and stimulation frequency (SF), referred to as detuning (detuning = SF-NF), will push the phase of both apart, slowly shifting the NF via entrainment. As SF and detuning get closer to cancelling each other out, NF decelerates, while it accelerates when SF and detuning are additive. This continues until SF and NF match in frequency, which not just affects phase but also amplitude of the neural oscillator, with the speed of the process and the magnitude of the change in both factors being determined by stimulation strength (Pikovsky, Rosenblum, and Kurths, 2001). Thut, Schyns and Gross (2011) hence conclude that sufficient evidence for successful entrainment of neuronal oscillations by any form of rhythmic stimulation would include a proof of synchronisation or phase alignment of the neural oscillator to rhythmic perturbation, that the effects of entrainment show effects of detuning (frequency-specificity), as well as spatial-specificity, so that the effects are strongest in the area of the brain that specialises in processing the sensory modality in which the stimulation is delivered.

In this study we deliver evidence in favour of all of these points and, for the first time, investigate the post-stimulation effects of photic stimulation in detail. Specifically, we show post-stimulatory alpha power suppression following alpha stimulation, and that this suppression coincides with changes in phase-lag-value (PLV) connectivity measures.

10 Hz is, on average, very close to individual alpha frequencies (IAF) (Williams, 2001; Thorpe, Cannon, and Fox, 2016) and is the center frequency of the alpha rhythm (Klimesch, 2012). This makes it a viable choice for using it as a fixed stimulation frequency of alpha activity, as stimulating in accordance with IAF makes photic driving maximally effective (Walter, 1963). For this reason, and to ensure that effects of stimulation could be compared easily across conditions, 10 Hz was chosen as the standard stimulation frequency in this study.

3.3 Methods

Building on past research on the effectiveness of photic stimulation (Walter, Dovey, and Shipton, 1946; Walter, 1963), we tested photic stimulation protocols in three conditions of 30 seconds, 60 seconds, and 120 seconds of stroboscopic 10 Hz photic stimulation at 6880 lux using the Lucia N°03 Hypnagogic stroboscope, comparing pre- and post-stimulation intervals of 25 seconds each. The order of conditions was randomised.

3.3.1 Procedure

Participants were seated in a dark and noise-proof electromagnetically shielded room facing the Lucia N°03 Hypnagogic stroboscope (Innsbruck, Austria), 50 cm away from the lamp, which contained an array of 8 high luminance LEDs arranged in two concentric circles forming a cross surrounding a single halogen light bulb (not used in this study). For reference, see Figure 3.1. At the position the participants had relative to the lamp, luminance was 6880 lux, which equalled 80of maximum LED output. Both brightness of the lamps as well as their flashing sequence and timing could be set by software supplied by the lamps manufacturer. The high luminance levels were important, as previous research had indicated that the contrast between on and off signals in rhythmic visual stimulation mediates effects, with higher contrast positively correlating with higher impact (Vialatte et al., 2010). Due to the brightness of the lights, all visual stimulation of participants occurred with their eyes closed. Prestimulus windows of 25 seconds gave a baseline against which the impact of photic driving could be compared, and a post-stimulation window of 25 seconds was used to investigate post-stimulatory effects.

FIGURE 3.1: The Lucia N°03 Hypnagogic stroboscope
This picture shows the Lucia N°03 Hypnagogic stroboscope used for photic stimulation, with a photodiode placed over one LED of the outer concentric circle in order to monitor and record the precise timing of flashes.

3.3.2 Conditions

Once setup had been completed the experimental conditions were as described in table 3.1

The order of conditions was randomised. Each condition was repeated four times, making for a total of 84 trials per condition across all 21 participants. In all conditions, pre- and post-stimulation intervals of 25 seconds were recorded, to establish baseline alpha levels (8-12 Hz) and post-stimulatory effects respectively. Pre- and post-stimulation intervals here are recorded immediately before and after photic stimulation intervals.

Conditions	Pre-stimulation	Stimulation	Post-stimulation
1		30 s	
2	25 s	60 s	25 s
3		20 s	

TABLE 3.1: Experimental conditions
Conditions were presented in a random order and repeated a total of four times

3.3.3 Participants

21 postgraduate students (9 males, 12 females) were recruited. Informed consent was obtained from them after the nature and potential consequences of the study had been explained. In addition, anxiety and epilepsy questionnaires were sent out for participants to fill in before they were invited to take part in the study, as the stroboscopic photic stimulation employed, in a very small percentage of susceptible individuals, may induce seizures or provoke anxiety. To screen participants for epileptic risk, a screening questionnaire based on Placenia et al. (1992) was used. To guard against the possibility of participants experiencing anxiety during the experiment, the State-Trait Anxiety Index, Trait Version (Spielberger, Gorsuch, and Lushene, 1970) was used (STAI). The STAI yields a total score between 20 and 80, with values above 50 indicating moderate anxiety. This study used a score above 60 on the STAI or a positive result on the epileptic questionnaire as exclusion criteria. However, in this study no participants were judged to be at risk for either epilepsy or anxiety. The protocol for this was approved by the Life Sciences & Psychology Cluster-based Research Ethics Committee of the University of Sussex (CREC).

3.3.4 Data

Data was collected using a 64 channel ANT Neuro amplifier, sampled at 2048 Hz. Electrical activity of the brain was recorded using ANT waveguard 64-channel caps, using standard Ag/AgCl electrodes placed according to the 10-20 system, using an average reference.

Eye movements were monitored with additional electrodes positioned vertically and horizontally around the participants' eyes and a photodiode was placed over one LED of the outer concentric circle of high-luminance LED's of the Lucia N°03 to provide information on precise timings of each delivered visual flash.

3.3.4.1 Recording

All signals were recorded using ASA-Lab 4.7.11 (ANT Neuro, Enschede), sampled at 2048 Hz without the use of analog filters during online-recording. Impedance values of individual electrodes were kept at $< 40k\Omega$, with sensors in the occipital region at $< 20k\Omega$.

3.3.4.2 Preprocessing

Data (pre-)processing was achieved using custom scripts in MATLAB R2017b (The Mathworks Inc., 2017), as well as select scripts from the EEGLAB toolbox (Delorme

and Makeig, 2004) with the MARA- (Winkler, Haufe, and Tangermann, 2011) and ERPLAB plugin (Lopez-Calderon and Luck, 2014).

For pre-processing, all data was downsampled to 250 Hz, channel-location was imported, eye- and photodiode channels were removed, and an infinite impulse response (IIR) Butterworth filter with a high-pass cut-off frequency of 0.1 Hz and a low-pass cut-off point at 30 Hz was used. Additionally, a notch filter at 50 Hz was applied in order to reduce the noise generated by electrical interference. An independent component analysis (ICA), using the pop_runica function of EEGLAB, was used to separate the signal into additive subcomponents. Using the CleanLine EEGLAB plugin, the data was then analysed for baselines drift via a frequency-domain regression (multi-tapering), using a Thompson F-statistic to identify and remove sinusoidal noise. This technique has been endorsed by Partha Mitra and Hemant Bokil (Mitra and Bokil, 2007) and is built on modified scripts from the Mitra Lab Chronux Toolbox (Bokil et al., 2010). Subsequently, the clean_rawdata EEGLAB plugin was used to clean the data by means of artifact subspace reconstruction, where a zero-phase and non-causal FIR filter is used to identify abnormal drifts in the data (a threshold of 5 standard deviations was used for artefact correction), and remove affected bad channels. Removed channels were interpolated using the pop_interp function of EEGLAB. MARA was then used to deal with left-over artifacts. Using supervised machine learning to automatically reject components based on extraction of six features from the spatial, spectral, and temporal domains, it ended up rejecting 9-14 components of the data. The data was then evaluated visually, and bad trials were removed. In total, out of 84 trials, 4 trials had to be removed from the dataset in the first condition. To keep the number of trials across conditions equal, corresponding trials were also removed from in all other conditions. Lastly, the data was re-referenced to a global average, and eye- and photodiode channels were added back into datasets, to keep data as complete as possible for future analysis. The photodiode data is also crucial for analysing any relationship between the light flashes during photic stimulation and the respective neural response - especially entrainment of neural oscillators by the stimulus measured via phase coherence.

The photodiode data was then analysed automatically using a custom script, sweeping through all samples in the time domain, looking for peaks of activity, identifying the first and last peak of photic stimulation, and automatically classifying them as the onset and end of photic stimulation, placing markers for epoching.

3.3.4.3 Analysis

In order to investigate the data in a time-frequency domain, complex Morlet wavelet convolution was used (Cohen, 2014). This allows an extraction of both power and phase from the data, which is important for analysing entrainment through assessing phase-similarity between EEG channels and PD data, and for the subsequent impact of entrainment effects on alpha amplitude. In short, Morlet wavelet convolution involves creating a sine wave and a Gaussian with a window of

$$ae^{-t/(2s^2)}, \tag{3.1}$$

and multiplying them point by point. The a stands for the amplitude of the Gaussian, the e for the base of its natural logarithm, t for time, and s is defined as

$$\frac{n}{2\pi f}, \tag{3.2}$$

where n is the number of wavelet cycles, and f is the frequency of interest in hertz. They are complex because they involve a real and imaginary part, occupying a three-dimensional space: time, real, and imaginary. This allows an extraction of both amplitude and phase of specific frequencies over time. Formally, this can be done via

$$M = \sqrt{(real^2 + imag^2)}\,, \tag{3.3}$$

where M is the magnitude of the line, representing the distance from the origin/zero value of the complex space to the point represented by the complex number in polar notation) and

$$\theta = arctan(imag/real)\,, \tag{3.4}$$

where *real* and *imag* refer to the real

$$real = M(cos(\theta)) \tag{3.5}$$

and imaginary

$$imag = M(sin(\theta)) \tag{3.6}$$

components respectively, and is the angle or phase that can be extracted.

For analysis with a focus on the alpha frequency window as it is commonly defined in the literature, the minimum frequency of interest was set to 8 Hz, and the maximum frequency to 12 Hz, but in order to investigate effects in the harmonic bands, the wavelet convolution included all frequencies between 1-50 Hz (for which a bandpass filter between 1-50 Hz was applied, instead of the 1-30 Hz bandpass filter used for the remaining analysis). A linearly spaced vector was created using these minimum and maximum parameters, with equally spaced points in between (500 were chosen for this study, so alpha had a step-resolution of 40). Wavelet parameters were chosen to cycle from four to ten as faster frequencies were approached during the convolution. A logarithmically spaced vector was then created for said process, pointwise dividing the base 10 logarithm of said range of cycles from start to end, given the total number of frequencies, by said points in the aforementioned linearly spaced vector times two times *pi*. With these starting parameters, wavelets were created for each frequency of interest (as defined above), taking the exponential of $2i$ times *pi*, the relevant point in the frequency vector pointwise multiplied with a vector ranging from minus two to two, in steps of one over the EEG sampling rate of 250 Hz, pointwise multiplying the result of the exponent of the negative of the same vector pointwise raised to the power of two, and then divided by two times the logarithmically spaced vector frequency point of interest, raised to the power of two. Formally, this can be expressed as

$$cmw = Ae^{-t^2/2s^2 e^{i2\pi ft}}\,, \tag{3.7}$$

where

$$A = 1\frac{1}{(s\sqrt{n})^{1/2}}\,. \tag{3.8}$$

Then, the fast Fourier transform (the Fourier transform of variable x being expressed as

$$X_f = \sum_{k=1}^{n} x_k e^{-2\pi f(k-1)n^{-1}}\,, \tag{3.9}$$

where n stands for the number of data points) is taken of each wavelet and the length of a vector running from minus two to two, at steps of one over the EEG sampling

rate and the same is done with the pre-processed EEG data for each channel. The result of the FFT of each wavelet is then pointwise divided by its maximum value, and the inverse Fourier transform, formally as

$$x_k = \sum_{k=1}^{n} X_k e^{i2\pi f(k-1)n^{-1}}, \tag{3.10}$$

is taken of its result pointwise multiplied with the Fourier transform result of the EEG data of each channel. Finally, the absolute power is taken of said result to the pointwise power of two, tapering the data via only considering the data points after onset and before end of each Gaussian window. In practice, this meant creating a window of exclusion ranging from the length of the linear vector from minus two to two, at steps equal to one over the EEG sampling rate minus one, divided by two, and applying this on both ends of the data, with an added excluded sample point at the start. This is done due to the Nyquist theorem, which states that at least two points per cycle are needed in measuring a sine wave, meaning that half the data points correspond to the fastest measurable frequency. Formally, the number of extractable frequencies from any signal of length N is $N/2+1$, with the $+1$ accounting for the zero frequency component, as, on each loop iteration, when going through relevant frequencies, the first one creates a sine wave of zero frequency, capturing the mean signal offset.

In order to create a second dataset with higher spatial accuracy for connectivity analysis, a copy of the resulting data was adjusted by smoothing it via a surface Laplacian. Being a form of a spatial bandpass filter, it increases selectivity by filtering out spatially broad data features, adjusting weights of data points based on interelectrode distance. This is done as broad topographical features (in a spatial sense) are likely reflections of volume-conducted potentials. Expressed formally, first G and H matrices need to be computed, where

$$G_{ij} = (4\pi)^{-1} \sum_{n=1}^{order} \frac{(2n+1)P_n(cosdist_{ij})}{(n(n+1))^m} \tag{3.11}$$

and

$$H_{ij} = (4\pi)^{-1} \sum_{n=1}^{order} \frac{(2n+1)P_n(cosdist_{ij})}{(n(n+1))^{m-1}}, \tag{3.12}$$

with i and j being electrodes, m a constant positive integer relating to data smoothness, which, for this thesis, was fixed at 4 as this is the recommended value (Perrin et al., 1989), P being the Legendre polynomial used to calculate spherical coordinate distances, n its order term, defining the spatial harmonic frequencies for each electrode, fixed at 10, which is the maximum accuracy possible for a 64 sensor cap (Cohen, 2014) and *cosdist* being the *coside* distance among all possible electrode pairs. It is expressed as

$$cosdist_ij = \frac{(X_i - X_j)^2 + (Y_i - Y_j)^2 + (Z_i - Z_j)^2}{2}, \tag{3.13}$$

The data of each electrode-pair is then weighted by distance via

$$Gs = G + \lambda, \tag{3.14}$$

and

$$d_i = data_i^{-1}(Gs)\,, \tag{3.15}$$

summing the diagonal elements of G with a smoothing parameter of 10-5, which is recommend for 64 electrodes (Cohen, 2014), and then applying the surface Laplacian with

$$C_i = d_i - \frac{\sum_{j=1}^{nelec} d_j}{\sum_{j=1}^{nelec} Gs_j^{-1}} Gs^{-1}\,. \tag{3.16}$$

Hence, to increase spatial accuracy, it attenuates low-spatial-frequency components, and boosts high-spatial frequency components. As this provides issues for any source reconstruction of deep sources of neural activity, the resulting surface Laplacian-smoothed data is only used for connectivity analysis in this thesis.

Both data sets (data before and after Laplacian smoothing) were then epoched in pre-stimulation intervals of 25 seconds, post-stimulation epochs of equal length, and stimulation windows of 30, 60, and 120 seconds respectively.

In order to assess relative changes in alpha amplitude in pre-stimulation and post-stimulation intervals, pre-stimulation activity served as a baseline against which post-stimulation activity was compared.

A two-tailed Wilcoxon signed-rank test was used to assess the significance of the difference between pre-, during-, and post-stimulation intervals and return associated p values. This test was chosen as the data is not normally distributed and samples are paired. Furthermore, the standard error of the mean (SEM) for average alpha power changes between EC1 and EC2 (ΔEC) with 95% confidence intervals was calculated to assess variability of results, with power measures being given in microvolt squared (μ^2). The SEM and confidence intervals are calculated as

$$\sigma_{\bar{x}} = \frac{\sigma}{\sqrt{n}} \times \sqrt{\frac{4}{9 \times \alpha}}\,. \tag{3.17}$$

where σ is the standard deviation and n the sample size of the group. The equation given here is based on the Vysochanskij–Petunin inequality theorem (Vysochanskij and Petunin, 1980), which gives an estimate about the upper and lower bounds of a sample falling within standard deviations of a group mean, which, here, are defined to be equal to 95%, with $\alpha = 0.05$. This way of calculating the SEM and confidence intervals is appropriate for data which is not normally distributed and is unimodal, as it is the case in this study.

Further, to compare pre- and during-stimulation levels of alpha power, as to validate whether there was a change in alpha power during stimulation, we, for every condition, used the last 25 seconds of the photic stimulation interval only, as to ensure that the during-stimulation window had the same number of data points as the pre-stimulation window. 25 seconds were chosen in order to ensure that pre-, during-, and post-stimulation intervals had an equal number of time points. The decision to use the last 25 seconds of stimulation was made because if stimulation duration had an impact on stimulation outcomes, as was one of the hypothesis we sought to investigate in this chapter, this would be most pronounced at the end of the stimulation time window.

When pre- and post-stimulation effects are compared on an individual basis, this is done using the standard mean difference formula (taking the standard mean difference - SDM_{all} - in alpha power over time) recommended for single-subject comparisons by Olive and Smith (2005). This test of effect size for independent data

(used in this chapter due to trial rejection) is formally written as

$$SDM_{all} = \frac{EC_1 - EC_2}{SD_{pooled}}, \tag{3.18}$$

where

$$SD_{pooled} = \sqrt{\frac{\sum(X_1 - \overline{X_1})^2 + \sum(X_2 - \overline{X_2})^2}{n_1 + n_2 - 2}}. \tag{3.19}$$

Here, EC_1 and EC_2 stand for pre- and post-stimulation conditions respectively, and X_1 and X_2 for alpha power at any time point of the respective intervals, with n_1 and n_2 giving the number of samples.

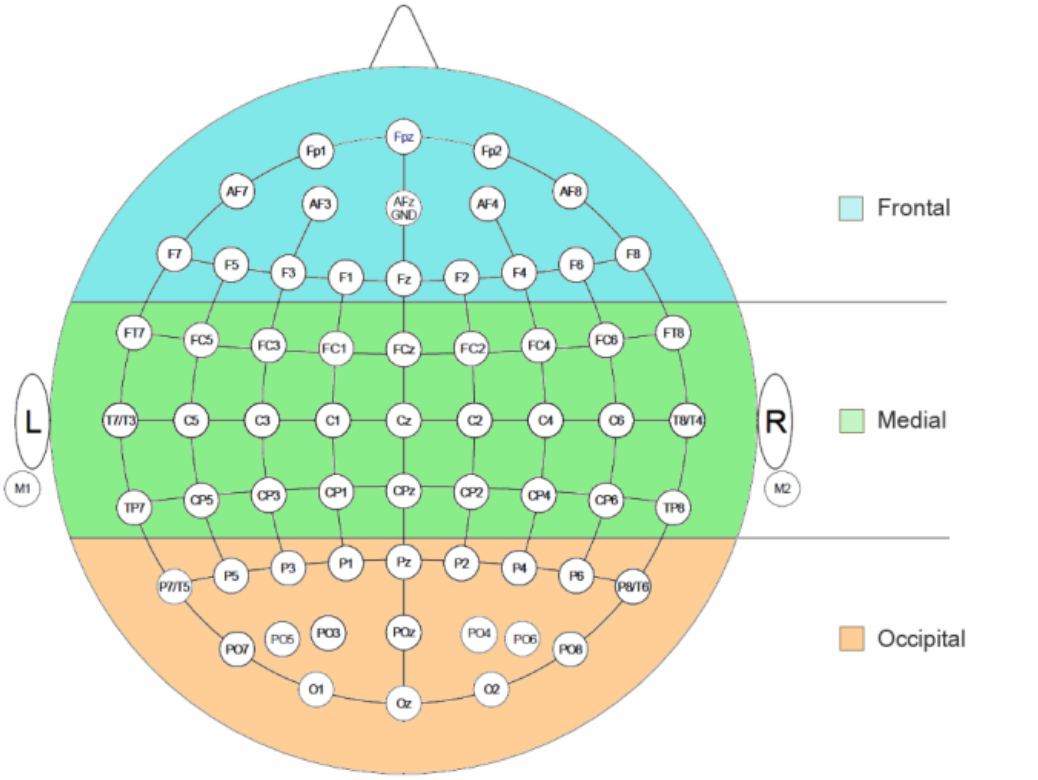

FIGURE 3.2: Sensor regions used.
For all future analysis, when frontal (top/blue), medial (middle/green), or occipital (bottom/orange) regions are referenced, averaged measures of electrodes within the coloured sections are used. There are 19 sensors in occipital-, 27 in medial-, and 16 in frontal regions.

For all but topographic and connectivity analysis, data was averaged across frontal, medial, and occipital areas as shown in 3.2.

In order to track entrainment of the neural oscillator by the photic stimulation signal over time, a coherence measure between alpha oscillations over occipital electrodes and the photic driving at 10 Hz was calculated, formally expressed as

$$Coher_{xy} = \left| \frac{S_{xy}}{S_{xx}(S_{yy})} \right|, \tag{3.20}$$

where S_{xy} is the cross-spectral density between electrodes x and y. Here, electrode activity is compared to the sequence of individual light flashes recorded by the photodiode (PD). In order to show actual entrainment effects, instead of just looking at the absence versus presence of the driving signal in relation to internal oscillations, the PD data was mirrored before and after stimulation, so that at any point the neural oscillations were assessed for coherence with a steady 10 Hz signal.

To investigate alpha power suppression effects over time, nonparametric permutation testing was used. Permutation testing is particularly well suited for time-frequency analysis of EEG data (Maris and Oostenveld, 2007), as it makes no assumptions about distribution of data, its parameters, and allows for corrections for multiple comparisons (Theiler et al., 1992). It allows for the creation of z-maps, showing significance of differences between intervals in a time-frequency domain, by iteratively shuffling interval trials to create null hypotheses distributions, and then testing the actual difference between conditions against them via their p-value distributions. Formally, this can be expressed as

$$Z = \frac{V_e - \overline{V}_n}{std(V_n)}, \tag{3.21}$$

with V_e being the observed-effect test statistic and V_n a null-hypothesis test statistic vector. This was done 1000 times, as this is the recommended value to reach high confidence in the validity of the shuffling process to generate a null hypotheses outcome (Cohen, 2014). Corrections for multiple comparisons are achieved by determining thresholds of significance by considering cluster size (groups of contiguous suprathreshold pixels) on each permutation, which allows to control for false alarms at a map level, using a p-value of 0.05 as the threshold for what clusters would be judged as significant (effectively cutting out the bottom 95% of the distribution).

Lastly, this study also employs connectivity analysis to investigate the degree of synchronisation of activity between different electrodes across the scalp. One way of assessing connectivity is measuring the phase differences between individual electrodes. Assuming that parts of the brain which fire in unison have greater connectivity, the phase-lag value (PLV) will give an absolute account of the mean phase difference between the signals from a channel-pair, expressed as a complex unit-length vector (Cohen, 2014). Assuming increasing uniform marginal distributions of signals and hence relative phase, the PLV will approach zero, while for the reverse it will approach one as the signals becomes more coupled. Formally it is expressed as

$$PLV_{xy} = \left| n^{-1} \sum_{t=1}^{n} sgn(imag(S_{xyt})) \right|, \tag{3.22}$$

with $imag(S)$ being the imaginary part of the cross-spectral density at time point t. Using the imaginary part of the complex number for estimating connectivity, also known as imaginary coherence, avoids dubious connectivity estimates based on volume conduction by ignoring phase lags of zero.

To assess the changes in connectivity in post- compared to pre-stimulation intervals, non-parametric permutation testing was employed. After creating a null hypothesis distribution with 1000 random permutations, the data was then corrected for multiple comparisons using pixel-based thresholding of significance. For the two-tailed test employed, it creates two distributions of the largest positive and negative value to be found under the null hypothesis condition, effectively defining

the statistical threshold for significance, with the lower bound corresponding to the lower 2.5th percentile of the negative distribution, and the higher bound being equal to the top 97.5th percentile of the maximum value distribution, if $p = 0.05$. Given that each pixel represents a channel-pair in a connectivity matrix figure, this is more appropriate than the cluster-size correction technique this study uses for the time-frequency domain.

3.4 Results

When comparing mean alpha power (8-12 Hz μV^2) during the last 25 seconds of photic stimulation (averaged) to a pre-stimulation 25 second baseline alpha power average in frontal, medial, and occipital sensor regions (refer to Figure 3.2 for sensor regions), we found significant during-stimulation alpha power increases in frontal ($p < 0.01$, $r \approx 0.318$, $Z \approx 2.844$, $W = 2213$) and occipital regions ($p < 0.05$, $r \approx 0.253$, $Z \approx 2.259$, $W = 2091$) for 120 seconds of stimulation, with effect sizes being largest across frontal and occipital regions for the longest stimulation period. Other stimulation conditions did not yield significant increases in alpha power. There were also no significant effects in medial regions for any condition.

We found the strongest effects of photic stimulation on alpha power over the frontal region, demonstrating photic stimulation can modulate alpha power in areas outside the visual system. Refer to table 3.2 for all p-values of changes in alpha power during photic stimulation, and table 3.3 for associated effect sizes.

Length of stim	**Frontal**	**Medial**	**Occipital**
30 s	0.8780	0.6976	0.4719
60 s	0.3208	0.2177	0.5080
120 s	0.0045	0.1614	0.0239

TABLE 3.2: Impact of photic stimulation across the scalp. 120 seconds of photic stimulation show significant frontal and occipital increases in mean alpha power (8-12 Hz μV^2), when comparing the last 25 seconds of stimulation (averaged) to an average of alpha power during their respective 25 seconds pre-stimulation baseline interval. To assess if there was a significant difference between pre- and during-stimulation intervals, a two-tailed Wilcoxon signed-rank test was used. Changes are averaged over channels, frequencies (within the alpha range), and time points (25 seconds). Length of stimulation for each condition is given in the leftmost column. Significance of the impact of photic stimulation is given for occipital, medial, and frontal regions of the scalp.

Length of stim	Frontal	Medial	Occipital
30 s	-0.0172	0.0434	0.0804
60 s	0.1110	0.1378	0.0740
120 s	0.3180	0.1566	0.2526

TABLE 3.3: Effect sizes for photic stimulation across the scalp. Effect sizes are small even for conditions in which alpha power was significantly enhanced during stimulation relative to pre-stimulation baselines (see table 3.2), when comparing mean alpha power (8-12 Hz μV^2) in the 25 seconds preceeding stimulation (pre-stimulation interval) to the last 25 seconds of the during-stimulation interval. Effect sizes were calculated by taking $Z\sqrt{N}$, with the z statistic being calculated by a two-tailed Wilcoxon signed-rank test. The length of stimulation applied during each condition is given in the leftmost column. Effect sizes are given for occipital, medial, and frontal regions of the scalp for 30-, 60-, and 120 seconds of photic stimulation.

The difference between alpha power during stimulation and pre-stimulation alpha power baselines can be seen in Figure 3.3. Error-bars (using 95% confidence intervals) also show the variation in data within intervals (pre-, during-, and post-stimulation). Specifically, the error-bars of the figure show, especially for 120 seconds of photic stimulation, there is big variation in alpha power changes post-stimulation. This variation in effect with both decreases and increases in mean alpha power during photic stimulation relative to pre-stimulation baseline mean alpha power levels is particularly pronounced in frontal and medial areas. Refer to section 3.3 for comments on the method used to calculate error bars (the Vysochanskij–Petunin inequality theorem).

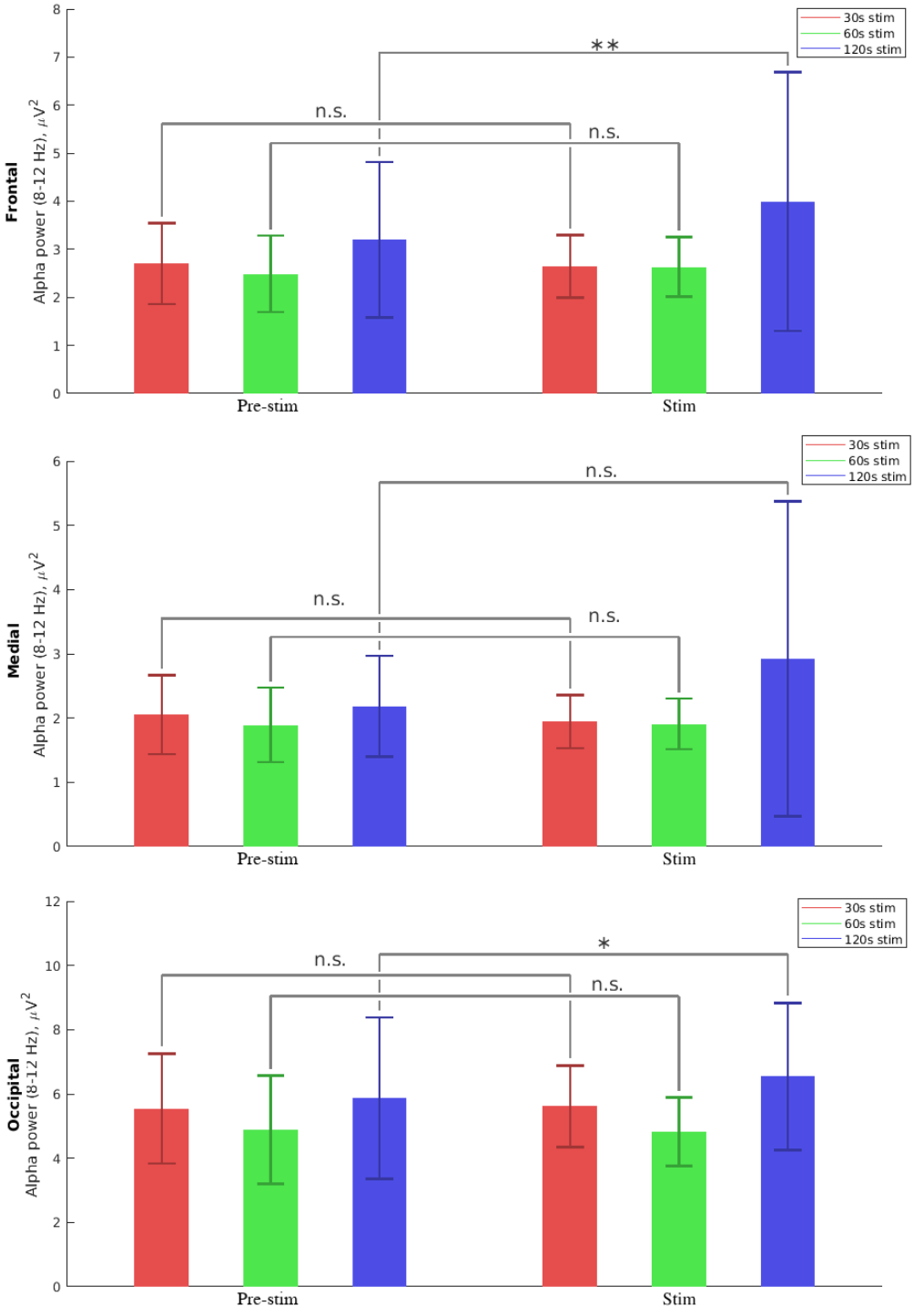

FIGURE 3.3: Changes in alpha power during photic stimulation at 10 Hz.

Occipital and frontal areas show significant mean alpha (8-12 Hz) power (μV^2) enhancements during 120 seconds of photic stimulation relative to pre-stimulation mean alpha power. Significance of alpha power difference between pre- and during-stimulation intervals, was tested using a two-tailed Wilcoxon signed-rank test. * denotes $p < 0.05$, ** for $p < 0.01$, and *n.s* for non-significant results. Red bars shows the effects of 30 seconds-, green bars of 60 seconds-, and blue bars the impact of 120 seconds of stimulation, using the full 25 seconds of pre- and the last 25 seconds of during-stimulation intervals. The results are given for frontal, medial, and occipital areas. Error-bars were calculated using the Vysochanskij–Petunin inequality theorem, and show the standard error of mean alpha power averaged across channels, frequencies and time points, using 95% confidence intervals.

Next we examined the coherence amplitude between Oz and a photodiode as a measure of entrainment of the photic signal (see Figure 3.4). We focused on the longest stimulation period of 120 seconds as this was where we found the greatest increase in alpha power during-stimulation. Results show phase alignment of the IAF to the SF over the occipital region during stimulation, which is one of the necessary effects given by Thut, Schyns, and Gross (2011) to be able to conclude that entrainment of endogenous neural oscillators by rhythmic external stimulation has occurred.

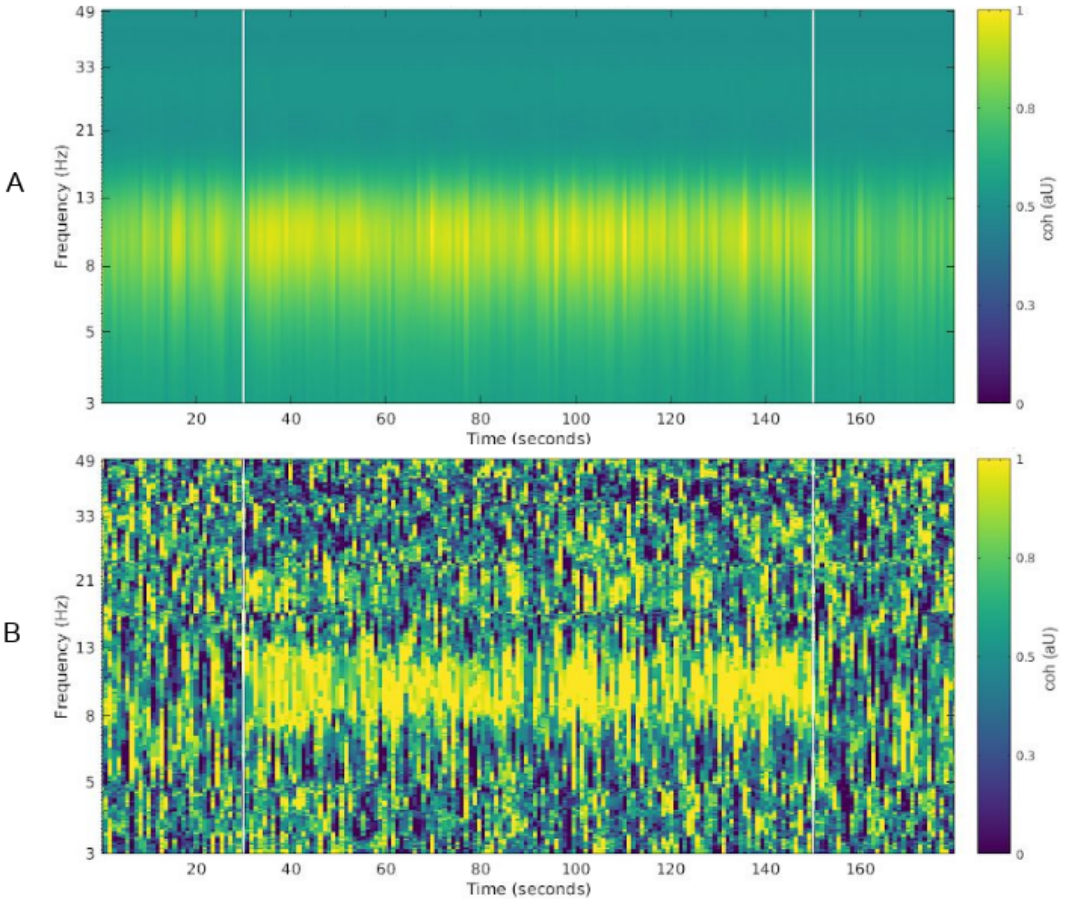

FIGURE 3.4: Coherence between channel Oz and photodiode (PD) before, during, and after 10 Hz photic stimulation.
Coherence measures provide evidence of entrainment. *A* shows coherence amplitude (coherence values are between 0 and 1) between Oz and photodiode (PD) activity, with onset and offset of photic stimulation being marked by white vertical lines. The PD signal was mirrored as to fill the pre- and post-stimulation period as well. This ensures that, rather than measuring the absence versus presence of the 10 Hz driving stimulus, we measure actual phase coherence of the exogenous and endogenous oscillator. *B* shows Oz-PD phase coherence (focusing on synchrony, ignoring amplitude), with vertical white lines showing the onset and end of photic stimulation. Entrainment effects can be seen within the alpha domain (8-12) Hz, centred at the 10 Hz driving signal, which is reflected both in coherence amplitude increase and greater phase coherence.

Next, we examined the amount of time required for the mean Oz-PD coherence amplitude to be reached after photic stimulation onset, which takes not just phase- but also amplitude-similarity between Oz (NF) and PD (SF) data into account. As can be seen in table 3.4, it took, on average, no longer than 2.4 seconds, for mean coherence amplitude to be reached after photic stimulation onset. Mean coherence, here, refers to the mean coherence amplitude value while photic stimulation is being applied (using the entire photic stimulation time window to calculate mean coherence values). This is a conservative estimate, as phase coherence (ignoring amplitude-similarity between Oz and PD and just assessing phase-similarity) is reached even faster, taking no longer than approximately 0.2 seconds across the scalp, albeit with a negative phase alignment in medial and frontal areas, as was shown in Figure 3.5. Entrainment effects drop sharply at the end of stimulation - both using measures of phase coherence and coherence amplitude measures. This drop in coherence entails that endogenous rhythms do not stay at the entrained speed or phase of the 10 Hz SF.

Length of stim	**Occipital**	**Medial**	**Frontal**
30 s	2.3641 s	1.4641 s	2.3641 s
60 s	1.3120 s	0.1120 s	0.7120 s
120 s	1.0120 s	1.9160 s	1.9160 s

TABLE 3.4: Time until mean coherence across the scalp (in seconds). Mean coherence being defined as the mean of the coherence amplitude during photic stimulation. For the occipital region, Oz was used. Cz was used as representative for the medial region, and Fz for the frontal area. Time is given in seconds. The leftmost column shows length of photic stimulation applied at each condition. Results are reported for occipital, medial, and frontal areas, taking an average of each area.

Although entrainment of the 10 Hz driving signal was visible across the scalp, we observed a negative phase correlation over medial and frontal areas, as can be seen in Figure 3.5, perhaps indicating endogenous alpha oscillations behaving as a travelling wave, as this would explain the reversal in phase alignment.

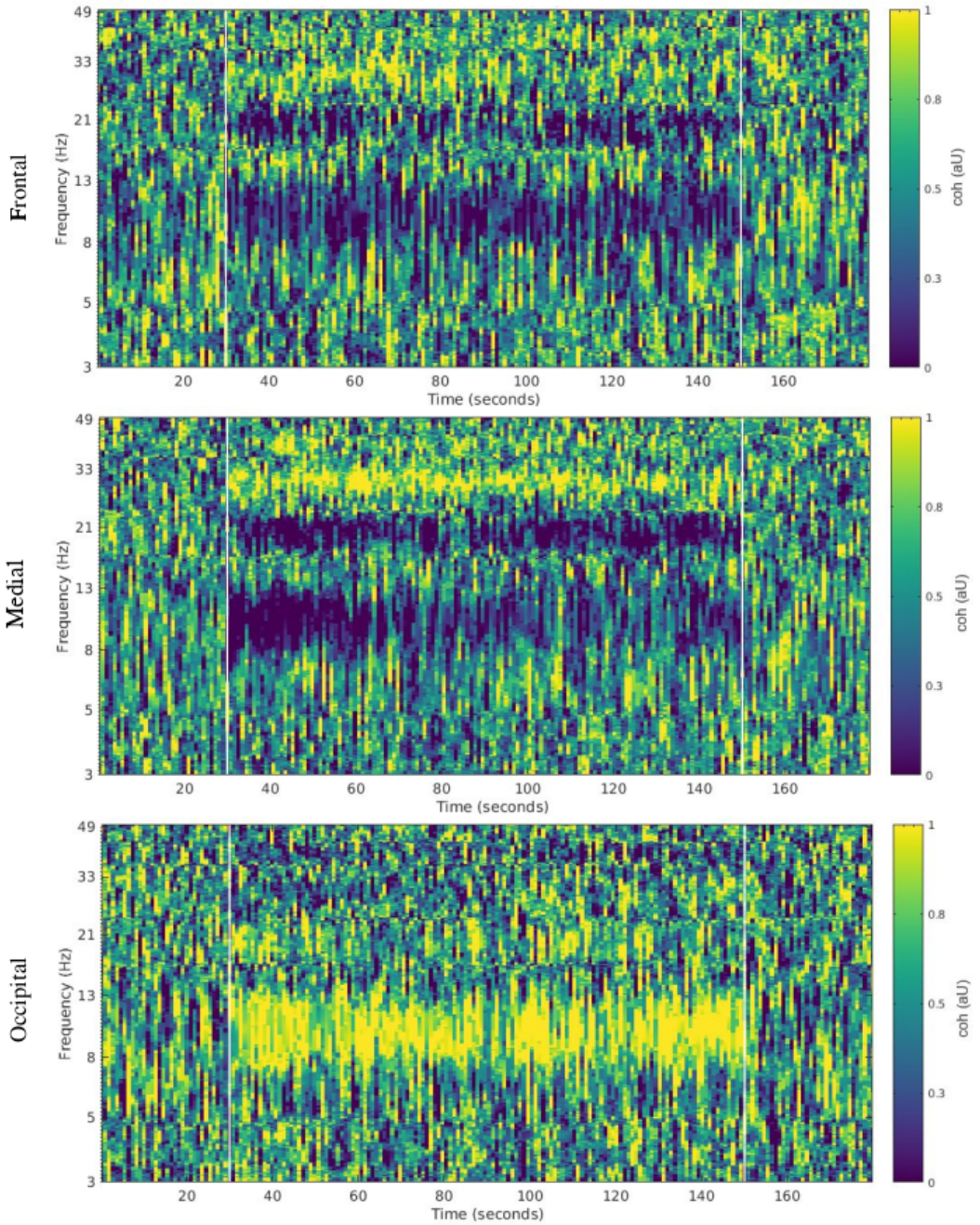

FIGURE 3.5: Phase coherence across the scalp during photic stimulation at 10 Hz.

While entrainment effects can be seen across the scalp for both the alpha domain and the harmonic beta phase in Fz-photodiode (PD)- (*Frontal*), Cz-PD- (*Medial*), and Oz-PD-coherence measures (*Occipital*), phase alignment is reversed in frontal and medial sensors compared to the occipital sensor. The figures here show data from trials using 120 second of photic stimulation, where the effects are most visually apparent. Entrainment effects can be seen for the alpha domain (8-12) Hz, and to a lesser extent within the harmonic beta band (12-30 Hz), which is reflected both in coherence amplitude increase and greater phase coherence.

Next, we focused on investigating the effects of photic stimulation on the post-stimulation window, which revealed a suppression of alpha activity (figure 3.6), coinciding with the end of entrainment (e.g. Figure 3.4). This finding demonstrates that photic stimulation affects brain dynamics even after the offset of stimulation and entrainment.

Figure 3.6 displays the topographic changes in alpha power during stimulation compared to pre- and post-stimulation intervals, as well as the topographic effect sizes for post-stimulation alpha power suppression.

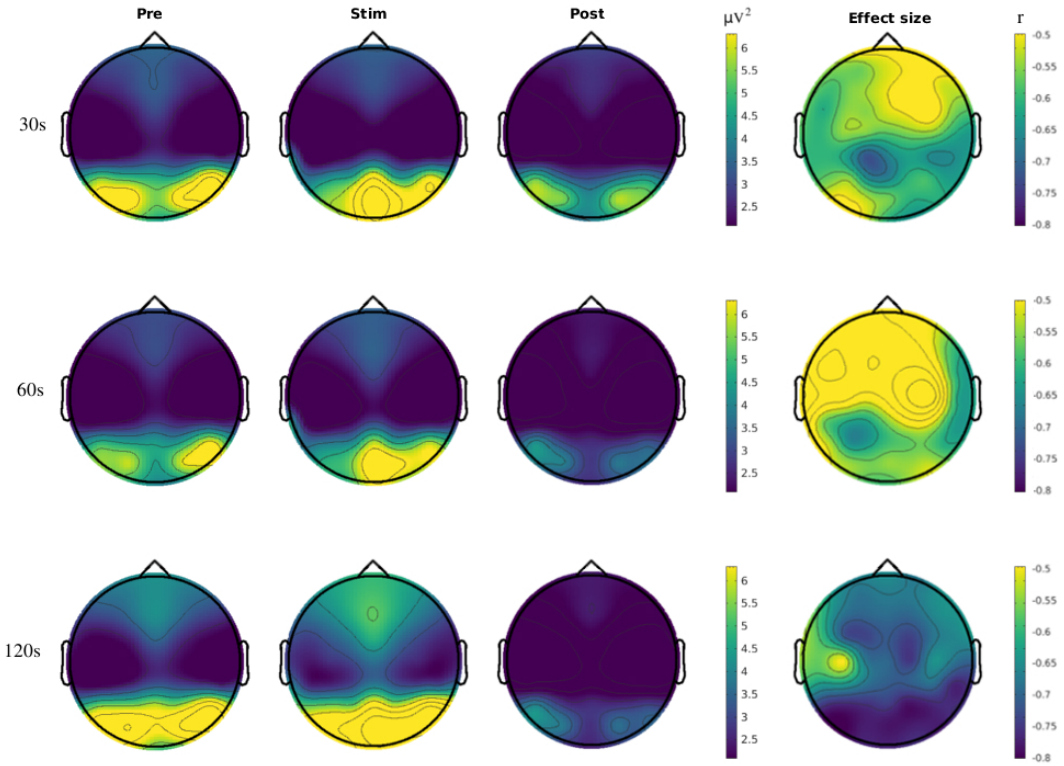

FIGURE 3.6: Topographic impact of 10 Hz photic stimulation on alpha power.
The topographic plots display an average of absolute alpha (8-12 Hz) power (μV^2). The *Pre* column shows mean alpha power activity during the 25 seconds pre-stimulation baseline interval, the *Stim* column (middle) shows the mean alpha power during the last 25 seconds of photic stimulation for 30-, 60-, and 120 seconds respectively, while the *Post* column shows the mean alpha power for a post-stimulation interval of 25 seconds. The rightmost column shows effect sizes derived from the z statistic of a two-tailed Wilcoxon signed-rank test of the difference between pre- and post-stimulation conditions, with greater numbers indicating greater significance of the post-stimulation alpha power suppression relative to baseline levels.

Post-stimulation alpha power suppression was highly significant across the scalp at $p < 0.0001$ for occipital, medial, and frontal areas in all conditions. Based on effect sizes, it was most prominent in occipital areas (30 seconds: $r \approx -0.6102$, $Z \approx -5.4582$, $W = 482$; 60 seconds: $r \approx -0.6279$, $Z \approx -5.6165$, $W = 449$; 120 seconds: $r = -0.7915$, $Z \approx -7.0793$, $W = 144$), but not restricted to it, as the medial region (30 seconds: $r \approx -0.6574$, $Z \approx -5.8802$, $W = 394$; 60 seconds: $r \approx -0.5727$, $Z \approx -5.1224$, $W = 552$; 120 seconds: $r \approx -0.7309$, $Z \approx -6.5373$, $W = 257$) and, to a lesser extent, the frontal region (30 seconds: $r \approx -0.5582$, $Z \approx -4.9929$, $W = 579$; 60 seconds: $r \approx -0.5266$, $Z \approx -4.7100$, $W = 638$; 120 seconds: $r \approx -0.6810$, $Z \approx -6.0913$, $W = 350$) showed a reduction in alpha levels after entrainment offset relative to pre-stimulation average baseline levels. Refer to table 3.5 for all p-values of changes in alpha power after photic stimulation, and table 3.6 for associated effect sizes.

Length of stim	Frontal	Medial	Occipital
30 s	< 0.0001	< 0.0001	< 0.0001
60 s	< 0.0001	< 0.0001	< 0.0001
120 s	< 0.0001	< 0.0001	<0.0001

TABLE 3.5: Statistical significance of alpha power suppression across the scalp.
Suppression of alpha power calculated by comparing average alpha power between post-stimulation and pre-stimulation alpha power time windows was strongly significant across occipital, medial and frontal regions. A two-tailed Wilcoxon signed-rank test comparing the mean alpha (8-12 Hz) power (microvolt squared values averaged across channels, frequencies, and time points) between pre and post-stimulation intervals was used to assess significance.

Length of stim	Frontal	Medial	Occipital
30 s	-0.5582	-0.6574	-0.6102
60 s	-0.5266	-0.5727	-0.6279
120 s	-0.6810	-0.7309	-0.7915

TABLE 3.6: Effect sizes of alpha power suppression across the scalp.
Effect sizes were calculated by taking $Z\sqrt{N}$, with the z statistic being calculated by a two-tailed Wilcoxon signed-rank test. The effect sizes are given for occipital, medial, and frontal regions for 30-, 60-, and 120 seconds of photic stimulation.

To see the variation in alpha power post-stimulation in comparison to pre-stimulation alpha power variation, refer to Figure 3.7. Contrary to the large variation in the changes in alpha power during photic stimulation at 10 Hz (Figure 3.3), we observed less variation in alpha power when comparing post-stimulation to pre-stimulation time windows (Figure 3.7).

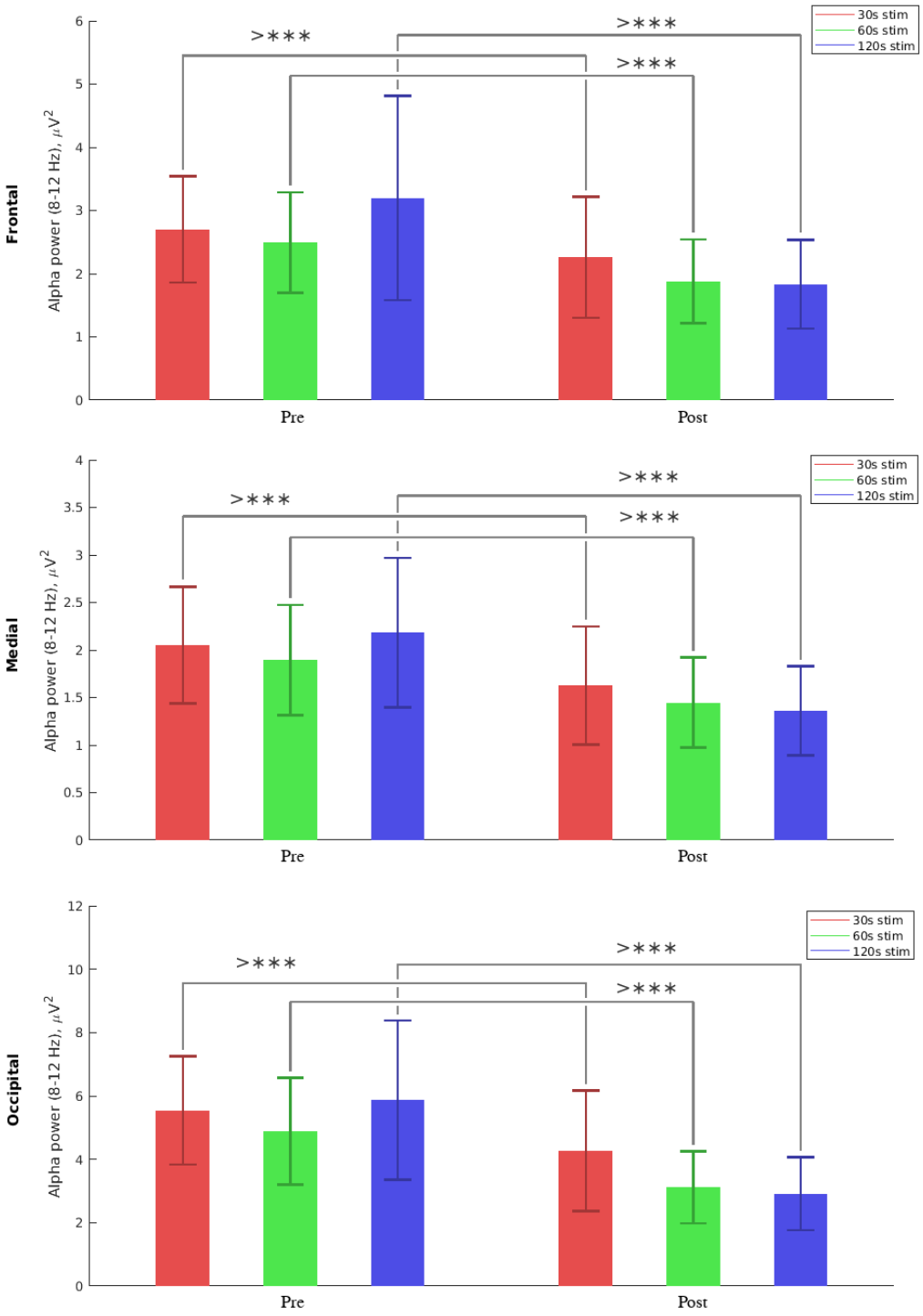

FIGURE 3.7: Comparison of alpha power for pre- and post-stimulation time-windows.

Post-stimulation alpha power is reduced significantly compared to pre-stimulation alpha power in occipital, medial, and frontal areas ($p < 0.001$). A two-tailed Wilcoxon signed-rank test was used to compare alpha power between pre- and post-stimulation time windows. * denotes p < 0.05, ** for p < 0.01, *** for p < 0.001, and *n.s* for non-significant results. The results are given for frontal, medial, and occipital areas, using the full 25 seconds of pre- and post-stimulation intervals after 30- (red bars), 60- (green bars) and 120 seconds (blue bars) of stimulation. Error-bars were calculated using the Vysochanskij–Petunin inequality theorem, and show the standard error of mean alpha (8-12 Hz) power (μV^2) measures averaged across channels, frequencies and time points, using 95% confidence intervals.

As this experiment used fixed 10 Hz stimulation, we were also able to investigate the relationship between effect sizes and the difference between stimulation frequency (SF) and individual alpha frequency (IAF) across the scalp. As shown in Figure 3.8, contrary to previous research (Walter, 1954), effectiveness of stimulation for alpha power enhancement is not maximised when $IAF = SF$. Rather, frontal, medial, and occipital areas show the most pronounced alpha power enhancements during stimulation when the stimulation frequency is 1-2 Hz above IAF (measured over Oz). SF-IAF alignment is more consistent across the brain for the effect size of post-stimulatory suppression: alpha is always most affected when SF more closely approaches IAF. The total effect size distribution was calculated by summing up individual contributions using the standard mean difference formula (see equation 3.18), as is recommended by Olive and Smith (2005).

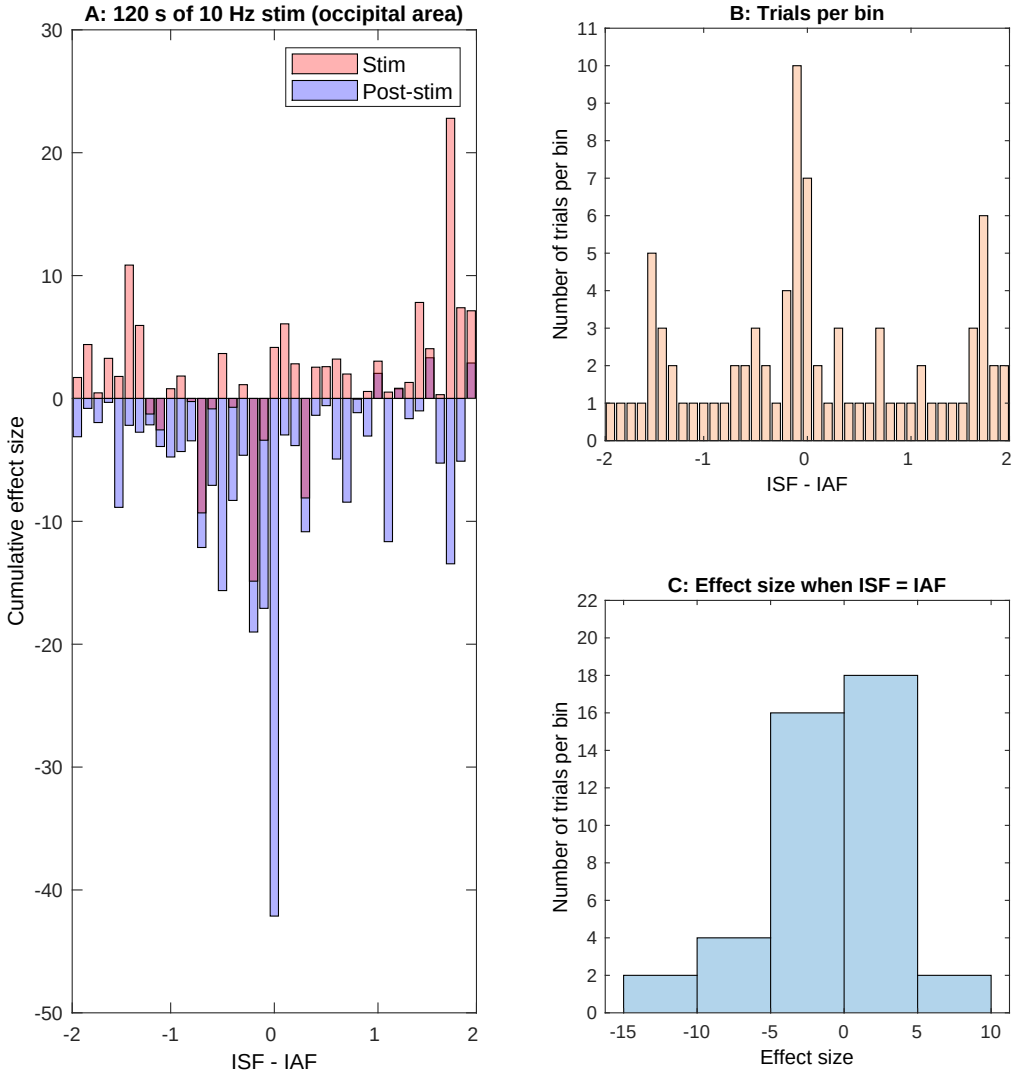

FIGURE 3.8: Occipital IAF-SF detuning and alpha power changes. Cumulative effect sizes are shown on the y-axis. The x-axis displays divergence between IAF and SF (10 Hz), with positive numbers indicating an SF that exceeds IAF, and negative numbers a slower SF compared to the IAF. Figure A: When SF equals IAF, some trials show a reduction rather than an enhancement of alpha power during stimulation, which has the effect of reducing their cumulative effect size. Alpha power suppression post-stimulation is most pronounced when detuning approaches zero. Figure B: Trials per bin for SF-IAF. The majority of trials show little divergence between SF and IAF, which suggests that the effect for strongest alpha power enhancement is driven by trials where the pre-stimulation IAF of participants was around 8 Hz (second biggest peak in the figure), with most participants having an IAF at 10 Hz. Figure C: Trials per bin and distribution of effect sizes for trials when SF equals IAF (blue), showing that for many trials photic stimulation yielded alpha power suppression during stimulation. IAF was calculated using pre-stimulation data recorded over occipital regions. Total effect size distribution was calculated by summing individual effect sizes of alpha power changes between either pre- and during-stimulation alpha power values, or between pre- and post-stimulation alpha power values. The standard mean difference formula was used to estimate differences in effect sizes of alpha (8-12 Hz) power for all time windows. This figure shows the effect of 120 seconds of photic stimulation over occipital areas.

Next, we further quantified the magnitude of increase in alpha power during stimulation and post-stimulation alpha power suppression using linear regression analysis. As can be seen in Figure 3.9, we found the magnitude of alpha power suppression was not related to the length of stimulation, confirmed by a linear regression analysis (Bonferroni-corrected $p > 0.05$). However, in contrast we found that the increase in overall alpha power during stimulation was more pronounced as stimulation time increases (Bonferroni-corrected $p < 0.01$).

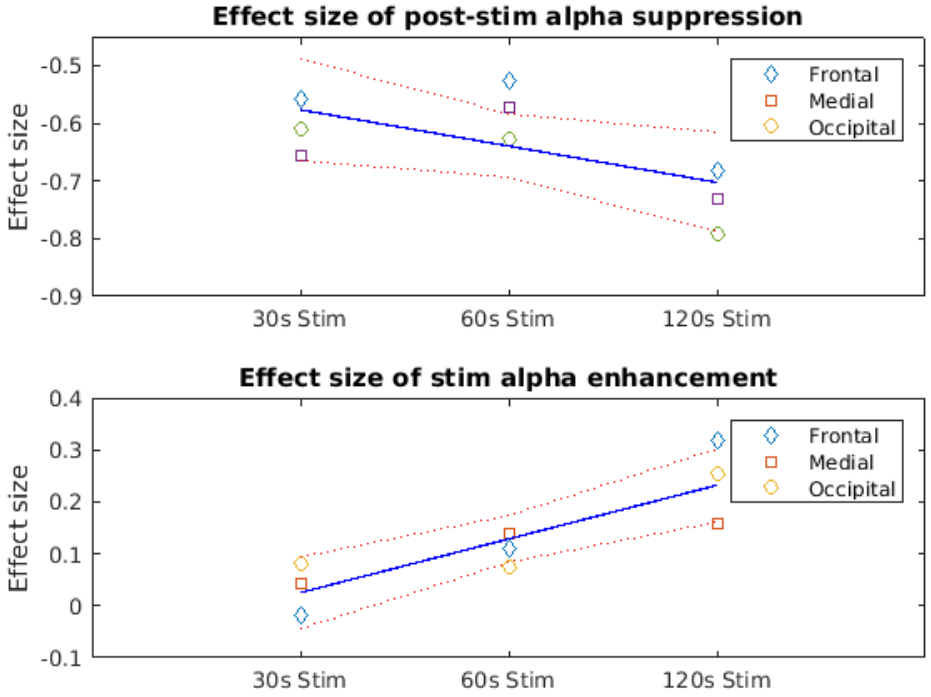

FIGURE 3.9: Linear regression analysis of post-stimulation alpha power suppression and photic stimulation alpha power enhancement for differing lengths of photic stimulation.
The top figure shows that the effect size of post-stimulatory alpha power suppression (8-12 Hz) does not increase significantly across the scalp as stimulation length increases, with a linear regression giving a significance value of $p > 0.05$ (averaged across frontal, medial, and occipital areas) after Bonferroni correction for multiple comparisons. In the bottom figure, during photic stimulation, longer stimulation durations significantly increases alpha (8-12 Hz) enhancement ($p < 0.01$ after Bonferroni correction). For both tests, the corrected alpha was 0.0125. If individual electrode regions are analysed in isolation (rather than using data points for all areas in conjunction, as it was done for this figure), however, length of stimulation is not significantly ($p > 0.05$) correlated with either during-stimulation alpha power enhancement or post-stimulation alpha power suppression for either frontal, medial or occipital areas. Effect sizes are calculated by $Z\sqrt{N}$, with the z statistic being calculated with the Wilcoxon sign-rank test. Orange dotted lines show polynomial confidence intervals of 95% calculated using the Matlab polyconf function.

Figure 3.10 shows the significance of the difference between pre- and post-stimulation intervals across the time-frequency domain, using z-maps which were generated using permutation testing (1000 permutations were used, as recommended by Cohen (2014)), and then corrected for multiple comparisons by zmap pixel-value-based cluster-size correction with $p < 0.05$. The figures shows significant alpha power suppression in the occipital region after 60 seconds of photic stimulation, and more pronounced alpha power suppression after 120 seconds of stimulation, which outlasts the post-stimulation window interval of 25 seconds.

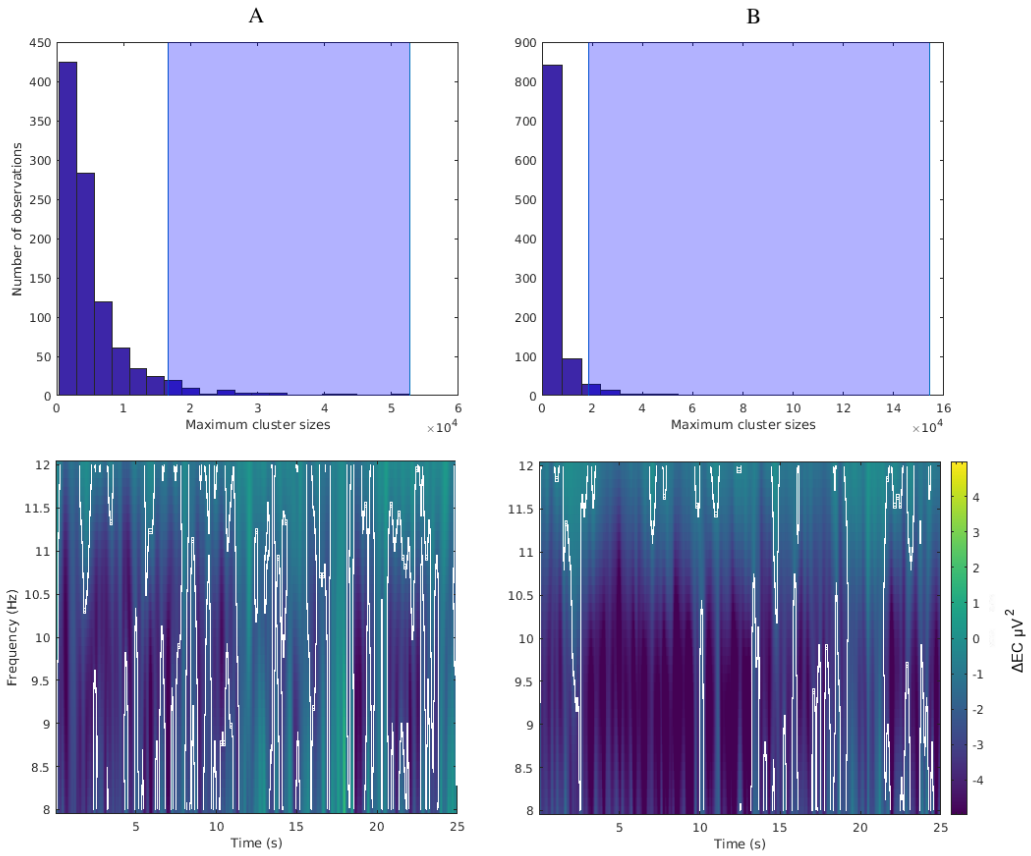

FIGURE 3.10: Thresholded difference maps during post-stimulation time windows following 60 and 120 seconds of photic stimulation. Thresholded difference maps (using z-maps) show greater post-stimulation alpha power suppression after 120 seconds of photic stimulation at 10 Hz compared to alpha power suppression levels following 60 seconds of photic stimulation. The top figure of column *A* shows the expected (based on the null hypothesis distribution) zmap pixel-value cluster sizes of changes in alpha (8-12 Hz) power (μV^2) in pre- and post-stimulation intervals for 60 seconds of photic stimulation, if the null hypothesis of there being no significant difference between conditions were true. The shaded area of the figure highlights the cluster sizes which would be judged as significant. The bottom figure of column *A* shows the difference map between pre- and post-photic-stimulation intervals, with areas of significant ($p < 0.05$, corrected for multiple comparisons with cluster size correction) decrease in amplitude (μV^2) in post- relative to pre-stimulation trials contoured by white lines. Column *B* shows the same analysis for 120 seconds of photic stimulation. Taken together, both columns show that post-stimulation alpha (8-12 Hz) suppression lasts for the entirety of the post-stimulation recording and that an increase in length of stimulation from 60 to 120 seconds also increases post-stimulation alpha power suppression. The data shown here uses an average of occipital sensors. For more detail on the statistical tests performed, refer to section 3.3.

If alpha is indeed acting as a brake on cognition (Mathewson et al., 2011), its down-regulation during post-stimulatory suppression would suggest greater cortical connectivity, as without said brake, neural activity could flow more freely. One

way of assessing connectivity is measuring the phase differences between individual electrodes, by assessing their phase-lag value. Phase-lag values lies between 0 and 1, and indicate the degree of synchronization between sensors. To help with the interpretation of subsequent connectivity figures, refer to Figure 3.11 to see which numbers correspond with what channels.

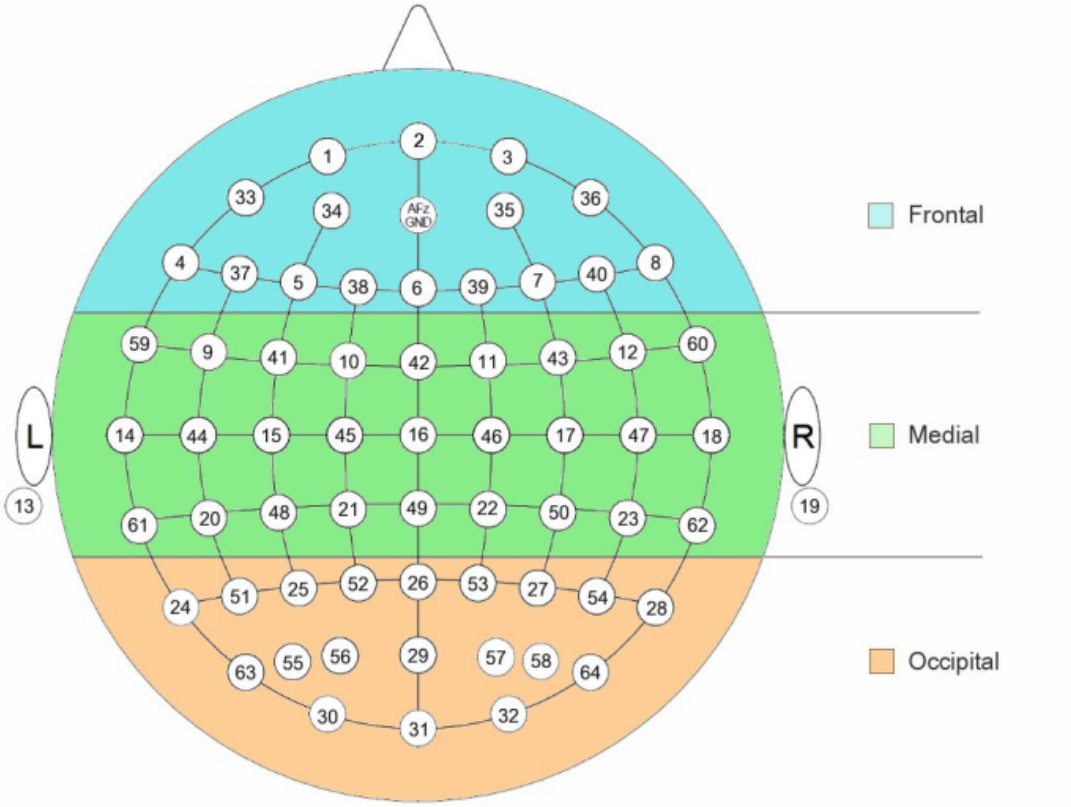

FIGURE 3.11: Sensor regions numbered.
For all analysis, when frontal (top/blue), medial (middle/green), or occipital (bottom/orange) regions are referenced, averaged measures of electrodes within the coloured sections are used. All electrodes are numbered according to the 10/20 system. Refer to this figure for interpreting successive connectivity matrices.

Figure 3.12 shows example data contrasting pre- and post-stimulation connectivity after 30 seconds of photic stimulation have been applied.The majority of these changes are over- and between occipital and lower medial regions, although effects can be seen across frontal, medial, and occipital areas (figure 3.13).

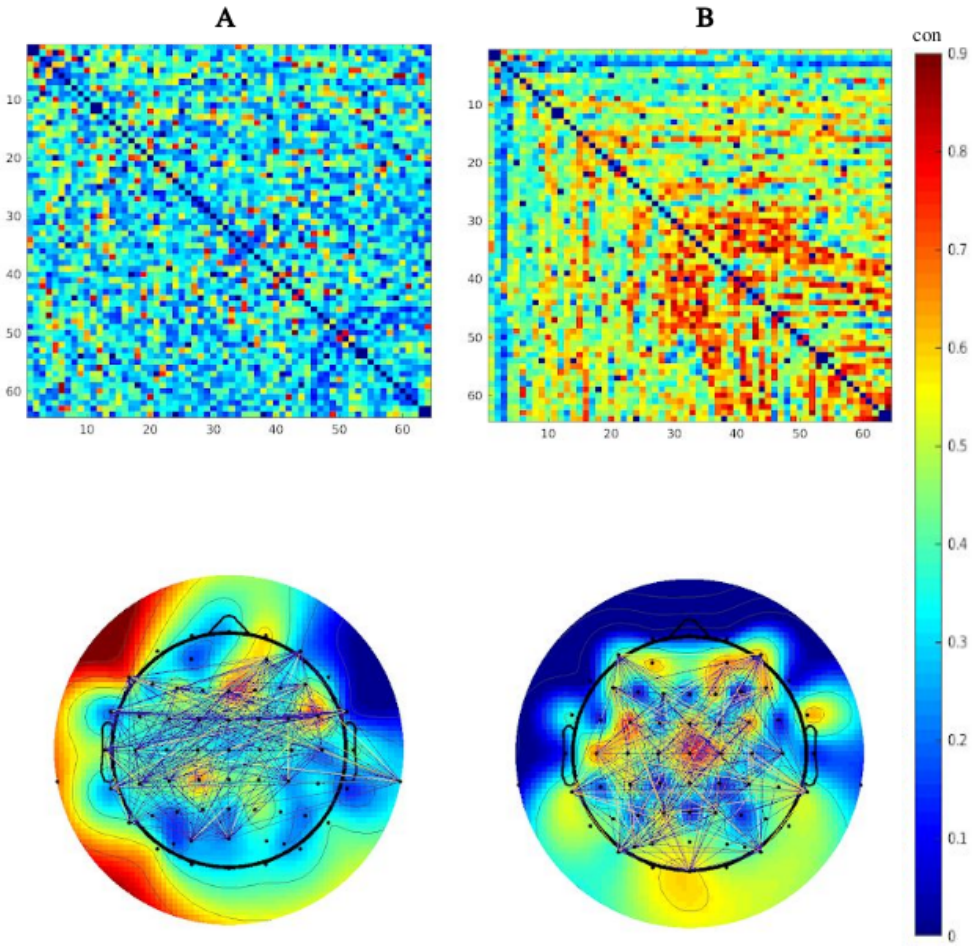

FIGURE 3.12: Phase-lag values pre and post photic stimulation
Phase-lag values are increased in post-stimulation intervals. The top row for columns *A* and *B* shows a connectivity matrix (64 by 64 channels) of phase-lag values (PLV), showing synchrony between channels (from zero to one), pre- (*A*) and post-stimulation (*B*). The bottom row shows a topographic representation of the top 5% of connection strengths for pre- (*A*) and post-stimulation (*B*) intervals. The data shown here compares pre- and post-stimulation intervals following 30 seconds of photic stimulation, as the topographic changes for this condition are most visually striking.

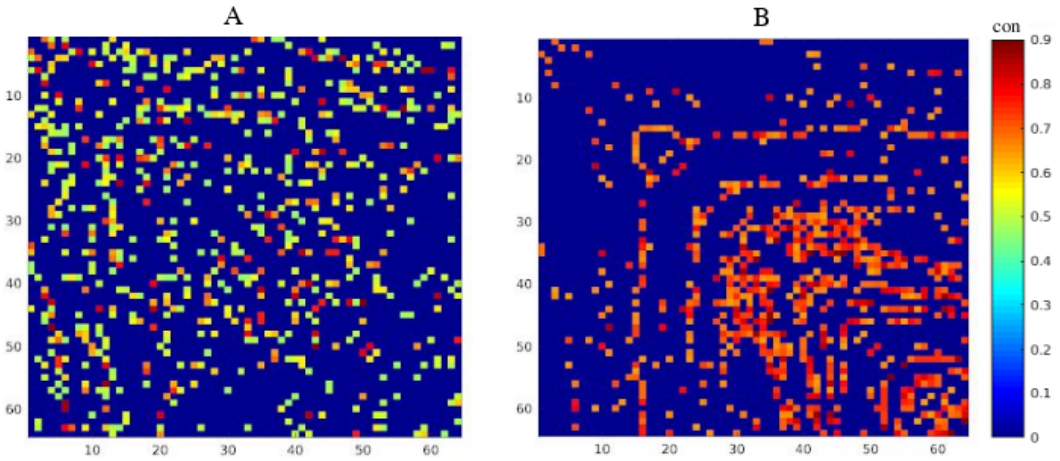

FIGURE 3.13: Thresholded connectivity phase-lag values across the scalp.
Phase-lag values are increased in post-stimulation intervals. The figure shows thresholded connectivity matrices for pre- (A) and post-stimulation (B) intervals, where any value within the distribution smaller than the median plus the standard deviation is set to zero, giving a clearer picture of where the main effects are to be found. This figure elaborates on the measures presented in Figure 3.12, and is consequently also showing data from trials which applied 30 seconds of photic stimulation. For reference about which number corresponds to which sensor, refer to Figure 3.2.

Figure 3.14 shows the significance of changes in connectivity in post- compared to pre-stimulation intervals as assessed by non-parametric permutation testing using pixel-based correction for multiple comparisons. Changes in PLV measures grow more pronounced as stimulation time lengthens, but also are increasingly focused on medial and occipital brain areas at $p < 0.05$. Conversely, there was no significant change in connectivity between pre-stimulation and stimulation conditions.

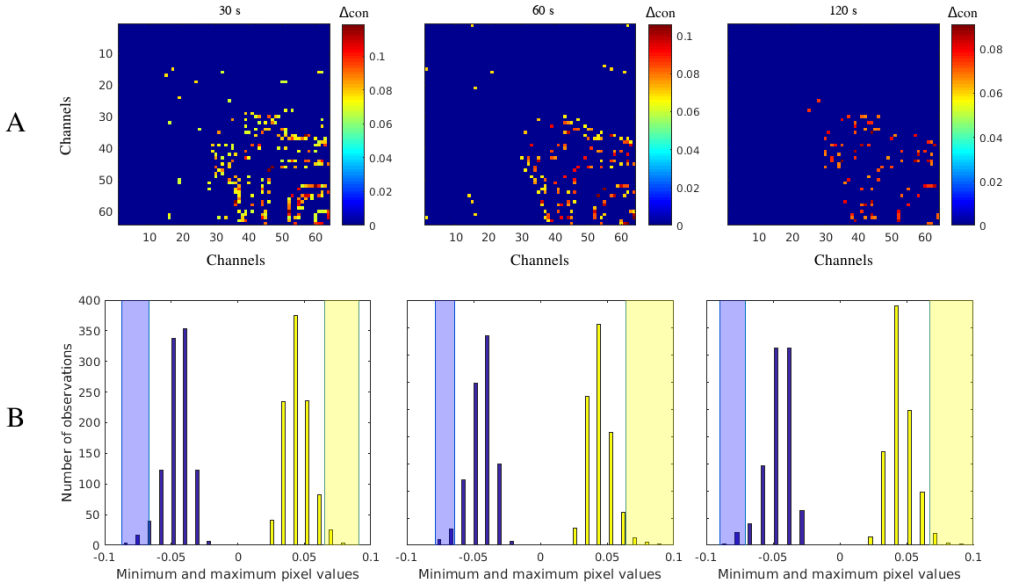

FIGURE 3.14: Changes in connectivity across conditions post photic stimulation at 10 Hz.
Connectivity increases are significant in all post-stimulation conditions. Row *A* shows thresholded connectivity (using z-maps) of the changes in connectivity measures (Δcon) between pre- and post-stimulation intervals, with all non-zero values showing significant ($p < 0.05$) post-stimulation increases in PLVs, indicating greater connectivity after 30-, 60-, and 120 seconds of photic stimulation. Row *B* shows the data distribution, according to which the lower (blue shading) and higher (yellow shading) areas of statistical significance for individual pixels are calculated, with each pixel representing a channel-pair.

3.5 Discussion

Thut, Schyns and Gross suggest that sufficient evidence for successful entrainment of neural oscillations by rhythmic stimulation has to include a proof of coherence between the endogenous and exogenous oscillator, that their interaction shows effects of detuning (frequency-specificity), with strongest effects of entrainment to be found in the area of the brain that specialises in the sensory modality of the stimulation signal (spatial-specificity) (Thut, Schyns, and Gross, 2011).

On the requirement of a proof of coherence between the endogenous and exogenous oscillator, we have demonstrated that there is indeed a strong increase in phase alignment over occipital electrodes in all conditions, setting in immediately at stimulation onset, and reaching its mean value after a maximum of 2.4 seconds. This is also in line with previous research by Adrian and Matthews who have shown that 10 Hz alpha stimulation shifts IAF frequency to synchronise with the SF (Adrian and Matthews, 1934). We also observed strong increases in coherence amplitude over medial and frontal areas, but the phase coherence for these areas was strongly negative, which might be a consequence of the underlying endogenous alpha rhythm exhibiting characteristics of a traveling wave across the scalp, causing the observed

phase-shift, explaining the observed reversal in polarity (Suzuki, 1974; Zhang et al., 2018; Patten et al., 2012).

The requirement of spatial-specificity is met only in part. Past research (Walter, 1963) reported that, aside from shifting the IAF, 10 Hz alpha stimulation would also enhance IAF power, as entrainment would cause resonance that would then further boost alpha amplitude. Consequently, as Thut, Schyns and Gross (2011) put forward that effect sizes of successful rhythmic brain stimulation ought to be strongest in the brain area that specialises in processing the sensory modality of the stimulus, we expected enhancements of alpha power during stimulation to be most pronounced over the occipital region. While we do find significant enhancements of alpha amplitude during stimulation in the occipital region, which houses the visual processing centre of the brain, for 120 seconds of stimulation ($p < 0.05$), frontal area alpha power changes during the same duration of photic stimulation were found to be more pronounced ($p < 0.01$). While this finding demonstrates that photic stimulation affects not just occipital areas, it also violates the expectation of area-specific effects. The reasons underlying this finding is unclear, although it is possible that this is a consequence of the fairly small sample size and number of trials in this study. It might also be the case that, if there is a homeostatic element keeping alpha power stable over time as is suggested by Kluetsch et al. (2014), successful enhancement of alpha power beyond a certain threshold (a sufficiently big deviation from pre-stimulation alpha power values) might bring about its own dampening. While highly speculative, the fact that, as will be discussed in more detail below, even non-significant changes in alpha power during stimulation (compared to pre-stimulation baseline values) are followed by strongly significant decreases in alpha power ($p < 0.0001$) across frontal, medial, and occipital areas in all conditions, which suggests the existence of just such a mechanism. Regardless, it is noteworthy that the effects of during-stimulation alpha power enhancement can be found outside of occipital areas, as this suggests an interaction between frontal and occipital alpha oscillators or alternatively a forward-boosting of occipital alpha power enhancements. In addition, when looking at the post-stimulation effects after stimulation offset, however, we find the strongest suppression over occipital areas, which is more in line with the area-specificity of effects required by Thut, Shyns and Gross (2011), and suggests that, to the extent that alpha is regulated by a homeostatic mechanism, perhaps strongest during-stimulation enhancement would have been found in the occipital region, would it not have been for its endogenous dampening in response to exogenous forcing.

The last piece of required evidence, as framed by Thut, Schyns and Gross, would include effects of detuning, where differences in the SF and IAF in turn affect efficiency of the stimulation approach (Thut, Schyns, and Gross, 2011). This view is in line with Walter, who found that, as the divergence between SF and IAF widened, the effectiveness of photic stimulation decreases, and that it could be maximised when $SF = IAF$ (Walter, Dovey, and Shipton, 1946; Walter, 1963). In contrast with this, we found that strongest alpha power enhancements across conditions and areas of the brain, occurred when SF was 1-2 Hz above IAF. We speculate that this may relate to the transit time of each flash from the retina to the visual cortex, which is estimated to take 100-150 milliseconds, and then another 100-200 milliseconds for the information to be decoded (Cauchoix et al., 2014; Nieuwenhuijzen et al., 2013; Carlson et al., 2013). This time-frame corresponds to 1-2 cycles of alpha-band oscillations, which could account for the disparity observed. Hence, in order to effectively

stimulate at IAF it would be necessary to stimulate at 1-2 Hz above the measured dominant frequency to maximise effectiveness, as only this would actually bring SF and IAF in alignment. Another observation allows us to put forward an alternative hypothesis, which brings our findings in alignment with those by previous research: the most pronounced post-stimulation alpha power suppression can be found after 120 seconds of photic stimulation where SF equals IAF, as shown in Figure 3.8. This is also the condition where we find greatest variation in during-stimulation alpha power as demonstrated by the error-bars in Figure 3.3 and also the right column of Figure 3.8, where, for a number of trials when IAF equals SF, photic stimulation results in a suppression of alpha power while stimulation is being applied instead of an alpha power increase, which does not happen to the same extent for trials where SF is 2 Hz above IAF. If alpha power is indeed regulated by a homeostatic mechanism, perhaps successful enhancement paradoxically also leads to more stringent endogenously regulated suppression. Put another way, alpha power might be, in line with findings by pioneers in this field, such as Walter (1946), most effectively enhanced when SF equals IAF, but this effect might be overshadowed by endogenous suppression. Perhaps it is exactly that homeostatic regulation that we see once exogenous forcing with photic stimulation is removed, and endogenous suppression becomes visible in the form of post-stimulation alpha power suppression.

In summary, the above constitutes evidence for successful entrainment and modulation of the alpha rhythm by rhythmic photic stimulation.

Going beyond these findings, we have shown for the first time that even in conditions where photic stimulation did not result in statistically significant changes in alpha power (Frontal: 30s, 60s; Medial: 30s, 60s, 120s; Occipital: 30s, 60s), the stimulation offset coincided with a significant ($p < 0.0001$ over frontal, medial, and occipital areas in all conditions) drop in alpha below pre-stimulation baseline levels with medium to large effect sizes. For the frontal area, post-stimulation alpha power suppression was significant after 30 seconds ($r \approx -0.56$), 60 seconds ($r \approx -0.53$), and 120 seconds ($r \approx -0.68$). Medial region alpha power suppression was significant for 30 seconds ($r \approx -0.66$), 60 seconds ($r \approx -0.57$), and 120 seconds ($r \approx -0.73$). Finally, occipital alpha power suppression was significant after 30 seconds ($r \approx -0.61$), 60 seconds ($r \approx -0.63$), and 120 seconds ($r \approx -0.79$) of photic stimulation. Significant changes in connectivity appear for all stimulation lengths, but were mostly restricted to the occipital and medial areas at $p < 0.05$.

We speculate, that alpha power suppression following the excitation during stimulation, might be part of a homeostatic control mechanism attempting to keep brain activity at a set point equilibrium of excitation and inhibition. As the suppression effect can also be found when the preceding stimulation did not result in a significant enhancement of alpha power, it might be the case that alpha power suppression happens concurrently with stimulation, in an attempt to counterbalance the exogenous forcing, as to keep alpha power stable. When stimulation is applied successfully, that is, with a significant increase in alpha power, as was the case over occipital regions, this endogenous homeostatic mechanism might be overpowered. This may explain why occipital sites that yielded greater (significant) alpha power enhancements during stimulation, also showed greater post-stimulatory alpha power suppression. Once the driving stimulus is removed, we speculate that it is due to the attempts of the brain to retain alpha power stability that their sudden and significant suppression results post-stimulation. If the post-stimulation alpha power suppression is indeed the result of a homeostatic mechanism, it is interesting to note that it is not a very transient phenomenon with alpha power levels quickly returning to

pre-stimulation baseline levels following the alpha power level correction post (or during) stimulation. One explanation for this might be that the time taken for alpha power levels to return to baseline values might be dependent on the extent of external forcing during stimulation, that is, on how strongly alpha power enhancement during photic stimulation would have to be balanced by endogenous suppression. The reasoning here is that stronger exogenous enhancement of alpha power brings about stronger endogenous suppression, which, as it increases in effect size, takes longer to level off post-stimulation, until baseline values of alpha power are reached. This could be investigated by using weaker photic stimulation, as according to this hypothesis it would bring about lesser alpha power suppression, and hence a quicker return to baseline alpha power levels. Another explanation for alpha power suppression lasting for the entirety of the 25 seconds post-stimulation time window might be that individual alpha levels are multi-stable (Van de Ville, Britz, and Michel, 2010; Mehrkanoon, Breakspear, and Boonstra, 2014; Ghosh et al., 2008), as elaborated in greater detail below. Perhaps, in the absence of a task which requires higher (or baseline) alpha power, lower alpha power too is a stable enough state. Note that even in this case, however, correction to pre-stimulation alpha power levels is possible without interference (even through random drift of alpha power) but quicker correction might be achieved by engagement in a task that facilitates higher alpha power. This hypothesis could be tested by giving participants cognitive tasks after alpha power suppression onset.

Further, we propose that the suppression effect, to the extent that it is the result of a homeostatic mechanism, brings the alpha power level and speed back to a set-state point that corresponds to a stable minima. This idea is building on Stam (2005), who conceptualises the brain as a multidimensional energy state-space. This state-space can be imagined as a simplified two-dimensional plane, with each oscillator traversing a number of low-potential valleys (basins of attraction) and hills (repellers). As it does so, it experiences more stability in the former, and less as he approaches the latter. There is, in fact, evidence that the alpha features properties in line with these projections (Freyer et al., 2009; Freyer et al., 2011; Pradhan et al., 1995; MacIver and Bland, 2014). A problem arises, however, when a local minima is stable enough for the oscillator to settle, but suboptimal for overall brain function. As alpha dysrhythmia is associated with negative impact on brain function (Arns et al., 2008; Wahbeh and Oken, 2013; Kan and Lee, 2015; Choi et al., 2011; Fink and Benedek, 2014; Babiloni et al., 2009), this might mean that dislodging pathological alpha minima might aid treatment of neuropathologies: With exogenous forcing through rhythmic brain stimulation using repetitive photic stimulation, this set point equilibrium might be shifted to a new one by shaking up the system. Local minima with greater depth might require greater forcing through longer stimulation times, but since we have shown that light stimulation does entrain and impact alpha rhythms, it is thinkable that, by enhancing alpha activity, we might allow the brain to settle in a new, hopefully better, minima. A NFB study by Kluetsch et al. (2014) gives some support for this interpretation. In an attempt to reduce post-traumatic stress disorder (PTSD) symptoms, they taught participants to suppress alpha power. This is a curious choice, as PTSD is associated with comparatively low alpha power to begin with, as it is the lack of its inhibitory potential which is thought to stand in relation to the cortical hyperarousal that characterises the disorder (Wahbeh and Oken, 2013). After training had finished which removed alpha power levels further from the normal range, they found that alpha levels had rebounded to levels significantly exceeding the low pre-NFB levels, more closely approximating normal alpha power

levels found in healthy subjects (Kluetsch et al., 2014). Taken together with our findings, this suggests that homeostatic correction might play a role in alpha dynamics.

3.6 Conclusion

This chapter shows the feasibility and effectiveness of photic driving for entrainment of neural oscillations in resonant alpha frequencies and demonstrates both their excitatory response to stimulation and their post-stimulatory suppression period. Besides demonstrating a proof of concept for the effect of photic stimulation across the brain, this study also shows that there is no positive relationship between stimulation length and effect size of photic stimulation (both during and post-stimulation). Further, it demonstrates that entrainment sets in after stimulation-onset after a maximum of 2.4 seconds. We have also shown that post-stimulatory signs of entrainment drop sharply in accordance with the alpha amplitude as stimulation ceases and that these reductions in alpha power are significant with small to medium effect sizes across the brain for 60 and 120 seconds of stimulation, with the largest effect sizes found in the occipital region. This alpha power suppression lasts for the entirety of the post-stimulation 25-second resting state measurement. Moreover, within the suppression period, we also show significant connectivity (PLV) across the scalp (relative to a pre-stimulation time window) - specifically in and between occipital and medial regions. Future research could focus on the length of alpha power suppression effects and its relationship to stimulation intensity (luminance). Further studies should also establish whether post-alpha-stimulation alpha power suppression also occurs in patients who suffer from neuropathologies associated with lowered alpha power, as the post-stimulation suppression we found might be specific to participants with alpha power levels in the normal range. If the same stimulation technique were applied to people with deficient alpha power levels, there might be no such post-stimulation downward-correction, but the alpha power enhancements during stimulation might carry over to post-stimulation intervals.

Chapter 4

Stimulation duration and post-stimulation alpha power suppression

4.1 Abstract

As we show in Chapter 3, photic stimulation at 10 Hz results in a significant post-stimulatory alpha power suppression across the scalp, for 30-, 60- and 120 seconds of stimulation. This follow-up study aims to replicate the finding of alpha power suppression post-stimulation this time using a custom LED-array instead of the light stimulation machine used in Chapter 3, as the LED-array allows us to directly control individual flashes rather than relying on pre-set flashing sequences. This study also aims to investigate the relationship between post-stimulation effects and stimulation lengths more deeply by contrasting a greater number of stimulation duration conditions. Specifically, we chose to test for during- and post-stimulation effects of photic stimulation at 10-, 20-, 30- and 60 seconds. When stimulating at 30 and 60 seconds, the setup mirrored the experimental conditions of Chapter 3, with the only difference being a reduced luminance of the photic driving signal from 6880 lux to 1810 lux. While the reduced luminance during stimulation still produced significant alpha power enhancement during stimulation and significant post-stimulation alpha power suppression, the post-stimulation suppression was not as pronounced or long-lived as found in Chapter 3. These findings suggest that the luminance of photic stimulation is an important consideration when attempting to use it as a tool to modulate brain activity. While we did not replicate our earlier finding of a relationship between length of stimulation and increases in alpha power during stimulation, we did find a statistically significant positive correlation between length of stimulation and post-stimulation effects, as longer stimulation lead to greater alpha power suppression relative to pre-stimulation baseline measures.

4.2 Introduction

In Chapter 3, we demonstrated that photic stimulation shows promise as a technique for modulating of alpha (8-12 Hz) activity. Using pulsing light flashes, it brings about steady-state visually evoked potentials (SSVEPs), which produce a train of visual evoked potential waves. We showed that this results in entrainment of occipital, medial, and frontal regions to the driving frequency, leading to an enhancement in alpha power during stimulation especially over occipital areas for 60 and 120 second of stimulation. Additionally, we found a post-stimulation alpha power suppression, which lasted the entirety of the 25-second post-stimulation interval.

In this study, we seek to investigate if there is a positive correlation between stimulation length and post-stimulation effects. For this purpose, we record over longer post-stimulation windows, as in Chapter 3 length of the post-stimulation window was not sufficient to observe the offset of suppression. Another reason to conduct this study was to test our new photic stimulation equipment which, in contrast to the stroboscopic light machine used in Chapter 3, allows for direct control of individual flashes (via Matlab). This will allow us to pursue our overall goal of developing a more complete control of alpha power by making light stimulation dependent on a real-time EEG signal in future Chapters. Hence, replicating- and expanding on our findings from Chapter 3 using a custom LED array is a necessary preamble for our later work in Chapter 7 and Chapter 8, which aim for phase-specific photic stimulation.

4.3 Method

Using a trial structure composed of pre- and post-stimulation time windows of equal length, and photic stimulation of varying duration, we tested photic stimulation protocols in four randomised conditions of 10-, 20-, 30-, and 60 seconds of stroboscopic 10 Hz photic stimulation at 1810 lux using a custom LED array with 100 fitted fan-cooled high-luminance LEDs. Post-stimulation resting states were recorded over 20-, 40-, 60, and 120 seconds respectively; pre-stimulation times were 20-, 40-, and 60, seconds, with the duration of pre-stimulation intervals being equal to the post-stimulation intervals, with the exception of the post-stimulation duration of 120 seconds following 60 seconds of photic stimulation being preceded by a shorter pre-stimulation interval of 60 seconds. For more detail on the conditions, refer to table 4.3.1 and table 4.1.

4.3.1 Procedure

Participants were seated in a dark and noise-proof electromagnetically shielded room opposite of a high-luminance fan-cooled custom LED array at a distance of 50 cm. It contained 100 LEDs arranged in 10 rows by 10 columns (see Figure 4.1). It was connected to a PC with a LabJack U3-HV with an added LJTick-DAC booster (Lab-Jack, USA) to control flashes with a custom Matlab script. Flashing at 10 Hz, the LED array had a luminance of 1810 lux at the participants eyes. All visual stimulation of participants occurred with their eyes closed.

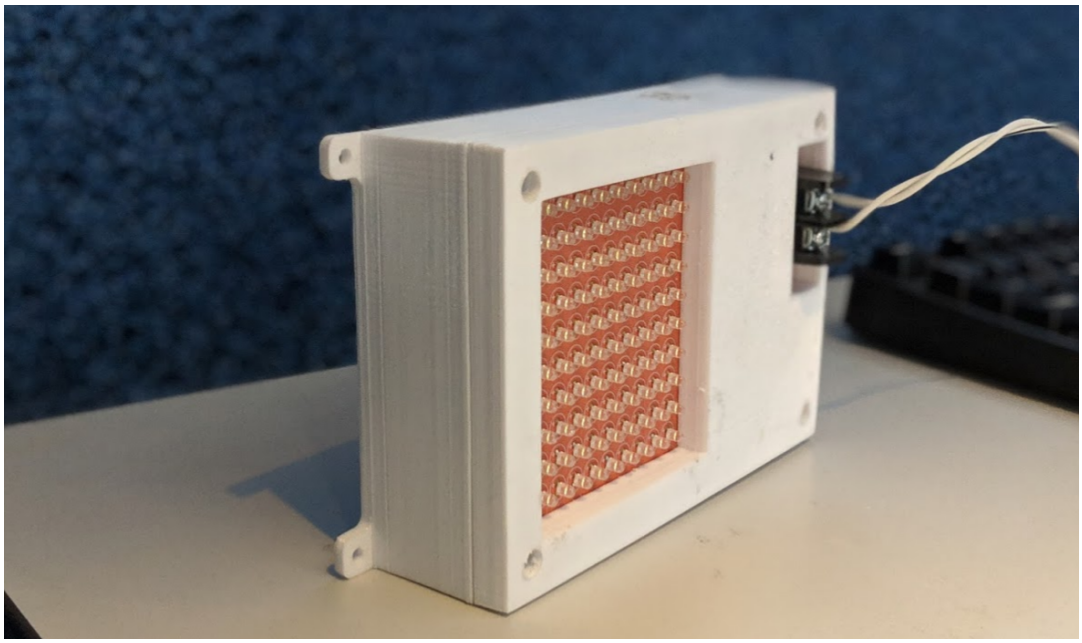

FIGURE 4.1: Custom LED array
Our custom LED array used for photic stimulation in this chapter, which allowed for precise manual control of individual flashes in real-time over Matlab.

4.3.2 Conditions

Condition	Pre-stimulation	Stimulation	Post-stimulation
1	20 s	10 s	20 s
2	40 s	20 s	40 s
3	60 s	30 s	60 s
4	60 s	60 s	60 s

TABLE 4.1: Each condition featured five trials, which were presented in a random order.

Experimental conditions as detailed in table 4.1 featured five trials, making for a total of 200 trials across all 10 participants. Trials were presented in a random order. In line with the findings of Chapter 3, 10 Hz was used as the photic stimulation frequency.

4.3.3 Participants

10 postgraduate students (2 males, 8 females) were recruited for this study. Informed consent was obtained from them after the nature and potential consequences of the study had been explained.

To screen participants for epileptic risk, a questionnaire based on Placenia et al. (1992) was used, while the State-Trait Anxiety Index, Trait Version (Spielberger, Gorsuch, and Lushene, 1970) screened for anxiety. More details on this procedure can be found in section 3.3.3.

The protocol for this study has been approved by the Life Sciences & Psychology Cluster-based Research Ethics Committee of the University of Sussex (CREC).

4.3.4 Data

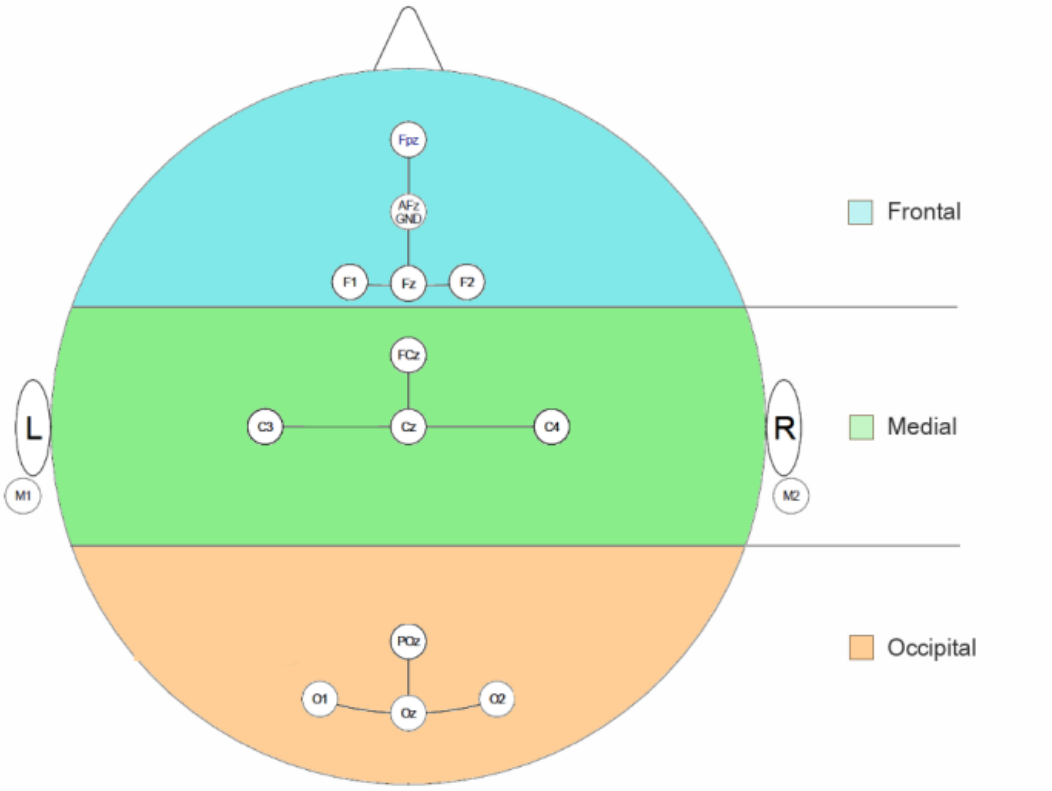

FIGURE 4.2: Sensor regions used.
For all future analysis, when frontal (top/blue), medial (middle/green), or occipital (bottom/orange) regions are referenced, averaged measures of electrodes within the coloured sections are used. There are 4 sensors over occipital-, 4 over medial-, and 5 over frontal regions (including the ground electrode). In addition, one electrode is placed at each mastoid (M1 and M2).

Data was collected using 12 channels (see Figure 4.2 for sensors used) on a 64 channel ANT Neuro amplifier, sampled at 2048 Hz. The channels were chosen as the areas covered by them showed the most pronounced changes in Chapter 3. Further, reducing the number of channels used allowed us to run a greater number of trials per participant, as it decreased set-up time, leaving more for data collection. Electrical activity of the brain was recorded using ANT waveguard 64-channel caps, using standard Ag/AgCl electrodes placed according to the 10-20 system, using an average reference.

Eye movements were monitored with additional electrodes positioned vertically and horizontally to the sides of the participants' eyes and a photodiode placed on one LED on the top right corner of the LED array provided information on precise timing of each delivered visual flash.

4.3.4.1 Recording

Details on recording procedures can be found in section 3.3.4.1.

4.3.4.2 Preprocessing

Data (pre-)processing was performed according to the same protocol used in section 3.3.4.2.

4.3.4.3 Analysis

Analysis techniques used were identical to those in section 3.3.4.3.

To contrast pre- and post-stimulation alpha power, the last 10 seconds before stimulation onset were compared against the first 10 seconds immediately following stimulation offset. In line with this time window size, to investigate differences in alpha power during stimulation relative to pre-stimulation alpha power baselines, we extracted the last 10 seconds of the photic stimulation interval, and compared it to the last 10 seconds of the pre-stimulation interval directly preceding stimulation onset. The time window size of 10 seconds was chosen as to make pre-, during- and post-stimulation intervals comparable, and 10 seconds as the shortest duration of photic stimulation applied. The last 10 seconds of the photic stimulation interval were chosen to represent the during-stimulation results in each condition, our thinking was that if there was a relationship between stimulation duration and stimulation outcomes, this would be most pronounced at the end of the stimulation interval.

4.4 Results

To investigate the effects 10 Hz photic stimulation on alpha power, we compared the last 10 seconds of photic stimulation in all conditions against the last 10 seconds of their respective pre-stimulation intervals directly preceding photic stimulation. Photic driving at 1810 lux at 10 Hz resulted in significant during-stimulation alpha power enhancement (mean values of 8-12 Hz μV^2), compared to pre-stimulation intervals for frontal- (20s: $p < 0.001$, $r \approx 0.3764$, $W = 3989$, $Z \approx 3.8570$; 60s: $p < 0.01$, $r \approx 0.2940$, $W = 3659$, $Z \approx 3.0126$), medial- (20s: $p < 0.0001$, $r \approx 0.3764$, $W = 3753$, $Z \approx 3.1025$), and occipital areas (10s: $p < 0.001$, $r \approx 0.2991$, $W = 4197$, $Z \approx 3.6264$; 20s: $p < 0.0001$, $r \approx 0.4809$, $W = 4324$, $Z \approx 4.9279$; 60s: $p < 0.01$, $r \approx 0.2741$, $W = 3596$, $Z \approx 2.8083$). Refer to table 4.2 for more detail on significance testing and table 4.3 for respective effect sizes.

Length of stim	Frontal	Medial	Occipital
10 s	0.0649	0.4746	0.0003
20 s	0.0001	0.0019	>0.0001
30 s	0.6776	0.3765	0.4878
60 s	0.0026	0.1332	0.0050

TABLE 4.2: Impact of photic stimulation across the scalp
Photic stimulation at 10 Hz achieved significant increases in alpha power for 20- and 60 seconds of stimulation over frontal and occipital areas, and at 10 seconds over the occipital region. To assess if there was a significant difference between mean alpha power (8-12 Hz μV^2) from pre-stimulation- to stimulation conditions, a two-tailed Wilcoxon signed-rank test was used. For details on the epoching of pre- and during stimulation data, refer to section 4.3.4.3. The data was then averaged over channels, frequencies (within the alpha range), and time points (of equal length) for the sake of significance testing. Length of stimulation for each condition is given in the leftmost column. Significance of the impact of photic stimulation is given for occipital, medial, and frontal regions.

Length of stim	Frontal	Medial	Occipital
10 s	0.1522	0.0590	0.2991
20 s	0.3764	0.3028	0.4809
30 s	0.0343	0.0729	0.0572
60 s	0.2940	0.1465	0.2741

TABLE 4.3: Effect sizes for photic stimulation across the scalp.
The largest effect sizes for alpha power enhancement accompanying photic stimulation were found over the occipital region, specifically following 20 seconds of stimulation. Effect sizes were calculated by taking $Z\sqrt{N}$, with the z statistic being calculated by a two-tailed Wilcoxon signed-rank test. The length of stimulation applied during each condition is given in the leftmost column. Effect sizes are given for occipital, medial, and frontal regions for 10-, 20-, 30-, and 60 seconds of photic stimulation.

Photic stimulation significantly enhanced alpha power across occipital, medial, and frontal areas, with most significant alpha power enhancements over the occipital region at $p < 0.001$, as can be seen in Figure 4.3.

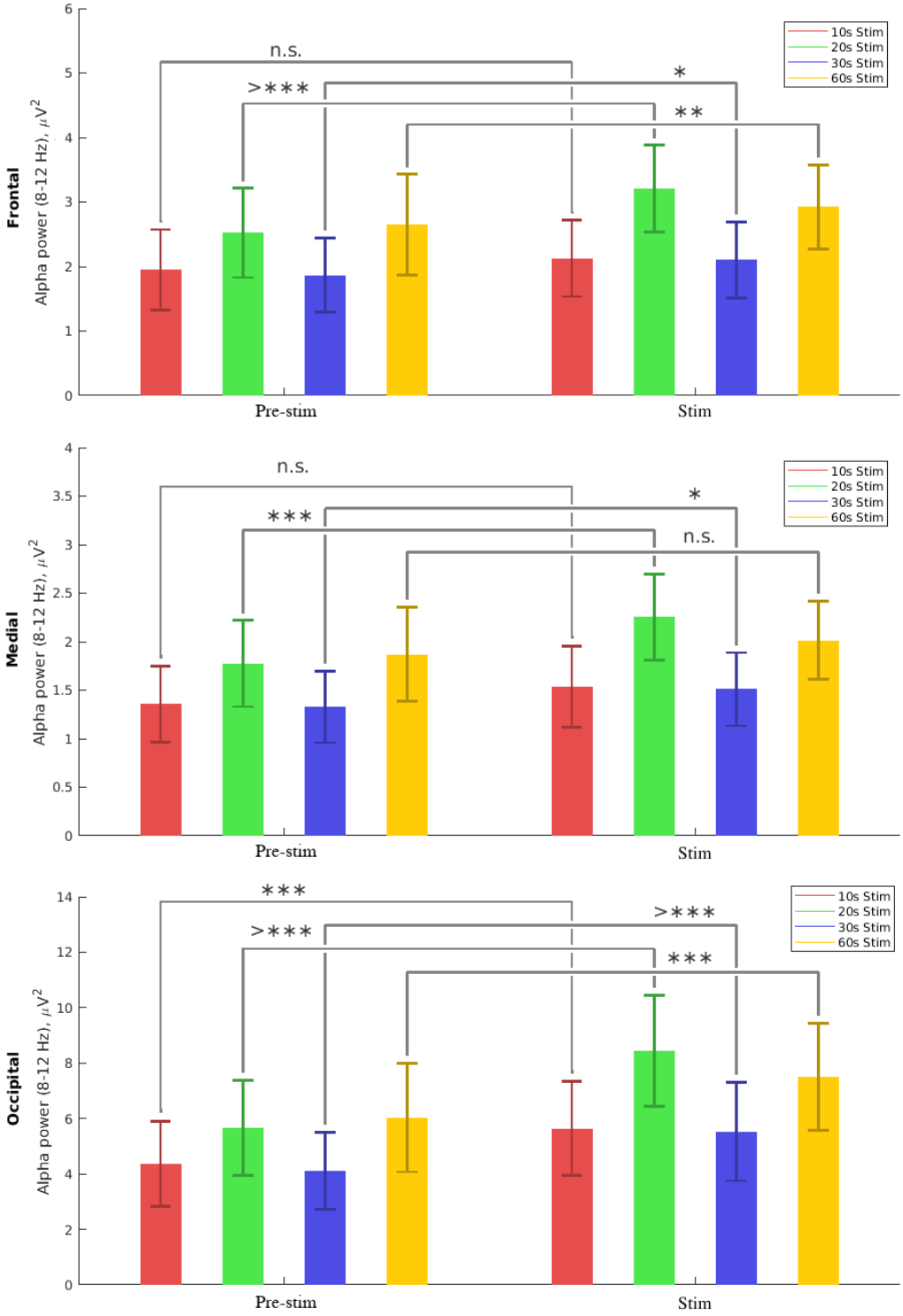

FIGURE 4.3: Changes in alpha power during photic stimulation Averaged across channels, frequencies and time points, we found increases in mean alpha (8-12 Hz) power (μV^2) during photic stimulation relative to pre-stimulation alpha power across the scalp; with strongest effects over the occipital region (refer to table 4.3). To test for alpha power differences between pre- and during-stimulation intervals, we used a two-tailed Wilcoxon signed-rank test. * denotes $p < 0.05$, ** for $p < 0.01$, *** for $p < 0.001$, and *n.s* for non-significant results. Red shows the effects of 10-, green of 20-, blue of 30-, and yellow the impact of 60 seconds of photic stimulation for frontal, medial, and occipital areas, comparing the last 10 seconds of photic stimulation with the last 10 seconds of their respective pre-stimulation intervals. Error-bars show the Vysochanskij–Petunin standard error of mean alpha power (μV^2), using 95% confidence intervals.

Next, to investigate post-stimulation alpha power suppression we compared the last 10 seconds of photic stimulation against the first 10 seconds of their respective post-stimulation intervals.

In line with our findings from Chapter 3 photic driving at 10 Hz resulted in significant post-stimulation alpha power suppression across the scalp. Specifically, post-stimulation alpha power suppression was significant across frontal, medial and occipital areas at $p < 0.0001$ (see table 4.4 and Figure 4.4), with medium to strong effect sizes at frontal- (10s:$r \approx -0.2966$, $W = 1808$, $Z \approx -3.5962$; 20s: $r \approx -0.3833$, $W = 1554$, $Z \approx -3.9273$; 30s: $r \approx -0.3387$, $W = 1639$, $Z \approx -4.1071$; 60s: $r \approx -0.5753$, $W = 912$, $Z \approx -5.8954$), medial- (10s:$r \approx -0.3442$, $W = 1617$, $Z \approx -4.1736$; 20s: $r \approx -0.4375$, $W = 1380$, $Z \approx -4.4835$; 30s: $r \approx -0.4021$, $W = 1385$, $Z \approx -4.8750$; 60s: $r \approx -0.5867$, $W = 876$, $Z \approx -6.0122$), and occipital areas (10s: $r \approx -0.3397$, $W = 1635$, $Z \approx -4.1192$; 20s: $r \approx -0.4731$, $W = 1266$, $Z \approx -4.8480$; 30s: $r \approx -0.4295$, $W = 1275$, $Z \approx -5.2075$; 60s: $r \approx -0.6358$, $W = 721$, $Z \approx -6.5148$). Hence, as measured by the effect sizes also listed in table 4.5, the strongest post-stimulation alpha power suppression is found over occipital areas after 60 seconds of 10 Hz photic stimulation ($r \approx -0.6358$, $W = 721$, $Z \approx -6.5148$).

Length of stim	Frontal	Medial	Occipital
10 s	< 0.0001	< 0.0001	< 0.0001
20 s	< 0.0001	< 0.0001	< 0.0001
30 s	< 0.0001	< 0.0001	< 0.0001
60 s	< 0.0001	< 0.0001	< 0.0001

TABLE 4.4: Statistical significance of post-stimulation alpha power suppression.
Post-stimulation alpha power suppression, calculated by comparing mean alpha power (8-12 Hz μV^2) between pre- and post-stimulation intervals, was found to be strongly significant across the scalp ($p < 0.0001$). A two-tailed Wilcoxon signed-rank test was used to compare the first 10 seconds of post-stimulation intervals immediately following stimulation offset with the last 10 seconds of their respective pre-stimulation intervals that directly precede photic stimulation. For significance testing, the data was then averaged over channels, frequencies (within the alpha range), and time points (of equal length). Length of stimulation for each condition is given in the leftmost column. Significance of the impact of photic stimulation is given for occipital, medial, and frontal regions.

Length of stim	Frontal	Medial	Occipital
10 s	-0.2966	-0.3442	-0.3397
20 s	-0.3833	-0.4375	-0.4731
30 s	-0.3387	-0.4021	-0.4295
60 s	-0.5753	-0.5867	-0.6358

TABLE 4.5: Effect sizes for post-stimulation alpha power suppression.
The largest effect size for post-stimulation alpha power suppression can be found over the occipital region for 60 seconds of stimulation. Effect sizes were calculated by taking $Z\sqrt{N}$, with the z statistic being calculated by a two-tailed Wilcoxon signed-rank test. The length of stimulation applied during each condition is given in the leftmost column. Effect sizes are given for occipital, medial, and frontal regions for 10-, 20-, 30-, and 60 seconds of photic stimulation.

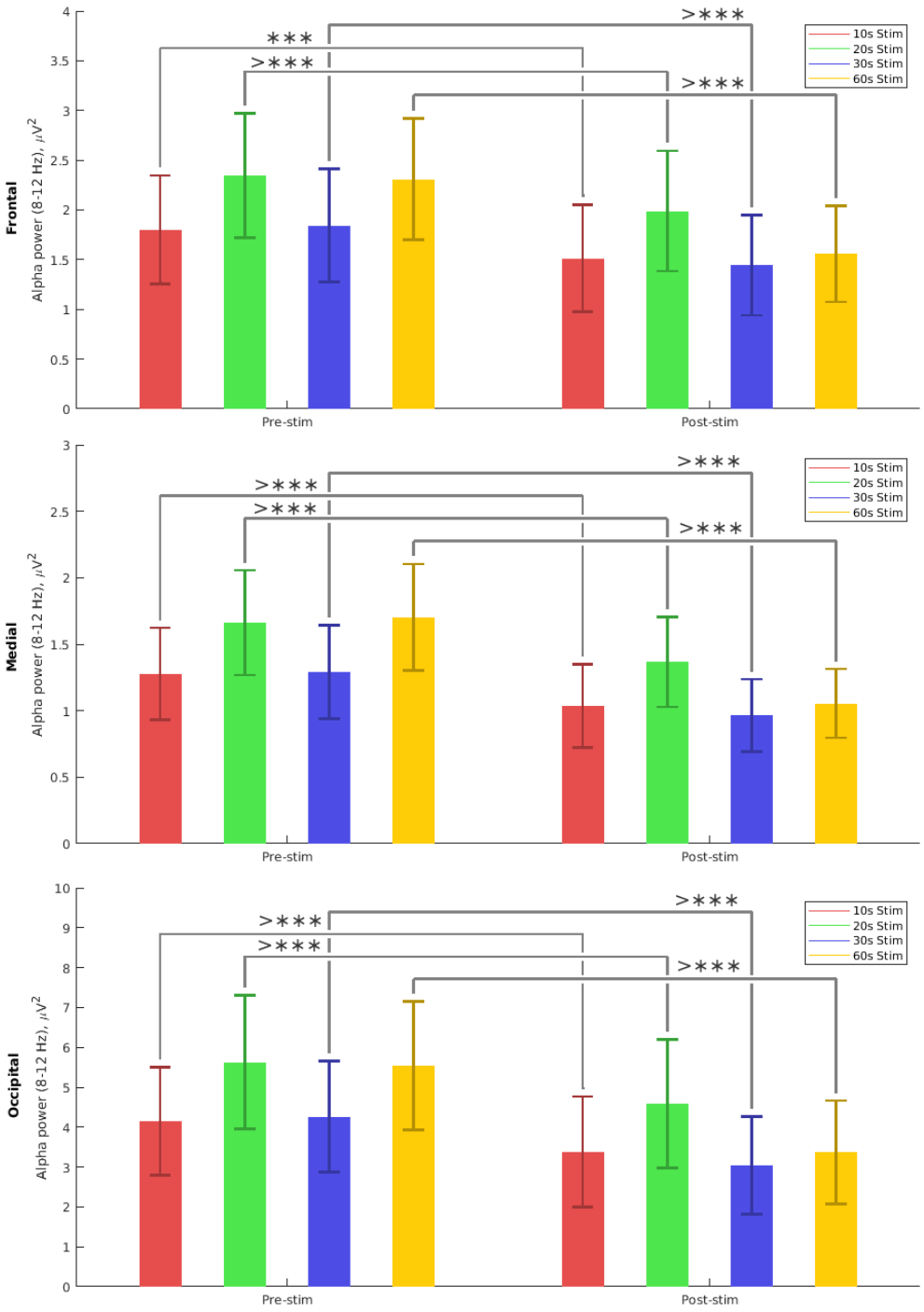

FIGURE 4.4: Comparisons of alpha power between pre- and post-stimulation intervals

Decreases in mean alpha (8-12 Hz) power (μV^2) averaged across channels, frequencies and time points in post-stimulation intervals relative to pre-stimulation alpha power were highly significant ($p < 0.0001$) across the scalp. To assess whether there were significant differences between pre- and post-stimulation intervals, we used a two-tailed Wilcoxon signed-rank test. * denotes p < 0.05, ** for p < 0.01, *** for p < 0.001, and *n.s* for non-significant results. Red shows the effects of 10-, green of 20-, blue of 30-, and yellow the impact of 60 seconds of photic stimulation for frontal, medial, and occipital areas, comparing the first 10 seconds of post-stimulation intervals with the last 10 seconds of their respective pre-stimulation intervals. Error-bars show the Vysochanskij–Petunin standard error of mean alpha power (μV^2) measures, using 95% confidence intervals.

In Chapter 3, we used stroboscopic light stimulation, which was significantly brighter (by 5770 lux) than the LED array used in this study. Because of this, we sought to compare the duration of alpha power suppression after 60 seconds of photic stimulation using 6880 lux (data taken from Chapter 3) to the alpha power suppression duration following the same stimulation duration at 1810 lux in this study. With this, we asked the question whether the lowered stimulation strength would affect alpha power suppression. We found that the reduced luminance used in this study led to a decrease in both the length and intensity of suppression, as can be seen in Figure 4.5. For a more in-depth comparison, contrast tables 3.6 listing effect sizes for alpha power suppression following stimulation at 6880 lux, and table 4.5 for effect sizes of stimulation at 1810 lux.

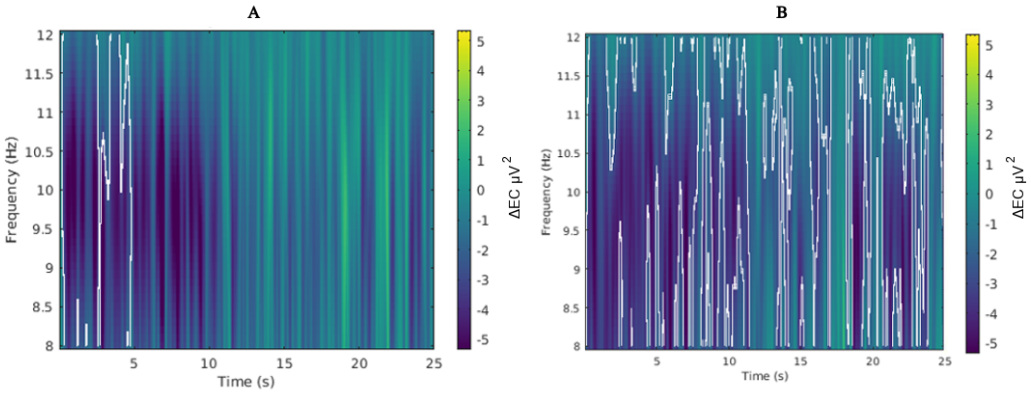

FIGURE 4.5: Alpha power suppression following low and high luminance photic stimulation.
Alpha power suppression after 60 seconds of 1810 lux 10 Hz stimulation is short-lived with reduced luminance. *A* shows a difference map between pre- and post-stimulation intervals in microvolts for 60 seconds of photic stimulation at 1810 lux, thresholded by a z-map as shown by white boundaries highlighting areas of significant alpha power suppression following photic stimulation. *B* shows the effects of equal length of photic stimulation at 6880 lux from Chapter 3. The thresholded difference map show the significance and direction of changes in alpha power after stimulation offset, with areas of significant decreases in alpha power being marked by white boundaries. Significance values are corrected for multiple comparisons using cluster size correction. Data is averaged across occipital electrodes, trials, and participants.

Lastly, to address whether there is a relationship between stimulation length when comparing pre-stimulation- and stimulation intervals, or pre-stimulation and post-stimulation epochs, we ran a linear regression analysis comparing these time intervals. The results reveal a positive correlation between post-stimulation alpha power suppression and length of stimulation, which is significant at a Bonferroni-corrected $p < 0.01$, see Figure 4.6. However, we were unable to replicate the finding of Chapter 3, where we showed a significant relationship between effect sizes of alpha-enhancement during stimulation and stimulation length.

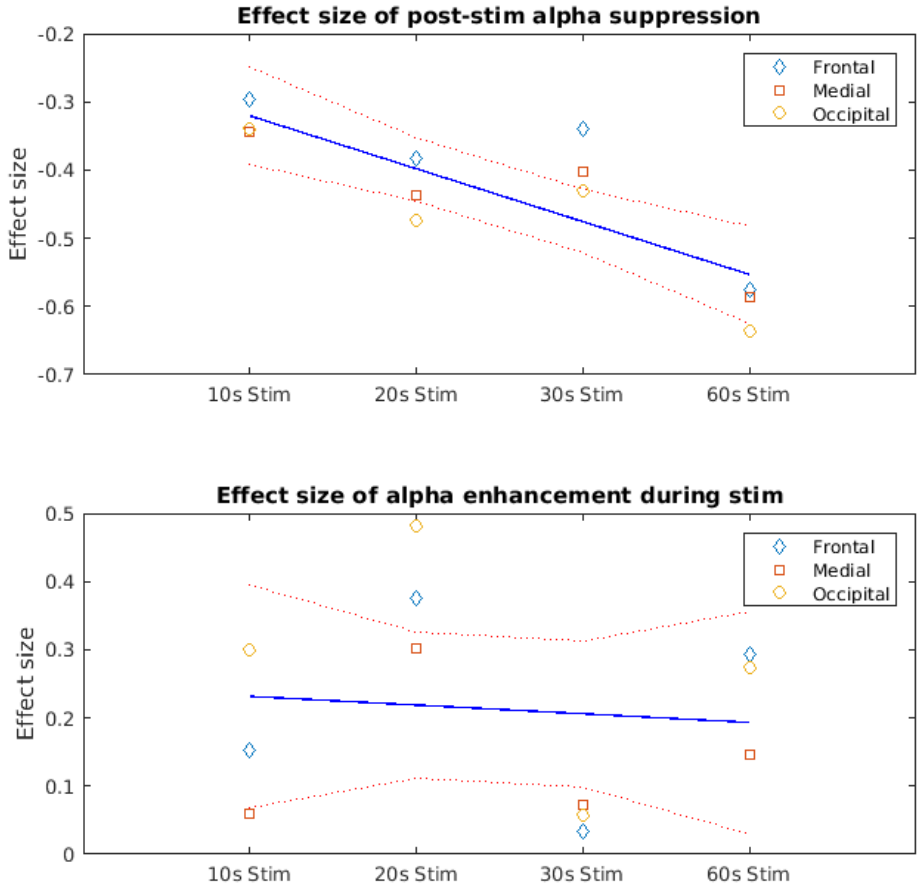

FIGURE 4.6: Linear regression analysis of post-stimulation alpha power suppression and photic stimulation alpha power enhancement for differing lengths of photic stimulation.
The top figure shows that the increase in effect sizes for post-stimulation alpha power suppression as stimulation lengthens is statistically significant at $p < 0.01$, after Bonferroni correction for multiple comparisons. However, as shown in the bottom figure, we did not find a significant relationship between length of stimulation and during-stimulation alpha power enhancement. For both tests, corrected alpha was set at 0.0125. When individual electrode areas were considered in isolation, there was no significant correlation between stimulation duration and either during-stimulation alpha power enhancement or post-stimulation alpha power suppression. Effect sizes are derived from the z statistic calculated with the Wilcoxon signed-rank test, via $Z\sqrt{N}$. The orange dotted lines show polynomial confidence intervals of 95% calculated using the Matlab polyconf function.

4.5 Discussion

We have tested four different lengths of photic stimulation at 10 Hz, assessing the differences in mean alpha power during stimulation relative to pre-stimulation baseline levels, as well as between pre- and post-stimulation time-windows. Setting out

to investigate whether there is a relationship between stimulation length and stimulation effects, we can now answer the question in cautious affirmation: Our results imply that there might be a positive relationship between stimulation length and post-stimulation alpha power suppression effect sizes. As the LED array used in this chapter had reduced luminance compared to the Lucia N°03 Hypnagogic stroboscope we used in Chapter 3, we also found that, under otherwise equal conditions using an equivalent duration of photic stimulation, there is a reduction in both effect sizes and duration, which might imply that there is a relationship between stimulation strength (luminance) and the degree to which photic stimulation can affect the alpha rhythm. Put differently, the findings from this and our previous investigation indicate that as luminance is increased, so is the during-stimulation alpha power enhancement and consequent post-stimulation alpha power suppression. This is in line with previous research, which found a relationship between luminance and SSVEP response for alpha stimulation, with brighter stimulation bringing about a more pronounced response (Mouli and Palaniappan, 2016). Interestingly, as in Chapter 3, the strength of during-stimulation alpha power enhancement was not predictive of post-stimulation alpha power suppression. As in Chapter 3, even when alpha power enhancement during stimulation was not significant, post-stimulation alpha power suppression effects might still be, as it was the case for frontal and medial photic stimulation of 10 seconds. Similarly, and in contrast to our previous finding in Chapter 3, we did not find a significant positive relationship between length of stimulation and during-stimulation alpha power enhancement. While this failure to replicate our earlier finding might be due to the reduction in stimulation strength (luminance), it still points to the complexity of the relationship between during-stimulation and post-stimulation effects, which are not as straightforward as they might initially seem. Perhaps contrary to intuition, the strongest alpha power enhancements during stimulation do not necessarily lead to equally strong post-stimulation alpha power suppression effects, as sometimes even non-significant during-stimulation changes can yield significant post-stimulation alpha power suppression results. One explanation for this might be the idea put forward in section 3.6, that when stimulation is applied, homeostatic mechanisms of the targeted oscillator might try to counteract the exogenous forcing via rhythmic stimulation, obscuring effective during-stimulation enhancement. Once the stimulation is removed, however, the balancing of alpha power, in the form of alpha power suppression, becomes visible. If true, then this would explain as to why in some conditions no significant change in alpha power is visible during stimulation, while still showing strongly significant alpha power suppression post-stimulation.

4.6 Conclusion

In combination with the results from our previous investigation, our findings imply that both length and stimulation strength (luminance) might matter for post-photic stimulation effects. While length of stimulation and effect sizes of post-stimulation alpha power suppression correlate positively, even in the longest stimulation condition of 60 seconds, decreasing luminance from 6880 lux to 1810 lux has also decreased duration and effect sizes of post-stimulation alpha power suppression as to not be equal to effects of identical stimulation lengths at higher luminance detailed in Chapter 3.

As this thesis' main focus is on finding a complete control of alpha power by means of closed-loop photic stimulation, we leave it to future research to probe the

direct relationship of luminance and effect size of photic stimulation in a more systematic manner, keeping all variables constant while varying luminance incrementally. However, as the more general finding of post-stimulation alpha power suppression is one of the core findings of this thesis, we do have a great interest in the potential cognitive effects of photic stimulation. With this in mind, the following Chapter investigates if post-stimulation alpha power suppression has an effect on cognition.

Chapter 5

Conscious attention and alpha power suppression

5.1 Abstract

Previous research has shown that pre-trial alpha power negatively correlates with reaction time (RT) speed, with lower pre-RT-trial alpha power being predictive of slower RT by participants (Nenert et al., 2012; Callaway and Yeager, 1960; Bompas et al., 2015; Haig and Gordon, 1998; Bastiaansen et al., 2001). As we have shown in Chapter 3 and Chapter 4, we are able to suppress post-stimulation alpha power levels using 10 Hz stimulation. Building on this finding, we sought to test participants' reaction time speeds immediately following photic stimulation in the alpha (10 Hz) and delta (3 Hz) frequency range. We presented RT trials both immediately before and after photic stimulation, assuming that post-stimulation alpha power suppression would lead to slower reaction times when compared to pre-stimulation baseline RT speeds. To ensure that increases in reaction times were frequency-specific (a result of alpha power suppression brought about by previous alpha power enhancement using 10 Hz photic stimulation), we employed a 3 Hz photic stimulation control condition, which we assumed would not lead to alpha power suppression. Our results show that surprisingly both conditions resulted in significant pre-RT-trial alpha power suppression at very small effect sizes, but we found no significant slowing of reaction times compared to a baseline condition, which did not involve any photic stimulation. These effects, which were observed across occipital, medial, and frontal areas of the scalp, show the complexity involved in studying photic stimulation, as any effects on the brain will be nonlinear, affecting frequency components beyond the driving signal (Pikovsky, Rosenblum, and Kurths, 2001).

As the effect sizes of post-stimulation alpha power suppression were only a fraction of those we found in Chapter 3 and 4, we wanted to test whether conscious engagement in the RT task was negating alpha power suppression. Therefore, in a follow-up experiment, we added two more conditions, in which we asked participants to ignore the reaction time task at hand after receiving photic stimulation at 10 Hz and 3 Hz. Here, we found that when participants did not engage in the RT task, we observed a significant reduction of alpha levels with medium effect sizes (comparable to prior findings in Chapter 3 and 4). The results show that whenever participants were asked to respond to the reaction time task, alpha levels immediately returned to their pre-stimulation baseline levels, but that when they ignored the task, alpha power suppression was visible across the scalp. These findings suggest that task- or other endogenous demands override exogenously induced alpha power suppression.

5.2 Introduction

Since it was first observed by Berger in 1929 (Berger, 1929), the alpha rhythm (8-12 Hz) has been one of the prominent features of electroencephalogram (EEG) brain activity (Williams, 2001). First thought to be an idling mechanism of the brain, as alpha power was found to, for example, increase as a consequence of closing one's eyes or increase by performing mental arithmetic (Adrian and Matthews, 1934; Berger, 1929), a more recent perspective has emerged that frames alpha as reflecting an attentional-inhibitory system regulating cortical excitation (Klimesch, 2018; Pfurtscheller and Silva, 2017; Mathewson et al., 2012). In favour of this framework, when attending to a particular task or stimulus, alpha power is increased in task-irrelevant- and decreased in task-relevant brain areas (Thut et al., 2006; Suffczynski et al., 2001). In consequence, alpha oscillations have been argued to reflect active inhibition of task-irrelevant stimuli, as to aid the processing of task-relevant stimuli (Suffcynski et al., 1999). Previous research has investigated the relationship between alpha power and behavioural performance during a reaction time task, and found that participants with higher pre-stimulus alpha power display faster reaction times, (Nenert et al., 2012; Callaway and Yeager, 1960; Bompas et al., 2015; Haig and Gordon, 1998; Bastiaansen et al., 2001). We speculate that this might be due to greater alpha power reflecting a greater enhanced potential to ignore task-irrelevant details, which might enhance the degree to which cognitive resources can be allocated to items in the attentional spotlight, making for faster responses.

The results of Chapter 3 and Chapter 4 show that it is possible to decrease alpha power through 10 Hz photic stimulation following stimulation offset. In this Chapter, we investigate whether this post-stimulation decrease in alpha power can negatively affect reaction time speeds. To do this, we presented a sequence of reaction time trials immediately following photic stimulation. Since we found that post-stimulation suppression of alpha power was most pronounced over the occipital region (see Chapter 3), we chose a visual reaction-task paradigm, in which participants had to, with their eyes closed, press a button once they were presented with a single light flash. As a control condition, we employed 3 Hz photic stimulation, as we assumed that it would not significantly modulate alpha power either during or post-stimulation, since 3 Hz is not a harmonic of 10 Hz. Rather than comparing reaction times after photic stimulation to reaction times in absence of stimulation, we chose to compare the difference between pre- and post-stimulation reaction times for a 10 Hz experimental conditions to the difference of reaction times pre- and post-3 Hz-photic stimulation, to control for the effects flashing lights might have on reaction times independent of their effect on the alpha frequency band.

5.3 Method

A visual reaction time task was used (see section 5.3.2 for a description of individual conditions), in which participants were asked to press the space-bar whenever they noticed a light flash of 100 ms. Trials were spaced out randomly between 1-2s, using intervals of 100 ms and a minimum spacing of 1s, in order to ensure that there would be no entrainment or formed expectancies impacting performance.

5.3.1 Procedure

For the presentation of the reaction time task, a custom array of 100 high-luminance LEDs was used, which we had used previously in Chapter 4. The LED array was

used for the RT trials, with participants having to respond to light flashes by pressing the spacebar of a keyboard placed in front of them. It was placed at a distance of 50 cm and produced a luminance of 1810 lux.

Aligned with the participant's eye level, directly above the LED array at a distance of 50 cm away from the participants, we positioned the Lucia N°03 Hypnagogic stroboscope, which we used for photic stimulation at 3 Hz and 10 Hz at 6880 lux for a duration of 60 seconds. This part of the setup mirrored the procedure from section 3.3.2.

5.3.2 Conditions

Three conditions were used in our original investigation. First, a baseline condition, which established RT values in absence of photic stimulation. Participants were told to close their eyes, rest for 60 seconds, and then respond to 40 light flashes of the LED array by pressing the space bar of a keyboard in front of them as quickly as they could manage.

Second, an experimental 10 Hz photic stimulation condition, which was designed to modulate alpha power post-stimulation in accordance with findings detailed in Chapter 3. Here, participants were also asked to close their eyes, but before the 40 RT trials ensued, 60 seconds of photic stimulation of 10 Hz were delivered using the Lucia N°03 Hypnagogic stroboscope.

Lastly, to ensure that changes in RT speeds following photic stimulation were a consequence of frequency-specific effects of 10 Hz, and not a general feature of photic stimulation, we included a control 3 Hz photic stimulation control condition, which otherwise functioned exactly like the experimental condition.

Each condition was presented in a random order and repeated 7 times. Conditions included 40 reaction time trials each, making for a total of 280 trials per condition (see table 5.1).

Conditions	**Stimulation length**	**RT trials**
Baseline	-	40
10 Hz stim	60 s	40
3 Hz stim	60 s	40

TABLE 5.1: Alpha power suppression and reaction times: Experimental and control conditions for initial investigation
Conditions were repeated seven times in a random order.

The 40 RT trials following photic stimulation in both the experimental- and control condition were performed by all participants in no more than 80 seconds.

Conditions	Stimulation length	RT trials
Pre-stim RRT (10 Hz)	-	40
Post-stim RRT (10 Hz)	60 s	40
Pre-stim RRT (3 Hz)	-	40
RRT (3 Hz)	60 s	40
FRT (10 Hz)	60 s	-
FRT (3 Hz)	60 s	-

TABLE 5.2: Alpha power suppression during faux RT tasks: Experimental and control conditions for follow-up investigation. Real reaction time tasks are abbreviated as RRT, faux reaction time tasks as FRT. Presentation of conditions was randomised, and each condition was repeated seven times.

In a follow-up investigation, in order to investigate whether conscious attention to the RT task would affect post-photic-stimulation effects on alpha power, we added two additional conditions, which included faux reaction time tests, which used the same visual reaction time tasks as in previous conditions, but asked participants to ignore all light flashes. These faux reaction time (FRT) trials were employed after 10 Hz photic stimulation conditions in order to ascertain whether conscious directing of attention would impact alpha power levels (see table 5.2). In addition, to ensure that baseline alpha power values and baseline reaction times to real reaction time (RTT) trials were minimally influenced by drifts of alpha over time, we replaced the baseline condition listed in table 5.1 with RRT trials that directly precede the photic stimulation. The pre-stimulation RRT trials then served as the baseline for analysis of post-stimulation RRT trials, as well as for FRT trials. This design also more closely mirrored previous investigations of alpha power suppression in Chapter 3 and 4.

Participants were instructed to keep their eyes closed throughout the experiment, including all conditions and RT trials.

Conditions were randomised and repeated 7 times each, with 40 RT trials each. In total, this means that for each condition (10 Hz photic stimulation, 3 Hz photic stimulation, as well as the two faux RT conditions in our follow-up investigation), we recorded 280 trials per participant. In the original investigation, baseline trials numbered 280 as well, while in the follow-up investigation there were two separate baseline trial sets with 280 trials each, one immediately preceding 3 Hz photic stimulation, and one just before onset of 10 Hz photic stimulation.

5.3.3 Participants

10 participants (2 males, 8 females) were recruited. Two participants (both female) took part in our follow-up investigation. Informed consent was obtained from them after the nature and potential consequences of the study had been explained.

Before participants were allowed to take part in the study, they were screened for epileptic risk using a questionnaire based on Placenia et al. (1992), and for anxiety using the State-Trait Anxiety Index, Trait Version (Spielberger, Gorsuch, and Lushene, 1970). More details on this procedure can be found in section 3.3.3.

The protocol for this study has been approved by the Life Sciences & Psychology Cluster-based Research Ethics Committee of the University of Sussex (CREC).

5.3.4 Data

EEG data was collected as described in section 4.3.4, with individual epochs being extracted from -1 to +1 second around each RT trial. In our follow-up investigation using faux RT trials, we extracted individual epochs around post-photic-stimulation light flashes, mirroring the RT conditions from -1 to +1 seconds around each FRT trial.

Reaction tests were administered with custom Matlab scripts, which also recorded reaction time speeds. Photic stimulation was administered manually according to protocols described in section 5.3.2.

5.3.4.1 Recording

The same recording montage and equipment was used that was also employed in section 4.3.4.1.

5.3.4.2 Preprocessing

All data was preprocessed in the manner described in section 3.3.4.2.

5.3.4.3 Analysis

Time-frequency and power analysis was performed as described in section 3.3.4.3.

Reaction time data was analysed using Bayesian estimation. The approach was chosen as reaction times are measured on a metric scale but do not necessarily follow a normal distribution due to outliers. T-tests require the assumption of normality to be satisfied, whereas the method used here does not (Kruschke and Vanpaemel, 2015; Kruschke, 2013).

For the analysis of the reaction time data, custom Matlab scripts were used. Bayesian estimation gives credible values for effect sizes, (differences of) group means and standard deviations, and evaluates the normality of the data. Here, it is applied to the analysis of pre- and post-stimulation reaction time data sets within conditions, and to the comparison reaction time speed changes between conditions.

Bayesian estimation is based on Bayes' rule, which derives the posterior probability of parameter values given prior data in terms of probability of the data given posterior parameter values and prior probabilities of the parameter values. The implementation used here is based on (Kruschke, 2013). The posterior distribution is approximated using a Markov chain Monte Carlo (MCMC) algorithm, which generates a chain of values providing thousands of combinations of parameter values fitting the observed data and prior distribution. This thesis uses a chain with 12000 values (3 chains with 4000 values each), with a burn-in of 1000, meaning that the first 1000 generated values are discarded to minimise the effect initial values have on posterior inference. In order to increase reliability of the estimate, no chain thinning is used. The high-density interval (HDI) limits were computed from the MCMC chain following section 25.2.3 and 7.5.2 of Kruschke (2015).

One advantage of Bayesian estimation is that it can also assess the credibility of a null value, via a region of practical equivalence (ROPE) around the null value. This thesis sets the ROPE value in line with Cohen's d from -0.1 to 0.1.

For the two groups, which are compared, effect sizes are then calculated via

$$\frac{\mu_1 - \mu_2}{\sqrt{(\sigma_1^2 + \sigma_2^2)/2}}, \tag{5.1}$$

where μ_1 and μ_2 are the means of group 1 and group 2 respectively, and σ_1 and σ_2 are their standard deviations. Their differences describe the magnitude of the difference between the variability of reaction times between the groups. The null hypothesis of there being no significant difference between conditions is then rejected when $< 5\%$ of the null value is in the ROPE. In this thesis, this approach is used to compare RT times without preceding photic stimulation to RT times following photic stimulation within conditions, and RT speeds between conditions, contrasting RT times following 10 Hz and 3 Hz photic stimulation.

To contrast alpha power changes as a result of photic stimulation, we compared alpha power during the last 10 seconds between the experimental (10 Hz stimulation) and control condition (3 Hz stimulation). For this, we used permutation-based z-map analysis with cluster (groups of contiguous suprathreshold pixel) size correction for multiple comparisons. In addition, we also compared FFT responses of the last 10 seconds of photic stimulation between conditions, using a nonparametric permutation-based paired ANOVA for each time point, adjusting for multiple comparisons using the Benjamini & Yekutieli (2001) procedure for controlling the false discovery rate (FDR). For the z-map permutation testing, permutations were set to 1000 in line with an alpha level of 0.05, and to 5000 for contrasting the FFT responses, which is appropriate for an alpha level of 0.01 (Manly, 2007).

For a comparison of alpha power between baseline and post-stimulation intervals, we compared mean alpha power during baseline and post-photic stimulation RT trials, using epochs of -1 to +1 seconds around the each RT trial.

To compare RT speeds over time, RT measures were separated into four segments of 10 trials each in chronological order. With this, each segment covered a time window of 10 seconds, with the first segment covering the period immediately after stimulation offset. This was done in order to investigate whether there is a trend in RT speeds over time using linear regression analysis. Specifically this analysis was done to ensure that, to the extent that there is an effect of alpha power suppression on RT performance, this could be detected even if alpha power suppression were to last only temporarily after stimulation offset and hence cover not all 40 RT trials.

5.4 Results

First, to assess post-stimulation alpha power suppression, we compared the changes in alpha power during RT trials following photic stimulation in both the experimental (10 Hz) and control (3 Hz) condition relative to alpha power during RT trials that lacked the preceding photic stimulation.

Comparing the alpha power during RT-trials with the alpha power during RT-trials that followed 60 seconds of photic stimulation, revealed significant ($p < 0.001$ across the scalp for both conditions) suppression over frontal (10 Hz stim: $r \approx -0.1109$, $W = 1064311$, $Z \approx -6.2274$; 3 Hz stim: $r \approx -0.1316$, $W = 1094291$, $Z \approx -5.2481$), medial (10 Hz stim: $r \approx -0.1728$, $W = 1010474$, $Z \approx -7.9860$; 3 Hz stim: $r \approx -0.1687$, $W = 1004557$, $Z \approx -8.1792$) and occipital areas (10 Hz stim: $r \approx -0.1412$, $W = 1014010$, $Z \approx -7.8705$; 3 Hz stim: $r \approx -0.1663$, $W = 1050412$, $Z \approx -6.6814$) for post-stimulation RT trials. Refer to table 5.3 for more information on significance values.

Sensor region	**Post 10 Hz-stim**	**Post 3 Hz-stim**
Frontal	< 0.0001	< 0.0001
Medial	< 0.0001	< 0.0001
Occipital	< 0.0001	< 0.0001

TABLE 5.3: Post-stimulation alpha power suppression across the scalp.
Alpha power suppression was strongly significant across the scalp during RT trials that followed photic stimulation at both 10 Hz (middle column) and 3 Hz (rightmost column). This was tested for using a two-tailed Wilcoxon signed-rank test, comparing the mean alpha power (8-12 Hz μV^2) between RT trials (-1 to +1 seconds around individual RT trials) without preceding photic stimulation to those that followed 60 seconds of either 10 Hz or 3 Hz stimulation. P values were corrected for multiple comparisons via Bonferroni-correction ($\alpha = 0.0056$). Significance of the impact of photic stimulation is given for occipital, medial, and frontal regions (see leftmost column).

Table 5.4 shows that effect sizes for post-stimulation suppression were most pronounced over the medial region. Effect sizes were very small across conditions and electrode regions. Moreover, effect sizes and significance of alpha changes were almost identical between 3 Hz and 10 Hz stimulation conditions, with effect sizes being a fraction of earlier findings of Chapter 3 and no significant difference in post-stimulation alpha power following 3 Hz or 10 Hz photic stimulation.

Sensor region	Post 10 Hz-stim	Post 3 Hz-stim
Frontal	-0.1109	-0.1316
Medial	-0.1728	-0.1687
Occipital	-0.1412	-0.1663

TABLE 5.4: Effect sizes for post-stimulation alpha power suppression across the scalp during RT trials.
Effect sizes are strongest over medial electrodes, with strongest alpha power suppression following 10 Hz stimulation (middle column). Effect sizes of alpha power suppression following 3 Hz photic stimulation can be seen in the rightmost column. Effect sizes were calculated by taking $Z\sqrt{N}$, with the z statistic being calculated by a two-tailed Wilcoxon signed-rank test. Effect sizes of the post-stimulation decrease in alpha power (mean 8-12 Hz μV^2) are given for occipital, medial, and frontal regions (see leftmost column).

As can be seen in Figure 5.1, both after 10 Hz and 3 Hz of photic stimulation, there is a significant alpha power suppression. It is interesting to note, that following the onset of the RT task at 0 seconds, there is an almost immediate reduction of alpha power suppression levels over all but the medial region. Further, 10 Hz stimulation results in the strongest post-stimulation alpha power suppression around the trial onset with a maximum decrease in alpha power at approximately $-6\mu V^2$, whereas the strongest alpha power suppression following 3 Hz stimulation can be seen over the frontal region, before trial onset close to 12 Hz at a maximum of roughly $-6\mu V^2$. Overall, we found the largest effect sizes over medial regions (see Figure 5.1 and Table 5.4).

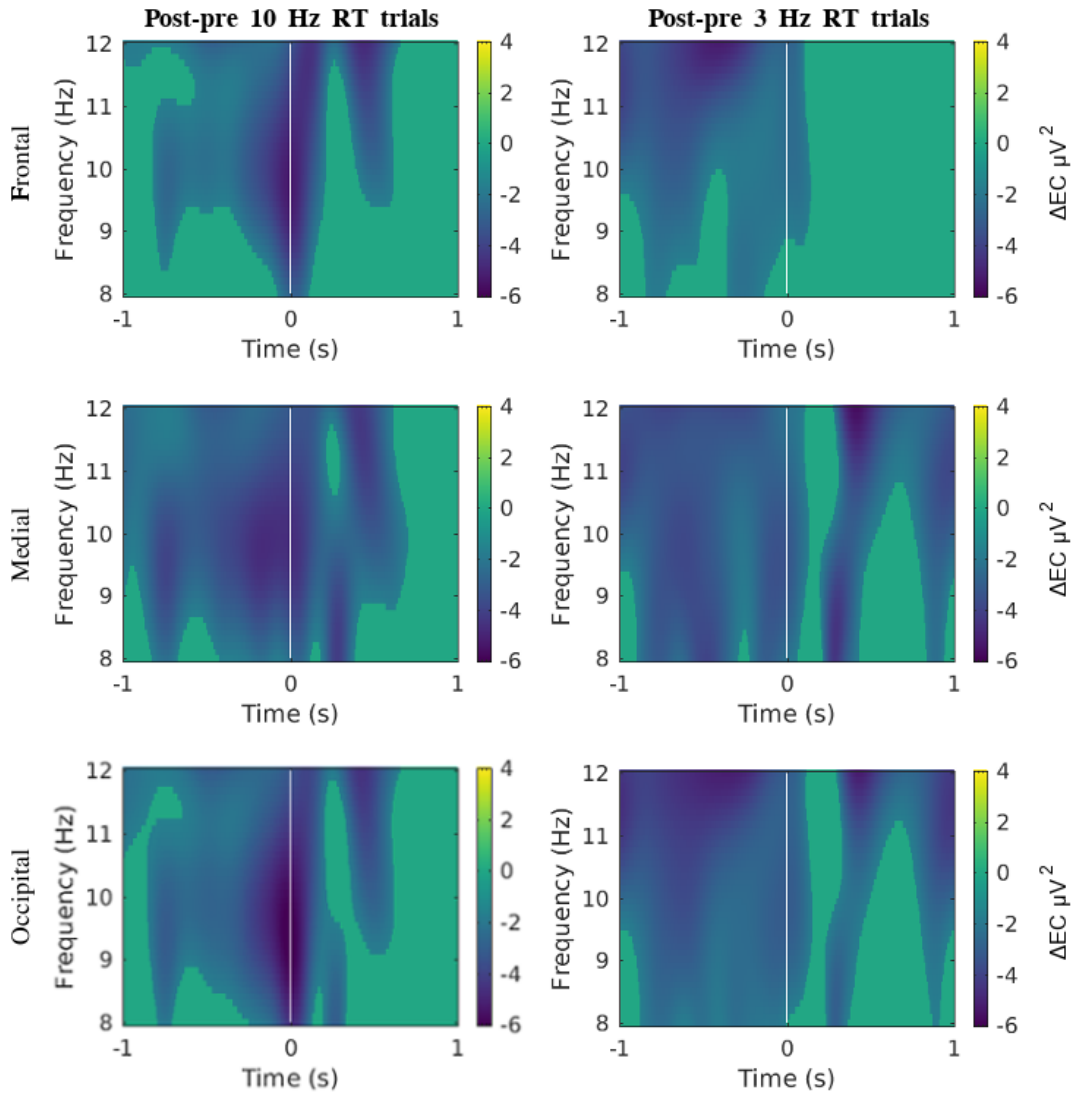

FIGURE 5.1: Post-photic-stimulation alpha power suppression during RT task

Post-photic-stimulation alpha power suppression during RT trials is visible across the scalp. Both columns show difference maps (between pre- and post-stimulation intervals - referred to as ΔEC in the legend) in microvolts, thresholded for significance by a z-map. The left column shows significant ($p < 0.05$) differences between baseline and post-10-Hz photic stimulation occipital alpha power during RT trial intervals. The right column does the same for post-3-Hz photic stimulation intervals. The thresholded difference maps show the significance and direction of changes in alpha power after stimulation offset, with blue shading showing significant alpha power suppression of $p < 0.05$, corrected for multiple comparisons via cluster correction. The vertical white line at 0 seconds shows the onset of the RT trials.

As we observed alpha power suppression following both 3 Hz and 10 Hz photic stimulation, we next investigated whether alpha power was also enhanced during stimulation for both conditions. Figure 5.2 shows that, for both conditions, alpha power was enhanced significantly ($p < 0.05$) during the last 10 seconds of photic

stimulation relative to a pre-stimulation baseline, although 10 Hz photic stimulation, on net, produced greater alpha power (for an interval of 2 seconds), as can be seen in the bottom plot. It is important to note that this figure does not show entrainment, that is the signal-similarity of the driving signal and neural oscillations, but rather entrainment effects. Consequently, as these are non-linear (Pikovsky, Rosenblum, and Kurths, 2001), the frequency (power) induced must not mirror the frequency applied. This explains why during 10 Hz photic driving, we find significant enhancements of alpha power centred around 11-12 Hz.

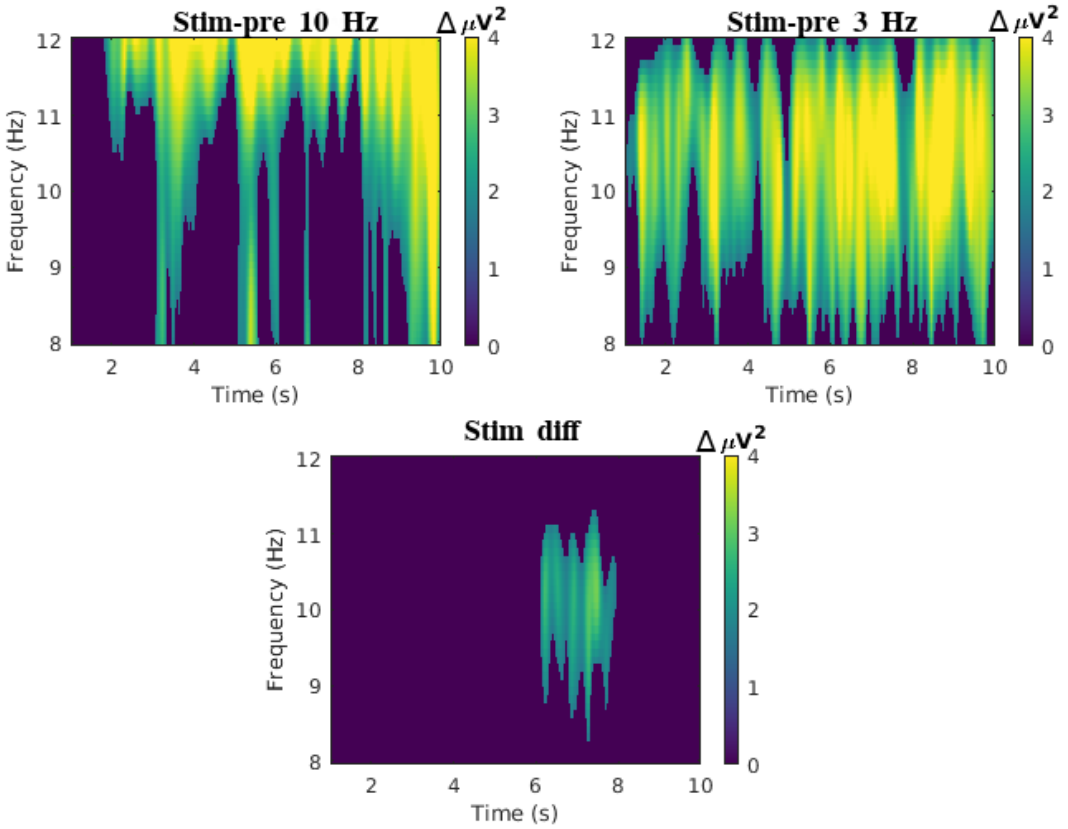

FIGURE 5.2: Significance of alpha power enhancement during photic stimulation at 10 Hz compared to 3 Hz.
Figures display microvolt measures in the alpha range (8-12 Hz) during photic stimulation compared to pre-stimulation measures thresholded for significance ($p < 0.05$) using z-maps. The top left figure shows the difference of alpha power levels between a 10 second pre-stimulation baseline directly preceding photic stimulation, and the last 10 seconds of a 60 second period of photic stimulation at 10 Hz. The top right figure does the same for the control condition employing 3 Hz photic stimulation. The bottom figure shows the difference of the total enhancement of alpha power between the experimental and control condition, showing that with the exception of a 2 second period in which 10 Hz stimulation brings about greater alpha power, there is no significant difference between conditions in during-stimulation alpha power enhancement. All thresholded difference maps show the significance and direction of changes in alpha power during the last 10 seconds of photic stimulation compare to pre-stimulation baselines of equal length, with shading showing significant alpha power enhancement of $p < 0.05$, corrected for multiple comparisons via cluster correction.

Next, to investigate whether the alpha power enhancement during 3 Hz photic stimulation was a consequence of a harmonic response at 9 Hz or 12 Hz, we plotted the FFT response of 10 Hz (blue) and 3 Hz (red) stimulation of the last 10 seconds of photic stimulation for each condition(Figure 5.3). As can be seen in red, we found that 3 Hz stimulation brought about a harmonic response at 12 Hz (as can be seen in red) in addition to a 3 Hz peak. Similarly, 10 Hz stimulation produces not just a peak at 10 Hz, but also a harmonic at 20 Hz (shown in blue).

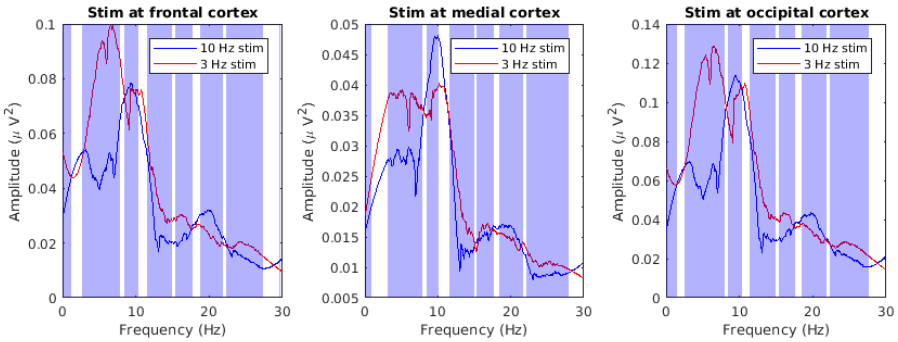

FIGURE 5.3: FFT responses to photic stimulation at 10 Hz and 3 Hz over frontal, medial, and occipital areas.
Points of significant difference in FFT response between conditions are highlighted in blue shading, with significant FFT differences between 10 Hz photic stimulation (blue line) and 3 Hz photic stimulation (red line) over frontal, medial, and occipital areas. 10 Hz stimulation displays a strong response at 10 Hz, and a second harmonic peak at 20 Hz. 3 Hz stimulation shows a peak at 3 Hz and a second harmonic peak at 12 Hz. This is in line with the results of Figure 5.2, that 3 Hz photic stimulation brings about significant alpha power enhancement during stimulation relative to pre-stimulation baselines. To compare FFT responses between conditions, we used the last 10 seconds of photic stimulation in each condition, and conducted non-parametric permutation-based ANOVA tests on each time point, controlling for multiple comparisons with the Benjamini & Yekutieli procedure. More detail of the analysis used here can be found in section 5.3.4.3.

Next, we turned to analysing differences in RT speeds within conditions comparing RT speeds after photic stimulation to baseline RT speeds without photic stimulation. In both experimental- and control conditions, we found that photic stimulation did not significantly affect RT speeds compared to baseline RT trials, with 23% of the values within the region of practical equivalence (ROPE) around the null value for the experimental condition, and 17% values within the ROPE for the control condition (see 5.4).

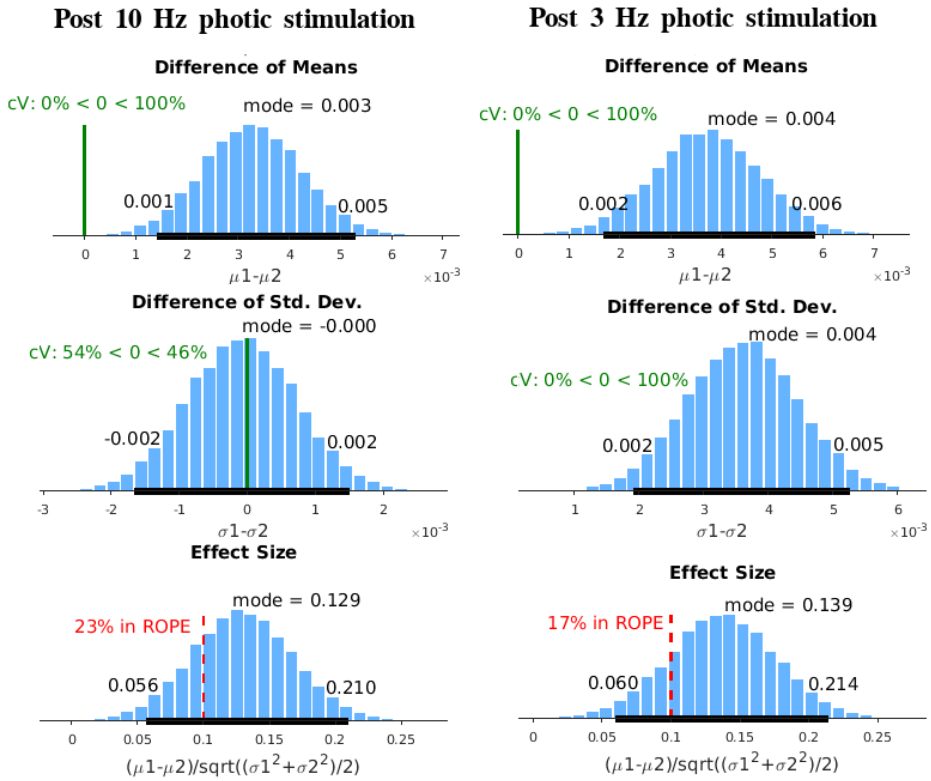

FIGURE 5.4: Bayesian estimate of RT speeds (post photic stimulation RT speeds vs pre photic stimulation RT baselines).
Both columns, from top to bottom, show the posterior distribution of the difference of means ($\mu_1 - \mu_2$), the posterior distribution of scales ($\sigma_1 - \sigma_2$) and the posterior distribution of the effect size ($\delta = (\mu_1 - \mu_2) / \sqrt{(\sigma_1^2 + \sigma_2^2)/2}$). The left-hand column compares post-10-Hz and baseline RT speeds, showing no significant change in RT speeds with 23% of the variation in effect size HDI within the ROPE of the null value. The right-hand columns shows a comparison between post-3-Hz and baseline RT speeds, showing no significant change in RT speeds with 17% of the effect size HDI within the ROPE of the null value. All posterior distributions are given with their 95% highest-density interval (HDI) and respective minimum, maximum, and modal values. The coefficient of variation (cV) further gives the variability of each distribution in relation to its mean. Refer to section 5.3.4.3 for how these measures were computed.

Finally, we also compared differences in RT speeds between conditions, contrasting RT speeds after 10 Hz photic stimulation with RT speeds after 3 Hz photic stimulation. As shown in Figure 5.9, there was no significant difference in RT speeds between the experimental 10 Hz photic stimulation-, and the 3 Hz photic stimulation control conditions.

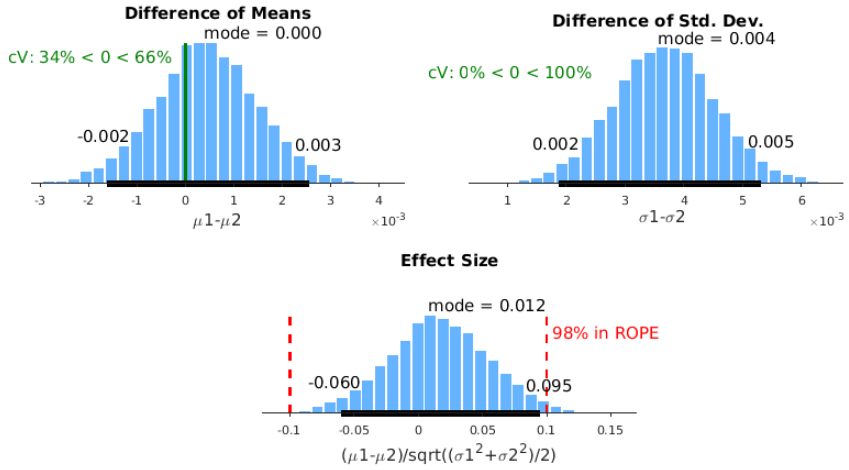

FIGURE 5.5: Bayesian estimate of RT speeds (control condition vs experimental condition).
The figure compares post-10-Hz- (group 1) and post-3Hz-photic stimulation (group 2) RT times. On the top left, the figure shows the posterior distribution of the difference of means ($\mu_1 - \mu_2$), on the top right the posterior distribution of scales ($\sigma_1 - \sigma_2$) and on the bottom the posterior distribution of the effect size ($\delta = (\mu_1 - \mu_2) / \sqrt{(\sigma_1^2 + \sigma_2^2)/2}$). With 98% of the effect size HDI within the ROPE of the null value, there is no significant difference in RT speed between conditions. All posterior distributions are given with their 95% highest-density interval (HDI) and respective minimum, maximum, and modal values. The coefficient of variation (cV) further gives the variability of each distribution in relation to its mean. Refer to section 5.3.4.3 for how these measures were computed.

As RT trials were presented over a maximum of 80 seconds post-stimulation and the post-stimulation alpha power suppression found in Chapter 3 only covered 25 seconds (since this was the maximum post-stimulation time interval recorded), we then segmented the RT speeds recorded into 4 blocks (each containing 10 RT trials in chronological order), to assess whether there was a trend in RT speeds over time (see section 5.3.4.3). This was done to address the issue of potentially diminishing alpha power suppression as RT trials got further removed from stimulation offset and its hypothetical effects on reaction times. However, we found no trend ($p > 0.05$)in the RT speeds over time, with RT measures remaining stable as revealed by a linear regression analysis.

Much to our surprise, the levels of alpha power suppression following 10 Hz photic stimulation (see Table 5.4) were only a fraction of those found in Chapter 3. To investigate this finding further, we ran a small pilot study to assess if the RT task demands were negating alpha power suppression. Using two participants, we added two conditions, in which people were given the same 60 seconds of photic stimulation (3 Hz and 10 Hz) as in the original experiment, but this time were asked to ignore the subsequent RT task (see table 5.2). This manipulation allowed us to investigate if we could observe alpha power suppression comparable to our findings in Chapter 3 and Chapter 4 in the absence of task demands.

First focusing on 3 Hz photic stimulation, the results displayed in Figure 5.6 show that, when participants were asked to engage with RT trials, there was no significant alpha power suppression following photic stimulation at 3 Hz. However, asking participants to ignore the RT trials brought about post-stimulation alpha power suppression over medial and occipital areas.

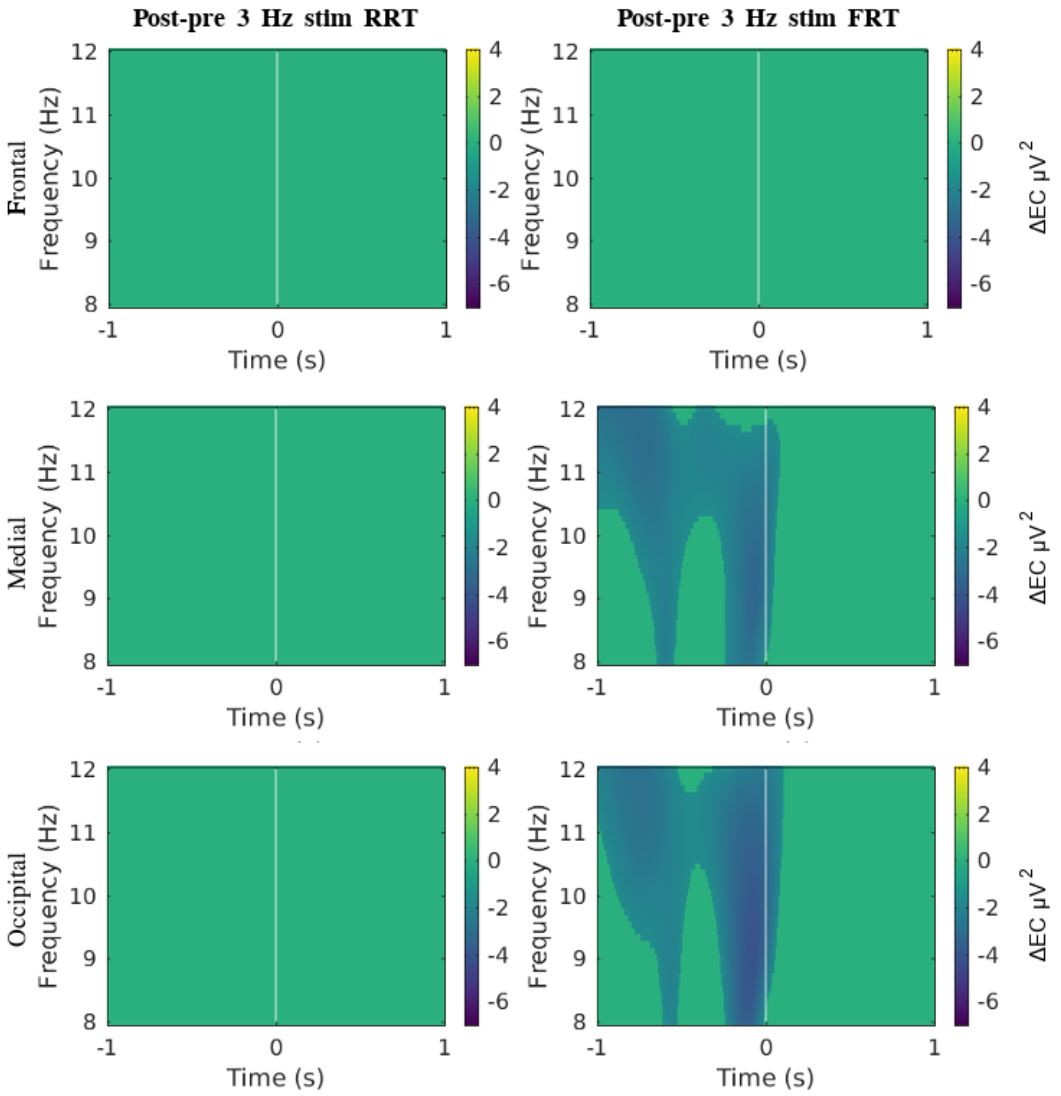

FIGURE 5.6: Post-stimulation alpha power suppression during faux RT trials (3 Hz).
Both columns show difference maps between pre- and post-stimulation intervals (abbreviated as ΔEC in the figure), thresholded by a z-map, with non-significant ($p > 0.05$) changes in mean alpha power (8-12 Hz μV^2) set to zero, corrected for multiple comparisons via cluster size correction (see section 5.3.4.3 for more details). The left-hand column shows that there are no significant differences in occipital alpha power between baseline and post-3 Hz photic stimulation during RT trial intervals, with all non-significant values set to zero. The right-hand column shows significant ($p < 0.05$) post 3-Hz photic stimulation alpha power suppression when participants were asked to ignore the RT trials over medial and occipital areas and no significant changes over frontal areas. Taken together, this shows that post-stimulation alpha power suppression during faux RT trials is more pronounced than during RT trials (following 3 Hz stimulation).

For RT trials following 10 Hz photic stimulation, alpha power suppression was only significant over medial and occipital areas, while, during FRT trials, it was also

significant over the frontal region. This can be seen in Figure 5.7. It is of note, however, that, like in Figure 5.1, both Figure 5.6 and 5.7 show a (at least temporary) decrease in alpha power suppression immediately following the flash presented as part of the RT trial - even when participants were told to ignore the task at hand. As this effect appears most strongly over medial areas, where the alpha rhythm, expressed as mu-waves, is thought to regulate the attentional demands of sensorimotor activity (Pfurtscheller and Neuper, 1994), this effect may might be an involuntary startling response.

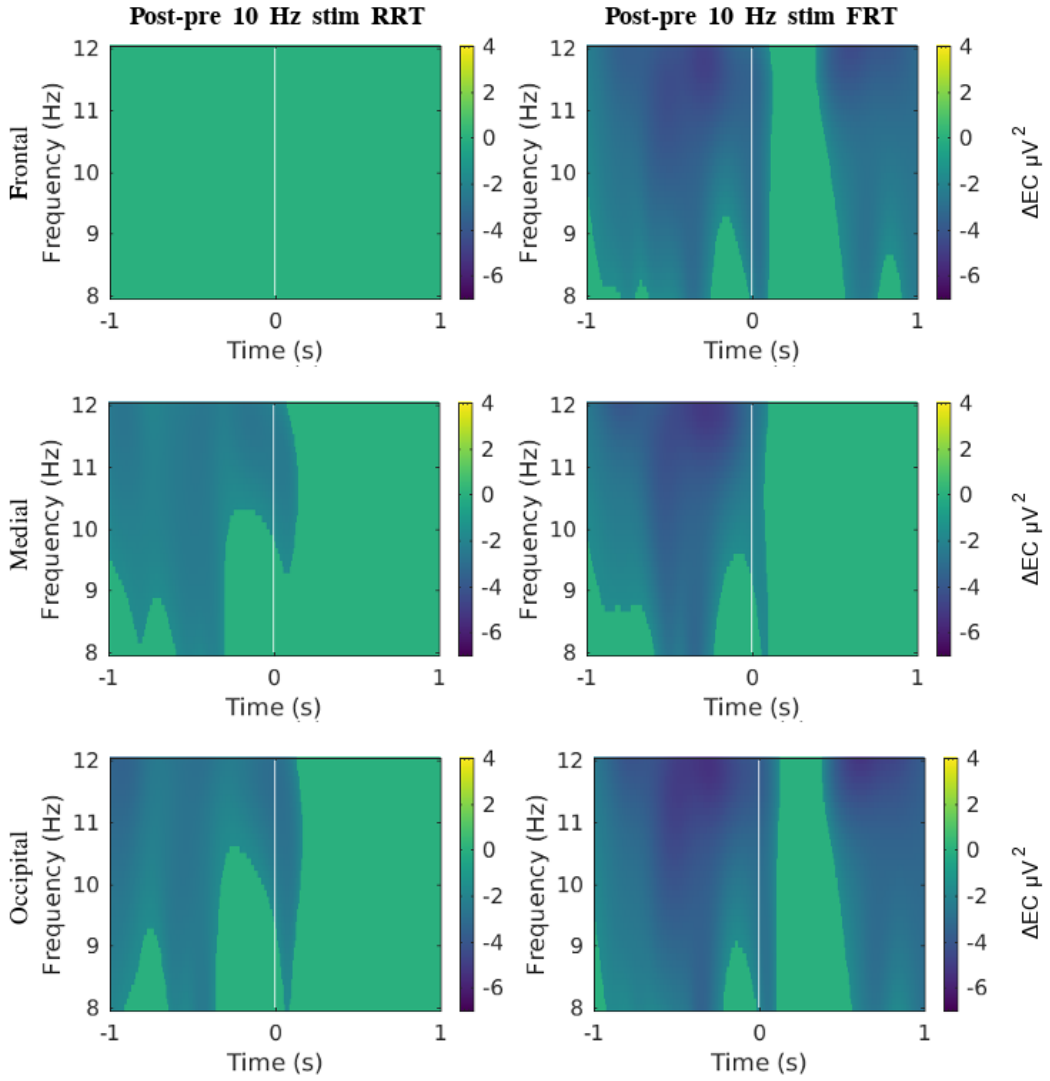

FIGURE 5.7: Post-stimulation alpha power suppression during faux RT trials (10 Hz).
The left-hand column shows alpha power (8-12 Hz μV^2) differences between baseline and post-10 Hz photic stimulation during RT trial intervals, thresholded by a z-map to highlight significant ($p < 0.05$) differences in alpha power (8-12 Hz μV^2), corrected for multiple comparisons using cluster size correction (for more detail see 5.3.4.3). Non-significant microvolt values were set to zero. Alpha power suppression is visible over medial and occipital areas during RT trials. The right-hand column shows significant alpha power suppression (the difference between baseline and post-stimulation alpha power values) when participants were asked to ignore the RT trials (FRT) over frontal, medial, and occipital areas. Post-10 Hz stimulation alpha power suppression during faux RT trials is more pronounced than during RT trials.

Next, we averaged alpha power across all time points and frequencies within the alpha range during post-stimulation RT and FRT trials and compared the resulting alpha power values to their respective pre-stimulation RT and FRT trial alpha

power baseline levels via a two-tailed Wilcoxon signed-rank test. Using this approach, we found significant ($p < 0.05$) alpha power suppression only after 10 Hz photic stimulation. Specifically, when participants were asked to respond to RT trials after 10 Hz stimulation, alpha power suppression during RT trials was significant over frontal ($p < 0.05$, $r \approx -0.2053$, $Z = -2.5967$, $W = 4850$), medial ($p < 0.01$, $r \approx -0.2381$, $Z = -3.0215$, $W = 4603$), and occipital ($p < 0.01$, $r \approx -0.2467$, $Z = -3.1298$, $W = 4540$) areas. When participants were asked to ignore reaction time tests during FRT trials, alpha power suppression was strongly significant across frontal ($p < 0.001$, $r \approx -0.3110$, $Z = -3.9457$, $W = 4124$), medial ($p < 0.0001$, $r \approx -0.3472$, $Z = -4.4056$, $W = 3854$), and occipital areas ($p < 0.0001$, $r \approx -0.3747$, $Z = -4.7549$, $W = 3649$).

Refer to table 5.5 for more information on significance values.

Conditions	**Frontal**	**Medial**	**Occipital**
3 Hz RT	2.6465	2.7760	2.7963
3 Hz FRT	0.3487	0.1207	0.1772
10 Hz RT	0.0282	0.0075	0.0052
10 Hz FRT	0.0002	<0.0001	<0.0001

TABLE 5.5: Statistical significance of alpha power suppression across the scalp during (F)RT trials.
To test for a difference in alpha power (mean 8-12 Hz μV^2) between post-stimulation (F)RT and pre-stimulation (F)RT alpha power, we used two-tailed Wilcoxon signed-rank test. Only 10 Hz photic stimulation caused significant post-stimulation alpha power suppression. In all conditions, 60 seconds of photic stimulation were applied. P-values were corrected for multiple comparisons via Bonferroni-correction. Post-stimulation RT and FRT trials took place in a 30 second window, and individual trials were extracted from -1 to +1 seconds around trigger values coinciding with individual (F)RT trials. Pre-stimulation (F)RT trials (extracted from -1 to +1 seconds around trigger values), gave alpha power baseline levels against which post-stimulation levels were compared. Significance of the impact of photic stimulation is given for occipital, medial, and frontal regions.

Table 5.6 shows that effect sizes for post-stimulation suppression were most pronounced over the occipital region. Photic stimulation brought about medium effects sizes for alpha power suppression across the scalp during FRT trials, and small effect sizes during RT trials. When participants were asked to ignore RT tasks during FRT trials, effect sizes and significance of alpha power suppression after 10 Hz photic stimulation were comparable to those detailed in Chapter 3. Due to the fact that 3 Hz stimulation did not bring about post-stimulation alpha power suppression, the associated effect sizes were negligible.

Conditions	Frontal	Medial	Occipital
3 Hz RT	0.0117	-0.0074	-0.0067
3 Hz FRT	-0.1238	-0.1617	-0.1488
10 Hz RT	-0.2053	-0.2381	-0.2467
10 Hz FRT	-0.3110	-0.3472	-0.3747

TABLE 5.6: Effect sizes for post-stimulation alpha power suppression across the scalp during (F)RT trials.
Effect sizes were most pronounced over the occipital region during FRT trials. They were calculated by taking $Z\sqrt{N}$, with the z statistic being calculated by a two-tailed Wilcoxon signed-rank test. Effect sizes of the post-stimulation decrease in alpha power (mean 8-12 Hz μV^2) are given for occipital, medial, and frontal regions.

Next, we compared reaction times within conditions, which is the difference between pre-stimulation RT trials and post-stimulation RT trials for both 3 Hz and 10 Hz photic stimulation.

As shown in Figure 5.8, neither experimental or control conditions significantly affected RT speeds compared to pre-stimulation baseline RT values, with 8% of the HDI in effect size values within the ROPE for 10 Hz of photic stimulation, and 25% for 3 Hz of stimulation.

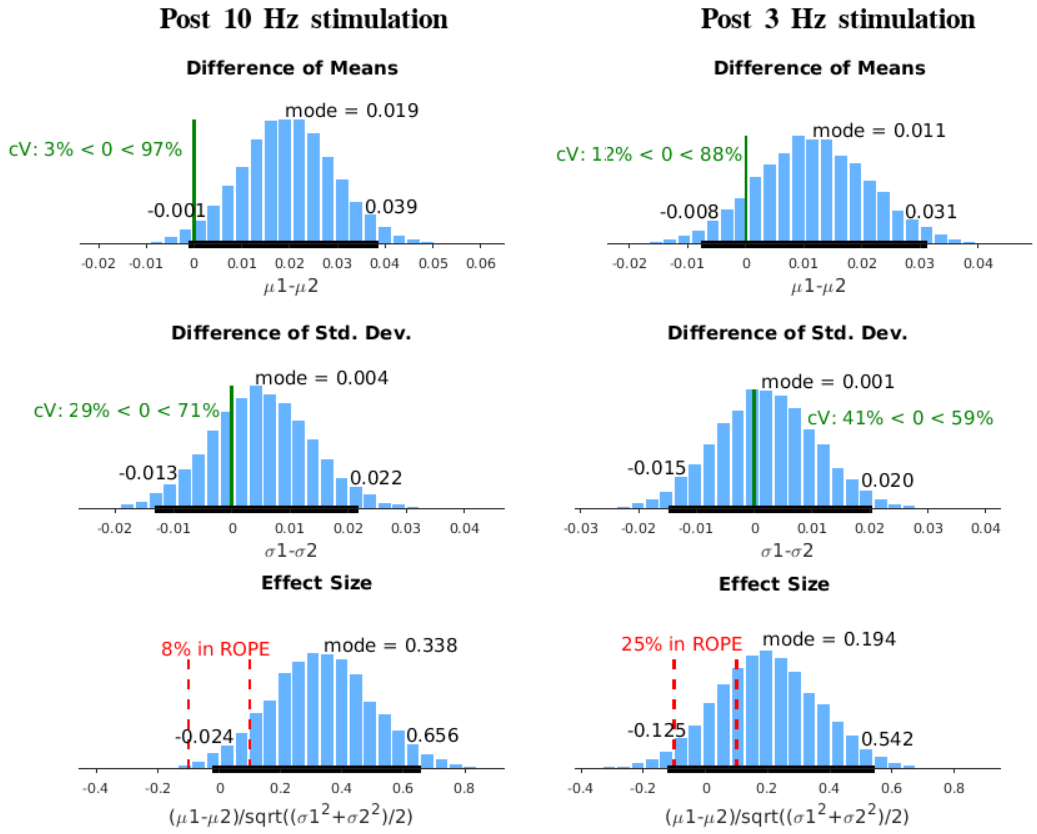

FIGURE 5.8: Bayesian estimate of (F)RT speeds (post photic stimulation RT speeds vs pre photic stimulation RT baselines)
For both columns, from top to bottom, the figure shows the posterior distribution of the difference of means ($\mu_1 - \mu_2$), the posterior distribution of scales ($\sigma_1 - \sigma_2$) and the posterior distribution of the effect size ($\delta = (\mu_1 - \mu_2) \,/\, \sqrt{(\sigma_1^2 + \sigma_2^2)\,/2}$). The left-hand column compares post-10-Hz and baseline RT speeds, showing no significant change in RT speeds with 23% of the variation in effect size HDI within the ROPE of the null value. The right-hand columns shows a comparison between post-3-Hz and baseline RT speeds, showing no significant change in RT speeds with 17% of the effect size HDI within the ROPE of the null value. Refer to section 5.3.4.3 for how these measures were computed. All posterior distributions are given with their 95% highest-density interval (HDI) and respective minimum, maximum, and modal values. The coefficient of variation (cV) further gives the variability of each distribution in relation to its mean.

Finally we contrasted reaction time speeds between conditions. As shown in Figure 5.9, RT speeds do not differ significantly between 10 Hz photic stimulation, and 3 Hz of photic stimulation, with 44% of the variation within the ROPE of the null value.

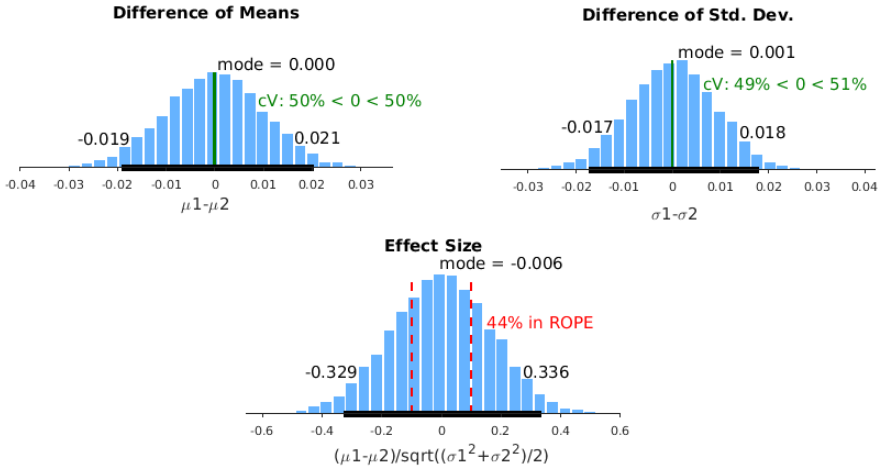

FIGURE 5.9: Bayesian estimate of (F)RT speeds (control condition vs experimental condition)
On the top left, the figure shows the posterior distribution of the difference of means ($\mu_1 - \mu_2$), on the top right the posterior distribution of scales ($\sigma_1 - \sigma_2$) and on the bottom the posterior distribution of the effect size ($\delta = (\mu_1 - \mu_2) / \sqrt{(\sigma_1^2 + \sigma_2^2)/2}$). Comparing post-10 Hz- (group 1) and post-3Hz photic stimulation (group 2) RT times, with 44% of the variation within the ROPE of the null value, there is no significant difference in RT speed between conditions. All posterior distributions are given with their 95% highest-density interval (HDI) and respective minimum, maximum, and modal values. The coefficient of variation (cV) further gives the variability of each distribution in relation to its mean. Refer to section 5.3.4.3 for how these measures are computed.

Like in our main investigation of this chapter, there was again no trend in RT speeds over time when RT measures were divided into 4 blocks with 10 RT trials each, as shown by a linear regression analysis ($p > 0.05$).

5.5 Discussion

In this chapter we sought to investigate the cognitive effects of post-stimulation alpha power suppression. Using a visual RT task following both 10 Hz and 3 Hz photic stimulation, we found that, while both 3 Hz and 10 Hz photic stimulation resulted in significant alpha power suppression during the RT trials, the resulting suppression was sparse with small effect sizes (see Table 5.4 and Figure 5.1). It could be argued that, since there was no significant difference in alpha power suppression between experimental and control photic stimulation conditions, the resulting decrease in alpha power during RT trials compared to the baseline condition is not due to frequency-specific effects (the result of prior exogenous alpha power enhancement). Rather, one might make the case that repetitive photic stimulation in general puts great demands on the inhibitory function of participants' alpha, with the stimulation offset coinciding with a release of the inhibition of exogenous forcing, and consequently with a decrease in alpha power. It is, however, more likely that the finding of alpha power suppression following both stimulation frequencies is due to the frequency-specific harmonic resonance of the 3 Hz photic signal. More precisely,

the modulation of alpha power might be a consequence of 3 Hz being two harmonic steps removed from the 8-12 Hz alpha frequency band (9 Hz and 12 Hz being a harmonic of 3 Hz), with photic stimulation at 3 Hz showing a second harmonic peak at 12 Hz (see Figure 5.3)

This latter hypothesis is further supported by the strongest alpha power suppression following 3 Hz photic stimulation being localised close to 12 Hz (Figure 5.1), whereas the same figure shows post-10-Hz-photic stimulation alpha power suppression effects to be most pronounced at around 10 Hz. Both explanations are consistent with our findings showing significant alpha power enhancement during 10 Hz and 3 Hz photic stimulation (see Figure 5.2), but the visible harmonic 9-12 Hz peak during 3 Hz stimulation in the FFT response in Figure 5.3 speaks in favour of the latter hypothesis only.

While we did find similar levels of alpha power suppression in both conditions, we found no significant slowing change in response time in RT trials following both 10 Hz and 3 Hz stimulation compared to the baseline condition lacking prior photic stimulation. When compared to each other, there is also no significant difference in response time following 3 Hz and 10 Hz photic stimulation. This is not surprising, since there was no significant difference in alpha power levels either.

Therefore, to investigate this question we performed a follow-up investigation, comparing alpha power suppression in absence and presence of RT task demands. During RT trials that participants were asked to engage with, only 10 Hz photic stimulation resulted in significant post-stimulation alpha power suppression, although these effects were restricted to medial and occipital regions. Effect sizes were small, with no significant changes in reaction times relative to pre-photic-stimulation RT trials. It was only during post-photic stimulation FRT trials, in which participants were asked to ignore the RT task, that the alpha power suppression was significant for both 3 Hz and 10 Hz photic stimulation. In fact, it was only when participants were asked to ignore the RT trials following 10 Hz photic stimulation that alpha power suppression returned to levels found in Chapter 3. Although we stress that these findings should be carefully considered due to the very small sample size, it is of note that the design of the task-free conditions in our follow-up investigations mirrored one condition in Chapter 3, including duration of stimulation and stimulation luminance. Consequently, we argue that the results from Chapter 3.3.4, showing strongly significant post-stimulation alpha power suppression in absence of a task mirror the findings of our follow-up investigation. Together, our findings provide evidence that pronounced alpha power suppression may only be expected when the participant is not asked to engage in any task following stimulation offset. This might be a consequence of how conscious top-down allocation of attention changes alpha dynamics, in order to effectively block out task-irrelevant information (Klimesch, 2018; Pfurtscheller and Silva, 2017; Mathewson et al., 2012; Thut et al., 2006; Suffczynski et al., 2001). In a visual attention task, such as our RT design, this would necessitate an increase in occipital alpha, perhaps explaining why we were unable to find strong alpha power suppression when participants were asked to attend to the RT task.

To further validate our hypothesis, future research is warranted, which repeats this study, using a greater number of participants. In addition, as the resetting of alpha power due to task demand might be a consequence of baseline alpha power levels being a local minima in the BSAP (see section 2.3), it might not occur when oscillations are pathological to start with. Hence, future research should study whether such alpha resetting due to task demand can also be observed in EEG signals from patients with pathologically low or high alpha before stimulation onset or if longer

stimulation intervals would ensure longer post-stimulation alpha power suppression.

5.6 Conclusion

In this chapter, we used a visual reaction time task during post-stimulation alpha power suppression in order to investigate whether alpha power suppression has a cognitive effect. Based on findings linking low alpha power power with longer reaction times (Nenert et al., 2012; Callaway and Yeager, 1960; Bompas et al., 2015; Haig and Gordon, 1998; Bastiaansen et al., 2001), we expected to find an increase in post-stimulation reaction times relative to pre-stimulation baseline RT measures. However, we found that 10 Hz did not lead to an increase in RT times. In addition, to our surprise, we found that the control condition which was used to test for post-photic stimulation RT changes in absence of post-stimulation alpha power suppression also resulted in a post-stimulation decrease in alpha power: Both 10 Hz and 3 Hz photic stimulation brought about significant levels of alpha power suppression post-stimulation relative to pre-stimulation baseline alpha power measures. In fact, alpha power levels post-stimulation did not differ significantly between conditions, with alpha power suppression being only a fraction of what we found in Chapter 3.

Our finding of post-3 Hz photic stimulation alpha power suppression calls into question whether photic stimulation fulfills the requirement of frequency-specificity outlined by Thut, Schyns and Gross (2011) as one key element of successful brain stimulation. After all, if stimulation at one frequency brings about a significant reaction in a separate frequency component, how reliable is the technique? Our result, could be, for example, taken to indicate that any kind of repetitive stimulation might bring about an increase in alpha power as a blocking response to exogenous forcing with a subsequent post-stimulation alpha power decrease to keep alpha power in a stable range. Things might not be as dire, however. Alternatively, as our analysis suggests, 3 Hz photic stimulation might affect the alpha band via harmonic effects. As is perhaps not surprising given the lack of significant differences in alpha power levels between conditions, we have shown that there is also no significant difference in reaction time speeds between conditions. It might need stronger post-stimulation alpha power suppression to bring about a slowing down of reaction times, as is indicated by previous findings showing a positive relationship between alpha power and reaction time speeds (Nenert et al., 2012; Callaway and Yeager, 1960). However, as the changes in alpha power are small and reaction time changes are not significant and also do not differ significantly between experimental and control conditions, we suggest that conscious top-down allocation of attention mostly negates previous exogenous forcing of neural oscillators by photic stimulation.

To further investigate this, in a follow-up pilot study, we introduced additional conditions in which participants were asked to ignore the RT trials. As a consequence, alpha power suppression returned to levels seen in Chapter 3, albeit RT task onset still (temporarily) reduced alpha power suppression, returning alpha power to baseline levels within a few milliseconds. The finding of a quick return to baseline levels of alpha power in both conditions (Figure 5.1) over occipital and frontal regions also gives evidence in the favour of there being an ideal minima in the BSAP which ensures optimal performance during specific cognitive operations (outlined in section 2.3). When photic stimulation removes it from this point, task-demands quickly bring it back to previous levels.

Assuming that alpha power is reset by task demands, one way to study the functional effects of alpha power suppression in healthy populations may be to investigate how it changes brain responses in absence of participants' conscious engagement. This could be done by studying whether alpha power suppression modulates the neural response to brain stimulation. As alpha power has been suggested to reflect inhibitory functions (Klimesch, 2012), in Chapter 6 we ask the question of whether alpha power suppression would lead to an increase in the amplitude and spread of transcranial magnetic stimulation evoked potentials.

Chapter 6

Alpha power suppression increases amplitude and spread of TMS-evoked potentials

6.1 Abstract

While past investigations have shown that 10 Hz repetitive photic stimulation can effectively increase electroencephalogram (EEG) alpha (8-12 Hz) activity during stimulation (Walter, Dovey, and Shipton, 1946; Adrian and Matthews, 1934), and that, as shown in Chapter 3, it can also decrease alpha power post-stimulation, it still remains an open question as to whether this alpha power suppression impacts brain function in any meaningful way. As we found that attentional demands reset alpha power suppression in Chapter 5, we aimed to investigate a more fundamental property of brain states by measuring the spread of transcranial magnetic stimulation evoked potentials (TEPs). This was motivated by the characterisation of alpha as reflecting processes of neural inhibition (Klimesch, 2018; Pfurtscheller and Silva, 2017; Mathewson et al., 2012). The "alpha as inhibition" framework seems especially plausible, as we, in 3, have shown that phase-lag connectivity values were significantly increased during post-stimulation alpha power suppression, suggesting reduced neural inhibition. Specifically, our hypothesis was that during alpha power suppression this decrease in inhibitory potential would lead to greater TEP amplitude and spread. To investigate this hypothesis, we compared the amplitude and spread of TEPs before and after 60 seconds of photic stimulation at 10 Hz. Here, TMS pulses in the post-photic stimulation time window were expected to fall within periods of alpha power suppression. TMS pulses before photic stimulation onset served as a baseline. We find that, compared to a control condition of photic stimulation at 3 Hz, 10 Hz photic stimulation significantly reduces alpha power post-stimulation, and increases both TEP amplitude and spread from the stimulation site. These findings give support to the notion that alpha power can be meaningfully modulated by photic stimulation, and that alpha oscillations are indeed a causal agent in inhibitory processes. With this, this study is the first to show that alpha power suppression affects brain function in a significant manner. More fundamentally, our findings give experimental evidence in favour of the "alpha as inhibition" hypothesis, building on previous correlational studies (e.g. Mathewson et al., 2011; Meeuwissen et al., 2011).

6.2 Introduction

In Chapter 3 we showed that post-stimulation alpha power suppression increases phase-lag-value (PLV) connectivity measures (see section 3.3.4.3). As the alpha frequency band (8-12 Hz) is thought to reflect, among others, inhibitory processes modulating neural responses and dynamics (Klimesch, 2018; Pfurtscheller and Silva, 2017; Mathewson et al., 2012), this makes intuitive sense. Following from this idea, in the present study we aim to test this hypothesis whether the increases in PLV connectivity measures that result from 10 Hz photic stimulation translate to a diminished inhibition of spread of neural activity. To do this, we employ transcranial magnetic stimulation (TMS), which uses magnetic pulses that elicit a neural response whose amplitude and spread we interpreted as an indication of the neural inhibitory levels.

In this study, we use rapid successive TMS pulses to the visual cortex and compare the spread and amplitude of the resulting transcranial evoked potentials (TEPs), both before and after photic stimulation at 10 Hz and 3 Hz respectively. We chose to stimulate over the visual cortex as it is the part of the brain which should be most affected by photic stimulation on theoretical grounds as laid out by Thut, Schyns and Gross, who pointed out that entrainment (and effects of entrainment) should be area-specific, so photic stimulation would be most pronounced in the part of the brain that primarily deals with visual information (Thut, Schyns, and Gross, 2011). In addition, in our previous investigations in Chapter 3, we found the occipital region to be most strongly affected by photic stimulation post-stimulation, giving more empirical support to this assumption. In the experimental condition, we use a stimulation frequency of 10 Hz, which we, in Chapter 3 and Chapter 4 have found to lead to significant post-stimulation alpha power suppression. In the control condition, to make sure the effects are frequency-specific, and not a result of photic stimulation in a more general sense, we employ 3 Hz of photic stimulation. We carried out this study in parallel with our previous investigation in Chapter 5, so only had partial knowledge of 3 Hz photic stimulation also affecting alpha power post-stimulation. However, as we have shown in Chapter 5, effect sizes of post-stimulation alpha power suppression following 3 Hz photic stimulation were significantly smaller than those resulting from 10 Hz photic stimulation (in absence of a RT task), leading to our decision to keep 3 Hz photic stimulation as the control condition of this experiment. Further, finding a stimulation frequency not leading to any alpha power suppression would have been a research project on its own outside the scope of this thesis which sought to find a complete method of alpha power modulation.

If we can in fact use photic stimulation to modulate TEPs in any significant manner, this would provide support to the notion that photic stimulation can affect endogenous oscillatory dynamics. More fundamentally, it would also give additional evidence to the proposition that alpha oscillations are indeed a causal agent in the regulation of neural inhibition, and not just an epiphenomenon of other processes. This is important, as it sheds light on general principles of brain organisation and function.

6.3 Method

TMS pulses pre and post photic stimulation at 10 Hz and 3 Hz were used in order to ascertain the impact of post photic-stimulation-alpha power suppression on TEPs.

6.3.1 Procedure

Participants were seated at a distance of 50 cm away of the Lucia N°03 Hypnagogic stroboscope, which was aligned with eye level and produced a total luminance of 6880 lux. To keep their head steady for subsequent TMS stimulation, a head-and-chin rest was used which prevented them from moving their head in any direction but backwards. To prevent them from moving their heads backwards, the TMS coil was attached to a stand, and placed directly behind them. Pressure was applied to the TMS coil from behind, as to press it against the head of the participant, to ensure pulse conduction and to minimise head movement. Participants were instructed to keep their eyes closed at all times and to not move their head.

TMS pulses were delivered using Magstim *Rapid*^{2} with an air-cooled coil (70 mm width, with a maximum field strength of 2.2T) (Magstim Ltd, Whitland, United Kingdom). Participants were asked to remove any metallic accessories before stimulation. To aid in locating the participant's visual cortex, we used the neuronavigation system Visor2 (ANT, Enschede, the Netherlands), by fitting a standard MNI coordinate system for each participant. For this purpose, a standard scan was transformed in line with the scanned anatomical coordinates, specifically the participant's nasion and notches posterior to the tragi of both ears as well as individual head shapes tracked by a Polaris infrared camera (Norther Digital, Waterloo, Canada). The same camera also monitored head movements via a head-tracker that we attached to the side of the EEG cap behind the ear of the participant. In addition, it traced the position of the TMS coil. Together, this allowed us to know the location and angle of both the specified target region of interest and the TMS coil in space. With this, once we had localised the participants' visual cortex - our target region - we were able to reliably stimulate the exact same spot with the same TMS coil position and angle repeatedly throughout all trials for each participant. The distance between actual location of the coil and its target position was kept at less than 1.5 mm for all TMS pulses. For stimulation, the coil was fitted to a stand, with its position being supported by the researcher who also applied pressure against the coil from behind, ensuring steady contact of the coil against the head of the participant.

To locate the visual cortex for each participant, we set out to find the area in which single TMS pulses most reliably brought about phosphenes for the participant. Phosphenes, in this context, were defined as the very subtle sensation of changes in visual awareness as a direct result of a single TMS pulse, where, with closed eyes, participants reported seeing a brief glimpse of light when the TMS pulse was delivered. As individual differences in the TMS intensity required to bring about phosphenes exists (Terhune et al., 2015), stimulation intensity was varied between participants. Stimulation intensity was set at 60% of maximum output initially and then increased incrementally to no more than 70% of maximum output to find the minimum stimulation intensity required to bring about phosphenes. This was repeated based on subjective report until participants gave three consecutive responses of seeing a phosphenes with high confidence. If no phosphenes could be elicited, the coil was placed in alignment with Oz and pulses were delivered at 65% of maximum output. The coil position was marked using Visor2 with a virtual head-marker, which was used as a reference point for subsequent stimulation. This meant that the coil did not change position or angle significantly throughout the experiment. Once set-up, 25 TMS pulses were applied both before and after 60 seconds of photic stimulation using either 10 Hz (experimental condition) or 3 Hz (control condition) as the stimulation frequency. Individual pulses were spaced out randomly between 1-2 seconds, using intervals of 100 ms and a minimum spacing of 1 second,

in order to ensure that there would be no entrainment or formed expectancies of a sequence of pulses.

6.3.2 Conditions

Conditions	Pre photic-stim TMS pulses	Photic stimulation	Post photic-stim TMS pulses
10 Hz stim	25	60 s	25
3 Hz stim	25	60 s	25

TABLE 6.1: Experimental and control condition. The presentation of each condition was randomised, and each condition was repeated seven times.

As table 6.1 shows, in the experimental condition, 25 TMS pulses were applied to the visual cortex, followed by 60 seconds of photic stimulation at 10 Hz, and then another 25 TMS pulses. In the control condition, the same procedure was used, with the photic stimulation being set to 3 Hz.

Individual trials occurred every 1-2 seconds. The spacing between the minimum (1 second) and maximum (2 seconds) inter-trial time window was incremented by a number of up to ten 100 ms intervals. The number of these 100 ms intervals was varied randomly, with each number occurring at equal distribution throughout the experiment. This "jitter" in inter-trial interval length was meant to avoid possible effects of entrainment or expectancies of the TMS pulses.

In total, there were 175 pre- and post-stimulation trials per condition.

6.3.3 Participants

20 postgraduate students (9 male, 11 female) were recruited. Informed consent was obtained from them after the nature and potential consequences of the study had been explained. In addition, anxiety and epilepsy questionnaires were sent out for participants to fill in before they were invited to take part in the study. Written consent was acquired by all participants, and participants were screened to ensure that they meet health requirements to participate in a TMS study (Keel, Smith, and Wassermann, 2001). The protocol for was approved by the Life Sciences & Psychology Cluster-based Research Ethics Committee of the University of Sussex (CREC).

6.3.4 Data

EEG data was collected as described in section 4.3.4.

6.3.4.1 Recording

The same recording montage and equipment was used as described in section 4.3.4.1.

6.3.4.2 Preprocessing

As TMS pulses bring about strong electrical interference, we used an automated correction algorithm of the Asalab TMS-EEG recording software (ANT, Enschede, The

Netherlands), which employs a backward infinite impulse response filter on a fixed interval (-25 ms to 10 ms around TMS pulse onset). It includes a low-pass filter of 100 Hz and a least-squares regression equation of that time interval which attempts to reconstruct the signal around the artifact, assuming that its voltage follows the parameters of exponential functions.

After correcting for TMS artifacts, all data was preprocessed in the manner described in section 3.3.4.2.

6.3.4.3 Analysis

Time-frequency and power analysis was performed as described in section 3.3.4.3.

ERPs for both pre- and post-photic stimulation TMS pulse intervals were epoched from -200 to 500 ms around TMS pulse onset, to assess the impact of TMS pulses. The data was then filtered with a butterworth filter from 1-30 Hz at an order of 2.

In order to assess and plot the significance of differences between pre- and post-photic-stimulation TEPs in control and experimental condition across time we calculated a nonparametric permutation-based paired ANOVA for each time point comparing both control and experimental conditions against their respective baselines. We adjusted for multiple comparisons using the Benjamini & Yekutieli (2001) procedure for controlling the false discovery rate (FDR), which is appropriate if data is paired as it is in this study. The number of permutations to estimate the null distribution was set to 5000, as this is the recommended value for an alpha level of 0.01 (Manly, 2007). In addition, to test for differences in absolute TEP amplitude between pre- and post-photic stimulation TEPs, both post-photic stimulation control and experimental condition TMS trials were baseline-corrected, based on pre-TMS pulse TEP power in trials without preceding photic stimulation in either condition.

6.4 Results

First, we looked at whether photic stimulation brought about alpha power suppression relative to pre-stimulation baselines. For this, we calculated the average alpha power of pre- and post-stimulation ERPs over all channels, alpha frequencies, and time points. As is shown in tables 6.2 and 6.3 alpha power suppression is significant across all electrode regions and for both 3 Hz (frontal: $p < 0.0001$, $r \approx -0.1618$, $W = 2490969$, $Z \approx -9.5741$; medial: $p < 0.0001$, $r \approx -0.1864$, $W = 2404176$, $Z \approx -11.0258$; occipital: $p < 0.0001$, $r = -0.1925$, $W = 2382492$, $Z \approx -11.3885$) and 10 Hz (frontal cortex: $p < 0.0001$, $r \approx -0.2651$, $W = 2125593$, $Z \approx -15.6855$; medial cortex: $p < 0.0001$, $r \approx -0.3067$, $W = 1978403$, $Z \approx -18.1474$; occipital: $p < 0.0001$, $r = -0.3145$, $W = 1950944$, $Z \approx -18.6067$) of photic stimulation. 10 Hz photic stimulation, however, yields significantly greater effect sizes (frontal: $p < 0.0001$, $r \approx 0.0919$, $W = 3388493$, $Z \approx 5.4380$; medial: $p < 0.0001$, $r \approx 0.0973$, $W = 3407642$, $Z \approx 5.7583$; occipital: $p < 0.0001$, $r = 0.0992$, $W = 3414115$, $Z \approx 5.8665$) than 3 Hz photic stimulation.

Conditions	**Frontal**	**Medial**	**Occipital**
Post 10 Hz stim	< 0.0001	< 0.0001	< 0.0001
Post 3 Hz stim	< 0.0001	< 0.0001	< 0.0001
Δ 10 Hz vs Δ 3 Hz	< 0.0001	< 0.0001	< 0.0001

TABLE 6.2: Alpha power suppression across the scalp during TMS pulses.
When comparing pre-photic-stimulation alpha power in TMS trials against post-photic-stimulation alpha power values during TMS trials, suppression of alpha power after photic stimulation is strongly significant ($p < 0.0001$) for both the experimental condition using 10 Hz and the control condition using 3 Hz as the stimulation frequency. Further, alpha power suppression is significantly ($p < 0.0001$) more pronounced after 10 Hz photic stimulation than after 3 Hz photic stimulation. To test for the significance of the difference of alpha power both between pre- and post-photic-stimulation alpha power within conditions as well as for the difference in alpha power suppression between conditions, we used a two-tailed Wilcoxon signed-rank test. The results reflect the significance of changes in mean alpha power (8-12 Hz μV^2 measurements) from pre-stimulation to post-stimulation TMS trials, using a time window from -200 to 500 ms for each trial, with 0 being the time point at which a TMS pulse was administered. Changes are averaged over channels, frequencies (within the alpha range), and time points (of equal length). The stimulation condition name is given in the leftmost column, with Δ 10 Hz vs Δ 3 Hz reflecting the significance of the degree to which 10 Hz photic stimulation yields more significant post-stimulation alpha power suppression than 3 Hz photic stimulation. Significance of alpha power suppression is given for occipital, medial, and frontal regions.

Length of stim	Frontal	Medial	Occipital
Post 10 Hz stim	-0.2651	-0.3067	-0.3145
Post 3 Hz stim	-0.1618	-0.1864	-0.1925
Δ 10 Hz vs Δ 3 Hz	0.0919	0.0973	0.0992

TABLE 6.3: Effect sizes for post-stimulation alpha power suppression during TMS pulses across the scalp.
Effect sizes were calculated by taking $Z\sqrt{N}$, with the z statistic being calculated by a two-tailed Wilcoxon signed-rank test. The stimulation condition name is given in the leftmost column, with Δ 10 Hz vs Δ 3 Hz reflecting the significance of the degree to which 10 Hz photic stimulation yields more significant post-stimulation alpha power suppression than 3 Hz photic stimulation. Significance of the impact of photic stimulation is given for occipital, medial, and frontal regions.

Figure 6.1 shows the significance ($p < 0.5$) of post-photic stimulation suppression of mean alpha power (mean 8-12 Hz μV^2) for both 10 Hz and 3 Hz photic stimulation relative to pre-stimulation baselines. The decrease in alpha power following 10 Hz stimulation was more pronounced than following 3 Hz stimulation, both before TMS onset at -100 ms, and after TMS administration between 200-400 ms. These results were controlled for multiple comparisons across 3500 trials using non-parametric permutation testing with pixel suprathresholding, providing a conservative estimate of the degree and time period of the significance of the difference between both experimental and control conditions. When cluster-size correction is used instead, which is a less conservative but still stringent method, the entire pre- and post-TMS pulse interval shows significantly stronger alpha power suppression in the experimental- than in the control condition.

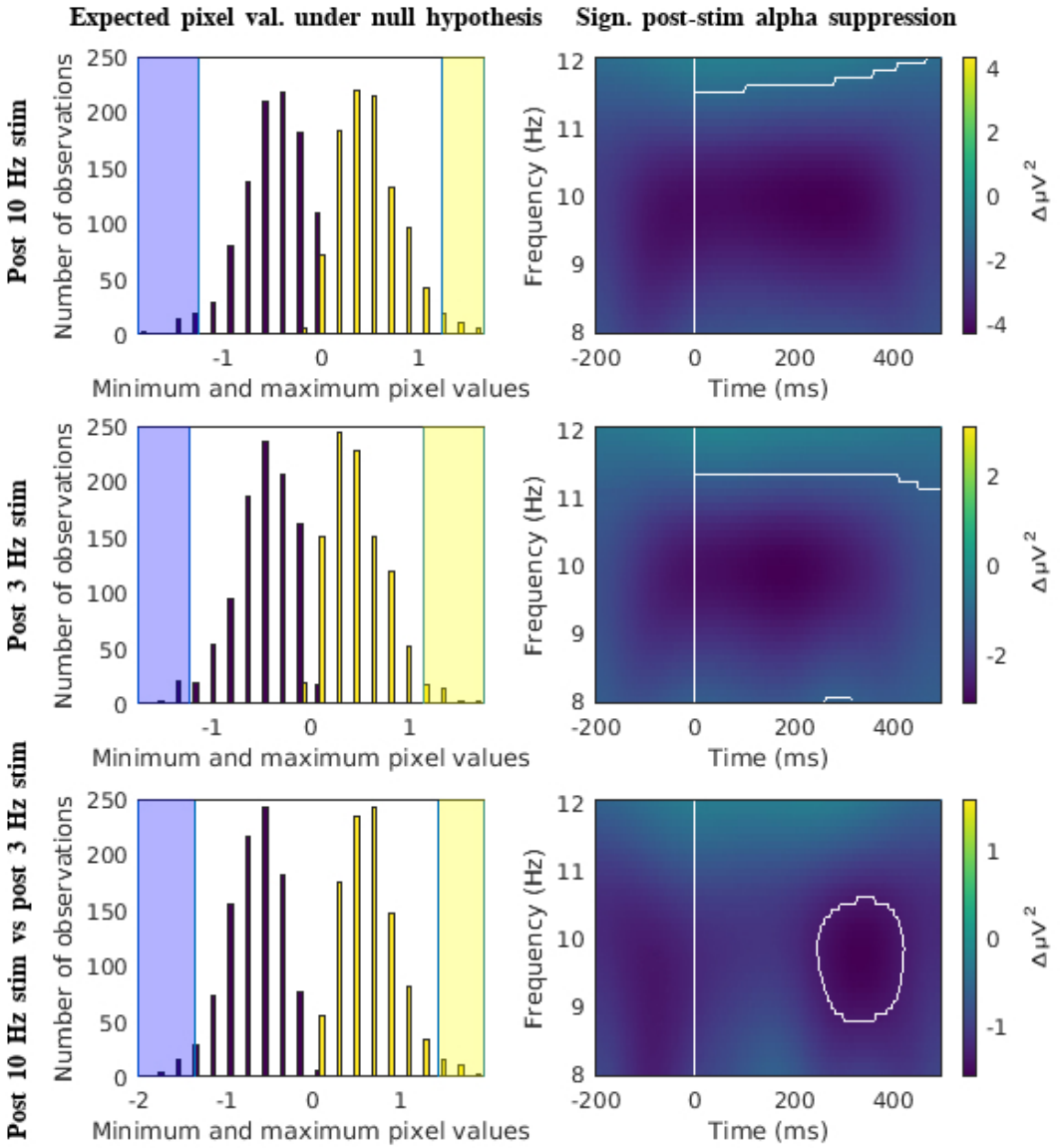

FIGURE 6.1: Alpha power suppression during TMS trials
Left-hand column: Data distribution according to which the lower (blue shading) and higher (yellow shading) thresholds for significance were calculated, with other values being within the range expected under the null hypothesis of no alpha power difference. Right-hand column: Thresholded z-maps of the differences between baseline and post photic stimulation occipital alpha power (mean 8-12 Hz μV^2) during TMS onset (shown by the vertical white line at time point 0), with all negative non zero values showing significant ($p < 0.05$, controlled for multiple comparisons via pixel suprathresholding) alpha power suppression. The first row in both columns assesses the change in alpha power that results from 10 Hz photic stimulation relative to pre-stimulation baselines, the second row displays the same the same for 3 Hz photic stimulation, and the third compares the difference of pre and post photic stimulation intervals over occipital alpha power between both conditions, and finds that 10 Hz photic stimulation yields significantly greater post-photic stimulation alpha-suppression than 3 Hz stimulation. Significant differences between pre- and post-stimulation alpha power before/at 0 ms are likely artefacts caused by the backwards-rolling filter employed to reduce post-TMS pulse artefacts and are hence not shown.

Next, we investigated if alpha power suppression brought about changes in TEP amplitude. We first compared TEP amplitude pre- and post-stimulation for experimental and control conditions using a non-parametric paired ANOVA for each time point, using the Benjamini & Yekutieli procedure to control for multiple comparisons. As shown in Figure 6.2, 10 Hz photic stimulation led to significant ($p < 0.05$) increases in TEP maximum peak amplitude compared to a pre-photic-stimulation baseline over medial and occipital areas. Significant increases in TEP amplitude in frontal areas were only visible at 0 ms, making them unlikely to reflect true changes in TEP spread, as the TMS pulse would be unable to propagate throughout the brain this fast (Buzsaki, 2006). In addition, in frontal and medial areas at -100 ms there was a period of significantly lower microvolt amplitude post 10 Hz photic stimulation compared to baseline trials. This is likely an artifact caused by the backwards-rolling filter described in section 6.3.4.3 meant to reduce post-TMS pulse artifacts and can hence be ignored. Following 3 Hz stimulation, there were no significant changes in either TEP amplitude or spread (non-significant results for each individual time point of the TEP).In the control condition, significant changes in the TEP peak enhancement were restricted to the very onset of TMS pulse administration at 0 ms, which are also likely artifacts of the backwards-rolling filter, and are hence ignored.

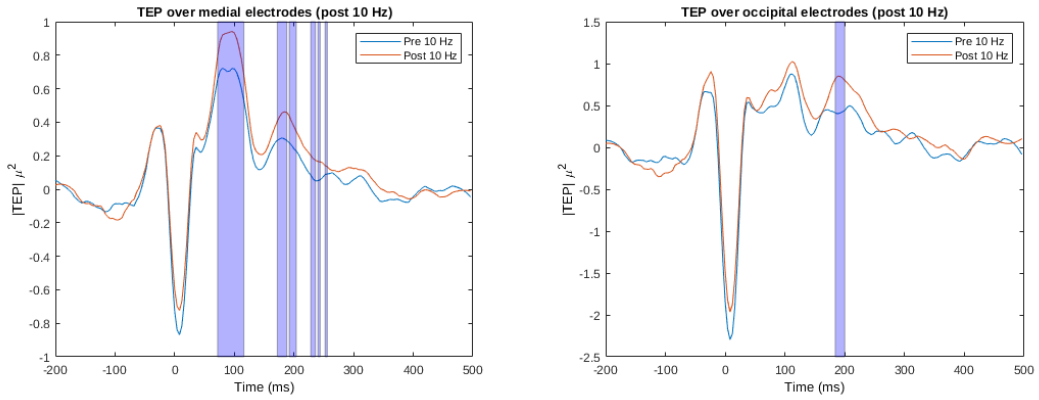

FIGURE 6.2: TEP amplitude pre- and post-photic stimulation at 10 Hz and 3 Hz.

This figure displays time points at which absolute TEP amplitude differs significantly for post-10 Hz photic stimulation compared to pre-photic-stimulation baseline TEPs from 0-250 ms. There was a significant increase in TEP amplitude over medial, and occipital regions (highlighted in blue). There were no significant changes in TEP amplitude over frontal regions. Similarly, there were no significant differences between pre- and post-photic stimulation TEP amplitude for the 3 Hz control condition. Significant differences between pre- and post-stimulation microvolt values before/at 0 ms are not shown as their interpretation is not possible due to artefacts caused by the backwards-rolling filter employed to reduce post-TMS pulse artefacts. Significance was calculated using a non-parametric paired ANOVA for each time point, controlling for multiple comparisons with the Benjamini & Yekutieli procedure. Thresholds for significance are set at $p < 0.05$, with a corrected alpha at 0.0009.

As there was concern that significant differences between pre- and post-photic stimulation TEP amplitudes might in part be due to a difference in baselines (pre-photic stimulation TEPs) between conditions, we also compared pre-photic stimulation baselines of the experimental and control conditions using the same method. Figure 6.3 shows that baselines between experimental and control condition trials do not differ significantly, further supporting the validity of the finding shown in Figure 6.2.

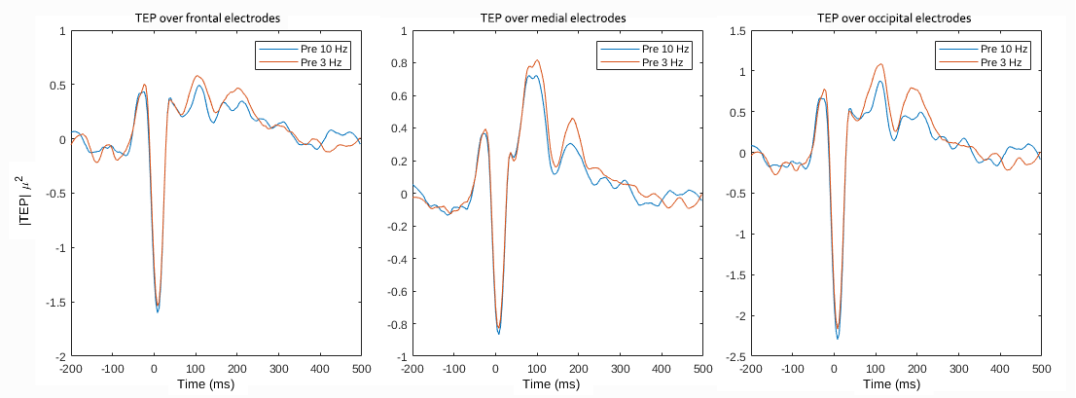

FIGURE 6.3: TEP baselines compared between conditions
Comparing the pre-stimulation baselines of the experimental (10 Hz photic stimulation) and control (3 Hz photic stimulation) conditions shows that there is no statistically significant difference between them over either frontal, medial, or occipital areas, when controlling for multiple comparisons via the Benjamini & Yekutieli procedure.

6.5 Discussion

In this chapter we sought to investigate if alpha power suppression affected the inhibitory process allowing greater TEP amplitude and spread. During individual TMS trials, both the experimental condition of 10 Hz photic stimulation and the control condition of 3 Hz photic stimulation resulted in strongly significant ($p < 0.0001$) post-photic-stimulation alpha power suppression across the scalp relative to pre-stimulation alpha power baseline trials. Effect size estimation demonstrated that this effect was significantly ($p < 0.0001$) stronger in the experimental condition, with medium instead of small effect sizes. Time-frequency zmap analysis based on pixel suprathreshold-corrected permutation testing showed that the experimental condition results in stronger alpha power suppression both before and after TMS pulse onset compared to the control condition. Based on the theorised inhibitory function of the alpha rhythm (Klimesch, 2018; Pfurtscheller and Silva, 2017; Mathewson et al., 2012), we expected that suppressing alpha power would increase the impact and spread of a TMS pulse. In line with this, the strongly significant reduction in alpha power in the experimental condition resulted in significant ($p < 0.01$) increases in TEP amplitude and spread across the scalp, with the occipital and medial areas exhibiting higher TEP peaks. This increase in TEP amplitude outside of occipital areas indicates a greater spread of the TMS pulse occured during alpha power suppression after 10 Hz photic stimulation. Our finding that there was no difference in TEPs in the control condition or between baselines of both conditions further supports this claim. We posit that these results support the notion that the small (but still

strongly significant) alpha power suppression of the control condition was not pronounced enough to affect changes in TEP amplitudes. This could suggest that there is a minimum level of alpha power suppression that needs to be reached before it significantly affects brain function. These results are noteworthy for three reasons: First, they show that post-stimulation alpha power suppression affects neural signal propagation in a measurable and significant manner. Second, they show that there might be a minimum threshold of post-photic-alpha power suppression that needs to be breached before these effects are significant, as the smaller alpha power suppression following 3 Hz photic stimulation did not bring about significant increases in TEP amplitude or spread. Third, it further demonstrates the inhibitory role alpha oscillations may play in brain function. This latter point suggests that aside from normalising brain function, photic stimulation might allow researchers to study potential functions of different frequency bands by enhancing their power or increasing or decreasing their speed, and then testing for changes in potential associated cognitive abilities or neural responses.

6.6 Conclusion

This chapter investigated the impact of photic stimulation to transcranial magnetic stimulation evoked potentials (TEPs). Based on the proposed inhibitory role alpha oscillations play on neural inhibition (Klimesch, 2018; Pfurtscheller and Silva, 2017; Mathewson et al., 2012), we assumed that the alpha power suppression following 10 Hz photic stimulation would lead to a modulation of TEP amplitude and propagation throughout the brain. Our investigation aimed to validate whether the post-photic stimulation alpha power suppression has a measurable effect on brain function. While we found that both 10 Hz and 3 Hz conditions resulted in post-photic stimulation alpha power suppression (relative to their respective baselines), alpha power suppression was significantly stronger following 10 Hz stimulation. Following 3 Hz photic stimulation we found no significant changes in TEP amplitude and spread between pre- and post-photic stimulation, except for the immediate effects of a higher TEP peak at 0 ms over frontal and occipital areas. For the 10 Hz experimental condition, we observed significant changes in TEP amplitude (relative to baseline measures) throughout occipital and medial. Together, these results suggest that post-photic stimulation alpha power suppression, as occurred in the 10 Hz experimental condition, led to a decrease in cortical inhibitory processes, which caused the increased spread of TEP across the scalp. These results further support alpha oscillations as being involved processes of neural inhibition, building on previous correlational studies (e.g. Mathewson et al., 2011; Meeuwissen et al., 2011).

Chapter 3-5 have dealt with validating photic stimulation as a means of noninvasive brain modulation, investigating both the during- and post-stimulation outcomes in the form of changes in alpha power. As we have shown in Chapter 3 and Chapter 4, we can increase alpha power during stimulation. This validates prior findings by e.g. Walter (Walter, 1963). There, however, exists no photic stimulation protocol of decreasing alpha power during stimulation. For this reason, to find a more complete control of alpha power, the next chapter investigates the phase-sensitivity of photic stimulation, asking the question of whether in- or out-of-phase stimulation differs in stimulation outcomes as suggested by Pikovsky et al. (2001).

Chapter 7

Phase-dependency of photic stimulation effects

7.1 Abstract

As demonstrated in Chapters 3 and 4, 10 Hz photic stimulation leads to entrainment of endogenous occipital alpha rhythms and in consequence enhances alpha power during stimulation across the scalp. In addition to enhancing alpha oscillations, suppressing alpha power during stimulation may also be necessary if photic stimulation is to be useful as a potential treatment method for correcting abnormal oscillations. Dynamical systems theory as applied to the issue of exogenous stimulation of endogenous neural oscillations gives the theoretical justification for the hypothesis that this more complete means of modulation of brain activity should be possible by changing the phase relationships between stimulation frequency (SF) and natural frequency (NF) (Pikovsky, Rosenblum, and Kurths, 2001). In order to study whether this holds empirically, this chapter seeks to investigate whether the ERP response to individual flashes of photic stimulation differ depending on their timing in relation to the phase of the endogenous oscillator. The results from this chapter show that presenting a single flash out of phase, with regards to pre-entrained endogenous oscillations results in significant ($p < 0.05$) changes in amplitude and speed of ERPs time-locked to the out-of-phase flash onset (-200 to 800 ms around the flash trigger event), with most pronounced differences occurring between 100-200 ms after out-of-phase stimulation and a complete phase shift from 200 ms onward. Further, depending on flash timings, shifting the stimulation phase through either an additional on-cycle or an added off-cycle in the stimulation sequence, we were able to both suppress the ERP amplitude and slow down its speed or enhance its amplitude and speed up the ERP response directly following flash presentation until entrainment again normalises flash response in line with pre-phase shift baseline values. With these findings of temporarily detailed moment to moment differences in ERP response to flashes depending on their phase relationship with neural oscillations, we are setting the groundwork for an investigation of whether phase-sensitive photic stimulation allows for a more complete means of alpha modulation (not just enhancing but also suppressing alpha oscillations by stimulation), which we will explore in more detail in Chapter 6 using a real-time closed-loop feedback photic stimulation protocol

7.2 Introduction

Rhythmic photic stimulation relies on how the rhythmic properties of neural oscillations change in response, and how temporal expectancies bring about phase locking

of those neural oscillations - a process called entrainment (Thut, Schyns, and Gross, 2011). EEG responses to photic stimulation have shown to display sharply peaked responses at the stimulation frequency, which are referred to as steady state visual evoked potentials (SSVEPs). Given how a series of flashes are presented in quick succession, the response to each flash superimposes their trailing ends on the start of their successors, creating a train of visual evoked potential waves which do not allow the brain frequency to settle back into its natural rhythm for the duration of photic stimulation (Herrmann, 2001).

As even basic processes of the brain, such as the mechanisms regulating the firing of a neuron's action potential are nonlinear (Hodgkin and Huxley, 1952), it is important to point out that the details of brain responses to individual flashes or sequence of flashes is more complicated than this explanation might imply, as the output (the response to photic stimulation, in our case) by the brain might not mirror the input exactly.

As outlined by Pikovsky et al. (2001), dynamics system theory describes an oscillatory system as having an internal source of energy - in other words, it is self-sustained, with NF being its natural frequency in the absence of exogenous forcing. When rhythmic stimulation is applied, it will eventually synchronise via entrainment or phase locking. A divergence between stimulation frequency (SF) and NF, referred to as detuning, will lead to divergent outcomes depending on whether their forces are additive, which leads to NF accelerating, or whether they cancel each other out, in which case NF slows down. Entrainment will hence involve both NF acceleration and deceleration in response to a SF, which will affect both phase and amplitude of the NF. As detuning increases, the effectiveness of rhythmic exogenous forcing decreases, requiring ever-greater stimulation strength to affect the NF. In short, the same stimulation applied should bring about different brain responses based on the amount and direction of detuning and it should be possible to both enhance and suppress speed and amplitude of the NF based on its phase relationship with the SF applied.

This highlights the potential importance of phase to rhythmic photic stimulation and its promise for a more complete control of brain activity, including not just enhancement but also suppression of neural oscillations during stimulation. This study seeks to investigate the empirical validity of this theory, by placing individual light flashes either in- or out-of-phase with regard to pre-entrained neural oscillations and comparing the resulting ERP responses.

7.3 Method

In order to observe potential differences in event-related potential (ERP) responses between in- and out-of-phase visual stimulation, we first entrained neural oscillations with a fixed 10 Hz signal for 30 seconds, and then shifted the phase to either send a second flash right after the preceding one, a "double-flash" condition, or prolong the space between two flashes by an additional "off-cycle - a "double-gap" condition. We then compared the ERP (-200 to 800 ms around the flash event trigger) response to a baseline condition of a single flash in line with a fixed 10 Hz photic stimulation frequency (-200 to 800 ms around the flash event trigger) to assess whether they differed significantly. Each baseline flash was picked randomly from the fixed 10 Hz stimulation interval preceding the phase shift trials.

7.3.1 Procedure

Procedure is detailed in section 4.3.1.

7.3.2 Conditions

Conditions	Stimulation	Stimulation sequence
Double-flash	30 s	flash-flash
Double-gap		off-off
Fixed stim		flash-off

TABLE 7.1: Experimental and control conditions. The order of conditions was randomised, and each condition was repeated 20 times. In double-flash conditions, a double-flash follows a 30 second sequence of fixed 10 Hz photic stimulation, in which the last flash of the sequence is followed up by another flash rather than an off signal. Conversely, in the double-gap condition, the last off signal of a 30 seconds sequence of photic stimulation at fixed 10 Hz is followed up by another off signal.

Once setup had been completed the experimental conditions were as described in table 7.1.

The order of conditions was randomised. Each condition was repeated 20 times, making for a total of 440 trials across all 22 participants. In all conditions, pre- and post-stimulation intervals of 25 seconds were recorded, to establish baseline alpha levels (8-12 Hz) and post-stimulatory effects respectively. Pre- and post-stimulation intervals here are recorded immediately before and after photic stimulation intervals.

7.3.3 Participants

22 postgraduate students were recruited. Informed consent was obtained from them after the nature and potential consequences of the study had been explained. In addition, anxiety and epilepsy questionnaires were sent out for participants to fill in before they were invited to take part in the study. More detailed information on the questionnaires can be found in section 4.3.3. The protocol for this has been approved by the Life Sciences & Psychology Cluster-based Research Ethics Committee of the University of Sussex (CREC).

7.3.4 Data

EEG data was collected as described in section 4.3.4.

7.3.4.1 Recording

The same recording montage and equipment was used that was also employed in section 4.3.4.1.

7.3.4.2 Preprocessing

All data was preprocessed in the manner described in section 3.3.4.2.

7.3.4.3 Analysis

First ERPs were computed to assess the difference in ERP response to out-of-phase compared to in-phase stimulation, by extracting data from -200 to 800ms around the flash event trigger. Baseline correction was done using the pre-stimulation (-200 to 0 ms) window. In order to assess the significance of the difference in ERPs between conditions, mass univariate within-subject t-tests were conducted on a butterfly plot of grand average ERPs, controlling for multiple comparisons via tmax permutation testing (Blair and Karniski, 1993; Westfall, Young, and Wright, 1993). For this, Matlab scripts based on the Mass Univariate ERP Toolbox were used (Groppe, Urbach, and Kutas, 2011).

Second, another set was of ERPs were extracted for coherence data analysis, covering a longer pre-stimulation interval, to show changes in entrainment after phase shift onset, ranging from -450 to 450ms. Coherence data was analysed as described in section 3.3.4.3.

7.4 Results

First, we looked at changes in coherence immediately following in- and out-of-phase stimulation. Before phase shift-onset, coherence between the photodiode (which recorded the timing of the sequence of flashes during photic stimulation) and channel Oz (refer to Figure 4.2 for a description of sensor regions) approximated 1 and hence perfect entrainment in the alpha range between 8-12 Hz. This can be seen in Figure 7.1. The figure also shows that after phase shift onset, there is an immediate decrease in coherence with temporary negative coherence at high alpha and low beta for a double-flash phase shift from 100-200 ms, and at theta for a double-gap phase shift between 0-400 ms. Entrainment in the alpha range is regained after 250 ms for a double-flash phase shift and at 150 ms for a double-gap phase shift.

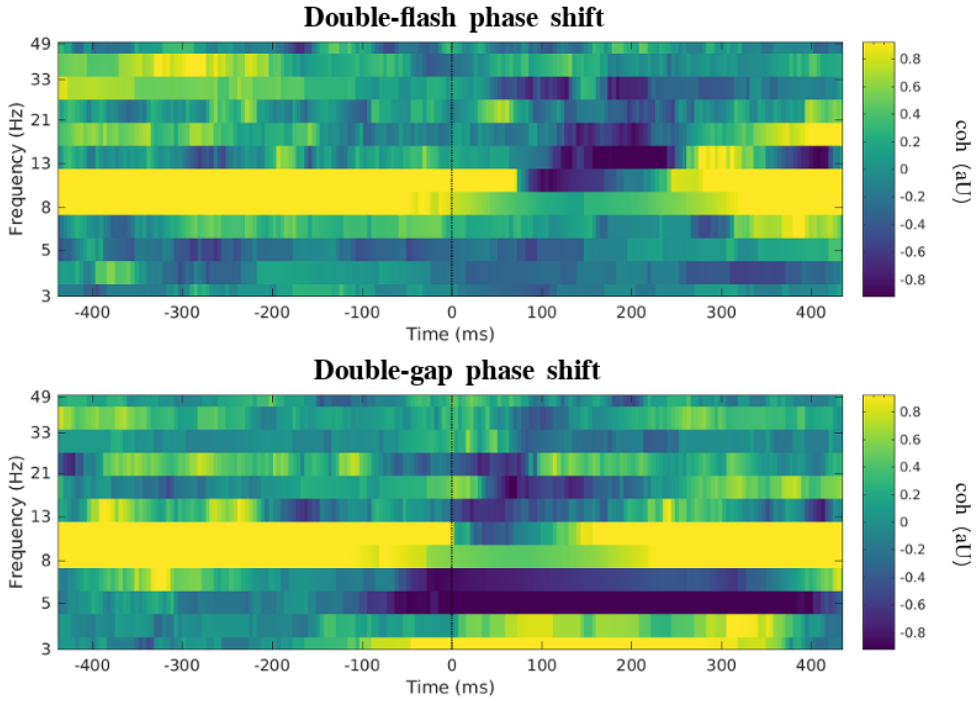

FIGURE 7.1: Coherence changes following double-gap and double-flash phase shifts after 30s of fixed 10 Hz stimulation.
Both top and bottom figure show coherence between the photodiode and channel Oz using a grand average across participants and trials. Coherence is given from -1 to 1, with 1 showing greatest phase similarity, and -1 negative phase alignment. Before phase shift onset at 0 ms approximates 1, which equates to perfect entrainment of neural oscillators to the 10 Hz photic stimulation signal captured by a photodiode before phase shift onset. From the phase shift onset there is a strong drop in coherence, with brief negative phase-alignment between driving stimulus and endogenous oscillator at high alpha and low beta for the double-flash phase shift (100-250 ms) and for the double-gap phase shift (0-150 ms). Entrainment within the alpha range at 10 Hz post-phase shift is regained for a double-flash phase shift at 250 ms, and at 150 ms for a double-gap phase shift.

Next, we looked at the photodiode data in relation to ERP oscillations to get an idea on the relationship between phase and phase-shifted stimulation in both conditions.

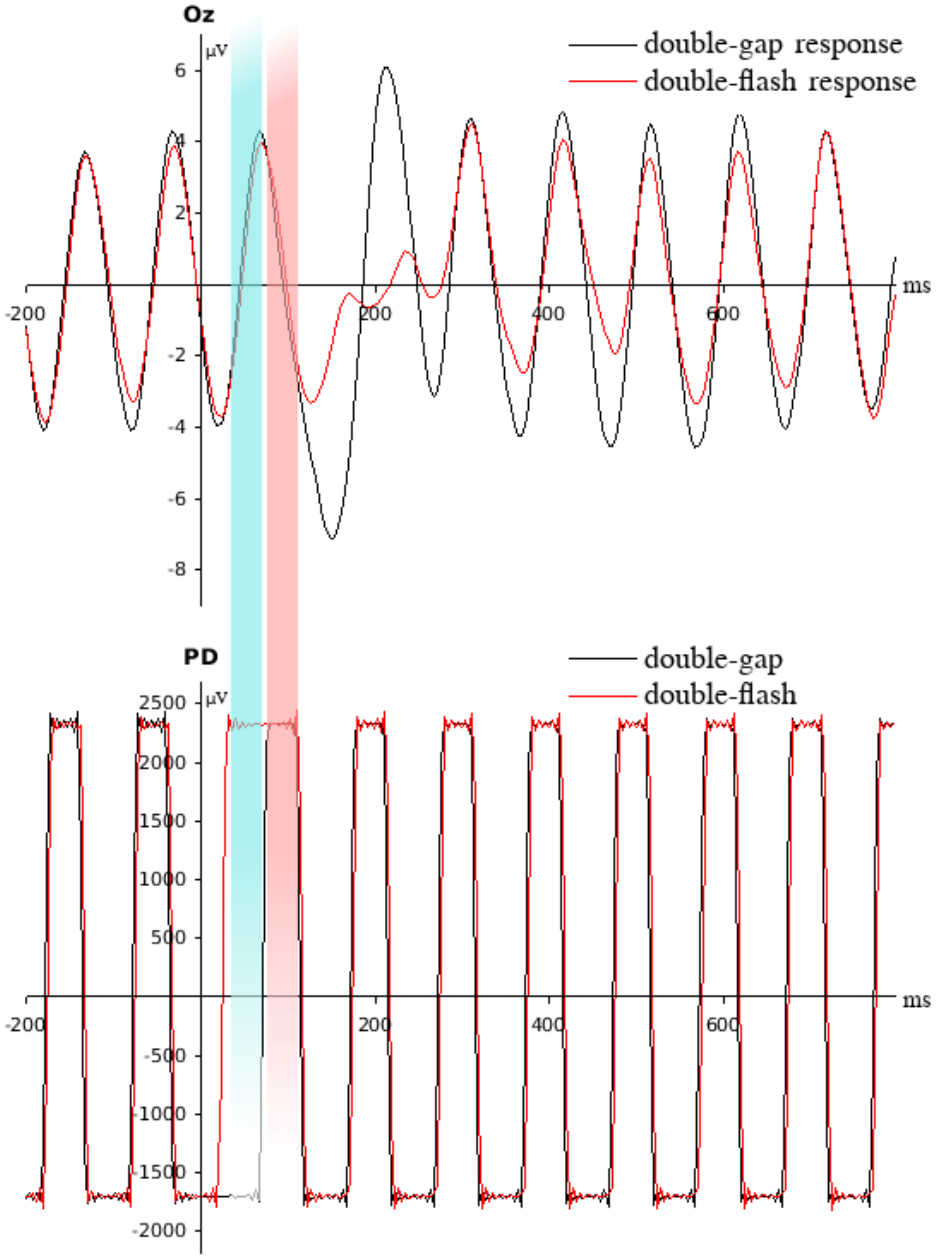

FIGURE 7.2: Relationship between ERP phase and placement of individual flashes during stimulation phase shifts.
The top figure shows the grand average (across trials and participants) ERP response to a double-gap (black) and a double-flash phase shift (red) as measured from channel Oz. The bottom figure shows the photodiode response as recorded from the outer ring of the light stimulation device, showing the flashes of both the double gap (black) and double flash (red) condition. The blue shading shows the second off cycle for the double-gap phase shift and the red shading shows the second on cycle for the double-flash phase shift.

Next, we analysed whether the phase shift also affected resulting ERPs. Figure 7.3 shows the significant changes in ERPs of phase shift conditions compared to baseline trials as well as the significance of differences in ERP responses between

double-flash and double-gap phase shifts. For double-gap phase shifts, after correcting for multiple comparisons with tmax permutation testing, using 2500 permutations, the estimated family-wise alpha level was 0.05 and critical t-scores ± 4.8683. All significant corrected p-values are between 0.0492 and < 0.0001. For double-flash phase shifts, using the same permutation testing procedure, critical t-scores were ± 5.0289, with significant corrected p-values ranging from 0.0488 to < 0.0001. For both conditions, the corrected test-wise alpha was < 0.0001. While the initial significant differences in ERP responses are interesting, it is noteworthy that, as Figure 7.1 shows, the phase shifted signals are perfectly entrained to the driving stimulus again at 150 ms (double gap) and 250 ms (double flash) after the phase shift onset, meaning that when comparing the ERP response at any time point beyond this, we are comparing two signals with inverse phase alignment. Hence, past the point of 150 ms and 250 ms respectively, these results do not say anything about differences about phase sensitivity of ERP responses to differing flash placements but rather just confirm the truism that two signals with perfectly inverted phase relationships are indeed different signals. For this reason it is informative to look a the bottom plot of Figure 7.3, which compares the ERP response between double-gap and double-flash phase shift trials. With this, it shows the time intervals in which the changes in ERP responses were a consequence not just of shifting the phase, as both of them do this and a significant difference between phase-shifted signals is a given as their respective phases have opposite polarity, but rather of the differing impact that the SF flash placement has with regards to the phase of pre-entrained NF.

The results show that double-gap and double-flash phase shifts significantly differed from each other, with critical t-scores of ± 4.7641 and corresponding corrected test-wise alpha levels of < 0.0001. Significant corrected p-values were between 0.0496 and < 0.0001. We can see significant differences in ERP response as they result from phase-specific photic stimulation from 100-250 ms, and then again between 450-500 ms, with any other significant changes in double-gap and double-flash conditions when compared to their respective baseline trials being a consequence only of a successfully phase-shifted signal, and hence not of great interest for our investigation.

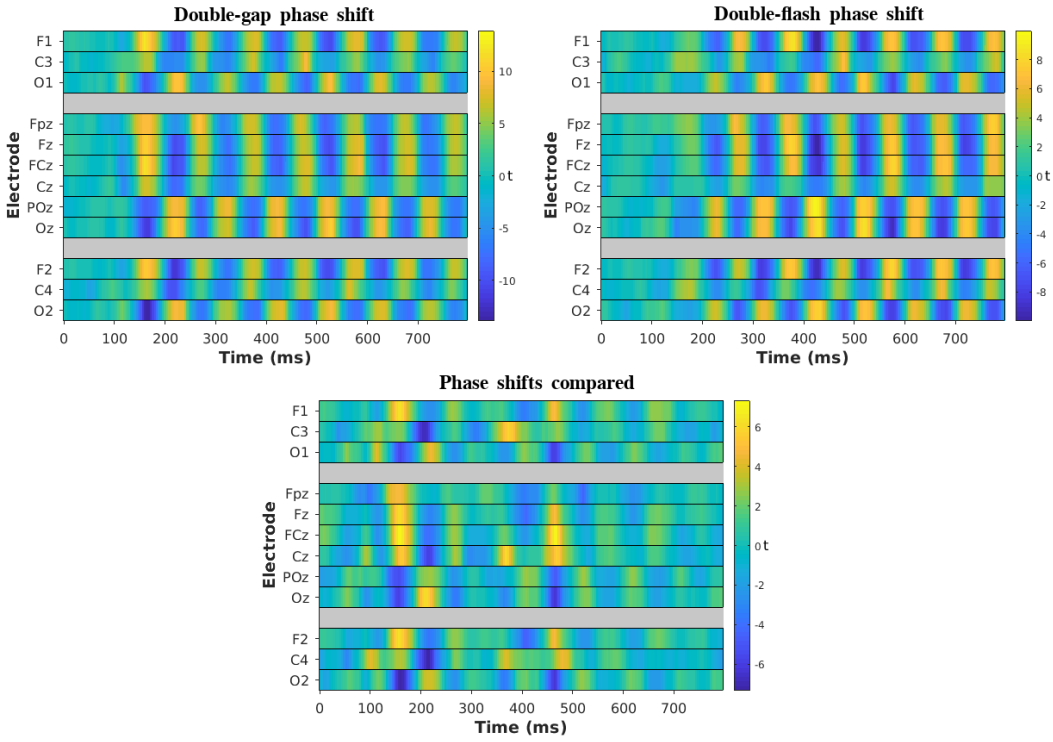

FIGURE 7.3: The effects of phase shifts on average trial responses (t-values via tmax permutation testing)
Data are t values of the difference in ERP response after phase shift onset (at 0 ms) either between phase shift- and baseline trials (top row) or between both conditions of phase shift trials (bottom row) calculated via tmax permutation testing. The bottom three rows in each figures show channels on the right side of the head (descending), the six rows in the middle the channels in the center of the EEG cap (descending), and the top three rows show the leftmost channels (descending). The top left figure shows the t values of a double-gap phase shift compared to baseline trials, where an additional half-cycle of an off signal causes a phase shift during 10 Hz photic stimulation. The top right figure shows the t values of a double-flash phase shift compared to baseline trials, where an additional on-signal, lasting for half a cycle of the 10 Hz photic stimulation shifts the phase of the driving signal. In both of the figures in the top row, significant differences to baseline trials can be seen from 150ms after phase shift onset. The bottom figure compares both means of shifting the phase, and finds that they differ significantly especially between 100-200 ms. With this, this figure shows the time intervals of significant ERP changes as a consequence of out-of-phase stimulation in absence of the effects of an already phase-shifted signal, which by its opposite polarity when compared to baseline trials always significantly differs from baseline trials following post-phase shift entrainment. Hence, the bottom figure highlights time intervals which give evidence to our hypothesis of photic stimulation being phase-sensitive.

As Figure 7.4 shows, the effects between in-phase and out-of-phase flashes diverge early on, with the most prominent differences being apparent between 100-200 ms. Both conditions also differ significantly from the baseline from 150-200 ms onward. The reason for the subsequent significant difference between baseline and

phase shift conditions is, of course, the negative phase relationship between them past the shift in phase that was initiated at 0 ms.

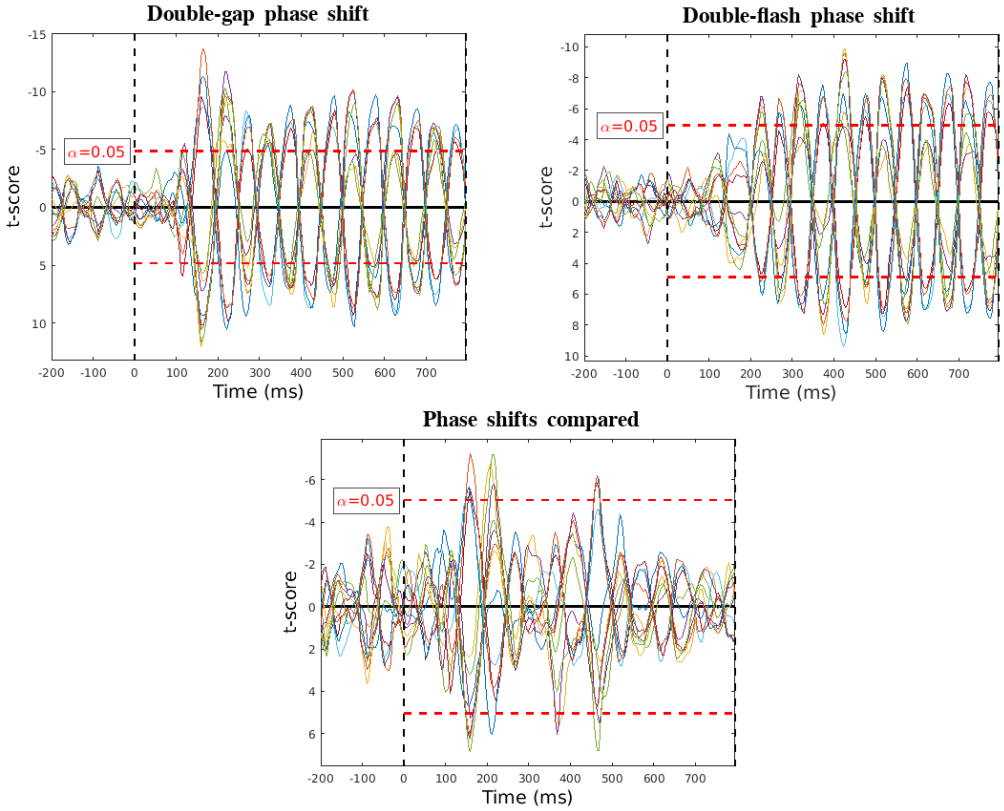

FIGURE 7.4: Phase shift effects on ERPs across time
The top-left figure shows the grand average (across trials and participants) ERP waveforms for each channel following a double-gap phase shift in photic stimulation. The butterfly plots show t values of the difference in ERP response to double-gap and double-flash trials (phase shift onset at 0 ms) in comparison to baseline trials (top row) and t values of the difference in ERP response between both phase shift conditions (bottom row), calculated via tmax permutation testing. The highest t-scores can be seen in the time period between 100-200 ms, while the effects of a double-flash phase shift are most pronounced from 200 ms onward, as can be seen in the top-right figure. Consequently, as shown by the bottom figure, effects of both phase shift methods diverge significantly early on between 100-200 ms.

Figure 7.5 highlights the divergence in effect between double-flash (red line) and double-gap phase shifts (black line) by showing the grand average ERP response of all channels in reference to fixed 10 Hz photic stimulation (blue line). Here, the in-phase stimulation yields a strong decrease in ERP amplitude (μV) between 150-200 ms, whereas out-of-phase stimulation brings about a more pronounced amplitude minima at 100-150 ms and a stronger amplitude maxima at 150-250 ms before returning to baseline levels from 250 ms onwards.

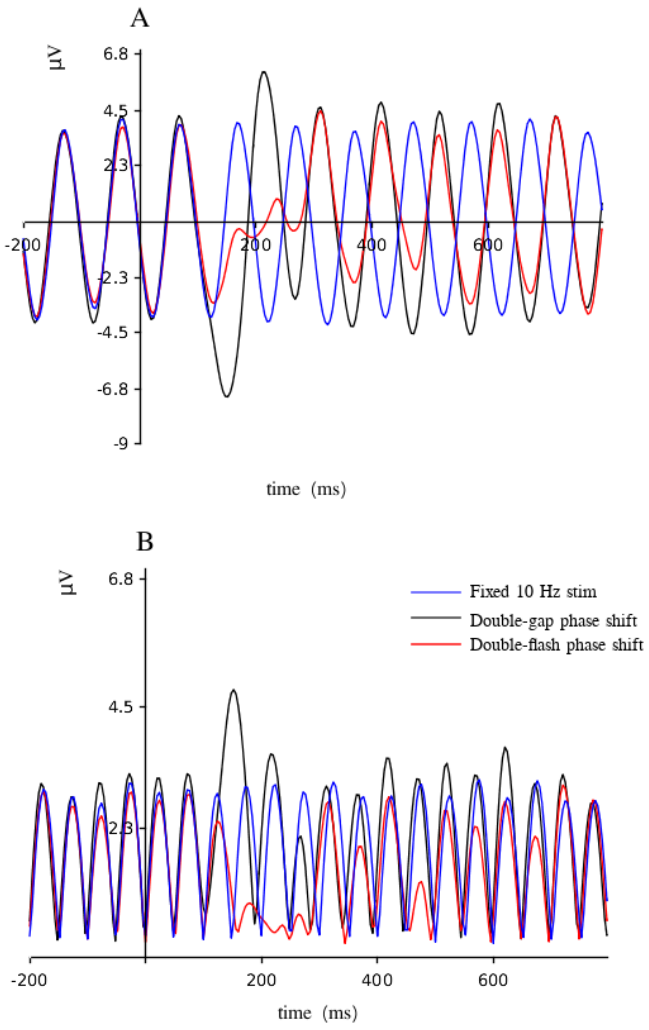

FIGURE 7.5: Grand average ERP responses to fixed 10 Hz, double-gap, and double-flash stimulation

The grand average (across participants and trials) ERP response to fixed photic stimulation at 10 Hz is given in blue, the grand average ERP response to a double-gap-phase shift in black, and to a double-flash-phase shift in red. About 100 ms after the phase shift at 0 ms, a response can be seen with the red double-flash ERP losing oscillatory speed and amplitude, as it slows down to catch up with the new photic stimulation rhythm. 300 ms in, the neural oscillator is again aligned with the external stimulation. The black double-gap ERP shows a similar response, with, in this case, speeding up and increasing the amplitude of the oscillation to catch up with the new rhythm at 300 ms in. Figure *A* shows this for the occipital sensor Oz, and figure *B* displays the global field potential averaged over all 12 channels.

The divergence in ERP responses following double-gap and double-flash phase shifts can also be seen topographically in Figure 7.6. As the figure shows, ERP changes were visible only across occipital and left medial areas for double-flash phase shift trials, but across occipital, left and right medial as well as frontal areas for double gap phase shift trials, with double-gap trials showing an overall stronger

ERP response. The figure shows channels with significant differences in ERPs between 100-200 ms following phase shift onset after correcting for multiple comparisons via tmax permutation testing using 2500 permutations, a desired family-wise alpha level of 0.05 and a corrected test-wise alpha of < 0.0001. Critical t-scores were ± 2.7051 for the double-gap phase shift seen in the top-left of Figure 7.6, with significant differences from zero (in order of earliest to latest) over electrodes Fpz, Fz, C3, Cz, C4, POz, O1, Oz, O2, F1, F2, FCz, which are highlighted in white. All significant corrected p-values were between 0.0316 and < 0.0001. The top-right of Figure 7.6 shows the t-values for the double-flash phase shift, with critical t-scores at ± 3.0281. All significant corrected p-values were between 0.03 and < 0.0001 over C3, POz, and Oz. The bottom part of Figure 7.6 shows the t-values of the difference between both phase shift methods with critical t-scores at ± 2.9652. Significant differences from zero (from earliest to latest) over Fpz, Fz, Cz, POz, O1, Oz, O2, F1, F2, and FCz, with significant corrected p-values between 0.04 and < 0.0001.

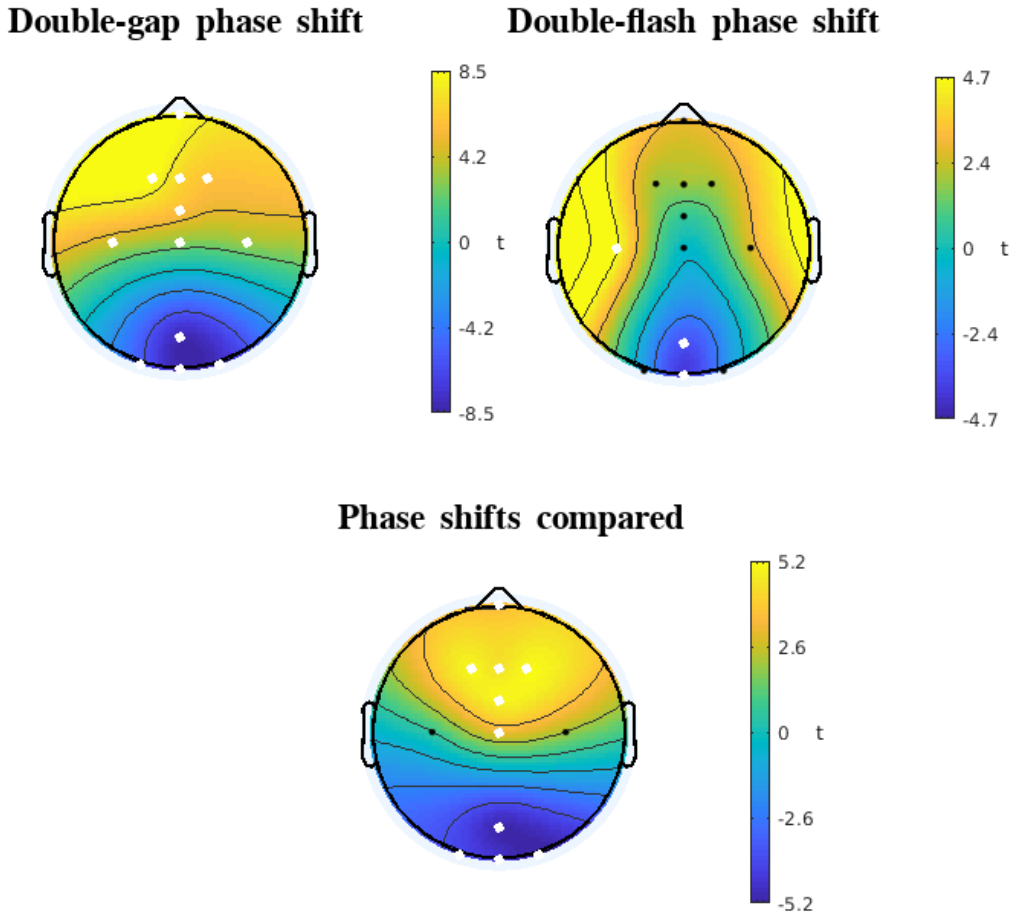

FIGURE 7.6: Topographic t-values 100-200 ms after phase shift
The topographic figures show the period of 100-200 ms (mean values across time) after phase shift-onset, and compare the ERP response between baseline trials and phase shift trials in the top row, and the ERP resopnse between both phase shift conditions in the bottom row. Significance of differences is given in t-values calculated via tmax permutation testing, with channels that have significant ($p < 0.05$) differences from zero being highlighted in white. The top-left figure shows the effects of a double-gap phase shift, the top-right figure shows the effects of a double-flash phase shift, and the bottom figure shows the t-values of the difference between both phase shift methods. Double-flash phase shifts only affect occipital and left medial areas, whereas double-gap phase shifts affect occipital, left and right medial, and frontal areas. When comparing both phase shift methods against each other, double gap phase shifts show an overall stronger response in occipital, center medial, and frontal regions.

7.5 Discussion

We found a significant divergence in ERP response to in- and out-of-phase stimulation immediately following phase shift onset. Both double-flash and double-gap phase shifts in stimulation brought about ERP changes that differed significantly

from fixed 10 Hz stimulation baselines, as well as from each other. A double-gap-phase shift led to a significantly more pronounced ERP amplitude between 100-250 ms after phase shift onset, as the oscillation sped up to catch up with the stimulation sequence. A double-flash-phase shift, on the other hand, decreased ERP amplitude as the oscillation slowed down from 100-250 ms to synchronise itself with the new stimulation rhythm. As Figure 7.6 shows, the effects of phase shifts on ERP amplitude and speed are also topographically distinct, with double flash phase shift effects being limited to occipital and left medial areas, whereas double-gap phase shifts impact occipital, left and right medial, as well as frontal areas, showing an overall more pronounced response across the scalp, but especially in occipital and frontal areas.

The difference in ERP response to in- and out-of-phase stimulation may be explained by reference to the theoretical work of Pikovsky et al. (2001), who describe the mechanisms of exogenous interference with an oscillatory system by means of dynamics system theory. Specifically, they describe an oscillatory as being powered by an internal energy source that keeps a self-sustained natural frequency (NF). When an external force is applied, such as a single flash of photic stimulation to a neural oscillator, the outcome of this interaction depends on the difference between stimulation frequency (SF) and NF. This difference in phase or frequency, referred to as detuning, will lead to different outcomes depending on whether the forces of the SF and NF are additive or cancel each other out. When we presented a double-flash phase shift, we observed a temporary increase in oscillatory speed of the ERP response with a greatly reduced amplitude. This increase in speed is possibly the result of detuning where NF and SF forces are additive, speeding up the oscillation in consequence. The double-gap phase shift, on the other hand, brought with it an ERP response that showed a slowing down of the oscillations in the ERP response with a greatly increased amplitude. Here, perhaps, NF and SF forces cancelled each other out, resulting in this slowdown.

In both cases, the effects of double-gap and double-flash phaseshifts show most pronounced effects between 100-250 ms, which is roughly in line with the estimated transit time a single flash takes from the retina to the visual cortex (taking between 100-150 ms) and the additional time needed to decode the information (an additional 100-200 ms) (Cauchoix et al., 2014; Nieuwenhuijzen et al., 2013; Carlson et al., 2013). Following this, we can see perfect entrainment to the phase-shifted signal from 250ms post phase shift onset in both conditions in Figure 7.1

Even though the precise dynamics underlying the effects of phase shifts need further investigation, this Chapter has demonstrated that phase of neural oscillations should be considered when devising photic stimulation protocols as, depending on flash placement, it is possible to both suppress and enhance brain activity.

7.6 Conclusion

We set out to investigate whether phase matters for photic stimulation. To achieve this, we first entrained neural oscillations using photic stimulation at a fixed 10 Hz for 30 seconds, before changing the stimulation sequence by adding in an additional on-cycle following an on-cycle - a "double flash" - or an additional off-cycle following an off-cycle - a "double gap". We found that resulting ERPs showed significant differences in changes in oscillation speed and amplitude, with double-flash-phase shifts decreasing ERP amplitude and speed, and double-gap-phase shifts increasing ERP amplitude and speed. This Chapter demonstrates that flash placement in

relation to the phase of neural oscillations matters for stimulation outcomes. Specifically, we have shown that brain activity can be both suppressed and enhanced given flash placement. Building on this, in the next chapter, we investigate whether phase-targeted photic stimulation might also allow for a more complete alpha power modulation by placing flashes in relation to peaks and troughs of a real-time EEG signal, thereby making SF and NF power additive (peak-based thresholding) or by making them cancel each other out (trough-based thresholding), increasing and decreasing brain activity respectively.

Chapter 8

Closed-loop photic stimulation using EEG

8.1 Abstract

Accumulating evidence points to the role aberrant neural oscillations may play in a number of neuropathologies, which might be effectively normalised through the use of non-invasive brain stimulation, which in theory should alleviate associated symptoms (Ros et al., 2014). One such approach is photic stimulation, which we have shown to increase electroencephalogram (EEG) alpha activity (8-12 Hz) during 10 Hz stimulation in Chapters 3 and 4. However, while this may allow for increasing alpha power in patients who are deficient in this particular frequency band, as of yet there exists no photic stimulation protocol which would bring about a decrease in alpha power during stimulation which could potentially be used in cases where patients exhibit excessive alpha activity. As we have shown in Chapter 7, out-of-phase stimulation can both increase and decrease ERP amplitude entrained by a 10 Hz photic signal depending on the precise timing of flashes. Therefore, in this chapter, we test a proof-of-concept closed-loop feedback-based photic stimulation protocol, which makes photic stimulation dependent on a real-time EEG signal.

The results show that, compared to a replay condition where the exact same sequence of flashes is played back to participants independently of their EEG response to said flashes, feedback-based photic stimulation is able to significantly ($p < 0.01$) enhance or suppress EEG activity within the alpha frequency range. Specifically, flashes triggered when the signal surpasses a dynamically established threshold value more effectively enhance-, and flashes triggered when the signal falls below a dynamic threshold more effectively suppress EEG activity.

8.2 Introduction

A number of neuropathologies are associated with either excessive or diminished brain activity when compared to healthy populations (Ros et al., 2014; Wahbeh and Oken, 2013; Kan and Lee, 2015; Choi et al., 2011; Babiloni et al., 2009; Arns et al., 2008). Photic stimulation may be one useful tool to noninvasively normalise brain activity in these conditions, as it has been shown to be able to modulate neural oscillators (Walter, 1963). Using repetitive light flashes, photic stimulation brings about a train of visual evoked potential waves which ultimately synchronise endogenous neural oscillations with the exogenous stimulation - a process referred to as entrainment (Thut, Schyns, and Gross, 2011). While this has been shown to enhance alpha

activity during stimulation (Walter, Dovey, and Shipton, 1946), a new photic stimulation protocol is necessary to allow for alpha power suppression during stimulation.

We propose that the findings of Chapter 7.3.4 may constitute a starting point for this endeavour. Specifically, we found that out-of-phase stimulation was able to both enhance and slow down resulting ERPs as well as both enhancing and suppressing their amplitude. In other words, we have shown that by manipulating the flash placement in relation to the phase of neural oscillations, we can modulate their power and speed in real-time in a more complete manner. This is because, until entrainment has succeeded in matching the natural frequency (NF) of the endogenous oscillator with the stimulation frequency (SF), the SF applied is not necessarily the one induced in the system. Rather, when the NF and the SF differ, the difference between both (referred to as detuning) will push their phase apart, slowly shifting the NF. If the forces of the SF and NF are additive, the NF will accelerate. Conversely, the NF will slow down when the forces of the SF and NF cancel each other out (Pikovsky, Rosenblum, and Kurths, 2001). While, in Chapter 7, we have shown that depending on where flashes are placed relative to the phase of endogenous oscillations, we are able to both slow down or speed up neural oscillations and to reduce or increase their amplitude, we were not able to do so in a sustained manner, as our method of out-of-phase stimulation necessitated the phase-shifting of a pre-entrained oscillator. Consequently, once the phase was shifted, stimulation once again entrained a fixed 10 Hz signal.

This chapter seeks to investigate phase-specific photic stimulation in a more direct manner, by making each flash phase dependent, rather than just stimulating out-of-phase for one flash every 30 seconds as in Chapter 7. Specifically, based on the idea of phase-sensitivity of neural responses to photic stimulation which was alluded to in the previous chapter, in this study we demonstrate the results of a proof-of-concept closed-loop feedback-based photic stimulation protocol. Rather than delivering a fixed sequence of flashes at 10 Hz, we make each flash dependent on whether a real-time EEG signal (filtered data from a single electrode corresponding to Oz in the 10-20 system) crosses a dynamically set threshold, as to place flashes either aligned with peaks or troughs of the signal. By setting flashes in alignment with peaks, we assume that the NF and SF forces would be additive, enhancing the amplitude of neural oscillator. Conversely, by setting flashes in alignment with troughs, we assume that NF and SF forces would cancel each other out, suppressing neural oscillator amplitude. Further, as we asked participants to close their eyes during the experiment, we assumed that the SF would approximate 10 Hz, as this is the predominant EEG component when eyes are closed (Berger, 1929), which in turn would be the predominant force in driving SF in our EEG-dependent stimulation protocol. Consequently, we assumed that the suppression and enhancement of brain activity during stimulation would be predominantly visible in the alpha frequency range.

In order to investigate if real-time feedback is effective, we devised a control condition where stimulation was not dependent on a real-time EEG signal, which we refer to as the replay condition. Specifically, we recorded the precise timing of all flashes during real-time feedback trials, and then replayed the exact sequence of flashes back to the participant independent of their EEG signal, consequently placing the flashes in no direct relation to actual signal peaks and troughs. We theorised that, if neural phase matters to photic stimulation outcomes, real-time feedback trials should differ significantly from their respective replay trials.

8.3 Method

In order to test whether photic stimulation driven by a real-time EEG signal can be used to enhance and suppress EEG activity, we devised a protocol according to which individual flashes were triggered when the EEG signal either surpassed (peak-based flashes) or fell below (trough-based flashes) a threshold. Chapter 7 shows that ERP response to individual flashes were phase dependent, and Pikovsky et al. (2001) provides a theoretical explanation for the differing response of the expected NF given the degree and direction of detuning it exhibits in relation to the SF. Hence we assumed that peak-based stimulation would result in additive forcing, enhancing brain activity, and trough-based stimulation would suppress activity, as NF and SF forces cancel each other out.

8.3.1 Procedure

Procedure for the set-up of the photic stimulation equipment is detailed in section 4.3.1. A modified version of the Lucia N°03 Hypnagogic stroboscope (Innsbruck, Austria) was used for this study, which could be connected to a PC using a LabJack U3-HV with an added LJTick-DAC booster (Lab-Jack, USA). This allowed for precise control of individual flashes, which could be triggered via a custom script in MATLAB R2017b (The Mathworks Inc., 2017).

Details for the hardware and software used to capture a real-time EEG signal are given in sections 8.3.4, 8.3.4.1, and 8.3.4.2.

The Matlab protocol for closed-loop photic stimulation proceeded as follows:

First, 30 seconds of baseline activity were collected from channel Oz, as this channel gave best estimate of visual cortex response central to our photic stimulation paradigm. The data was stored as an array, which we will refer to as the "pre-stimulation array". The data in this array was detrended using the least-squares fit method (via the Matlab detrend function), which is phase-preserving but factored out the data drift. Next, the data was filtered with a custom bandpass filter between 1-30 Hz using the Matlab designfilt and filtfilt functions to reduce signal noise and limit the SF to a minimum of 1 Hz, and a maximum of 30 Hz. From this initial array, the last 6 samples were extracted and saved separately to serve as a starting point for a moving average window of EEG activity for the photic stimulation condition, immediately following the pre-stimulation window. We will refer to this as "moving average array". The size of this moving average array was calculated on the basis of dividing the sampling rate of 250 Hz by 40, which effectively served as a low-pass 40 Hz filter. In addition, the last one second time window of the pre-stimulation condition was saved in a separate array, which will be referred to as the "one second moving window".

A 60 seconds photic stimulation condition followed this pre-stimulation window (the pre-stimulation array). Photic stimulation used either "positive" feedback, in which flashes were triggered by the average value of the EEG signal surpassing a threshold value, or "negative" feedback, in which flashes were triggered only when said value fell below a threshold. The rationale behind this peak- and trough-based thresholding of flashes is given in section 8.3.

The dynamic thresholding value was calculated as follows: The script, with a loop-around-time of 4 ms, requested and received a new single sample on every loop. This sample was added to the one second moving window, removing the oldest sample in the array. This was done so that enough data points would be given by the one second moving window so that the data could be detrended and

filtered as described above for the pre-stimulation array. The last data point of the filtered and detrended data in the one second moving window was then added to the moving average array, again removing the oldest entry to the array in the process. This latency, which includes the time needed for all the operations described, meant that the loop was sampled at 250 Hz, which is sufficient for alpha modulation (8-12 Hz). At every loop, the previous version of the updated moving average window was then stored separately as the "old moving average array", the mean of which was then subtracted from the current mean of the moving average array (to filter out additional noise). If the resulting value, from now on simply referred to as the difference value, was then, depending on the condition, either above ("positive" feedback) or below ("negative feedback") the threshold value, a flash was triggered.

The threshold value was calculated as follows: Every time all 6 samples of the moving average window had been replaced, a new threshold value was set. Specifically, the Matlab function prctile was used to calculate the 50th percentile of the moving average window, which was then set as the threshold value. The rationale behind this is that the resulting value would have led to flashes 50% of the time for the current moving average window, providing sufficiently steady photic stimulation (by ensuring the threshold value does not result in a steady "on" or "off" signal). The result of this calculation was set as the new threshold value for the next six loops, as on the seventh loop all six samples in the moving average array are replaced again, triggering the setting of the next new threshold value. Given the loop-around-times, this means a new threshold value was set every 24 ms. This sets the stimulation rate at any value between 1-20 Hz (given the size of the window used), with a natural tendency towards 10 Hz as this will be the dominant eyes-closed EEG signal component for any participant (Berger, 1929).

See Figure 8.1 for a flowchart of the procedure.

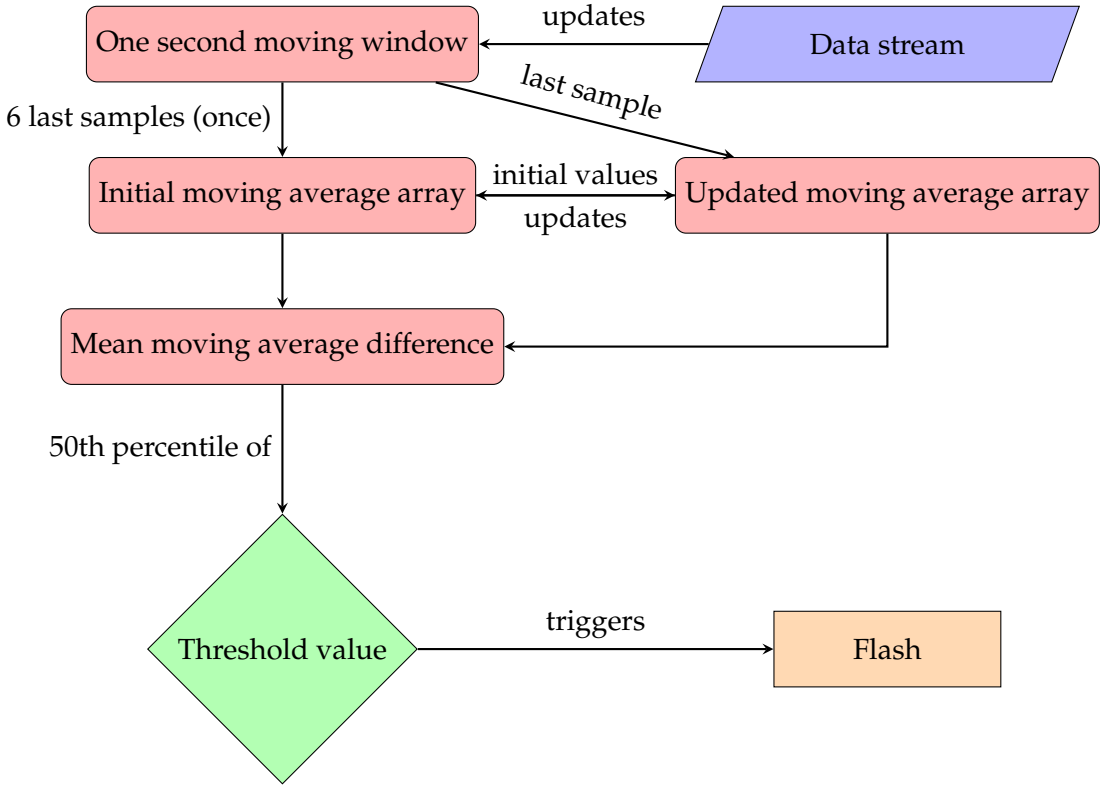

FIGURE 8.1: Photic feedback procedure flowchart
First, the most recent 250 data points (1 second) were extracted from the pre-stimulation array to serve as the initial values of a one second moving window during photic feedback. The last six samples of one second moving window made up an initial moving average array, of which a copy was created (the "updated moving average array"), which, on every loop, received a new sample from the data stream (every 4 ms) via the one second moving window (in which all data was filtered and detrended). On every loop, the preceding updated moving average array then became the initial moving average array. Next, the difference was taken between the initial and updated moving average array. If their difference value exceeded the threshold value, a flash was triggered. The threshold value was set to be equal to the 50th percentile of their mean difference (of both moving average arrays) every every six loops (once the updated moving average array had replaced all six data points from the previous threshold value calculation instance).

The resulting sequence of flashes for the entirety of the stimulation trial (60 seconds) was stored in a Matlab array along with respective time points.

Photic stimulation was followed by a 30 seconds post-stimulation window.

Next, either the same closed-loop feedback (either "positive" or "negative" feedback) was presented again, or participants were presented with a "replay condition", in which the photic stimulation followed the exact same sequence of flashes that were previously presented in one of the feedback conditions using the stored sequence and time stamps of individual flashes.

All conditions, both feedback and replay, were presented in a random order for each participant, with the only exception being the very first photic stimulation trial,

which, by necessity, used the described feedback protocol. Whether positive feedback or negative feedback was used was also randomised. During replay conditions, each specific sequence of flashes was only presented once. With that, every feedback condition had its replay counterpart. All feedback and replay conditions also had their respective pre- and post-stimulation intervals. Specifically, the first photic stimulation trial was preceded by a pre-stimulation time window and followed by a post-stimulation window. The post-stimulation window of first trial was then used as the pre-stimulation window of the second photic stimulation trial. This pattern was repeated until the last photic stimulation trial, which was followed by a post-stimulation window which did not serve as the pre-stimulation window of any subsequent photic stimulation trials.

8.3.2 Conditions

Conditions	**Threshold**
Positive feedback (PF)	Flash if X > threshold
Negative feedback (NF)	Flash if X < threshold
Positive replay (PR)	Replay PF flash sequence
Negative replay (NR)	Replay NR flash sequence

TABLE 8.1: Experimental and control conditions
The first condition presented was always either PF or NF (randomised). The order of all subsequent conditions was randomised. All conditions, including the one presented at the start of the experimental session, were presented a total of four times, with no specific replay condition being presented more than once, so that every PF and NF trial had its respective replay trial. In PF trials, flashes were triggered when the EEG difference value surpassed a EEG threshold value (see section 8.3.1 for details on how both are defined). In NF trials, flashes were triggered when the difference value went below a threshold value. PR trials replayed one of the yet un-replayed flash sequences from a previous PF trial, using the exact same timing of flashes but presenting them regardless of EEG activity. NR trials did the same for un-replayed previous NF trials.

Once setup had been completed the experimental conditions were as described in table 8.1.

Each condition was repeated a total of 4 times. While their order was randomised, the first condition presented was either a negative feedback (NF) or a positive feedback (PF) trial. Further, any subsequent positive replay (PR) or negative replay (NR) trials only used a specific flash sequence from a previous feedback trial once, so that every feedback trial had its respective replay condition. All photic stimulation conditions lasted 60 seconds and featured pre- and post-stimulation intervals of 30 seconds, which were recorded immediately before and after stimulation intervals.

8.3.3 Participants

5 (4 males, 1 female) postgraduate students were recruited. The low subject number was due to time pressure, the high degree of stress placed on the test subjects by the feedback-based photic stimulation, and the EEG headset used requiring very specific head-size and head-shape to ensure good signal quality, limiting the pool

of available participants. Informed consent was obtained from all participants after the nature and potential consequences of the study had been explained. In addition, anxiety and epilepsy questionnaires were sent out for participants to fill in before they were invited to take part in the study. More detailed information on the questionnaires can be found in section 4.3.3. The protocol for this has been approved by the Life Sciences & Psychology Cluster-based Research Ethics Committee of the University of Sussex (CREC).

8.3.4 Data

Data was acquired using a prototype EEG headset by Augmind (Augmind, UK) at a sampling rate of 250 Hz from a single channel corresponding to Oz in the 10-20 system.

The headset used a modified OpenBCI Cyton featuring a 32 bit-processor, a Bluetooth RFduino module, and a PIC32MX250F128B microcontroller with a ADS1299 24-bit analog-to-digital converter. The device featured three custom gold-plated spring-loaded electrodes. Two of them were positioned just above each ear, serving as ground (left) and reference (right) electrodes respectively. The third channel was placed in alignment with Oz in accordance with the 10-20 system.

The headset was fitted to the head of the participant by the researcher and adjusted to ensure good signal quality. This judgment was done by eye, based on the experience the researcher had acquired in conducting the research for all preceding Chapters of this thesis, as the system used did not have an ability to calculate impedance values.

This setup was used as it was the only available means of streaming EEG data to Matlab at a loop-around-time fast enough to modulate alpha power (requiring <50ms per loop), where it could then be used to trigger individual flashes of photic stimulation following the outlined feedback protocol (see 8.3.1).

8.3.4.1 Recording

Data was streamed to Matlab using custom Python (Python Software Foundation, 2018) and Matlab scripts based on a customised LSL protocol (Kothe, 2014) supplied by Augmind.

8.3.4.2 Preprocessing

During data collection described in section 8.3.1 the data was already detrended using the Matlab detrend function, and bandpass filtered between 1-30 Hz using the Matlab designfilt and filtfilt functions.

8.3.4.3 Analysis

Wavelet convolutions for time-frequency and power analysis were performed as discussed in section 3.3.4.3.

Further, to test for differences between FFT power spectra between photic stimulation conditions (see section 8.3.2) as well as between pre- and post-stimulation intervals, we used a nonparametric permutation-based paired ANOVA correcting for multiple comparisons using the Benjamini & Yekutieli (2001) procedure for controlling the false discovery rate (FDR), using 5000 permutations, as this is appropriate for an alpha level of 0.01 (Manly, 2007).

8.4 Results

First, we calculated the amplitude spectrum of the photic stimulation output in both feedback conditions in order to identify the average photic stimulation frequency for each condition. For this, we averaged across trials for either condition, divided their fast Fourier transform (FFT) spectra by the length of their runtime and plotted the absolute values (Figure 8.2). As can be seen in Figure 8.2, for positive feedback, stimulation frequency tended to be around 9 Hz while for negative feedback stimulation frequency tended to be around 7 Hz. In pre-stimulation intervals average IAF peaks tended towards 9 Hz for both conditions.

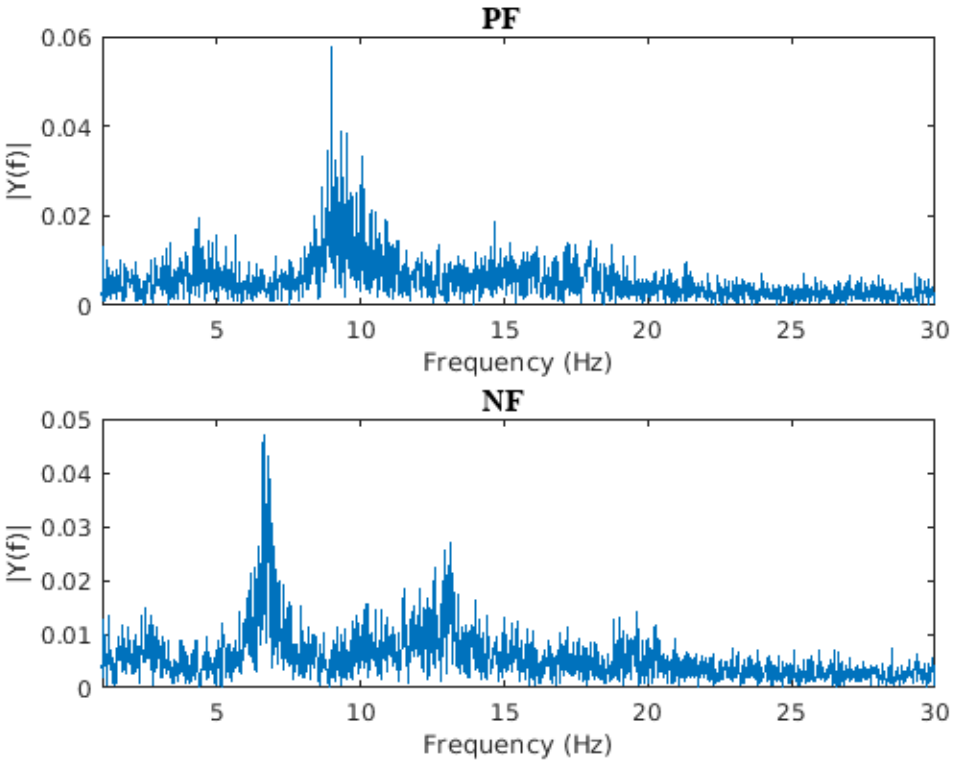

FIGURE 8.2: Grand average amplitude spectrum for positive and negative feedback-based photic stimulation
The top figure shows the grand average amplitude spectrum (across trials, participants, and time) of the photic stimulation signal derived from the positive feedback stimulation (PF) protocol, which triggered a light flash once EEG activity over Oz surpassed a dynamic threshold. The bottom figure shows the same for negative feedback (NF), where a light flash was triggered only if the EEG activity recorded from Oz fell below a dynamic threshold. For the top figure, the signal tended towards 9 Hz, while for the bottom figure, there was a trend towards 7 Hz.

Next, we compared the FFT spectra of pre- and post-stimulation intervals as well as of PR, NR, PF, and NF trials using a permutation-based paired ANOVA, correcting for multiple comparisons using the Benjamini and Yekutieli implementation of the false-discovery rate (FDR) with $p < 0.01$. The only comparison that exhibited significant difference were PF trials and their respective replay conditions (PR), and

NF trials and their associated NR trials (Figure 8.3). Specifically, PF trials show a significantly ($p < 0.01$) greater amplitude at 9 Hz than PR trials, and NF trials show a significantly ($p < 0.01$) decreased amplitude at 9 Hz compared to NR trials.

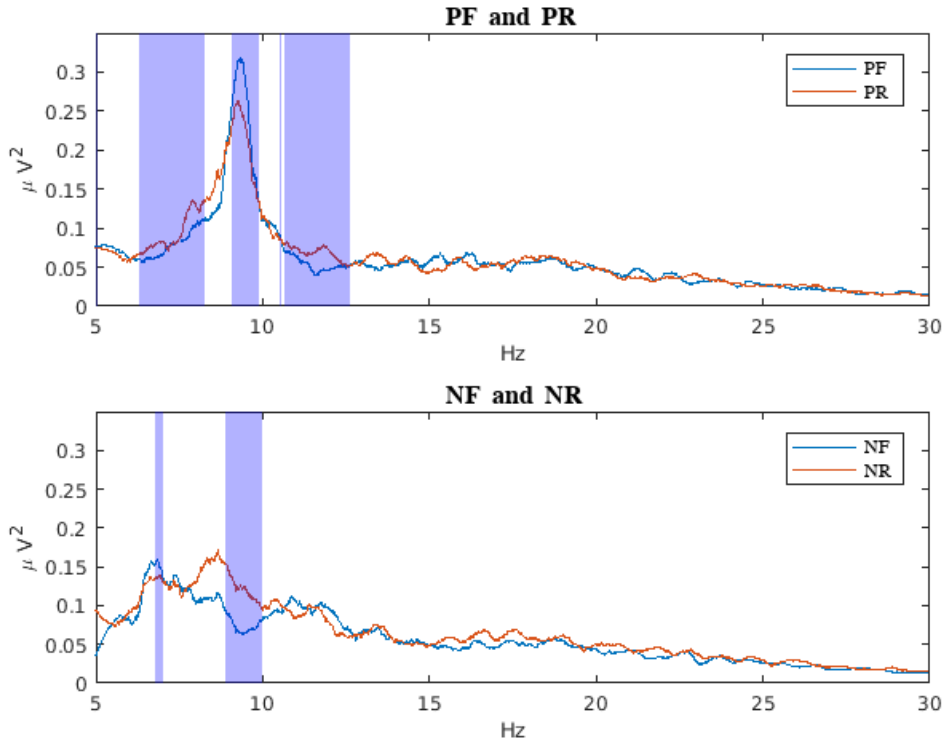

FIGURE 8.3: Average FFT profile for feedback and replay conditions. The top figure contrasts the average FFT (across trials participants, and time) response for positive-feedback (PF) in blue and its respective replay condition (PR) in orange, showing that positive feedback yields a significantly (corrected alpha = 0.0018) stronger alpha peak at 9 Hz than replay trials. The bottom figure shows the average FFT EEG frequency profile for negative-feedback (NF) based photic stimulation trials in blue, and its respective replay condition (NR) in orange, with feedback-based stimulation yielding significantly (corrected alpha = 0.0030) stronger suppression in the alpha domain (8-12 Hz) during stimulation than the replay condition. Areas shaded in blue show frequencies in which feedback and replay conditions differ significantly ($p < 0.01$). To correct for family-wise errors, p-values were adjusted using the Benjamini & Yekutieli implementation of the false-discovery rate (FDR) with $p < 0.01$.

A more comprehensive comparison of mean alpha power (mean 8-12 Hz μV^2) differences between pre- and post photic stimulation intervals in both feedback (PF/NF) and replay (PR/NR) conditions can be seen in Figure 8.4 (for details see table 8.2). Figure 8.4 also shows a comparison of mean alpha power differences between pre- and during-stimulation intervals, and of the differences between feedback and replay conditions. We find that compared to pre-stimulation intervals, during-stimulation alpha power changes were significant for both PF ($p < 0.0001$, $W = 202$, $Z \approx 3.6213$, $r \approx 0.8097$) and PR ($p < 0.0001$, $W = 210$, $Z \approx 3.9199$, $r \approx 0.8765$), with PF overall bringing about a significantly greater alpha power enhancement during stimulation than PR ($p < 0.05$, $W = 164$, $Z \approx 2.2026$, $r \approx 0.4925$). Changes were also significant for NF ($p < 0.0001$, $W = 5$, $Z \approx -3.7333$, $r \approx -0.8348$) with a strong effect size, but did not reach significance in its replay condition NR, with the difference in during-stimulation alpha power suppression between both being strongly significant ($p < 0.0001$, $W = 0$, $Z \approx -3.9199$, $r \approx -0.8765$), with NF reducing alpha activity more effectively during stimulation.

Comparisons	**P**	**W**	**Z**	**R**
NF pre/post	0.1169	63	-1.5680	-0.3506
NR pre/post	0.5016	123	0.6720	0.1503
NF pre/stim	<0.0001	5	-3.7333	-0.8348
NR pre/stim	0.5503	89	-0.5973	-0.1336
PF pre/post	0.4781	124	0.7093	0.1586
PR pre/post	0.6813	94	-0.4107	-0.0918
PF pre/stim	<0.0001	202	3.6213	0.8097
PR pre/stim	<0.0001	210	3.9199	0.8765
NR/NF stim	<0.0001	0	-3.9199	-0.8765
PR/PF stim	0.0276	164	2.2026	0.4925

TABLE 8.2: Significance of changes in photic feedback and replay conditions compared to either pre-stimulation windows or to each other To test whether differences in mean alpha (8-12 Hz) power (μV^2) between pre-, during-, or post-stimulation stimulation intervals exist within or between conditions, we used a two-tailed Wilcoxon signed-rank test. Photic feedback has a significantly stronger effect on mean alpha (8-12 Hz) power (μV^2) than respective replay conditions, as can be seen when comparing mean alpha power changes between both PF and PR ($p < 0.05$) and NF and NR trials ($p < 0.0001$). The table lists significance values under the P column, the W column gives the value of the sign rank test statistic, Z gives the associated z-statistic, and R the effect size calculated with $Z\sqrt{N}$

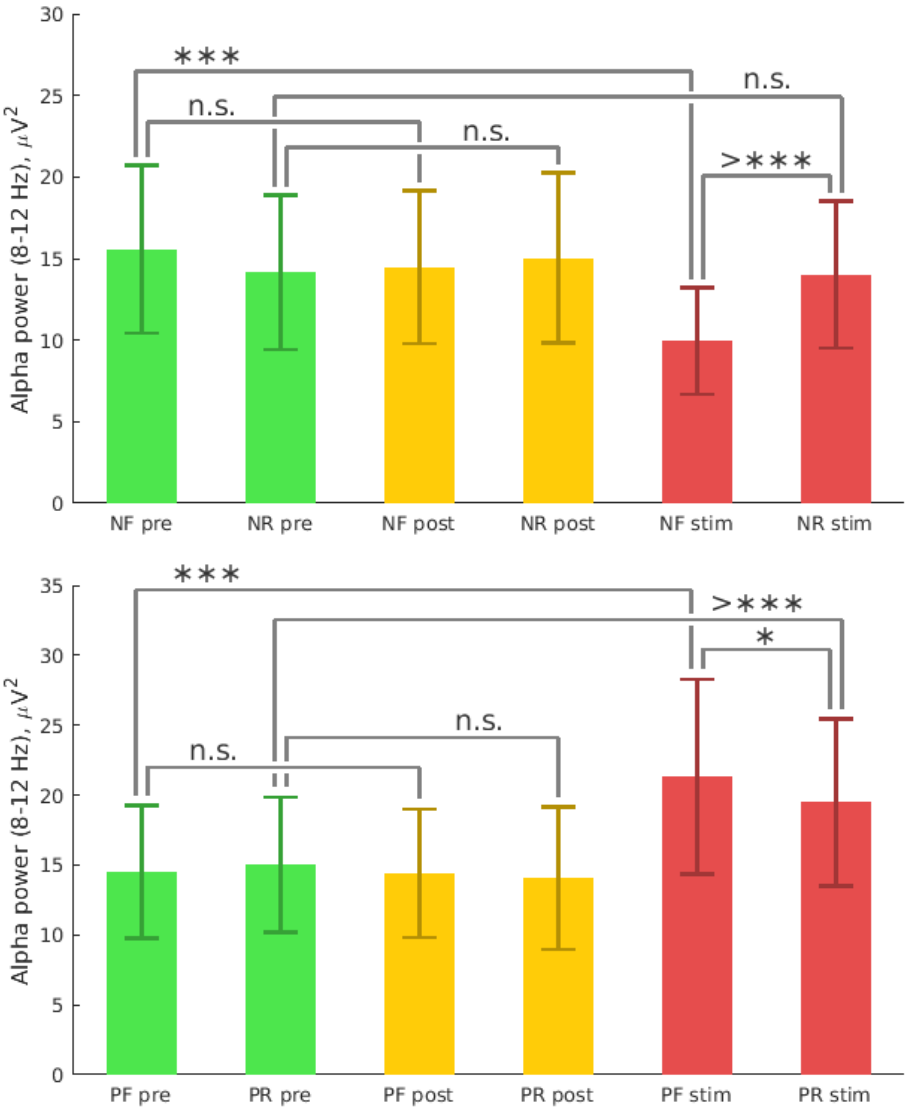

FIGURE 8.4: Grand average alpha power pre, post, and during photic feedback.

To compare mean alpha (8-12 Hz) power (μV^2) between intervals, we used a two-tailed Wilcoxon signed-rank test. * is displayed for $p < 0.05$, ** for $p < 0.01$, *** for $p < 0.001$, and $n.s$ for non-significant results. Instead of ****, >*** is displayed when the maximum measured precision ($p < 0.0001$) has been exceeded. Green bars show pre-stimulation intervals, yellow show post-stimulation intervals, and red during-stimulation intervals for both feedback and replay conditions. Significant ($p < 0.0001$) increases in mean alpha power during photic stimulation can be seen for NF, and both PF and PR trials, with PF trials showing a significantly stronger enhancement effect ($p < 0.05$) than PR trials. The error-bars given show the Vysochanskij–Petunin standard error of mean alpha power measures averaged across frequencies and time points, using 95% confidence intervals.

8.5 Discussion

In this chapter we have built on the findings from Chapter 7 which demonstrated the divergent effects of out-of-phase photic stimulation relative to fixed frequency photic stimulation, by testing a proof-of-concept protocol that makes each flash dependent on a real-time EEG signal. In a "positive feedback" (PF) condition, flashes were triggered when a moving average window of EEG activity surpassed a dynamically set threshold, as to place the flash in line with an activity peak. In a "negative feedback" (NF) condition, conversely, a flash was triggered only when that same moving average window of EEG activity fell below the dynamic threshold, as to place the flash in line with the signals troughs. Replay trials for both positive and negative feedback (PR and NR) then replayed the identical sequence of flashes back to the participants independent of their EEG signal as a control conditions.

Using the same sequence of flashes, PF trials enhanced alpha activity more significantly ($p < 0.05$) than PR trials. During NF, alpha power is suppressed significantly (< 0.0001), with NR showing no significant difference in alpha power between pre- and during-stimulation time windows.

We found that the predominant stimulation rate using positive feedback tended towards 9 Hz. This may be a consequence of 9 Hz being the pre-stimulation IAF dominant in the five participants (on average). Consequently, the dynamic thresholding of the EEG signal would be mostly dependent on the IAF peak, as its reduction or enhancement would constitute a significant source of variation in difference values. The significantly ($p < 0.05$) greater increase in the IAF peak during positive feedback stimulation when compared to their respective replay trials is possibly a consequence of SF and NF forces being additive. Negative feedback, on the other hand, tended to produce a stimulation frequency close to 7 Hz. This is likely due to the SF and NF forces cancelling each other out, shifting the IAF downwards and reducing IAF amplitude.

In summary, we were not just able to enhance alpha power more effectively in PF trials compared to PR trials, but we were also able to suppress alpha power during stimulation using negative thresholding during NF trials, with respective NR trials showing no significant effect on mean alpha power relative to pre-stimulation baseline alpha power levels. These results demonstrate a proof-of-concept, that it is possible to use real-time feedback to alter ongoing oscillations in a direct manner, which can both enhance and diminish these oscillations. Similarly, other frequency bands could be targeted with this feedback-based protocol. This could be achieved by filtering out all but the desired frequency range during data acquisition. This, at least theoretically, allows for a complete modulation (enhancement and suppression) of all frequency bands inside the scope of the loop-around-time of the EEG acquisition method used divided by two (the Nyquist frequency). The current setup would theoretically allow for the modulation of 1-125 Hz. As previously mentioned, this approach has potential clinical application, as a treatment method to normalise aberrant oscillations associated with certain neuropathologies, by either reducing excessive- or enhancing deficient neural frequency components (Ros et al., 2014). For example, excessive beta activity has been associated with Parkinson's (Little and Brown, 2014; Engel and Fries, 2010), and deficient alpha activity with ADHD (Deiber et al., 2019). We, however, want to stress again that, as highlighted in section 2.2.1, that it is unlikely that a neuropathology can be treated by simply modulating a single frequency band, as there is likely interplay between different frequency components, which have to be considered in combination. This setup could be adopted to target more global measures such as inter-frequency-band activity ratios, coherence

or phase-synchrony, although the processing of these would increase loop-around-times and consequently decrease the range of frequencies that can be targeted. In addition, using feedback-based stimulation makes the signal intermittent by definition (which also applies to replay conditions), which our participants reported as being immensely stressful and uncomfortable. Given that, in a clinical context, patients might not respond well to this, we suggest that perhaps oscillating Newton rings - a steady-state motion visual evoked potential (SSMVEP) technique - could be used instead of a photic stimulation lamp, which too evoke a significant SSVEP response but bring about less visual discomfort (Xie et al., 2012) in participants.

8.6 Conclusion

In this chapter, we demonstrated a proof-of-concept that phase-targeted photic stimulation can lead to both enhancement and suppression of brain activity during stimulation. In order to ensure that the results we observed were not just a consequence of the light flash sequence used (independent of the EEG signal), but more specifically as result of the exact flash placement in relation to neural oscillations captured by EEG, we recorded the precise flash sequence in both feedback conditions, and replayed them to the participants in two additional conditions, which we had dubbed "negative replay" and "positive replay" respectively. We found that positive feedback and positive replay both significantly enhanced alpha amplitude during stimulation, stimulating at an average stimulation frequency of 9 Hz. This is due to the average pre-stimulation IAF exhibiting a defined peak at 9 Hz, which meant that stimulation approximated a 9 Hz fixed driving signal as well. Given our findings in Chapters 3 and 4, which demonstrated that photic stimulation at 10 Hz enhanced alpha power during stimulation, the finding that a signal approximating 9 Hz does the same (independent of the EEG signal) should not come as a surprise. However, positive feedback did enhance alpha power to a significantly ($p < 0.05$) greater extent than its otherwise identical positive replay counterpart. This shows that alpha power can be enhanced more effectively if stimulation is phase dependent (and hence dependent on a real-time EEG signal). Negative feedback trials showed a significant suppression of alpha during stimulation at an average of 7 Hz, whereas their respective negative replay trials did not significantly change alpha activity relative to pre-stimulation baseline levels. Together these findings show promise for feedback-based photic stimulation as a potentially more complete method of modulation of alpha activity. Future research should use similar protocols for in-depth large-scale investigations using a greater number of participants, and, if successful, deploy them in a clinical context, to hopefully assist in the correction of aberrant neural oscillations and ease symptoms associated with neuropathologies.

Chapter 9

Conclusion and future directions

Accumulating evidence points to a close relationship between abnormalities in brain oscillations and various neuropathologies, including attention-deficit hyperactivity (ADHD) (Arns et al., 2008), post-traumatric stress disorder (PTSD) (Wahbeh and Oken, 2013), and Parkinson's disease (Little and Brown, 2014; Engel and Fries, 2010). In line with this, some (e.g. Ros et al., 2014) have suggested that non-invasive brain modulation could be applied as a potential treatment method, by normalising pathological oscillations.

One potential technique for this purpose is neurofeedback (NFB), which works by allowing the user to self-regulate their oscillatory patterns by means of guiding an audio-visual representation of their brain activity to a desired goal state. As self-regulation requires a certain amount of skill and conscious control on part of the user, this might not always be a practical solution. For this reason, in this thesis, we have considered photic stimulation as an alternative. Traditionally, it works by applying a fixed rhythmic sequence of light flashes, which entrain brain activity (Herrmann, 2001), and in consequence enhance the power of targeted frequency bands such as alpha (8-12 Hz) (e.g. Walter, 1963; Adrian and Matthews, 1934) in the absence of conscious effort of the participant. By enhancing diminished alpha power, for example, photic stimulation might be able to increase - and hence normalise - deficient alpha power in various neuropathologies. For example, patients with Alzheimer's show diminished alpha power when compared to healthy populations (Babiloni et al., 2009). Here photic stimulation might be applied to potentially alleviate negative symptoms. For other neuropathologies, however, it may be required to reduce excessive brain activity, rather than to enhance the power of deficient frequency bands. For example, patients with Parkinson's generally exhibit excessive beta power when compared to healthy populations (Little and Brown, 2014). Consequently, there is a need to not just enhance, but also to decrease the power of specific frequency components. Photic stimulation, however, has so far only been shown to be able to enhance alpha frequency power during stimulation. This, of course, limits potential clinical application. For this reason, in this thesis we set out to assess the feasibility of an alternative photic stimulation protocol that allows for a complete modulation of alpha (and potentially other frequency bands). In other words, we wanted to develop a protocol that allows to both increase and decrease alpha power by photic stimulation. To set the groundwork for this, we first investigated the effects of fixed - traditional - photic stimulation at 10 Hz, including the immediate post-stimulatory effects on alpha power, as the literature up until this point had focused on the during-stimulation effects of photic driving. As alpha is often seen as reflecting inhibitory processes (Klimesch, Sauseng, and Hanslmayr, 2007), we also assessed changes in connectivity measures as given by phase-lag values (PLVs), and transcranial magnetic stimulation evoked potentials (TEPs) in post-photic stimulation time windows compared to pre-photic stimulation baseline measures. We then turned to our main

objective of assessing the feasibility of a photic stimulation protocol allowing for a more complete control of alpha power (and potentially other frequency bands) by studying the phase-dependency of photic stimulation, as the work by Pikovsky et al. (Pikovsky, Rosenblum, and Kurths, 2001) had given the theoretical basis for the idea that the direction of detuning between an endogenous oscillator and an exogenous stimulus would either lead to additive forcing or a cancelling out of either forces. Finally, we closed with a proof-of-concept of a novel real-time closed-loop-feedback photic stimulation protocol, which either stimulated at the peaks of a real-time processed EEG signal (additive forcing) or placed the flash at the troughs of the signal (canceling it out).

At the start of this thesis, in Chapter 3 and Chapter 4, we sought to replicate findings of previous research (e.g. Walter, 1963), which had shown that repetitive photic stimulation at 10 Hz resulted in entrainment of neural oscillations (Herrmann, 2001), which in turn allowed for shifting (Adrian and Matthews, 1934) and enhancing (Walter, Dovey, and Shipton, 1946) of endogenous alpha rhythms. Beyond finding entrainment in occipital areas (specifically of the visual cortex) by photic stimulation (in line with e.g. Herrmann, 2001), we found evidence of strong scalp-wide entrainment. Further, we showed that entrainment effects exhibited a phase shift from occipital to medial and frontal areas of the scalp, which is in line with the expectation of occipital alpha oscillations behaving as a travelling wave (Zhang et al., 2018), as the phase relationship between the stimulation frequency (SF) of 10 Hz and the entrained natural (or dominant) individual alpha frequency (IAF) flips in polarity from approximating perfect positive coherence over occipital areas, and approximating perfect negative coherence over medial and frontal areas of the scalp. Still, while we found that not all stimulation durations resulted in significant changes in alpha power during stimulation relative to pre-stimulation alpha power baselines, we found that significant alpha power modulation displayed positive enhancement regardless of entrainment polarity across the scalp over frontal, medial and occipital areas, with most pronounced changes being visible over frontal and occipital regions. The fact that during-stimulation alpha power enhancements were almost identical between these areas is noteworthy. In Chapter 3, frontal enhancements were slightly more pronounced, whereas in Chapter 4, enhancements were largest for occipital areas. According to Thut, Schyns and Gross (2011) it is to be expected that effect sizes for brain stimulation should be biggest in the area specialised for the specific stimulation-modularity, which, in the case of photic stimulation, would be the visual cortex. It is consequently surprising that frontal area alpha power was affected (at least) just as much. To some extent this might be due to overall fairly small sample sizes and number of trials employed in individual chapters in this thesis, but if findings from Chapter 3 and Chapter 4 are combined, this argument seems less convincing, as it increases the total amount of evidence that speaks to this observation. Consequently, it seems as if there might be some direct connection between occipital and frontal alpha oscillators which does not extend to the medial sensorimotor rhythm (SMR) oscillators to the same extent. This is something future research could investigate in more detail by, for example, stimulating occipital, frontal, and medial alpha individually through neurofeedback and then observing relative changes in supra-areal alpha power.

Much more surprising to us, however, was the novel finding of strongly pronounced post-stimulation alpha power suppression over occipital, medial, and frontal areas, which had not been reported in the literature before. Even though, on their own, the chapters feature only a small number of participants, taken together the

findings from both Chapters 3 and 4 make a compelling case for the phenomenon of alpha power suppression. We hypothesised that the post-stimulation alpha power suppression occurs as a the result of a homeostatic control mechanism that tries to keep alpha power stable at a set point equilibrium of excitation and inhibition. As evidence for this, we point to the fact that post-stimulation alpha power suppression occurs reliably, even when alpha power was not enhanced significantly during the preceding photic stimulation. Specifically, we propose that counterbalancing of alpha power occurs from the onset of exogenous forcing onwards, and that post-stimulation alpha power suppression is only the effect of removing the exogenous alpha power enhancement while exogenous mechanisms suppress alpha power. The reason for why this is not a transient phenomenon, with alpha power quickly returning to pre-stimulation baseline levels after photic stimulation is removed, may be due to the strength of photic stimulation applied and the absence of endogenous demands for higher alpha power levels. This is backed up by our findings in Chapter 4, that with a shorter stimulation duration and a reduced stimulation strength (luminance) we do find reduced alpha power suppression effects, and the results in Chapter 5, which shows that a task-demand immediately resets post-stimulation alpha power to pre-stimulation baseline levels. Further, by thinking about alpha power as being governed by homeostatic mechanisms, we are building on Stam (2005), who proposes the framework to think of the brain as a multidimensional energy state-space, where each oscillator traverses a number of basins of attraction and repellers (in the form of low-potential valleys and hills), with the latter giving less stability than the former. Once an oscillator finds itself in a low-potential valley, it might get stuck until disruption (either endogenous or exogenous) destabilises the arrangement and forces it to find a new minima. In line with this, research indicates that alpha power is indeed multi-stable (Van de Ville, Britz, and Michel, 2010; Mehrkanoon, Breakspear, and Boonstra, 2014; Ghosh et al., 2008), with any valley in the brain state-space exhibiting its own homeostatic mechanisms. A study by Kluetsch et al. (2014) gives further experimental support in favour of this framework. Specifically, Kluetsch et al. (2014) used neurofeedback to decrease the alpha power of participants with post-traumatic stress disorder (PTSD) symptoms, only to find a strong increase in alpha power immediately following NFB training. This might be due PTSD patients already exhibiting deficient alpha power (Wahbeh and Oken, 2013) compared to healthy populations. In line with this reasoning from homeostatic principles, the during-NFB training induced alpha power decrease was followed with a significant post-NFB alpha power increase beyond pre-stimulation baseline levels and more in line with healthy populations (Kluetsch et al., 2014). A similar finding was made by Deiber et al. (2019), who applied NFB to reduce alpha power in participants with ADHD, who often show deficient alpha power (Arns et al., 2008) when compared to healthy populations, only to find significant increases in alpha power post-NFB training in the ADHD group. With this we are making two main points: First, alpha power is likely governed by homeostatic mechanisms, which we suggest are also the cause of the post-photic stimulation alpha power suppression we found in Chapters 3 4. Second, alpha power is multi-stable, with some minima in the state-space of the brain being more ideal for brain function than others. For example, lower alpha power in PTSD and ADHD does not self-correct in absence of exogenous forcing, so it is stable. After exogenous forcing, however, alpha is stable at a different minima, exhibiting greater alpha power (Kluetsch et al., 2014; Deiber et al., 2019). This points to the potential usefulness of photic stimulation

for clinical application: disrupting stable but suboptimal brain dynamics and pushing brain activity towards oscillatory patterns more closely resembling healthy populations in order to alleviate symptoms associated with various neuropathologies. Although speculative, if photic stimulation could be used to dislodge pathological oscillations stuck in suboptimal local minima of the BSAP, then we might observe long-lasting normalisations of EEG frequency profiles following photic stimulation of participants with abnormal EEG spectra. In this way, rather than brain activity returning to its previous default state after stimulation offset, it would settle in a new minima in closer approximation of normal activity. The degree of forcing necessary for this might depend on the depth of trough of the BSAP minima in which the oscillator got stuck, meaning that this would be increasingly difficult as the oscillator approaches a global minima as represented by normal ranges of oscillatory activity. We thus speculate that in the absence of sufficiently strong forcing or regular repeated exposure to photic stimulation (resulting in greater cumulative forcing) brain activity will eventually return to its previous default state - perhaps driven by endogenous demands - while pathological activity might perhaps be normalised in a more long-lasting manner.

Next, we pondered the question as to what functional impact post-stimulation alpha power suppression might have. As alpha is often seen as reflecting inhibitory processes (Klimesch, Sauseng, and Hanslmayr, 2007), we looked at changes in connectivity as indexed by phase-lag-values (PLV), and found that, during alpha power suppression, connectivity is increased significantly across the scalp. To further validate whether this finding represented a functional shift in brain function compared to baseline conditions, we next investigated potential alpha power suppression effects on a measure of cognitive processing using a visual reaction time (RT) test. This technique was chosen, as RT performance had previously been linked to pre-trial alpha power, with higher alpha power being predictive of faster reaction times (Nenert et al., 2012; Callaway and Yeager, 1960; Bompas et al., 2015; Haig and Gordon, 1998; Bastiaansen et al., 2001). Consequently, we reasoned that post-stimulation alpha power suppression should also bring about a reduction of reaction times (relative to baseline reaction time speeds). To control for the effects photic stimulation may have on participants outside of frequency effects specific to the stimulation frequency of 10 Hz, we decided to employ a control condition of 3 Hz photic stimulation. Our results showed no significant change in RT speeds after photic stimulation in either condition. In addition, much to our surprise, while 10 Hz photic stimulation created significant alpha power enhancement during stimulation, we found that 3 Hz photic stimulation did so too, perhaps as a consequence of a harmonic response at around 9 Hz. Both conditions also featured significant alpha power suppression during RT trials post-photic stimulation across the scalp. Effect sizes for that suppression, however, were at best just over a fifth of those we found for the same stimulation setup and length in Chapter 3, which gave us reason to think that the attentional demands of the RT task may have to some extent negated the post-stimulation alpha power suppression. Our finding of a lack of alpha power suppression to the same degree as our investigation in Chapter 3 may also explain why we failed to find significant changes in RT speeds between conditions or compared to baseline RT measures, as greater alpha power suppression in line with findings in Chapter 3 may very well induce changes in RT speeds.

To test whether conscious attention to the RT task was to blame for the reduction in alpha power suppression effect size, we ran a follow-up investigation using

two participants, in which we made two major changes to the experimental protocol: First, we removed the baseline condition, in which participants engaged with RT tests in absence of photic stimulation, and instead presented two baseline conditions - one specific to the experimental condition, where we used photic stimulation at 10 Hz, and one specific to the control condition, using 3 Hz. With this we wanted to reduce the chances of alpha power level drift throughout the experiment to give a false positive of alpha power suppression. Secondly, we also added in two additional conditions, in which, both for 10 Hz and 3 Hz photic stimulation, participants were asked to ignore subsequent RT trials. With this protocol, we found that alpha power suppression following 3 Hz photic stimulation was now no longer significant at all when participants engaged with the RT task, and restricted to occipital and medial areas when they were told to ignore RT trials. When averages were taken of the entire RT epoch of both baseline and post-stimulation intervals, however, not a single case of 3 Hz photic stimulation resulted in significant post-stimulation alpha power suppression. 10 Hz photic stimulation, on the other hand, still showed significant post-stimulation alpha power suppression even when participants were asked to attend to the RT task. Effect sizes of post-photic stimulation alpha power suppression when attending RT tasks, however, were still very small and the reduction in reaction time speeds did not reach significance. When participants, however, were asked to ignore RT trials following 10 Hz stimulation, alpha power suppression was again strongly significant, with an increase in effect sizes, which were now over one half the size of those reported in Chapter 3. Overall, the finding that alpha power suppression is strongly significant only in the absence of task-demands implies that conscious attention might negate alpha power suppression. If true, this would make it difficult to investigate potential cognitive effects alpha power suppression might have on potential cognitive correlates, as any test of it would make alpha power suppression less pronounced or even void. It is important to stress that given the very small sample size of this follow-up investigation these results should be treated with caution. For this reason, we encourage attempts to replicate these results using a greater number of participants. In addition, task-demands negating alpha power suppression might indicate that brain function returned to default state after the intervention. This suggests that to affect behavioural measures either greater stimulation intensity or longer repeated exposure to photic stimulation might be necessary.

Following on from the results of Chapter 5, we had reasons to believe that conscious engagement with a task might at least partially negate the effects of post-stimulation alpha power suppression. Therefore we decided to investigate if we could observe the effects of alpha power suppression at the neural level. Specifically, since we found evidence of alpha power suppression enhancing neural connectivity, we decided to investigate if alpha power suppression would lead to enhanced neural signal propagation, as measured via transcranial magnetic stimulation evoked potentials (TEPs). For this, we administered 40 transcranial magnetic stimulation (TMS) pulses both before and after photic stimulation at 10 Hz (experimental condition) and 3 Hz (control condition). In line with the follow-up investigation to our RT study (Chapter 4), we found that alpha power suppression during TMS pulse administration was significantly more pronounced across the scalp following photic stimulation at 10 Hz compared to 3 Hz stimulation. This greater degree of post-stimulation alpha power suppression translated to significant changes in TEP amplitudes in the experimental condition of 10 Hz stimulation over medial and occipital areas, with no significant changes in the control condition (using 3 Hz) relative

to pre-stimulation baseline TEPs. There was no significant change in frontal TEP amplitude in either condition. We argue that this finding is important for three reasons: First, it shows that post-stimulation alpha power suppression does indeed affect neural signal propagation in a manner that is both measurable and significant. Second, it implies that there might be a minimum amount of alpha power suppression necessary before its effect can be detected, as significant (but lesser, compared to post-10 Hz photic stimulation alpha power suppression) alpha power suppression following 3 Hz photic stimulation did not result in significant TEP amplitude changes. This is interesting also with a look back at our findings from Chapter 4, where significant, but comparably modest, post-stimulation alpha power suppression did not bring about changes in RT speeds. As we speculated then, perhaps greater post-stimulation alpha power suppression would have resulted in a significant change in RT speeds. Given this, our finding is of more general importance to the study of alpha, as our finding of alpha power suppression enhancing TEP amplitude further supports the role of alpha activity in inhibitory processes. This also points to photic stimulation as a means to study the cognitive correlates of oscillatory brain dynamics in general, as photic stimulation might allow researchers to study potential frequency band functions by enhancing and suppressing their power and then testing changes in a number of cognitive abilities.

Both for normalising brain function and to use photic stimulation as a research device, it would be useful to be able to not just enhance alpha power during stimulation, but also to suppress it while stimulation is applied. For this reason, we investigated the impact of in- compared to out-of-phase photic stimulation, by placing individual flashes in or out of sync with pre-entrained endogenous neural oscillations. Our goal was to leverage the potential differing responses of a self-sustained oscillator to exogenous perturbation based on their phase difference - as described by Pikovsky et al. (2001) - to allow for a more complete control of alpha oscillations. The findings of Chapter 7 show that there is a significant difference in ERP response to out-of-phase relative to in-phase stimulation using a fixed stimulation frequency of 10 Hz. Specifically, after first entraining neural oscillations using a 10 Hz photic signal, we created a phase shift in photic stimulation by inserting either one additional off-cycle or one added on-cycle to the stimulation 10 Hz stimulation signal. When an additional off-cycle was added to shift the phase of the stimulation frequency, the resulting ERP response showed a significant increase in amplitude between 100-250 ms after phase shift onset, with the ERP oscillation speeding up - possibly to catch up with the phase shifted stimulation frequency. If another on-cycle was added to achieve the phase shift, the opposite happened. That is, it caused a significant decrease in ERP amplitude compared to baseline ERP responses to fixed in-phase stimulation from 100-250 ms after phase shift onset, with the ERP oscillation slowing down until it synchronised itself with the stimulation signal. Although the precise dynamics underlying this difference in response still need further investigation, it demonstrates that it is possible to, depending on flash placement, bring about both enhancement and suppression of brain activity during stimulation, hence making a more complete control of alpha at least theoretically feasible.

Finally, given the finding in Chapter 5, that, depending on flash placement in relation to endogenous neural oscillations, both suppression or enhancement of ERP amplitude could come about, we built and tested a proof-of-concept photic stimulation protocol which made every flash dependent on a real-time electroencephalogram (EEG) signal, as to place flashes in line with its peaks and troughs. Through

this, we aimed at bringing about both increases and decreases in the EEG signal amplitude - specifically in its alpha component. To ensure that changes in the signal as a result of feedback-based stimulation were indeed a consequence of its signal specificity, that is, of the flash placement relative to brain activity (EEG) peaks and troughs, we recorded the precise sequence and timing of flashes during feedback conditions and then replayed those back to the participants. Our results show that trials where a peak in the signal triggered a flash brought about significant enhancement of alpha activity, with their replay trials doing the same, although replay trials resulted in significantly weaker alpha power enhancement than feedback-based trials. The fact that replay trials for "peak-based" positive feedback photic stimulation brought about alpha power enhancement during stimulation as well is not surprising, as average (across participants and trials) pre-stimulation IAF tended towards 9 Hz, which the photic signal approximated during stimulation. This means that, in replay conditions, participants were stimulated at roughly 9 Hz (with an intermittent signal), which would, similarly to the fixed 10 Hz signal we used in Chapters 3 4 entrain and enhance alpha power. That "positive feedback" trials, in which flashes were triggered by peaks in the processed real-time EEG signal, enhanced alpha power to a significantly greater extent is also expected, as this would make SF and NF forces additive. Conversely, feedback conditions where a trough in the signal triggered a flash brought about a significant decrease in alpha amplitude relative to pre-stimulation baselines, whereas there was no significant change in alpha power when that same sequence of flashes was played back to the participant independent of their brain activity as measured by EEG. Here, the forces of the SF and NF cancelled each other out in the feedback condition, with the resulting signal having significantly diminished alpha power. The stimulation frequency in this condition approximated 7 Hz, as the IAF peak was reduced in amplitude and shifted downwards from a pre-stimulation measure of 9 Hz. This is the first time photic stimulation has reliably brought about significant alpha power suppression during stimulation. The fact that the replay trials of negative feedback trials did not bring about any significant changes in alpha power compared to pre-stimulation windows is further supporting the effectiveness of real-time feedback photic stimulation. While there was no difference between pre- and post-stimulation alpha power for any condition, this is a hugely promising result that deserves further study, as it holds potential for treatment of neuropathologies as well as for the study of potential relationships between neural oscillations and their cognitive correlates.

In conclusion to this thesis, we want to recapitulate our initial objectives, to what degree we met them, reiterate the novelty of our main findings, and suggest where future research could put its focus in order to build on our work. This thesis set out to investigate the during- and post-stimulation effects of photic stimulation, and further test the feasibility of a new photic stimulation protocol allowing for more complete modulation of brain activity, where traditional fixed stimulation only allows for enhancement of frequency band power. We, for the first time, show that the alpha power enhancement during photic stimulation is followed by significant alpha power suppression across occipital, medial, and frontal areas of the scalp. We propose that this is due to homeostatic mechanisms, with the post-stimulation alpha power suppression being dependent on length of photic stimulation, luminance, and the presence of task-demands that bring about endogenous resetting of alpha power to pre-stimulation baselines. We also, for the first time, show that alpha power suppression has functional relevance, as it affects neural signal propagation as shown by significantly increased TEP amplitudes during post-photic stimulation alpha power

suppression time-windows compared to pre-photic stimulation TEP responses. This greater neural connectivity during alpha power suppression is also shown by greater PLV values. Further, we, for the first time, show phase dependency of 10 Hz entrained ERP responses for photic stimulation, with in- or out-of-phase stimulation bringing about significant differences in ERP amplitude and speed. Specifically, we show that ERP amplitude can be increased or decreased, and sped up or slowed down depending on flash placement in relation to ERP phase. Most importantly, building on this finding, and in line with Pikovsky et al. (2001), we show that using a real-time closed-loop feedback photic stimulation protocol, we can more effectively enhance alpha power by making the NF and SF forces additive by aligning individual flashes with peaks in a real-time EEG signal. Further, by making the NF and SF forces cancel each other out through aligning flashes with troughs in the real-time EEG signal we can also significantly decrease alpha power during stimulation, which, up until now, had not been achieved. With this, we have demonstrated a more complete control of alpha - and potentially all other frequency bands up to 125 Hz - and hence achieved the aim of this thesis. This photic stimulation protocol could be used to normalise pathological oscillations to alleviate symptoms of neuropathologies, or to enhance or suppress frequency band activity in order to then study their functional significance. We hope that other researchers will build on the foundation we have laid out in order to provide a noninvasive means of brain modulation for the purpose of the scientific study of function or cognitive correlates of neural oscillations, the correction of aberrant oscillations in neuropathologies and for general brain function optimisation in healthy populations.

Bibliography

Adrian, E. D. and B. H. C. Matthews (1934). "THE BERGER RHYTHM: POTENTIAL CHANGES FROM THE OCCIPITAL LOBES IN MAN". In: *Brain* 57.4, pp. 355–385. ISSN: 0006-8950. DOI: 10.1093/brain/57.4.355. URL: https://academic.oup.com/brain/article-lookup/doi/10.1093/brain/57.4.355.

Arns, Martijn et al. (2008). "EEG phenotypes predict treatment outcome to stimulants in children with ADHD." In: *Journal of integrative neuroscience* 7.3, pp. 421–38. ISSN: 0219-6352. URL: http://www.ncbi.nlm.nih.gov/pubmed/18988300.

Babiloni, C et al. (2009). "Hippocampal volume and cortical sources of EEG alpha rhythms in mild cognitive impairment and Alzheimer disease". In: *NeuroImage* 44.1, pp. 123–135. ISSN: 10538119. DOI: 10.1016/j.neuroimage.2008.08.005. URL: http://linkinghub.elsevier.com/retrieve/pii/S1053811908009105.

Baddeley (2000). "The episodic buffer: a new component of working memory?" In: *Trends in cognitive sciences* 4.11, pp. 417–423. ISSN: 1879-307X. URL: http://www.ncbi.nlm.nih.gov/pubmed/11058819.

Baddeley, Alan (1996). "Exploring the Central Executive". In: *The Quarterly Journal of Experimental Psychology Section A* 49.1, pp. 5–28. ISSN: 0272-4987. DOI: 10.1080/713755608. URL: http://journals.sagepub.com/doi/10.1080/713755608.

— (2012). "Working Memory: Theories, Models, and Controversies". In: *Annual Review of Psychology* 63.1, pp. 1–29. ISSN: 0066-4308. DOI: 10.1146/annurev-psych-120710-100422. URL: http://www.annualreviews.org/doi/10.1146/annurev-psych-120710-100422.

Bak, Per, Chao Tang, and Kurt Wiesenfeld (1988). "Self-organized criticality". In: *Physical Review A* 38.1, pp. 364–374. ISSN: 0556-2791. DOI: 10.1103/PhysRevA.38.364. URL: https://link.aps.org/doi/10.1103/PhysRevA.38.364.

Bastiaansen, M C et al. (2001). "Event-related desynchronization during anticipatory attention for an upcoming stimulus: a comparative EEG/MEG study." In: *Clinical neurophysiology : official journal of the International Federation of Clinical Neurophysiology* 112.2, pp. 393–403. ISSN: 1388-2457. URL: http://www.ncbi.nlm.nih.gov/pubmed/11165546.

Becerra, J. et al. (2006). "Follow-Up Study of Learning-Disabled Children Treated with Neurofeedback or Placebo". In: *Clinical EEG and Neuroscience* 37.3, pp. 198–203. ISSN: 1550-0594. DOI: 10.1177/155005940603700307. URL: http://www.ncbi.nlm.nih.gov/pubmed/16929704http://journals.sagepub.com/doi/10.1177/155005940603700307.

Benedek, Mathias et al. (2014). "Alpha power increases in right parietal cortex reflects focused internal attention". In: *Neuropsychologia* 56, pp. 393–400. ISSN: 00283932. DOI: 10.1016/j.neuropsychologia.2014.02.010. URL: http://www.ncbi.nlm.nih.gov/pubmed/24561034http://www.pubmedcentral.nih.gov/articlerender.fcgi?artid=PMC3989020https://linkinghub.elsevier.com/retrieve/pii/S0028393214000621.

Berger, Hans (1929). "Über das Elektrenkephalogramm des Menschen". In: *Archiv für Psychiatrie und Nervenkrankheiten* 87.1, pp. 527–570. ISSN: 0003-9373. DOI: 10.1007/BF01797193. URL: http://link.springer.com/10.1007/BF01797193.

Blair, R C and W Karniski (1993). "An alternative method for significance testing of waveform difference potentials." In: *Psychophysiology* 30.5, pp. 518–24. ISSN: 0048-5772. URL: http://www.ncbi.nlm.nih.gov/pubmed/8416078.

Bokil, Hemant et al. (2010). "Chronux: A platform for analyzing neural signals". In: *Journal of Neuroscience Methods* 192.1, pp. 146–151. ISSN: 01650270. DOI: 10.1016/j.jneumeth.2010.06.020. URL: http://www.ncbi.nlm.nih.gov/pubmed/20637804http://www.pubmedcentral.nih.gov/articlerender.fcgi?artid=PMC2934871https://linkinghub.elsevier.com/retrieve/pii/S0165027010003444.

Bompas, Aline et al. (2015). "The contribution of pre-stimulus neural oscillatory activity to spontaneous response time variability". In: *NeuroImage* 107, pp. 34–45. ISSN: 10538119. DOI: 10.1016/j.neuroimage.2014.11.057. URL: http://www.ncbi.nlm.nih.gov/pubmed/25482267http://www.pubmedcentral.nih.gov/articlerender.fcgi?artid=PMC4306532https://linkinghub.elsevier.com/retrieve/pii/S1053811914009872.

Bullmore, Ed and Olaf Sporns (2009). "Complex brain networks: graph theoretical analysis of structural and functional systems". In: *Nature Reviews Neuroscience* 10.3, pp. 186–198. ISSN: 1471-003X. DOI: 10.1038/nrn2575. URL: http://www.ncbi.nlm.nih.gov/pubmed/19190637http://www.nature.com/articles/nrn2575.

Busch, Niko A, Julien Dubois, and Rufin VanRullen (2009). "The phase of ongoing EEG oscillations predicts visual perception." In: *The Journal of neuroscience : the official journal of the Society for Neuroscience* 29.24, pp. 7869–76. ISSN: 1529-2401. DOI: 10.1523/JNEUROSCI.0113-09.2009. URL: http://www.ncbi.nlm.nih.gov/pubmed/19535598.

Buyck, Inez and Jan R. Wiersema (2015). "Task-related electroencephalographic deviances in adults with attention deficit hyperactivity disorder." In: *Neuropsychology* 29.3, pp. 433–444. ISSN: 1931-1559. DOI: 10.1037/neu0000148. URL: http://doi.apa.org/getdoi.cfm?doi=10.1037/neu0000148.

Buzsaki, G. and Andreas Draguhn (2004). "Neuronal Oscillations in Cortical Networks". In: *Science* 304.5679, pp. 1926–1929. ISSN: 0036-8075. DOI: 10.1126/science.1099745. URL: http://www.ncbi.nlm.nih.gov/pubmed/15218136http://www.sciencemag.org/cgi/doi/10.1126/science.1099745.

Buzsáki, György, Costas A. Anastassiou, and Christof Koch (2012). "The origin of extracellular fields and currents — EEG, ECoG, LFP and spikes". In: *Nature Reviews Neuroscience* 13.6, pp. 407–420. ISSN: 1471-003X. DOI: 10.1038/nrn3241. URL: http://www.ncbi.nlm.nih.gov/pubmed/22595786http://www.pubmedcentral.nih.gov/articlerender.fcgi?artid=PMC4907333http://www.nature.com/articles/nrn3241.

Buzsaki, G. (2006). *Rhythms of the brain*. Oxford University Press, p. 448. ISBN: 9780199828234. URL: https://global.oup.com/academic/product/rhythms-of-the-brain-9780199828234?cc=gb{\&}lang=en{\&}.

Callaway, E and C L Yeager (1960). "Relationship between reaction time and electroencephalographic alpha phase." In: *Science (New York, N.Y.)* 132.3441, pp. 1765–6. ISSN: 0036-8075. DOI: 10.1126/SCIENCE.132.3441.1765. URL: http://www.ncbi.nlm.nih.gov/pubmed/13689987.

Carlson, T. et al. (2013). "Representational dynamics of object vision: The first 1000 ms". In: *Journal of Vision* 13.10, pp. 1–1. ISSN: 1534-7362. DOI: 10.1167/13.10.1. URL: http://jov.arvojournals.org/Article.aspx?doi=10.1167/13.10.1.

Cauchoix, Maxime et al. (2014). "The Neural Dynamics of Face Detection in the Wild Revealed by MVPA". In: *Journal of Neuroscience* 34.3, pp. 846–854. ISSN: 0270-6474.

DOI: 10.1523/JNEUROSCI.3030-13.2014. URL: http://www.ncbi.nlm.nih.gov/pubmed/24431443.

Choi, Sung Won et al. (2011). "Is Alpha Wave Neurofeedback Effective with Randomized Clinical Trials in Depression? A Pilot Study". In: *Neuropsychobiology* 63.1, pp. 43–51. ISSN: 1423-0224. DOI: 10.1159/000322290. URL: https://www.karger.com/Article/FullText/322290.

Cohen, Michael X (2017). "Where Does EEG Come From and What Does It Mean?" In: *Trends in Neurosciences* 40.4, pp. 208–218. ISSN: 01662236. DOI: 10.1016/j.tins.2017.02.004. URL: http://www.ncbi.nlm.nih.gov/pubmed/28314445https://linkinghub.elsevier.com/retrieve/pii/S0166223617300243.

Cohen, Mike X. (2014). *Analyzing neural time series data : theory and practice*, p. 578. ISBN: 9780262019873. URL: https://mitpress.mit.edu/books/analyzing-neural-time-series-data.

Deiber, Marie-Pierre et al. (2019). "Linking alpha oscillations, attention and inhibitory control in adult ADHD with EEG neurofeedback". In: *bioRxiv*, p. 689398. DOI: 10.1101/689398. URL: https://www.biorxiv.org/content/10.1101/689398v1?ct=.

Delorme, Arnaud and Scott Makeig (2004). "EEGLAB: an open source toolbox for analysis of single-trial EEG dynamics including independent component analysis". In: *Journal of Neuroscience Methods* 134.1, pp. 9–21. ISSN: 01650270. DOI: 10.1016/j.jneumeth.2003.10.009. URL: http://www.ncbi.nlm.nih.gov/pubmed/15102499http://linkinghub.elsevier.com/retrieve/pii/S0165027003003479.

Engel, Andreas K and Pascal Fries (2010). "Beta-band oscillations—signalling the status quo?" In: *Current opinion in neurobiology* 20.2, pp. 156–165.

Evans, James R. (2007). *Handbook of neurofeedback : dynamics and clinical applications*. Haworth Medical Press, p. 378. ISBN: 0789033607.

Fairchild, M. D. and M. B. Sterman (1974). *Unilateral Sensory-Motor-Rhythm (SMR) Training in Cats: A Basis for Testing Neurophysiological and Behavioral Effects of Monomethylhydrazine (MMH)*. Tech. rep. US Dept of the Air Force. DOI: 10.21236/ADA011578. URL: http://www.dtic.mil/docs/citations/ADA011578.

Fetz, E E (1969). "Operant conditioning of cortical unit activity." In: *Science (New York, N.Y.)* 163.3870, pp. 955–8. ISSN: 0036-8075. URL: http://www.ncbi.nlm.nih.gov/pubmed/4974291.

Fingelkurts, Alexander A. et al. (2006). "Stability, reliability and consistency of the compositions of brain oscillations". In: *International Journal of Psychophysiology* 59.2, pp. 116–126. ISSN: 01678760. DOI: 10.1016/j.ijpsycho.2005.03.014. URL: http://www.ncbi.nlm.nih.gov/pubmed/15946755http://linkinghub.elsevier.com/retrieve/pii/S0167876005001017.

Fink, Andreas and Mathias Benedek (2014). "EEG alpha power and creative ideation." In: *Neuroscience and biobehavioral reviews* 44.100, pp. 111–23. ISSN: 1873-7528. DOI: 10.1016/j.neubiorev.2012.12.002. URL: http://www.ncbi.nlm.nih.gov/pubmed/23246442http://www.pubmedcentral.nih.gov/articlerender.fcgi?artid=PMC4020761.

Freyer, Frank et al. (2009). "Bistability and non-Gaussian fluctuations in spontaneous cortical activity." In: *The Journal of neuroscience : the official journal of the Society for Neuroscience* 29.26, pp. 8512–24. ISSN: 1529-2401. DOI: 10.1523/JNEUROSCI.0754-09.2009. URL: http://www.ncbi.nlm.nih.gov/pubmed/19571142.

Freyer, Frank et al. (2011). "Biophysical mechanisms of multistability in resting-state cortical rhythms." In: *The Journal of neuroscience : the official journal of the Society for*

Neuroscience 31.17, pp. 6353–61. ISSN: 1529-2401. DOI: 10.1523/JNEUROSCI.6693-10.2011. URL: http://www.ncbi.nlm.nih.gov/pubmed/21525275.

Ghaziri, Jimmy et al. (2013). "Neurofeedback Training Induces Changes in White and Gray Matter". In: *Clinical EEG and Neuroscience* 44.4, pp. 265–272. ISSN: 1550-0594. DOI: 10.1177/1550059413476031. URL: http://www.ncbi.nlm.nih.gov/pubmed/23536382http://journals.sagepub.com/doi/10.1177/1550059413476031.

Ghosh, Anandamohan et al. (2008). "Noise during Rest Enables the Exploration of the Brain's Dynamic Repertoire". In: *PLoS Computational Biology* 4.10. Ed. by Karl J. Friston, e1000196. ISSN: 1553-7358. DOI: 10.1371/journal.pcbi.1000196. URL: https://dx.plos.org/10.1371/journal.pcbi.1000196.

Giraud, Anne-Lise and David Poeppel (2012). "Cortical oscillations and speech processing: emerging computational principles and operations". In: *Nature Neuroscience* 15.4, pp. 511–517. ISSN: 1097-6256. DOI: 10.1038/nn.3063. URL: http://www.ncbi.nlm.nih.gov/pubmed/22426255http://www.pubmedcentral.nih.gov/articlerender.fcgi?artid=PMC4461038http://www.nature.com/articles/nn.3063.

Gratton, Gabriele et al. (1992). "Functional correlates of a three-component spatial model of the alpha rhythm". In: *Brain Research* 582.1, pp. 159–162. ISSN: 0006-8993. DOI: 10.1016/0006-8993(92)90332-4. URL: https://www.sciencedirect.com/science/article/pii/0006899392903324.

Groppe, David M., Thomas P. Urbach, and Marta Kutas (2011). "Mass univariate analysis of event-related brain potentials/fields I: A critical tutorial review". In: *Psychophysiology* 48.12, pp. 1711–1725. ISSN: 00485772. DOI: 10.1111/j.1469-8986.2011.01273.x. URL: http://doi.wiley.com/10.1111/j.1469-8986.2011.01273.x.

Gross, Joachim et al. (2013). "Speech Rhythms and Multiplexed Oscillatory Sensory Coding in the Human Brain". In: *PLoS Biology* 11.12. Ed. by David Poeppel, e1001752. ISSN: 1545-7885. DOI: 10.1371/journal.pbio.1001752. URL: http://dx.plos.org/10.1371/journal.pbio.1001752.

Gruzelier, John H. (2014). "EEG-neurofeedback for optimising performance. I: A review of cognitive and affective outcome in healthy participants". In: *Neuroscience & Biobehavioral Reviews* 44, pp. 124–141. ISSN: 01497634. DOI: 10.1016/j.neubiorev.2013.09.015. URL: http://www.ncbi.nlm.nih.gov/pubmed/24125857https://linkinghub.elsevier.com/retrieve/pii/S0149763413002248.

Haig, A R and E Gordon (1998). "Prestimulus EEG alpha phase synchronicity influences N100 amplitude and reaction time." In: *Psychophysiology* 35.5, pp. 591–5. ISSN: 0048-5772. URL: http://www.ncbi.nlm.nih.gov/pubmed/9715102.

Hanslmayr, Simon et al. (2011). "The role of alpha oscillations in temporal attention". In: *Brain Research Reviews* 67.1-2, pp. 331–343. ISSN: 01650173. DOI: 10.1016/j.brainresrev.2011.04.002. URL: http://www.ncbi.nlm.nih.gov/pubmed/21592583https://linkinghub.elsevier.com/retrieve/pii/S0165017311000233.

Hebb, DO (1949). *The organization of behavior. A neuropsychological theory*. URL: https://pure.mpg.de/rest/items/item{_}2346268/component/file{_}2346267/content.

Héliot, R et al. (2010). "Learning in Closed-Loop Brain–Machine Interfaces: Modeling and Experimental Validation". In: *IEEE Transactions on Systems, Man, and Cybernetics, Part B (Cybernetics)* 40.5, pp. 1387–1397. ISSN: 1083-4419. DOI: 10.1109/TSMCB.2009.2036931. URL: http://ieeexplore.ieee.org/document/5353750/.

Hellyer, Peter J et al. (2014). "The control of global brain dynamics: opposing actions of frontoparietal control and default mode networks on attention." In: *The Journal*

of neuroscience : the official journal of the Society for Neuroscience 34.2, pp. 451–61. ISSN: 1529-2401. DOI: 10.1523/JNEUROSCI.1853-13.2014. URL: http://www.ncbi.nlm.nih.gov/pubmed/24403145http://www.pubmedcentral.nih.gov/articlerender.fcgi?artid=PMC3870930.

Herrmann, Christoph S. (2001). "Human EEG responses to 1-100 Hz flicker: resonance phenomena in visual cortex and their potential correlation to cognitive phenomena". In: *Experimental Brain Research* 137.3-4, pp. 346–353. DOI: 10.1007/s002210100682. URL: http://link.springer.com/10.1007/s002210100682.

Herrmann, Christoph S. et al. (2016). "EEG oscillations: From correlation to causality". In: *International Journal of Psychophysiology* 103, pp. 12–21. ISSN: 01678760. DOI: 10.1016/j.ijpsycho.2015.02.003. URL: http://www.ncbi.nlm.nih.gov/pubmed/25659527https://linkinghub.elsevier.com/retrieve/pii/S0167876015000331.

Hesse, Janina and Thilo Gross (2014). "Self-organized criticality as a fundamental property of neural systems". In: *Frontiers in Systems Neuroscience* 8, p. 166. ISSN: 1662-5137. DOI: 10.3389/fnsys.2014.00166. URL: http://journal.frontiersin.org/article/10.3389/fnsys.2014.00166/abstract.

Hills, Thomas T., Peter M. Todd, and Robert L. Goldstone (2010). "The central executive as a search process: Priming exploration and exploitation across domains." In: *Journal of Experimental Psychology: General* 139.4, pp. 590–609. ISSN: 1939-2222. DOI: 10.1037/a0020666. URL: http://www.ncbi.nlm.nih.gov/pubmed/21038983http://www.pubmedcentral.nih.gov/articlerender.fcgi?artid=PMC2974337http://doi.apa.org/getdoi.cfm?doi=10.1037/a0020666.

Hodgkin, A L and A F Huxley (1952). "A quantitative description of membrane current and its application to conduction and excitation in nerve." In: *The Journal of physiology* 117.4, pp. 500–44. ISSN: 0022-3751. URL: http://www.ncbi.nlm.nih.gov/pubmed/12991237http://www.pubmedcentral.nih.gov/articlerender.fcgi?artid=PMC1392413.

Hutcheon, B and Y Yarom (2000). "Resonance, oscillation and the intrinsic frequency preferences of neurons." In: *Trends in neurosciences* 23.5, pp. 216–22. ISSN: 0166-2236. URL: http://www.ncbi.nlm.nih.gov/pubmed/10782127.

Iaccarino, Hannah F. et al. (2016). "Gamma frequency entrainment attenuates amyloid load and modifies microglia". In: *Nature* 540.7632, pp. 230–235. ISSN: 0028-0836. DOI: 10.1038/nature20587. URL: http://www.ncbi.nlm.nih.gov/pubmed/27929004http://www.pubmedcentral.nih.gov/articlerender.fcgi?artid=PMC5656389http://www.nature.com/doifinder/10.1038/nature20587.

Ismail, Rola et al. (2018). "The Effect of 40-Hz Light Therapy on Amyloid Load in Patients with Prodromal and Clinical Alzheimer's Disease". In: *International Journal of Alzheimer's Disease* 2018, pp. 1–5. ISSN: 2090-8024. DOI: 10.1155/2018/6852303. URL: https://www.hindawi.com/journals/ijad/2018/6852303/.

Jensen, Ole and Laura L. Colgin (2007). "Cross-frequency coupling between neuronal oscillations". In: *Trends in Cognitive Sciences* 11.7, pp. 267–269. ISSN: 13646613. DOI: 10.1016/j.tics.2007.05.003. URL: http://www.ncbi.nlm.nih.gov/pubmed/17548233http://linkinghub.elsevier.com/retrieve/pii/S1364661307001271.

Jensen, Ole et al. (2002). "Oscillations in the alpha band (9-12 Hz) increase with memory load during retention in a short-term memory task." In: *Cerebral cortex (New York, N.Y. : 1991)* 12.8, pp. 877–82. ISSN: 1047-3211. URL: http://www.ncbi.nlm.nih.gov/pubmed/12122036.

Kamiya, Joe (2011). "The First Communications About Operant Conditioning of the EEG". In: *Journal of Neurotherapy* 15.1, pp. 65–73. ISSN: 1087-4208. DOI: 10.1080/10874208.2011.545764. URL: http://www.isnr-jnt.org/article/view/16584.

Kan, Donica Pei Xin and Pok F. Lee (2015). "Decrease alpha waves in depression: An electroencephalogram(EEG) study". In: *undefined*. URL: https://www.semanticscholar.org/paper/Decrease-alpha-waves-in-depression{\%}3A-An-study-Kan-Lee/be6d0e808076881b4a70ac3ca31ebd2cf391867e.

Kay, Leslie M (2015). "Olfactory system oscillations across phyla." In: *Current opinion in neurobiology* 31, pp. 141–7. ISSN: 1873-6882. DOI: 10.1016/j.conb.2014.10.004. URL: https://linkinghub.elsevier.com/retrieve/pii/S0959438814002049http://www.ncbi.nlm.nih.gov/pubmed/25460070http://www.pubmedcentral.nih.gov/articlerender.fcgi?artid=PMC4374988.

Keel, John C, Mark J Smith, and Eric M Wassermann (2001). "A safety screening questionnaire for transcranial magnetic stimulation." In: *Clinical neurophysiology: official journal of the International Federation of Clinical Neurophysiology* 112.4, pp. 720–720.

Kim, Shinheun et al. (2016). "Rhythmical Photic Stimulation at Alpha Frequencies Produces Antidepressant-Like Effects in a Mouse Model of Depression". In: *PLOS ONE* 11.1. Ed. by Per Svenningsson, e0145374. ISSN: 1932-6203. DOI: 10.1371/journal.pone.0145374. URL: https://dx.plos.org/10.1371/journal.pone.0145374.

Klimesch, Wolfgang (1997). "EEG-alpha rhythms and memory processes." In: *International journal of psychophysiology : official journal of the International Organization of Psychophysiology* 26.1-3, pp. 319–40. ISSN: 0167-8760. URL: http://www.ncbi.nlm.nih.gov/pubmed/9203012.

— (2012). "Alpha-band oscillations, attention, and controlled access to stored information". In: *Trends in Cognitive Sciences* 16.12, pp. 606–617. ISSN: 13646613. DOI: 10.1016/j.tics.2012.10.007. URL: http://www.ncbi.nlm.nih.gov/pubmed/23141428http://www.pubmedcentral.nih.gov/articlerender.fcgi?artid=PMC3507158https://linkinghub.elsevier.com/retrieve/pii/S1364661312002434.

— (2013). "An algorithm for the EEG frequency architecture of consciousness and brain body coupling." In: *Frontiers in human neuroscience* 7, p. 766. ISSN: 1662-5161. DOI: 10.3389/fnhum.2013.00766. URL: http://www.ncbi.nlm.nih.gov/pubmed/24273507http://www.pubmedcentral.nih.gov/articlerender.fcgi?artid=PMC3824085.

— (2018). "The frequency architecture of brain and brain body oscillations: an analysis". In: *European Journal of Neuroscience* 48.7, pp. 2431–2453. ISSN: 0953816X. DOI: 10.1111/ejn.14192. URL: http://www.ncbi.nlm.nih.gov/pubmed/30281858http://doi.wiley.com/10.1111/ejn.14192.

Klimesch, Wolfgang, Paul Sauseng, and Simon Hanslmayr (2007). "EEG alpha oscillations: The inhibition–timing hypothesis". In: *Brain Research Reviews* 53.1, pp. 63–88. ISSN: 01650173. DOI: 10.1016/j.brainresrev.2006.06.003. URL: http://www.ncbi.nlm.nih.gov/pubmed/16887192http://linkinghub.elsevier.com/retrieve/pii/S016501730600083X.

Kluetsch, R. C. et al. (2014). "Plastic modulation of PTSD resting-state networks and subjective wellbeing by EEG neurofeedback". In: *Acta Psychiatrica Scandinavica* 130.2, pp. 123–136. ISSN: 0001690X. DOI: 10.1111/acps.12229. URL: http://www.ncbi.nlm.nih.gov/pubmed/24266644http://www.pubmedcentral.nih.gov/articlerender.fcgi?artid=PMC4442612http://doi.wiley.com/10.1111/acps.12229.

Kornmeier, Jürgen and Michael Bach (2012). "Ambiguous Figures – What Happens in the Brain When Perception Changes But Not the Stimulus". In: *Frontiers in Human Neuroscience* 6, p. 51. ISSN: 1662-5161. DOI: 10.3389/fnhum.2012.00051. URL: http://journal.frontiersin.org/article/10.3389/fnhum.2012.00051/abstract.

Kothe, C (2014). "Lab streaming layer (LSL)". In: *https://github. com/sccn/labstreaminglayer. Accessed on December 2018* 26, p. 2015.

Kruschke, John K. (2013). "Bayesian estimation supersedes the t test." In: *Journal of Experimental Psychology: General* 142.2, pp. 573–603. ISSN: 1939-2222. DOI: 10.1037/a0029146. URL: http://www.ncbi.nlm.nih.gov/pubmed/22774788http://doi.apa.org/getdoi.cfm?doi=10.1037/a0029146.

Kruschke, John K and Wolf Vanpaemel (2015). "Bayesian estimation in hierarchical models". In: *The Oxford handbook of computational and mathematical psychology*, pp. 279–299.

Lakatos, Peter et al. (2016). "Global dynamics of selective attention and its lapses in primary auditory cortex". In: *Nature Neuroscience* 19.12, pp. 1707–1717. ISSN: 1097-6256. DOI: 10.1038/nn.4386. URL: http://www.ncbi.nlm.nih.gov/pubmed/27618311http://www.pubmedcentral.nih.gov/articlerender.fcgi?artid=PMC5127770http://www.nature.com/articles/nn.4386.

Little, Simon and Peter Brown (2014). "The functional role of beta oscillations in Parkinson's disease". In: *Parkinsonism & related disorders* 20, S44–S48.

Llinás, R R et al. (1999). "Thalamocortical dysrhythmia: A neurological and neuropsychiatric syndrome characterized by magnetoencephalography." In: *Proceedings of the National Academy of Sciences of the United States of America* 96.26, pp. 15222–7. ISSN: 0027-8424. URL: http://www.ncbi.nlm.nih.gov/pubmed/10611366http://www.pubmedcentral.nih.gov/articlerender.fcgi?artid=PMC24801.

Loomis, A. L., E. N. Harvey, and G. Hobart (1935). "FURTHER OBSERVATIONS ON THE POTENTIAL RHYTHMS OF THE CEREBRAL CORTEX DURING SLEEP". In: *Science* 82.2122, pp. 198–200. ISSN: 0036-8075. DOI: 10.1126/science.82.2122.198. URL: http://www.sciencemag.org/cgi/doi/10.1126/science.82.2122.198.

Loomis, A. L., E. N. Harvey, and G. A. Hobart (1937). "Cerebral states during sleep, as studied by human brain potentials." In: *Journal of Experimental Psychology* 21.2, pp. 127–144. ISSN: 0022-1015. DOI: 10.1037/h0057431. URL: http://content.apa.org/journals/xge/21/2/127.

Lopes da Silva, Fernando (2013). "EEG and MEG: Relevance to Neuroscience". In: *Neuron* 80.5, pp. 1112–1128. ISSN: 08966273. DOI: 10.1016/j.neuron.2013.10.017. URL: http://www.ncbi.nlm.nih.gov/pubmed/24314724https://linkinghub.elsevier.com/retrieve/pii/S0896627313009203.

Lopez-Calderon, Javier and Steven J Luck (2014). "ERPLAB: an open-source toolbox for the analysis of event-related potentials." In: *Frontiers in human neuroscience* 8, p. 213. ISSN: 1662-5161. DOI: 10.3389/fnhum.2014.00213. URL: http://www.ncbi.nlm.nih.gov/pubmed/24782741http://www.pubmedcentral.nih.gov/articlerender.fcgi?artid=PMC3995046.

Lőrincz, Magor L. et al. (2009). "Temporal Framing of Thalamic Relay-Mode Firing by Phasic Inhibition during the Alpha Rhythm". In: *Neuron* 63.5, pp. 683–696. ISSN: 08966273. DOI: 10.1016/j.neuron.2009.08.012. URL: http://www.ncbi.nlm.nih.gov/pubmed/19755110http://www.pubmedcentral.nih.gov/articlerender.fcgi?artid=PMC2791173http://linkinghub.elsevier.com/retrieve/pii/S0896627309006242.

MacIver, M. B. and Brian H. Bland (2014). "Chaos analysis of EEG during isoflurane-induced loss of righting in rats". In: *Frontiers in Systems Neuroscience* 8, p. 203. ISSN: 1662-5137. DOI: 10.3389/fnsys.2014.00203. URL: http://www.ncbi.nlm.nih.gov/pubmed/25360091http://www.pubmedcentral.nih.gov/articlerender.fcgi?artid=PMC4199270http://journal.frontiersin.org/article/10.3389/fnsys.2014.00203/abstract.

Manly, Bryan F. J. (2007). *Randomization, bootstrap and Monte Carlo methods in biology*. Chapman & Hall/ CRC, p. 455. ISBN: 9781584885412.

Maris, Eric and Robert Oostenveld (2007). "Nonparametric statistical testing of EEG- and MEG-data". In: *Journal of Neuroscience Methods* 164.1, pp. 177–190. ISSN: 01650270. DOI: 10.1016/j.jneumeth.2007.03.024. URL: http://www.ncbi.nlm.nih.gov/pubmed/17517438http://linkinghub.elsevier.com/retrieve/pii/S0165027007001707.

Marzbani, H., H. Marateb, and M. Mansourian (2016). "Methodological Note: Neurofeedback: A Comprehensive Review on System Design, Methodology and Clinical Applications". In: *Basic and Clinical Neuroscience Journal* 7.2, pp. 143–58. ISSN: 22287442. DOI: 10.15412/J.BCN.03070208. URL: http://www.ncbi.nlm.nih.gov/pubmed/27303609http://www.pubmedcentral.nih.gov/articlerender.fcgi?artid=PMC4892319http://bcn.iums.ac.ir/browse.php?a{_}id=608{\&}sid=1{\&}slc{_}lang=en.

Mathewson, Kyle E. et al. (2011). "Pulsed Out of Awareness: EEG Alpha Oscillations Represent a Pulsed-Inhibition of Ongoing Cortical Processing". In: *Frontiers in Psychology* 2, p. 99. ISSN: 1664-1078. DOI: 10.3389/fpsyg.2011.00099. URL: http://journal.frontiersin.org/article/10.3389/fpsyg.2011.00099/abstract.

Mathewson, Kyle E. et al. (2012). "Making Waves in the Stream of Consciousness: Entraining Oscillations in EEG Alpha and Fluctuations in Visual Awareness with Rhythmic Visual Stimulation". In: *Journal of Cognitive Neuroscience* 24.12, pp. 2321–2333. ISSN: 0898-929X. DOI: 10.1162/jocn_a_00288. URL: http://www.ncbi.nlm.nih.gov/pubmed/22905825http://www.mitpressjournals.org/doi/10.1162/jocn{_}a{_}00288.

Mazzoni, Alberto et al. (2010). "Understanding the relationships between spike rate and delta/gamma frequency bands of LFPs and EEGs using a local cortical network model". In: *NeuroImage* 52.3, pp. 956–972. ISSN: 10538119. DOI: 10.1016/j.neuroimage.2009.12.040. URL: http://www.ncbi.nlm.nih.gov/pubmed/20026218http://linkinghub.elsevier.com/retrieve/pii/S1053811909013299.

Meeuwissen, Esther B. et al. (2011). "Increase in posterior alpha activity during rehearsal predicts successful long-term memory formation of word sequences". In: *Human Brain Mapping* 32.12, pp. 2045–2053. ISSN: 10659471. DOI: 10.1002/hbm.21167. URL: http://www.ncbi.nlm.nih.gov/pubmed/21162031http://doi.wiley.com/10.1002/hbm.21167.

Mehaffey, W Hamish et al. (2008). "Ionic and neuromodulatory regulation of burst discharge controls frequency tuning." In: *Journal of physiology, Paris* 102.4-6, pp. 195–208. ISSN: 0928-4257. DOI: 10.1016/j.jphysparis.2008.10.019. URL: http://www.ncbi.nlm.nih.gov/pubmed/18992813http://www.pubmedcentral.nih.gov/articlerender.fcgi?artid=PMC4529324.

Mehrkanoon, Saeid, Michael Breakspear, and Tjeerd W. Boonstra (2014). "Low-Dimensional Dynamics of Resting-State Cortical Activity". In: *Brain Topography* 27.3, pp. 338–352. ISSN: 0896-0267. DOI: 10.1007/s10548-013-0319-5. URL: http://www.ncbi.nlm.nih.gov/pubmed/24104726http://link.springer.com/10.1007/s10548-013-0319-5.

Mitra, Partha and Hemant Bokil (2007). *Observed Brain Dynamics*. Oxford University Press. ISBN: 9780195178081. DOI: 10.1093/acprof:oso/9780195178081.001.0001. URL: http://www.oxfordscholarship.com/view/10.1093/acprof:oso/9780195178081.001.0001/acprof-9780195178081.

Montez, Teresa et al. (2009). "Altered temporal correlations in parietal alpha and prefrontal theta oscillations in early-stage Alzheimer disease." In: *Proceedings of the National Academy of Sciences of the United States of America* 106.5, pp. 1614–9. ISSN: 1091-6490. DOI: 10.1073/pnas.0811699106. URL: http://www.ncbi.nlm.nih.gov/pubmed/19164579http://www.pubmedcentral.nih.gov/articlerender.fcgi?artid=PMC2635782.

More, Max and Natasha Vita-More (2013). *The transhumanist reader: Classical and contemporary essays on the science, technology, and philosophy of the human future*. John Wiley & Sons.

Mouli, Surej and Ramaswamy Palaniappan (2016). "Eliciting higher SSVEP response from LED visual stimulus with varying luminosity levels". In: *2016 International Conference for Students on Applied Engineering (ICSAE)*. IEEE, pp. 201–206.

Murakami, Shingo, Akira Hirose, and Yoshio C Okada (2003). "Contribution of ionic currents to magnetoencephalography (MEG) and electroencephalography (EEG) signals generated by guinea-pig CA3 slices." In: *The Journal of physiology* 553.Pt 3, pp. 975–85. ISSN: 0022-3751. DOI: 10.1113/jphysiol.2003.051144. URL: http://www.ncbi.nlm.nih.gov/pubmed/14528026http://www.pubmedcentral.nih.gov/articlerender.fcgi?artid=PMC2343617.

Nagengast, Arne J., Daniel A. Braun, and Daniel M. Wolpert (2009). "Optimal Control Predicts Human Performance on Objects with Internal Degrees of Freedom". In: *PLoS Computational Biology* 5.6. Ed. by Konrad Kording, e1000419. ISSN: 1553-7358. DOI: 10.1371/journal.pcbi.1000419. URL: https://dx.plos.org/10.1371/journal.pcbi.1000419.

Nenert, Rodolphe et al. (2012). "Modulations of ongoing alpha oscillations predict successful short-term visual memory encoding." In: *Frontiers in human neuroscience* 6, p. 127. ISSN: 1662-5161. DOI: 10.3389/fnhum.2012.00127. URL: http://www.ncbi.nlm.nih.gov/pubmed/22586390http://www.pubmedcentral.nih.gov/articlerender.fcgi?artid=PMC3347628.

Neuper, Christa. and Wolfgang. Klimesch (2006). *Event-related dynamics of brain oscillations*. Elsevier, p. 448. ISBN: 9780444521835. URL: https://graz.pure.elsevier.com/en/publications/event-related-dynamics-of-brain-oscillations.

Nieuwenhuijzen, M.E. van de et al. (2013). "MEG-based decoding of the spatiotemporal dynamics of visual category perception". In: *NeuroImage* 83, pp. 1063–1073. ISSN: 10538119. DOI: 10.1016/j.neuroimage.2013.07.075. URL: http://www.ncbi.nlm.nih.gov/pubmed/23927900https://linkinghub.elsevier.com/retrieve/pii/S1053811913008446.

Niv, Sharon (2013). "Clinical efficacy and potential mechanisms of neurofeedback". In: *Personality and Individual Differences* 54.6, pp. 676–686. ISSN: 01918869. DOI: 10.1016/j.paid.2012.11.037. URL: https://linkinghub.elsevier.com/retrieve/pii/S0191886912006241.

Norman, Donald A. and Tim Shallice (1986). "Attention to Action". In: *Consciousness and Self-Regulation*. Boston, MA: Springer US, pp. 1–18. DOI: 10.1007/978-1-4757-0629-1_1. URL: http://link.springer.com/10.1007/978-1-4757-0629-1{_}1.

Olive, Melissa L. and Benjamin W. Smith (2005). "Effect size calculations and single subject designs". In: *Educational Psychology* 25.2-3, pp. 313–324. ISSN: 01443410.

DOI: 10.1080/0144341042000301238. URL: https://www.tandfonline.com/doi/full/10.1080/0144341042000301238.

Palva, Satu and J. Matias Palva (2007). "New vistas for α-frequency band oscillations". In: *Trends in Neurosciences* 30.4, pp. 150–158. ISSN: 01662236. DOI: 10.1016/j.tins.2007.02.001. URL: http://www.ncbi.nlm.nih.gov/pubmed/17307258http://linkinghub.elsevier.com/retrieve/pii/S0166223607000264.

— (2012). "Discovering oscillatory interaction networks with M/EEG: challenges and breakthroughs". In: *Trends in Cognitive Sciences* 16.4, pp. 219–230. ISSN: 13646613. DOI: 10.1016/j.tics.2012.02.004. URL: http://www.ncbi.nlm.nih.gov/pubmed/22440830https://linkinghub.elsevier.com/retrieve/pii/S1364661312000472.

Panzeri, Stefano et al. (2010). "Sensory neural codes using multiplexed temporal scales". In: *Trends in Neurosciences* 33.3, pp. 111–120. ISSN: 01662236. DOI: 10.1016/j.tins.2009.12.001. URL: http://www.ncbi.nlm.nih.gov/pubmed/20045201http://linkinghub.elsevier.com/retrieve/pii/S0166223609002008.

Park, Hyojin et al. (2014). "Blocking of irrelevant memories by posterior alpha activity boosts memory encoding". In: *Human Brain Mapping* 35.8, pp. 3972–3987. ISSN: 10659471. DOI: 10.1002/hbm.22452. URL: http://www.ncbi.nlm.nih.gov/pubmed/24522937http://doi.wiley.com/10.1002/hbm.22452.

Pastukhov, Alexander et al. (2013). "Multi-stable perception balances stability and sensitivity". In: *Frontiers in Computational Neuroscience* 7, p. 17. ISSN: 1662-5188. DOI: 10.3389/fncom.2013.00017. URL: http://journal.frontiersin.org/article/10.3389/fncom.2013.00017/abstract.

Patten, Timothy M. et al. (2012). "Human Cortical Traveling Waves: Dynamical Properties and Correlations with Responses". In: *PLoS ONE* 7.6. Ed. by Pedro Antonio Valdes-Sosa, e38392. ISSN: 1932-6203. DOI: 10.1371/journal.pone.0038392. URL: https://dx.plos.org/10.1371/journal.pone.0038392.

Perrin, F. et al. (1989). "Spherical splines for scalp potential and current density mapping". In: *Electroencephalography and Clinical Neurophysiology* 72.2, pp. 184–187. ISSN: 0013-4694. DOI: 10.1016/0013-4694(89)90180-6. URL: https://www.sciencedirect.com/science/article/abs/pii/0013469489901806.

Pfurtscheller, G and F H Lopes da Silva (1999). "Event-related EEG/MEG synchronization and desynchronization: basic principles." In: *Clinical neurophysiology : official journal of the International Federation of Clinical Neurophysiology* 110.11, pp. 1842–57. ISSN: 1388-2457. DOI: 10.1016/S1388-2457(99)00141-8. URL: http://www.ncbi.nlm.nih.gov/pubmed/10576479.

Pfurtscheller, Gert and Christa Neuper (1994). "Event-related synchronization of mu rhythm in the EEG over the cortical hand area in man". In: *Neuroscience Letters* 174.1, pp. 93–96. ISSN: 0304-3940. DOI: 10.1016/0304-3940(94)90127-9. URL: https://www.sciencedirect.com/science/article/abs/pii/0304394094901279?via{\%}3Dihub.

Pfurtscheller, Gert and Fernando Lopes da Silva (2017). *EEG Event-Related Desynchronization and Event-Related Synchronization*. Ed. by Donald L. Schomer and Fernando H. Lopes da Silva. Vol. 1. Oxford University Press. DOI: 10.1093/med/9780190228484.003.0040. URL: http://www.oxfordmedicine.com/view/10.1093/med/9780190228484.001.0001/med-9780190228484-chapter-40.

Pikovsky, Arkady, Michael Rosenblum, and J. (Jurgen) Kurths (2001). *Synchronization : a universal concept in nonlinear sciences*. Cambridge University Press, p. 411. ISBN: 052153352X.

Placencia, M. et al. (1992). "Validation of a screening questionnaire for the detection of epileptic seizures in epidemiological studies". In: *Brain*. ISSN: 00068950. DOI: 10.1093/brain/115.3.783.

Pletzer, Belinda, Hubert Kerschbaum, and Wolfgang Klimesch (2010). "When frequencies never synchronize: The golden mean and the resting EEG". In: *Brain Research* 1335, pp. 91–102. ISSN: 0006-8993. DOI: 10.1016/J.BRAINRES.2010.03.074. URL: https://www.sciencedirect.com/science/article/pii/S0006899310007092?via{\%}3Dihub.

Poil, Simon-Shlomo et al. (2012). "Critical-state dynamics of avalanches and oscillations jointly emerge from balanced excitation/inhibition in neuronal networks." In: *The Journal of neuroscience : the official journal of the Society for Neuroscience* 32.29, pp. 9817–23. ISSN: 1529-2401. DOI: 10.1523/JNEUROSCI.5990-11.2012. URL: http://www.ncbi.nlm.nih.gov/pubmed/22815496http://www.pubmedcentral.nih.gov/articlerender.fcgi?artid=PMC3553543.

Pradhan, N. et al. (1995). "Patterns of attractor dimensions of sleep EEG". In: *Computers in Biology and Medicine* 25.5, pp. 455–462. ISSN: 0010-4825. DOI: 10.1016/0010-4825(95)00032-Y. URL: https://www.sciencedirect.com/science/article/pii/001048259500032Y.

Puil, E., H. Meiri, and Y. Yarom (1994). "Resonant behavior and frequency preferences of thalamic neurons". In: *Journal of Neurophysiology* 71.2, pp. 575–582. ISSN: 0022-3077. DOI: 10.1152/jn.1994.71.2.575. URL: http://www.ncbi.nlm.nih.gov/pubmed/8176426http://www.physiology.org/doi/10.1152/jn.1994.71.2.575.

Rohenkohl, Gustavo and Anna C. Nobre (2011). "Alpha Oscillations Related to Anticipatory Attention Follow Temporal Expectations". In: *Journal of Neuroscience* 31.40, pp. 14076–14084. ISSN: 0270-6474. DOI: 10.1523/JNEUROSCI.3387-11.2011. URL: http://www.jneurosci.org/content/31/40/14076.

Ros, Tomas et al. (2014). "Tuning pathological brain oscillations with neurofeedback: a systems neuroscience framework". In: *Frontiers in Human Neuroscience* 8, p. 1008. ISSN: 1662-5161. DOI: 10.3389/fnhum.2014.01008. URL: http://journal.frontiersin.org/article/10.3389/fnhum.2014.01008/abstract.

Russo, R, H J Herrmann, and L de Arcangelis (2014). "Brain modularity controls the critical behavior of spontaneous activity." In: *Scientific reports* 4, p. 4312. ISSN: 2045-2322. DOI: 10.1038/srep04312. URL: http://www.ncbi.nlm.nih.gov/pubmed/24621482http://www.pubmedcentral.nih.gov/articlerender.fcgi?artid=PMC3952147.

Saalmann, Y. B. et al. (2012). "The Pulvinar Regulates Information Transmission Between Cortical Areas Based on Attention Demands". In: *Science* 337.6095, pp. 753–756. ISSN: 0036-8075. DOI: 10.1126/science.1223082. URL: http://www.ncbi.nlm.nih.gov/pubmed/22879517http://www.pubmedcentral.nih.gov/articlerender.fcgi?artid=PMC3714098http://www.sciencemag.org/cgi/doi/10.1126/science.1223082.

Shephard, Elizabeth et al. (2019). "Oscillatory neural networks underlying resting-state, attentional control and social cognition task conditions in children with ASD, ADHD and ASD+ ADHD". In: *Cortex* 117, pp. 96–110.

Shew, Woodrow L. and Dietmar Plenz (2013). "The Functional Benefits of Criticality in the Cortex". In: *The Neuroscientist* 19.1, pp. 88–100. ISSN: 1073-8584. DOI: 10.1177/1073858412445487. URL: http://www.ncbi.nlm.nih.gov/pubmed/22627091http://journals.sagepub.com/doi/10.1177/1073858412445487.

Siebenhühner, Felix et al. (2016). "Cross-frequency synchronization connects networks of fast and slow oscillations during visual working memory maintenance".

In: *eLife* 5. ISSN: 2050-084X. DOI: 10.7554/eLife.13451. URL: https://elifesciences.org/articles/13451.

Siegel, Markus, Tobias H. Donner, and Andreas K. Engel (2012). "Spectral fingerprints of large-scale neuronal interactions". In: *Nature Reviews Neuroscience* 13.2, pp. 121–134. ISSN: 1471-003X. DOI: 10.1038/nrn3137. URL: http://www.ncbi.nlm.nih.gov/pubmed/22233726http://www.nature.com/articles/nrn3137.

Singer, W (1993). "Synchronization of Cortical Activity and its Putative Role in Information Processing and Learning". In: *Annual Review of Physiology* 55.1, pp. 349–374. ISSN: 0066-4278. DOI: 10.1146/annurev.ph.55.030193.002025. URL: http://www.ncbi.nlm.nih.gov/pubmed/8466179http://www.annualreviews.org/doi/10.1146/annurev.ph.55.030193.002025.

Sohn, Hansem et al. (2010). "Linear and non-linear EEG analysis of adolescents with attention-deficit/hyperactivity disorder during a cognitive task." In: *Clinical neurophysiology : official journal of the International Federation of Clinical Neurophysiology* 121.11, pp. 1863–70. ISSN: 1872-8952. DOI: 10.1016/j.clinph.2010.04.007. URL: http://www.ncbi.nlm.nih.gov/pubmed/20659814.

Spielberger, C. D., R. L. Gorsuch, and R. E. Lushene (1970). *The State-Trait Anxiety Inventory Manual*. DOI: 10.1037/t06496-000.

Sporns, Olaf and Christopher J Honey (2006). "Small worlds inside big brains." In: *Proceedings of the National Academy of Sciences of the United States of America* 103.51, pp. 19219–20. ISSN: 0027-8424. DOI: 10.1073/pnas.0609523103. URL: http://www.ncbi.nlm.nih.gov/pubmed/17159140http://www.pubmedcentral.nih.gov/articlerender.fcgi?artid=PMC1748207.

Stam, C J (2005). "Nonlinear dynamical analysis of EEG and MEG: review of an emerging field." In: *Clinical neurophysiology : official journal of the International Federation of Clinical Neurophysiology* 116.10, pp. 2266–301. ISSN: 1388-2457. DOI: 10.1016/j.clinph.2005.06.011. URL: http://www.ncbi.nlm.nih.gov/pubmed/16115797.

Stein, Astrid von and Johannes Sarnthein (2000). "Different frequencies for different scales of cortical integration: from local gamma to long range alpha/theta synchronization". In: *International Journal of Psychophysiology* 38.3, pp. 301–313. ISSN: 0167-8760. DOI: 10.1016/S0167-8760(00)00172-0. URL: https://www.sciencedirect.com/science/article/abs/pii/S0167876000001720?via{\%}3Dihub.

Steriade, M. et al. (1990). "Basic mechanisms of cerebral rhythmic activities". In: *Electroencephalography and Clinical Neurophysiology* 76.6, pp. 481–508. ISSN: 00134694. DOI: 10.1016/0013-4694(90)90001-Z. URL: http://linkinghub.elsevier.com/retrieve/pii/001346949090001Z.

Sterman, M B, R C Howe, and L R Macdonald (1970). "Facilitation of spindle-burst sleep by conditioning of electroencephalographic activity while awake." In: *Science (New York, N.Y.)* 167.3921, pp. 1146–8. ISSN: 0036-8075. URL: http://www.ncbi.nlm.nih.gov/pubmed/5411633.

Sterman, M. B., R. W. LoPresti, and M. D. Fairchild (2010). "Electroencephalographic and Behavioral Studies of Monomethyl Hydrazine Toxicity in the Cat". In: *Journal of Neurotherapy* 14.4, pp. 293–300. ISSN: 1087-4208. DOI: 10.1080/10874208.2010.523367. URL: http://www.isnr-jnt.org/article/view/16596.

Sterman, M.B and L Friar (1972). "Suppression of seizures in an epileptic following sensorimotor EEG feedback training". In: *Electroencephalography and Clinical Neurophysiology* 33.1, pp. 89–95. ISSN: 0013-4694. DOI: 10.1016/0013-4694(72)90028-4. URL: https://www.sciencedirect.com/science/article/abs/pii/0013469472900284.

Sterman, MB, RW LoPresti, and MD Fairchild (1969). *Electroencephalographic and behavioral studies of monomethylhydrazine toxicity in the cat*. Tech. rep. CALIFORNIA UNIV LOS ANGELES BRAIN RESEARCH INST.

Suffcynski, P. et al. (1999). *Event-related dynamics of alpha band rhythms: A neuronal network model of focal ERD/surround ERS*. URL: https://graz.pure.elsevier.com/en/publications/event-related-dynamics-of-alpha-band-rhythms-a-neuronal-network-m.

Suffczynski, P et al. (2001). "Computational model of thalamo-cortical networks: dynamical control of alpha rhythms in relation to focal attention." In: *International journal of psychophysiology : official journal of the International Organization of Psychophysiology* 43.1, pp. 25–40. ISSN: 0167-8760. DOI: 10.1016/S0167-8760(01)00177-5. URL: http://www.ncbi.nlm.nih.gov/pubmed/11742683.

Suzuki, H (1974). "Phase relationships of alpha rhythm in man." In: *The Japanese journal of physiology* 24.6, pp. 569–86. ISSN: 0021-521X. URL: http://www.ncbi.nlm.nih.gov/pubmed/4464361.

Terhune, Devin B et al. (2015). "Phosphene perception relates to visual cortex glutamate levels and covaries with atypical visuospatial awareness". In: *Cerebral cortex* 25.11, pp. 4341–4350.

Thatcher, Robert Wayne, Duane Michael North, and Carl John Biver (2009). "Self-organized criticality and the development of EEG phase reset". In: *Human Brain Mapping* 30.2, pp. 553–574. ISSN: 10659471. DOI: 10.1002/hbm.20524. URL: http://doi.wiley.com/10.1002/hbm.20524.

The Mathworks Inc. (2017). *MATLAB - MathWorks*. DOI: 2016-11-26.

Theiler, James et al. (1992). "Testing for nonlinearity in time series: the method of surrogate data". In: *Physica D: Nonlinear Phenomena* 58.1-4, pp. 77–94. ISSN: 0167-2789. DOI: 10.1016/0167-2789(92)90102-S. URL: https://www.sciencedirect.com/science/article/pii/016727899290102S.

Thorpe, Samuel G., Erin N. Cannon, and Nathan A. Fox (2016). "Spectral and source structural development of mu and alpha rhythms from infancy through adulthood". In: *Clinical Neurophysiology* 127.1, pp. 254–269. ISSN: 13882457. DOI: 10.1016/j.clinph.2015.03.004. URL: http://www.ncbi.nlm.nih.gov/pubmed/25910852http://www.pubmedcentral.nih.gov/articlerender.fcgi?artid=PMC4818120https://linkinghub.elsevier.com/retrieve/pii/S1388245715001698.

Thut, G. et al. (2006). "Alpha-Band Electroencephalographic Activity over Occipital Cortex Indexes Visuospatial Attention Bias and Predicts Visual Target Detection". In: *Journal of Neuroscience* 26.37, pp. 9494–9502. DOI: 10.1523/JNEUROSCI.0875-06.2006. URL: http://www.ncbi.nlm.nih.gov/pubmed/16971533http://www.ncbi.nlm.nih.gov/pubmed/16971533.

Thut, Gregor, Carlo Miniussi, and Joachim Gross (2012). "The Functional Importance of Rhythmic Activity in the Brain". In: *Current Biology* 22.16, R658–R663. ISSN: 09609822. DOI: 10.1016/j.cub.2012.06.061. URL: http://www.ncbi.nlm.nih.gov/pubmed/22917517https://linkinghub.elsevier.com/retrieve/pii/S0960982212007373.

Thut, Gregor, Philippe G. Schyns, and Joachim Gross (2011). "Entrainment of Perceptually Relevant Brain Oscillations by Non-Invasive Rhythmic Stimulation of the Human Brain". In: *Frontiers in Psychology* 2, p. 170. ISSN: 1664-1078. DOI: 10.3389/fpsyg.2011.00170. URL: http://journal.frontiersin.org/article/10.3389/fpsyg.2011.00170/abstract.

Todorov, Emanuel (2004). "Optimality principles in sensorimotor control." In: *Nature neuroscience* 7.9, pp. 907–15. ISSN: 1097-6256. DOI: 10.1038/nn1309. URL: http:

//www.ncbi.nlm.nih.gov/pubmed/15332089http://www.pubmedcentral.nih.gov/articlerender.fcgi?artid=PMC1488877.

Van de Ville, Dimitri, Juliane Britz, and Christoph M Michel (2010). "EEG microstate sequences in healthy humans at rest reveal scale-free dynamics." In: *Proceedings of the National Academy of Sciences of the United States of America* 107.42, pp. 18179–84. ISSN: 1091-6490. DOI: 10.1073/pnas.1007841107. URL: http://www.ncbi.nlm.nih.gov/pubmed/20921381http://www.pubmedcentral.nih.gov/articlerender.fcgi?artid=PMC2964192.

Vialatte, François-Benoît et al. (2010). "Steady-state visually evoked potentials: Focus on essential paradigms and future perspectives". In: *Progress in Neurobiology* 90.4, pp. 418–438. ISSN: 03010082. DOI: 10.1016/j.pneurobio.2009.11.005. URL: http://www.ncbi.nlm.nih.gov/pubmed/19963032http://linkinghub.elsevier.com/retrieve/pii/S0301008209001853.

Vysochanskij, DF and Yu I Petunin (1980). "Justification of the 3σ rule for unimodal distributions". In: *Theory of Probability and Mathematical Statistics* 21.25-36.

Wahbeh, Helané and Barry S. Oken (2013). "Peak High-Frequency HRV and Peak Alpha Frequency Higher in PTSD". In: *Applied Psychophysiology and Biofeedback* 38.1, pp. 57–69. ISSN: 1090-0586. DOI: 10.1007/s10484-012-9208-z. URL: http://www.ncbi.nlm.nih.gov/pubmed/23178990http://www.pubmedcentral.nih.gov/articlerender.fcgi?artid=PMC3578126http://link.springer.com/10.1007/s10484-012-9208-z.

Walter, W. Grey. (1963). *The living brain*. W. W. Norton. ISBN: 9780393001532. URL: http://books.wwnorton.com/books/The-Living-Brain/.

Walter, W. Grey, V. J. Dovey, and H. Shipton (1946). "Analysis of the Electrical Response of the Human Cortex to Photic Stimulation". In: *Nature* 158.4016, pp. 540–541. ISSN: 0028-0836. DOI: 10.1038/158540a0. URL: http://www.nature.com/articles/158540a0.

Wang, Xiao-Jing (2010). "Neurophysiological and Computational Principles of Cortical Rhythms in Cognition". In: *Physiological Reviews* 90.3, pp. 1195–1268. ISSN: 0031-9333. DOI: 10.1152/physrev.00035.2008. URL: http://www.ncbi.nlm.nih.gov/pubmed/20664082http://www.pubmedcentral.nih.gov/articlerender.fcgi?artid=PMC2923921http://www.physiology.org/doi/10.1152/physrev.00035.2008.

Westfall, P. H., S. S. Young, and S. Paul Wright (1993). "On Adjusting P-Values for Multiplicity". In: *Biometrics* 49.3, p. 941. ISSN: 0006341X. DOI: 10.2307/2532216. URL: https://www.jstor.org/stable/2532216?origin=crossref.

Williams, J H (2001). "Frequency-specific effects of flicker on recognition memory." In: *Neuroscience* 104.2, pp. 283–6. ISSN: 0306-4522. URL: http://www.ncbi.nlm.nih.gov/pubmed/11377833.

Winkler, Irene, Stefan Haufe, and Michael Tangermann (2011). "Automatic Classification of Artifactual ICA-Components for Artifact Removal in EEG Signals". In: *Behavioral and Brain Functions* 7.1, p. 30. ISSN: 1744-9081. DOI: 10.1186/1744-9081-7-30. URL: http://behavioralandbrainfunctions.biomedcentral.com/articles/10.1186/1744-9081-7-30.

Wyrwicka, Wanda and Maurice B. Sterman (1968). "Instrumental conditioning of sensorimotor cortex EEG spindles in the waking cat". In: *Physiology & Behavior* 3.5, pp. 703–707. ISSN: 00319384. DOI: 10.1016/0031-9384(68)90139-X. URL: http://linkinghub.elsevier.com/retrieve/pii/003193846890139X.

Xie, Jun et al. (2012). "Steady-state motion visual evoked potentials produced by oscillating newton's rings: implications for brain-computer interfaces". In: *Plos one* 7.6, e39707.

Yekutieli, Daniel and Yoav Benjamini (2001). "The control of the false discovery rate in multiple testing under dependency". In: *The Annals of Statistics* 29.4, pp. 1165–1188. DOI: 10.1214/aos/1013699998. URL: http://projecteuclid.org/euclid.aos/1013699998.

Zhang, Honghui et al. (2018). "Theta and Alpha Oscillations Are Traveling Waves in the Human Neocortex". In: *Neuron* 98.6, 1269–1281.e4. ISSN: 08966273. DOI: 10.1016/j.neuron.2018.05.019. URL: http://www.ncbi.nlm.nih.gov/pubmed/29887341https://linkinghub.elsevier.com/retrieve/pii/S0896627318304173.